

Oxamate-containing palladium(II) complexes: An open gate in fundamental and applied chemistry



Tesis Doctoral - Programa de doctorado en Química (3056)
Instituto de Ciencia Molecular - Departamento de Química Inorgánica
Facultad de Química - Universidad de Valencia

2015

Francisco Ramón Fortea Pérez

Dirigida por los Dres. Miguel Julve Olcina y Salah-Eddine Stiriba

Miguel Julve Olcina, Doctor en Ciencias Químicas, Catedrático de Universidad y **Salah-Eddine Stiriba** Doctor en Ciencias Químicas, Profesor contratado Doctor ambos miembros del Instituto de Ciencia Molecular (ICMol) y de los Departamento de Química Inorgánica y Orgánica respectivamente, de la Facultad de Química de la Universidad de Valencia.

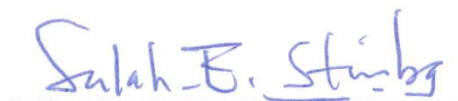
CERTIFICAN:

Que el trabajo que presenta D. **Francisco Ramón Fortea Pérez** en esta Memoria, con el título "*Oxamate-containing palladium(II) complexes: An open gate in fundamental and applied chemistry*", en el marco del programa de doctorado de Químicas ha sido realizado bajo nuestra dirección en el Instituto de Ciencia Molecular y el Departamento de Química Inorgánica de la Universidad de Valencia para optar al título de Doctor en Química.

Y para que así conste, firmamos el presente certificado en Burjassot a 30 de septiembre de 2015.



Fdo.: **Miguel Julve Olcina**



Fdo.: **Salah-Eddine Stiriba**

D. **Francisco Ramón Fortea Pérez**, Licenciado en Ciencias Químicas de la Universidad de Valencia, presenta esta memoria con el título "*Oxamate-containing palladium(II) complexes: An open gate in fundamental and applied chemistry*", en el marco del programa de doctorado en Química (3056) con el fin de optar al grado de Doctor en Ciencias Químicas.

Y para que así conste, firma la presente en Burjassot a 30 de septiembre de 2015.



Fdo.: **Francisco Ramón Fortea Pérez**

A mis tres princesas

Agradecimientos

Claramente, la parte más difícil de una tesis doctoral es plasmar los agradecimientos en una hoja de papel. Nunca sabes por quien empezar o a quien te puedes dejar olvidado...

*En mi caso, no tengo ningún problema, voy a empezar por aquella persona que me ha servido de guía y ejemplo. Es una persona que cuando la miras piensas “alguna vez seré la mitad de bueno que él”, por supuesto me estoy refiriendo a **Miguel Julve**. Para mí, esta tesis no hubiese sido posible sin su constante e incondicional ayuda y apoyo. Siempre ha estado a mi lado cuando lo he necesitado y ha sacado este proyecto adelante, así como cada uno de mis artículos. Un pequeño párrafo se queda corto para intentar explicar lo agradecido que estoy. ¡GRACIAS!*

A Salah-Eddine Stiriba por haberme propuesto este tema de trabajo e introducirme en el grupo de Química de Coordinación.

Por ello no quiero olvidarme del resto de los integrantes del grupo. Paco Lloret, que siempre está ahí para escuchar al “roget” y ayudarme en estos duros años de tesis. A Emilio con el cual conseguí mi primer artículo como primer autor y espero que sea el primero de muchos. A Joan, por dejarme participar en la tesis de Julia y mantenerme ocupado cuando más lo necesitaba. A Rafa por ayudarme de manera totalmente desinteresada siempre que ha tenido la posibilidad. A Isabel que me brindó la posibilidad de descubrir y trabajar en el sincrotrón y la última incorporación llegada de Leiden, Marta que no hemos podido trabajar juntos pero espero que tenga muchos éxitos en este grupo.

Una parte muy importante de tu tiempo de tesis son tus compañeros de laboratorio que te han acompañado día a día, por eso quiero dar las gracias a Julia, Alex, Zulema, Martita, Lucía, Manu, Cristian y Javi por los buenos momentos en el laboratorio (sobre todo a ti Alex, que fuiste un chorro de aire fresco), la desconexión del laboratorio en las comidas, por saber escuchar nuestras penas pre-doctorales y por siempre preocuparnos los unos por los otros. A las Erasmus Isabel y Berit que me ayudaron a desarrollar parte de esta tesis.

Julia necesita un párrafo para ella sola. Mi compañera de laboratorio desde el principio, una trabajadora nata con una paciencia sobrehumana (aunque no lo parezca) demostrándolo: enseñándome magnetismo, el squid, tratar las medidas del mismo (una y otra vez) y diga lo que diga; ella me ha ayudado más de lo que yo he podido ayudarle. Por siempre, estar ahí ¡GRACIAS!

No todos los agradecimientos se quedan en casa, también hay una parte muy importante que se ha elaborado fuera, en Calabria, con el **Prof. Giovanni De Munno** y la **Dra. Donatella Armentano** quienes han sido mis maestros en la resolución y descripción de las estructuras cristalinas de esta Tesis Doctoral y de cualquier artículo nuestro. Grazie Tonino por preocuparse por un servidor, como si fuese un “mono” suyo, así como por el desarrollo de mis artículos.

La Dra. Donatella Armentano (con la que se que me voy a quedar corto en agradecimientos) porque es también una persona que te sirve de ejemplo a seguir. Donatella que lucha cada cristal (mío o de mis compañeros), cada estructura y saca de manera incansable el trabajo hacía delante. ¡Grazie mille!

Por último y no por ello menos importante quiero agradecer esta tesis a mi familia. Primero a mis padres que me han estado guiando desde siempre y fueron mi primer apoyo cuando elegí hacer la tesis. Y por supuesto a **Bea** (mi mujer), que siempre está ahí, para oírme y algunas veces para escucharme, apoyarme y la parte más difícil: aguantarme. Y por supuesto a **Eli** y a **Bea**, que **sois** las alegrías de la casa, a **mis** dos princesas, que me han enseñado (y estoy intentando asimilar) lo importante que es la **vida** e intentar estar siempre feliz.

*No enseñar a un hombre que está dispuesto a aprender
es desaprovechar a un hombre.*

Confucio

Index

Agradecimientos		
Contents		
Abstract	i	
List of publications	iii	
Glossary	v	
I	Introduction	1
	<i>Oxamate ligand: a suitable choice</i>	
	I.1. Coordination chemistry overview	3
	I.2. Metallo-supramolecular approach	5
	I.3. Oxalate vs. Oxamidate in molecular magnetism	7
	I.4. Oxamate ligand in crystal and magnetic engineering	8
	I.5. Oxamate-containing palladium(II) complexes:	13
	I.6. References	16
II	Chapter 1	25
	<i>Structural versatility of bis(oxamato)palladate(II) complexes</i>	
	<i>Part I: Cis-trans isomerism in solid state of bis(oxamato)palladate(II) complexes: X-ray structures and catalytic properties</i>	27
	II.1. Aim	29
	II.2. Synthesis and characterization	30
	II.3. Results and discussion	32
	II.4. Catalytic properties	63
	II.5. Conclusions	67
	<i>Part II: Halogen derivatives of bis(N-substituted oxamato)-palladate(II) complexes: structural and supramolecular features</i>	69
	II.6. Halogen bonding in crystal engineering	71
	II.7. Aim	73
	II.8. Synthesis and characterization	74
	II.9. Results and discussion	76
	II.10. Conclusions	90
	II.11. References	91

III	Chapter 2	95
	<i>Study of the influence of the substituents and solvent on the catalytic properties of bis(oxamato)palladate(II) complexes</i>	
	III.1. Carbon-carbon cross coupling reactions	97
	III.2. Aim	99
	III.3. Synthesis and characterization	100
	III.4. Results and discussion	104
	III.5. Catalytic properties	114
	III.5.1. Heck reaction – Homogeneous catalysis	114
	III.5.2. Heck reaction – Ionic liquids medium	118
	III.5.3. Suzuki reaction – Homogeneous catalysis	127
	III.5.4. Suzuki reaction – Ionic liquids medium	129
	III.6. Conclusions	132
	III.7. References	134
IV	Chapter 3	139
	<i>From serendipity to rational design</i>	
	<i>Part I: X-ray characterization of the $[Pd(H_2O)_4]^{+2}$ cation</i>	141
	IV.1. Aquapalladium(II) complexes	143
	IV.2. Aim	144
	IV.3. Synthesis and characterization	145
	IV.4. Results and discussion	146
	IV.5. Catalytic properties	154
	IV.6. Conclusions	156
	<i>Part II: Trapping the $[Pd(H_2O)_4]^{+2}$ cation</i>	157
	IV.7. The nitrile hydration reaction	159
	IV.8. Aim	160
	IV.9. Synthesis and characterization	161
	IV.10. Results and discussion	163
	IV.11. Conclusions	174
	IV.12. References	175

V	Chapter 4	179
	<i>Dinuclear palladium(II) oxamate metallacyclophanes</i>	
	V.1. Searching new functionalities	181
	V.2. Aim	184
	V.3. Synthesis and characterization	185
	V.4. Results and discussion	188
	V.5. Catalytic properties	201
	V.6. Photochemistry studies	208
	V.7. Cytotoxicity studies	219
	V.8. Conclusions	222
	V.9. References	224
VI	Conclusions and new horizons	229
VII	Appendixes	239
	Appendix A <i>Supporting information for Chapter 1</i>	241
	Appendix B <i>Supporting information for Chapter 2</i>	255
	Appendix C <i>Supporting information for Chapter 3</i>	279
	Appendix D <i>Supporting information for Chapter 4</i>	291

Abstract

La versatilidad que ofrece el ligando oxamato funcionalizado con distintos sustituyentes en forma aniónica, ha permitido desarrollar una química de coordinación muy extensa y variada. Sus inicios datan de los años ochenta, a cargo del Profesor O. Kahn y colaboradores, con una atención particular en estudios de propiedades magnéticas y estructuras cristalinas. La continuación y profundización de dicha química, desde la perspectiva del magnetismo molecular, es una línea de trabajo que nuestro grupo de investigación viene desarrollando en el ICMol durante las últimas dos décadas. Su mayor interés radica en la obtención de oxamato complejos multifuncionales.

En esa Tesis Doctoral, hemos tratado de extender el uso de los complejos con ligandos oxamato substituidos hacia nuevos campos tales como la química supramolecular (ingeniería molecular y cristalina) y la catálisis orgánica. Para ello, hemos elegido el paladio(II) como centro metálico diamagnético universalmente conocido por su aplicabilidad en procesos catalíticos.

Los resultados obtenidos en esta Tesis se han agrupado en cuatro capítulos:

(i) Un primer capítulo que se centra en la preparación, caracterización estructural y un estudio preliminar de las propiedades catalíticas (reacción de Suzuki: formación de enlaces carbono-carbono) de complejos paladio(II)-oxamato con cationes alcalinos. Se completa este capítulo con el estudio de la influencia del sustituyente halogenado del ligando oxamato en el empaquetamiento cristalino de las entidades mononucleares bis(oxamato)palladato(II).

(ii) Un segundo capítulo en el cual se han sintetizado y caracterizado mediante difracción de Rayos X sobre monocristal un total de quince oxamatocomplejos de paladio(II), los cuales se han utilizado para el estudio catalítico de reacciones de Heck y Suzuki (formación de enlaces carbono-carbono), usando mayoritariamente medios de reacción alternativos como sales iónicas (*ionic liquids*) con objeto de lograr una química más sostenible con el medio ambiente.

(iii) Un tercer capítulo donde se ha conseguido capturar cristalográficamente, por primera vez en química de coordinación, el catión $[\text{Pd}(\text{H}_2\text{O}_4)]^{+2}$ de dos maneras distintas: como contra-catión del complejo aniónico palladio(II)-oxamato y como especie activa en la hidrólisis catalítica del acetonitrilo a acetamida.

(iv) Un cuarto y último capítulo en el cual se han preparado y caracterizado estructuralmente complejos dinucleares de palladio(II)-oxamato con ligandos bis-oxamato diseñados a la carta en donde la distancia intramolecular palladio-palladio se controla con los espaciadores orgánicos entre los dos fragmentos oxamato; esta estrategia nos ha permitido estudiar las reacciones catalíticas de Heck y Suzuki, su reactividad fotoquímica y aspectos relacionados con su posible toxicidad.

List of publications

The work which was carried out in this Thesis has given rise to the following publications, some described in this dissertation:

- (1) Castellano, M.; Fortea-Pérez, F. R.; Stiriba, S.-E.; Julve, M.; Lloret, F.; Armentano, D.; De Munno, G.; Ruiz-García, R.; Cano, J. *Inorg. Chem.* **2011**, *50*, 11279.
- (2) Fortea-Pérez, F. R.; Schlegel, I.; Julve, M.; Armentano, D.; De Munno, G.; Stiriba, S.-E. *J. Organomet. Chem.* **2013**, *743*, 102. (*Chapter 2*)
- (3) Fortea-Pérez, F. R.; Vallejo, J.; Julve, M.; Lloret, F.; De Munno, G.; Armentano, D.; Pardo, E. *Inorg. Chem.* **2013**, *52*, 4777.
- (4) Fortea-Pérez, F. R.; Vallejo, J.; Inclán, M.; Déniz, M.; Pasán, J.; García-España, E.; Julve, M. *J. Coord. Chem.* **2013**, *66*, 3349.
- (5) Castellano, M.; Fortea-Pérez, F. R.; Bentama, A.; Stiriba, S.-E.; Julve, M.; Lloret, F.; De Munno, G.; Armentano, D.; Li, Y.; Ruiz-García, R.; Cano, J. *Inorg. Chem.* **2013**, *52*, 7645.
- (6) Fortea-Pérez, F. R.; Armentano, D.; Julve, M.; De Munno, G.; Stiriba, S.-E. *J. Coord. Chem.* **2014**, *67*, 4003. (*Chapter 3*)
- (7) Fortea-Pérez, F. R.; Marino, N.; Armentano, D.; De Munno, G.; Julve, M.; Stiriba, S.-E. *CrystEngComm* **2014**, *16*, 6971. (*Chapter 1*)
- (8) Martínez-Lillo, J.; Armentano, D.; Fortea-Pérez, F. R.; Stiriba, S.-E.; De Munno, G.; Lloret, F.; Julve, M.; Faus, J. *Inorg. Chem.* **2015**, *54*, 4594.
- (9) Castellano, M.; Ruiz-García, R.; Cano, J.; Ferrando-Soria, J.; Pardo, E.; Fortea-Pérez, F. R.; Stiriba, S.-E.; Julve, M.; Lloret, F. *Acc. Chem. Res.* **2015**, *48*, 510.
- (10) Castellano, M.; Ruiz-García, R.; Cano, J.; Ferrando-Soria, J.; Pardo, E.; Fortea-Pérez, F. R.; Stiriba, S.-E.; Barros, W. P.; Stumpf, H. O.; Cañadillas-Delgado, L.; Pasán, J.; Ruiz-Pérez, C.; de Munno, G.; Armentano, D.; Journaux, Y.; Lloret, F.; Julve, M. *Coord. Chem. Rev.* **2015**, *303*, 110.

- (11) Fortea-Pérez, F. R.; Rothenpieler, B. L.; Marino, N.; Armentano, D.; De Munno, G.; Julve, M.; Stiriba, S.-E. *Inorg. Chem. Front.* **2015**, DOI: 10.1039/C5QI00093A. (Chapter 2)
- (12) Fortea-Pérez, F. R.; Marino, N.; Armentano, D.; De Munno, G.; Julve, M.; Stiriba, S.-E. *Inorg. Chem.* **2015**, Manuscript ID: ic-2015-02063g. (Chapter 3)
- (13) Fortea-Pérez, F. R.; Marino, N.; De Munno, G.; Stiriba, S.-E.; Julve, M.; Armentano, D. *To be submitted to RSC Advances* (Chapter 1)

Glossary

List of abbreviations in this Thesis:

The numbering of the complexes is as follows: only digits in bold style to denote single crystals and the *a* label them indicates powder samples.

H ₂ pma	<i>N</i> -phenyloxamic acid
H ₂ -ppba	<i>N,N'</i> -1,4-phenylenebis(oxamic acid)
H ₂ -dpvba	<i>N,N'</i> -4,4'-diphenylethenebis(oxamic acid)
H ₂ -dpazba	<i>N,N'</i> -4,4'-diphenyldiazenebis(oxamic acid)
H ₂ -dpeba	<i>N,N'</i> -4,4'-diphenylethynebis(oxamic acid)
H ₂ -tpeba	<i>N,N'</i> -1,4-di(4-phenylethynyl)phenylenebis(oxamic acid)
Me-	Methyl
<i>i</i> -Pr-	Isopropyl
OMe-	Methoxy
F-	Fluoro
Cl-	Chloro
Br-	Bromo
Ph-	Phenyl
DMF	Dimethylformamide
MeOH	Methanol
MeCN	Acetonitrile
Et ₃ N	Triethylamine
OAc	Acetate
dba	dibenzylideneacetone
bzac	benzoylacetate
OEt	ethoxide
(C ₂ O ₄) ²⁻	Oxalate
<i>n</i> -Bu ₄ N ⁺	Tetra- <i>n</i> -butylammonium cation
<i>n</i> -Bu ₄ NOH	Tetra- <i>n</i> -butylammonium hydroxide
<i>n</i> -Bu ₄ NBr	Tetra- <i>n</i> -butylammonium bromide
<i>n</i> -Bu ₄ NCl	Tetra- <i>n</i> -butylammonium chloride
AsPh ₄ Cl	Tetraphenylarsonium chloride
PPh ₄ Cl	Tetraphenylphosphonium chloride
AsPh ₄ ⁺	Tetraphenylarsonium cation
As(OH) ₃	Arsenous acid
BMIMBr	1-Butyl-3-methylimidazolium bromide
BIMIMPF ₆	1-butyl-3-methylimidazolium hexafluorophosphate
Cat.	Catalyst
Reflec.	Reflections
Indep.	Independent

Glossary

Diff.	Diffractions
GC	Gas chromatography
PFTBA	Perfluorotributylamine (GC internal standard)
NMR	Nuclear magnetic resonance
TON	Turn over number $TON = \frac{mol_{Aryl\ halide} \times \frac{yield(\%)}{100}}{mol_{cat.}}$
TOF	Turn over frequency $TOF = \frac{TON}{time\ (h)}$
IC ₅₀	Concentration required to inhibit 50% of cellular growth.

I

Introduction

Oxamate ligand: a suitable choice

I.1. Coordination chemistry overview

Since the foundation of coordination chemistry by Werner in 1893¹ a remarkable effort has been devoted to the study of coordination complexes, including discrete species and coordination polymers (CPs), their functional properties and fascinating structures being two main points for this interest.²⁻⁹ The development of materials science and crystal engineering has enhanced the use of the concepts of chemistry to achieve functional materials such as catalysts, magnetic objects, non-linear optical materials and porous frameworks.¹⁰⁻¹⁸ Therefore, it is not unexpected that inorganic chemists have been betrothed to the research of coordination complexes for magnetic, catalytic, photochemical and medical applications, for instance.¹⁹⁻³⁹

This outline is intended to provide an overview from the chemistry of coordination complexes to metal-organic frameworks, focusing on supramolecular chemistry and together with the relevance of complexes as building blocks. In this respect, the choice of suitable ligands to develop this chemistry is a key point.

Coordination complexes play an important role in the design and synthesis of molecules that are able to assemble into large, well-defined supermolecules joined by non-covalent intermolecular interactions, a topic which remains one of the foremost challenges in supramolecular chemistry.⁴⁰

The spectacular development of supramolecular coordination chemistry (termed metallosupramolecular chemistry) in the late 1980s and 1990s has set up the guiding principles for the self-assembly of well-defined multimetallic coordination architectures of increasing structural complexity that are based on metal-ligands interactions.⁴¹⁻⁴⁵ Discrete zero-dimensional (0D) entities⁴⁶⁻⁴⁹ as well as one- (1D), two- (2D), or three-dimensional (3D) coordination polymers (CPs),^{15,50-52} are included in this category (Figure 1).

At the beginning of this new century, the introduction of functionality into these metallosupramolecular compounds has become one of the aims of a large number of research groups working in metallosupramolecular chemistry.⁵³⁻⁵⁸

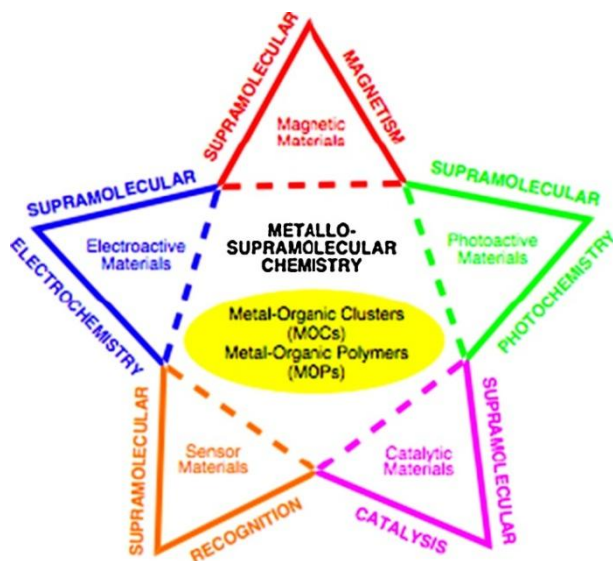


Figure 1. Relationships between metallosupramolecular chemistry and other research fields.

The unique properties exhibited by these hybrid inorganic-organic systems are not the sum of those from the cooperative interactions between the metal ions through the organic bridging ligands. The study of the supramolecular structure-function correlations will then orientate the rational design and synthesis of self-assembled supramolecular functional materials. They display interesting physicochemical properties that could be exploited in supramolecular recognition, catalysis,⁵³⁻⁵⁵ supramolecular photo-, electro-, and magnetochemistry⁵⁶⁻⁵⁸ (Figure 1).

In the search for molecular and metallosupramolecular materials, a “bottom-up” metallosupramolecular approach appears as an advantageous alternative to the classical “top-down” one toward functional magnetic, catalytic or photo-active materials. The coordination chemistry-based on the rational design and synthesis of chemical compounds with previously fixed specific properties such as magnetism,⁵⁹⁻⁶⁵ molecular recognition,^{40,66} biological activity,^{17,67} chemical sensing,⁶⁸ chirality,⁶⁹⁻⁷¹ ion conductivity or transport,⁷² conductivity,⁷³ catalysis,^{74,75} etc. are research fields of remarkable interest.

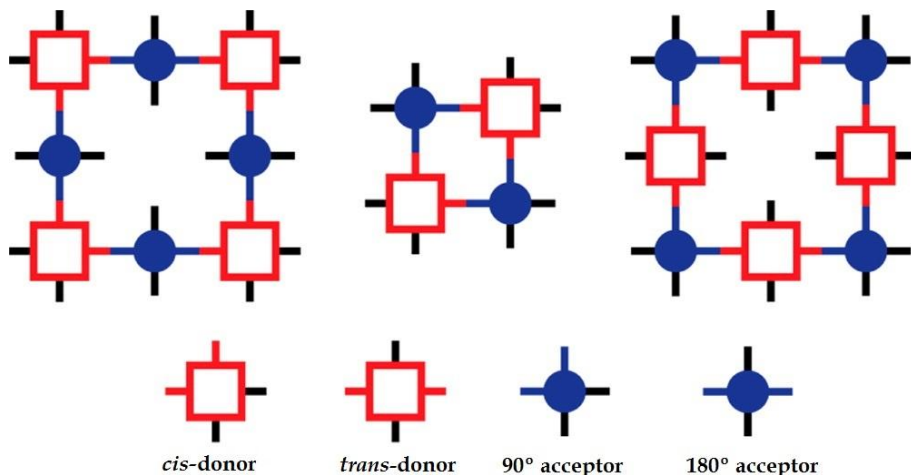
I.2. Metallosupramolecular approach

In this respect our research group focus on the design and preparation of mono- and dinuclear complexes as Lewis bases. Two possible synthetic routes have been proposed:

(i) the use of a discrete and stable entity that can be connected through linkers in a prefixed manner (node-and-spacer strategy, Scheme 1)^{76,77} or

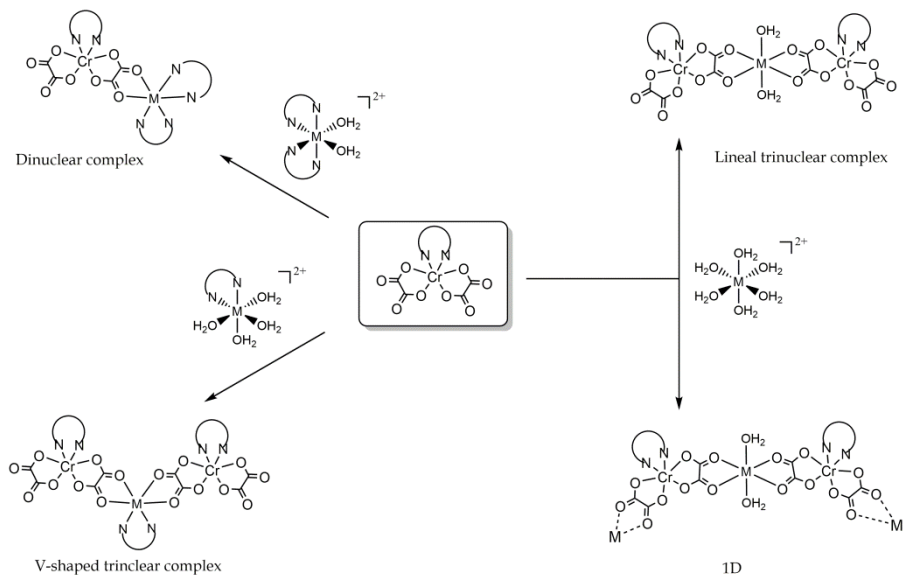
(ii) the use of such a unit as ligand towards either a fully solvated metal ion or a preformed complex whose coordination sphere is unsaturated (complex-as-ligand strategy, Scheme 2).³³

It deserves to be pointed out that these strategies are among the most established routes towards the achievement of multifunctional molecule-based materials. Two latest review articles have been devoted to the first one,^{78,79} which was inspired by the seminal studies of Robson during the nineties.^{80,81} As far as the second one is concerned, the richness and variety of polymetallic assemblies obtained through the use of cyanidometallate⁸²⁻⁸⁵, and bis(oxalato)-³³ and tris(oxalato)chromate(III)⁸⁶⁻⁹⁴ units as building blocks illustrate their potential in designing well-defined polymetallic species (see for instance Scheme 2).



Scheme 1. Topological representation of the node-and-spacer strategy.

The oxalate ligand can lead to different structures by using the strategies explained above. However, aiming at creating new structures that enrich the coordination chemistry, the oxalate as ligand has been thoroughly used over the years, as it would be summarized by Julve and Verdaguer in an up-coming oxalate review.⁹⁵



Scheme 2. Synthetic route with the complex-as-ligand strategy focusing on the complex $[\text{Cr}(\text{N}^{\wedge}\text{N})(\text{C}_2\text{O}_4)_2]^-$ as ligand.

In the light of the rich chemistry of oxalate, the coordination possibilities for related ligands have focused the attention of different research groups.

(i) Firstly, because if one has in mind that this thesis consist of finding new coordination complexes with remarkable properties by their own and as future candidates for the complex-as-ligand strategies, the use of an overworked ligand versus the palladium(II) metal ion lacks of originality see examples on literature about oxalate-palladium(II) complexes⁹⁶⁻¹⁰³.

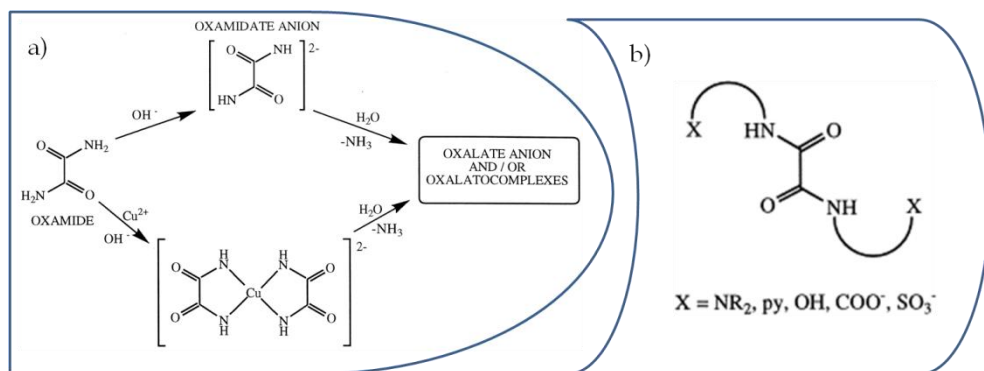
(ii) Secondly, keeping in mind that this Thesis has been carried out in a research group that focuses on the magnetic properties in coordination chemistry, the oxalate has some limitations over other ligands such as the functionalized oxamidate and oxamate ones.

I.3. Oxalate *versus* Oxamide in Molecular Magnetism

It is well-known that multiatom bridges can propagate magnetic exchange interactions between paramagnetic metal ions.⁵⁹ The dependence of the magnetic exchange on the nature of the bridging species and/or stereochemical factors has been thoroughly investigated in the 80's,^{104,105} focusing mainly on copper(II) complexes the aim being understanding of the magnitude of superexchange interactions.^{59,104}

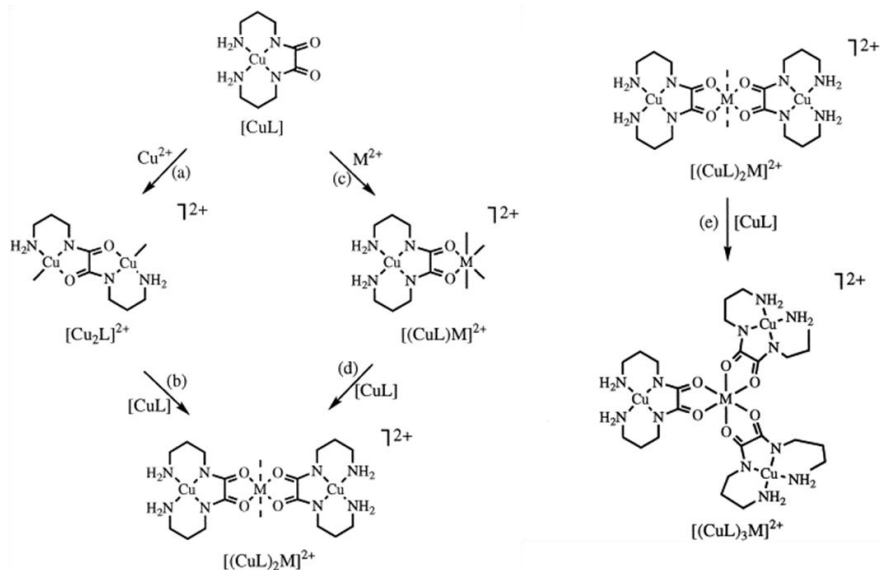
Envisaging stronger magnetic interactions between metal centers, the oxamate bridge is a better candidate than the oxalate bridge because of the lower electronegativity of the nitrogen atoms respect to the oxygen ones.¹⁰⁶⁻¹⁰⁹ For that reason, magnetic studies on oxamate-containing complexes were undertaken. Bidentate and bis-bidentate coordination modes of oxamate occurs in its metal complexes, yielding either mono-^{110,111} or polynuclear^{106,107,109,112,113} compounds, as for the parent oxalate ligand.

Compared to the oxalate ligand, the complexes with oxamate exhibit a greater stability caused by the strong electron-donating capability of its deprotonated amidate-nitrogen-atoms.¹¹⁴ However, some problems of oxamide in its use as ligand are its insolubility in common solvents and the hydrolytic reaction which it undergoes under deprotonation, yielding oxalate¹⁰⁸⁻¹¹⁰ (Scheme 3a). These problems are overcome by using *N,N'*-bis(coordinating group substituted) oxamides (Scheme 3b).



Scheme 3. a) Hydrolytic reaction of oxamide. b) Oxamide functionalization.

A great variety of substituted oxamides is available *via* simple synthetic routes which allow modifying charge, polarity, coordination capability and solubility due to the X group (Scheme 3b). An example of the diversity of species which can be designed and prepared by reaction of copper(II) and oxamate ligand is shown in Scheme 4.



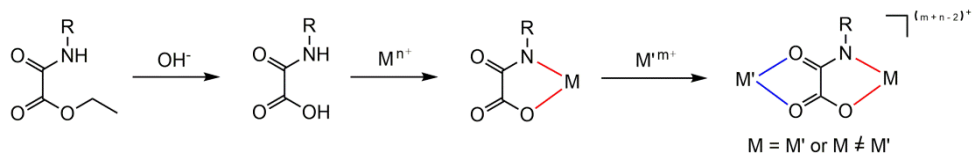
Scheme 4. Oxamate-containing copper(II) complexes as building blocks.

Both oxalate and oxamate ligands have played an important role in the rational design of heterotrinnuclear complexes and molecule-based magnets as illustrated by the great number of reports which have been devoted to these systems.^{59,60,104,115,116}

I.4. Oxamate ligand in crystal and magnetic engineering

The parent oxamate ligand raised up in 1987 when Kahn and coworkers pointed out that it was possible to have a state of high-spin multiplicity in ABA trinuclear species with local spins $2S_A > S_B + \frac{1}{2}$ without imposing ferromagnetic interactions between the nearest neighbor magnetic centers.¹¹⁵ Complexes with oxamate ligand appeared to be appropriate as bridging units for the design of this kind of magnetic systems.

As for the parent oxalate and oxamidate ligands, the oxamate dianion can adopt bidentate and bis-bidentate coordination modes in its metal complexes, to yield either mono-⁸ or polynuclear¹¹⁷ compounds (Scheme 5).



Scheme 5. Simplified route for the coordination of the oxamate ligand, where M^{n+} and M'^{m+} are metal ions.

The strong electron-donating capability of its deprotonated amide-nitrogen atom together with the good donor properties of the carboxylate-oxygen atom account for the greater stability of its metal complexes compared to the one with oxalate. Another issue to be considered is the asymmetric donor set of the oxamate, a feature that makes easier the preparation of heterometallic species.

The first bis-oxamato complex was synthesized by Nonoyama's group in 1976,¹¹⁸ and as commented above, their development was carried out by Kahn and coworkers in the late 1980s,^{60,115} and continued by Journaux's and Lloret's research groups in the late 1990s.^{8,114,119}

Our research group has taken advantage of the remarkable ability of oxamate dianion to mediate magnetic interactions between the paramagnetic metal ions bridged by them¹²⁰ to get deeper insights on the rational approach to molecule based magnets¹²¹⁻¹²⁷ and the concept of irregular spin state¹²⁸⁻¹³⁰ as well as to extend the spin polarization mechanism to coordination compounds¹³¹.

Over the years, the *N*-substituted oxamate ligands have proved to be an excellent tool to prepare mono- and dinuclear complexes (Figure 2), because of the high stability of their complexes with transition metal ions such as copper(II) ions in aqueous solution.¹¹⁴ The knowledge of the species formed in this medium has allowed the rational preparation of a great variety of homo- and heterometallic species.^{8,117}

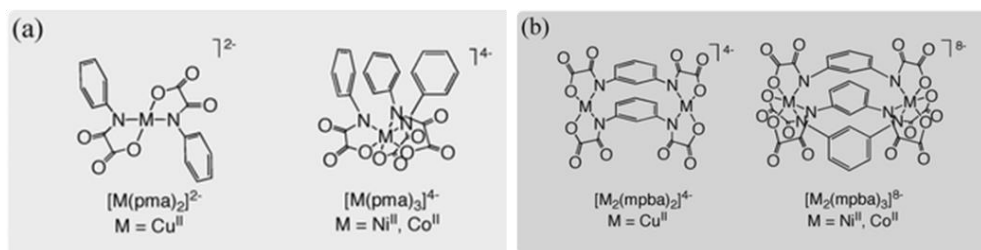


Figure 2. Self-assembling metallosupramolecular oxamato complexes with late 3d divalent metal ions of different preferred coordination geometries: (a) double and triple, *trans* and *cis* mononuclear complexes, (b) double- and triple-stranded dinuclear metallacyclic complexes.

In this pioneering work, aliphatic or aromatic group-substituted bis(oxamato)^{-60,115} and related bis(oxamidato)copper(II) complexes^{8,114,119} were used as ligands, being referred to as metal-organic ligands (MOLs).

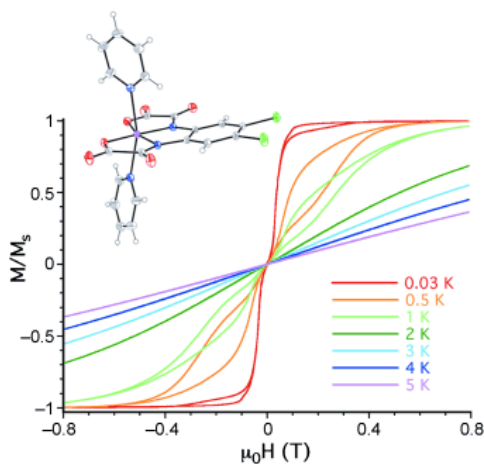


Figure 3. The first mononuclear manganese(III) complex exhibiting a slow relaxation of the magnetization (that is, a species with a single slow-relaxing, highly anisotropic Mn^{III} ion), as confirmed by very low-temperature micro-SQUID magnetization and high-field EPR spectroscopic measurements.⁹

More recent efforts with specifically substituted oxamate ligands have been directed towards the achievement of Molecule-based Multifunctional Magnetic Materials (MMMMs),¹³² illustrative examples being the preparation and characterization of Single Ion Magnets (SIMs) (Figure 3),^{9,133} Single Molecule Magnets (SMMs),^{134,135} and Chiral Single Chain Magnets (CSCMs).^{136,137}

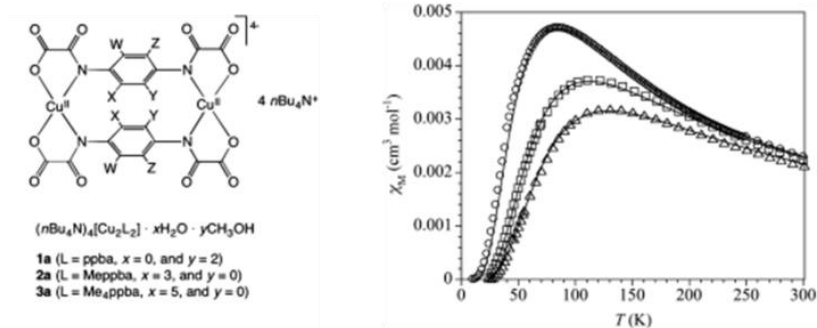


Figure 4. Dicopper(II) metallacyclophanes with electroswitchable polymethyl-substituted *para*-phenylene spacers and their antiferromagnetically coupled Cu^{II}_2 pairs.¹³⁸

Recent achievements deserve to be pointed out such as electroswitchable magnetic systems (Figure 4),¹³⁸ porous/luminescent magnets,¹³⁹ magnetic sensors of small guest molecules,^{18,140} pH-controlled switches for the reversible formation of emulsions,¹⁴¹ and chiral three-dimensional metal-organic polymers (CMOPs),¹⁴² and single crystal to single crystal transmetallation (Figure 5),¹⁴³ demonstrating the potentiality of the substituted oxamate-containing systems in the design of multifunctional materials.

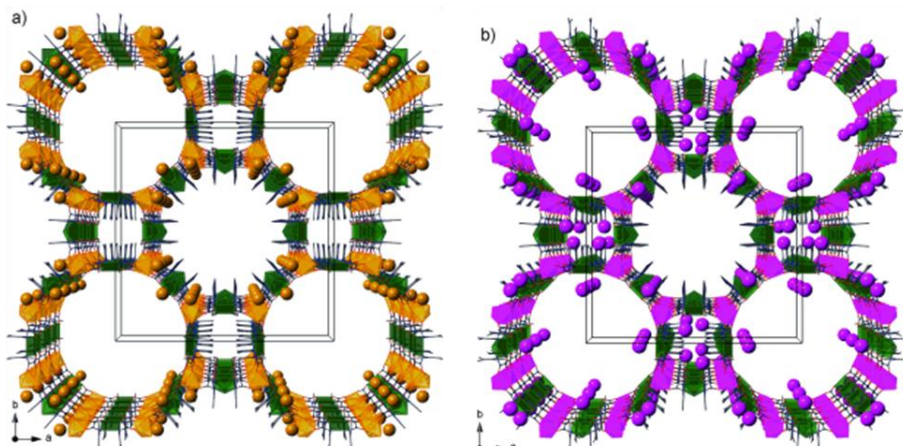
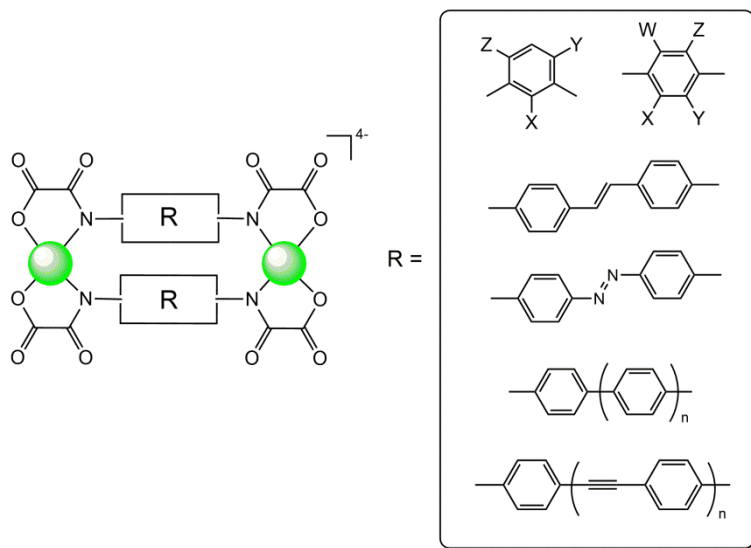


Figure 5. Anionic 3D $\text{M}^{\text{II}}_4\text{Cu}^{\text{II}}_6$ networks using the oxamate ligand 2,4,6-Me₃pma (L) a) $\text{Mg}^{\text{II}}_2\{\text{Mg}^{\text{II}}_4[\text{Cu}^{\text{II}}_2(\text{L})_2]_3\} \cdot 45 \text{H}_2\text{O}$ and b) $\text{Co}_2^{\text{III}}\{\text{Co}^{\text{II}}_4[\text{Cu}^{\text{II}}_2(\text{L})_2]_3\} \cdot 56 \text{H}_2\text{O}$ or $\text{Ni}_2^{\text{III}}\{\text{Ni}^{\text{II}}_4[\text{Cu}^{\text{II}}_2(\text{L})_2]_3\} \cdot 54 \text{H}_2\text{O}$.¹⁴³

Lately, our research group has prepared new dinucleating ligands possessing two oxamate donor groups separated by more or less rigid, extended π -conjugated aromatic spacers that are able to self-assemble with Cu(II) ions to form double-stranded dicopper(II) metallacyclic complexes of the cyclophane type. These compounds possess electro- and photoactive chemical properties and then, they are of potential interest in molecular spintronics and quantum computing, as illustrated in Scheme 6.^{144,145}



Scheme 6. Oxamate-based metal(II) metallacyclophanes with extended π -conjugated aromatic spacers.¹⁴⁴

I.5. Oxamate-containing palladium(II) complexes

Aiming at increasing the functionality of the oxamate-containing complexes, we focused on the diamagnetic square planar palladium(II) as metal center. The importance of using palladium to carry out a new oxamate coordination chemistry is based on the large number of well-known catalyzed-organic reactions accomplished by this element.¹⁴⁶⁻¹⁴⁹ Among others, the versatile palladium center enables carbonylation, hydrogenation,¹⁵⁰ hydrogenolysis,¹⁵¹ formation of carbon-carbon,¹⁵²⁻¹⁵⁷ carbon-hydrogen,¹⁰ carbon-oxygen,¹⁵⁸⁻¹⁶⁰ carbon-nitrogen^{12,37} and carbon-sulfur^{161,162} bond reactions.

There is a large variety of available commercial palladium(II)/(0) complexes used in organic and catalysis chemistry. Some of them are:

(i) $[\text{PdCl}_2]$ which is very stable but its solubility in water or organic solvents is very low;¹⁴⁷

(ii) the compounds of general formula $\text{M}_2[\text{PdCl}_4]$ ($\text{M} = \text{Li}, \text{Na}$ and K) which are very soluble in water but sparingly soluble in alcohols or other organic solvents;¹⁴⁷

(iii) $[\text{Pd}_3(\text{OAc})_6]$ which is stable in the solid state and soluble in organic solvents but it is sparingly soluble in water;¹⁴⁷

(iv) $[\text{Pd}_3(\text{OAc})_6]$ combined with $\text{P}(n\text{-But})_3$ which is a very active catalyst but it must be used immediately because it undergoes a fast oxidation to phosphine oxide together with a phosphine-free $\text{Pd}(0)$ species;¹⁴⁷

(v) $[\text{Pd}(\text{PPh}_3)_4]$ which is light-sensitive and unstable in the open air;¹⁴⁷

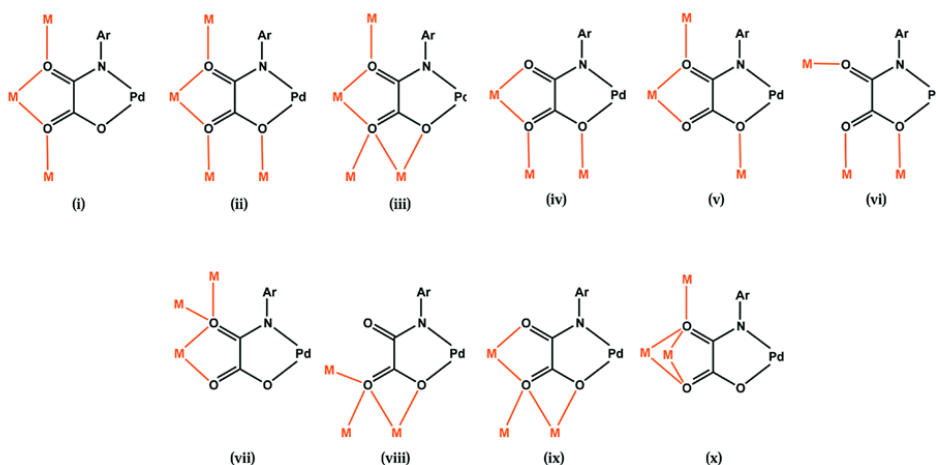
(vi) $[\text{Pd}(\text{dba})_2]$ which is an active catalyst but nanoparticles of palladium(0) are formed sometimes during the synthesis of the compound.¹⁶³

In the light of these features and having in mind the need of implementing an ecologically benign chemistry, new palladium complexes with the following requirements are needed:

- (a) soluble in water and other alcoholic solvents,
- (b) light-insensitive and stable in the open air,
- (c) easily accessible, handling and structurally versatile.
- (d) environmentally friendly avoiding for example the use of phosphine ligands,

In the present PhD Thesis work, we have discovered that the oxamate-containing palladium(II) complexes fulfill all these requirements.

The first structure of this type of complexes was published in 1999 by Colacio *et. al.*¹⁶⁴ and during the materialization of this Thesis, additional structures have been reported by Pereira *et. al.*¹⁶⁵⁻¹⁶⁷ These last works have shown that oxamate-containing palladium(II) complexes exhibit cytotoxic activity against leukemia cells,¹⁶⁶ and also act as suitable diamagnetic spacers (Scheme 7) in heterobimetallic magnetic one-dimensional compounds.^{165,167}



Scheme 7. Possible coordination modes of the mono-oxamate-palladate(II) unit.

The main achievements of this Thesis on the oxamate-containing palladium(II) complexes are summarized hereunder:

(i) crystallographic studies on the structural topology of bis(oxamate)palladate(II) complexes of formula $M_2[PdL_2]$ (L = oxamate ligand and M = alkaline element),¹⁶⁸ and the investigation of hydrogen bonding and supramolecular halogen-halogen interactions in halogen derivatives of bis(oxamate)palladate(II) complexes,

(ii) studies of the catalytic activity of bis(oxamate)palladate(II) complexes of formula $(n\text{-Bu}_4\text{N})_2[PdL_2]$, in the carbon-carbon cross-coupling reactions (Heck and Suzuki reactions) using alternative greener solvents such as *ionic liquids*,¹⁶⁹

(iii) combined crystal structure determination and catalytic activity studies (Suzuki reaction¹⁷⁰ and nitrile hydration) of bis(oxamate)palladate(II) complexes of formula $[Pd(H_2O_4)][PdL_2]$,

(iv) synthesis, structural characterization of dinuclear oxamate-containing palladium(II) metallacyclophanes of formula $(n\text{-Bu}_4\text{N})_2[Pd_2L_2]$ and their catalytic (Heck and Suzuki reactions in *ionic liquids*), cytotoxicity (on leukemia cells) and photochemical (preliminary investigation) activities.

I.6. References

- (1) Cotton, F. A.; Wilkinson, G. In *Advanced Inorganic Chemistry - A Comprehensive Text*; John Wiley & Sons, 1972; p. p 620.
- (2) Johnson, L. K.; Killian, C. M.; Brookhart, M. J. *Am. Chem. Soc.* **1995**, *117*, 6414–6415.
- (3) Holliday, B. J.; Mirkin, C. a. *Angew. Chem. Int. Ed. Engl.* **2001**, *40*, 2022–2043.
- (4) Eddaoudi, M.; Moler, D. B.; Li, H.; Chen, B.; Reineke, T. M.; O’Keeffe, M.; Yaghi, O. M. *Acc. Chem. Res.* **2001**, *34*, 319–330.
- (5) Evans, M.; O’Neil, J.; Komma, B. *Ion Implant. Technol. 2002. Proc. 14th Int. Conf.* **2002**.
- (6) Kitagawa, S.; Kitaura, R.; Noro, S. *Angew. Chem. Int. Ed. Engl.* **2004**, *43*, 2334–2375.
- (7) Braga, D.; Grepioni, F.; Maini, L.; Brescello, R.; Cotarca, L. *Cryst. Eng. Comm.*, 2008, *10*, 469.
- (8) Pardo, E.; Ruiz-García, R.; Cano, J.; Ottenwaelder, X.; Lescouëzec, R.; Journaux, Y.; Lloret, F.; Julve, M. *Dalt. Trans.* **2008**, 2780–2805.
- (9) Vallejo, J.; Pascual-Álvarez, A.; Cano, J.; Castro, I.; Julve, M.; Lloret, F.; Krzystek, J.; De Munno, G.; Armentano, D.; Wernsdorfer, W.; Ruiz-García, R.; Pardo, E. *Angew. Chem. Int. Ed.* **2013**, *52*, 14075–14079.
- (10) Wang, X.; Gribkov, D. V.; Sames, D. J. *Org. Chem.* **2007**, *72*, 1476–1479.
- (11) Hasegawa, S.; Horike, S.; Matsuda, R.; Furukawa, S.; Mochizuki, K.; Kinoshita, Y.; Kitagawa, S. *J. Am. Chem. Soc.* **2007**, *129*, 2607–2614.
- (12) Biscoe, M. R.; Fors, B. P.; Buchwald, S. L. *J. Am. Chem. Soc.* **2008**, *130*, 6686–6687.
- (13) Ferrando-Soria, J.; Pardo, E.; Ruiz-García, R.; Cano, J.; Lloret, F.; Julve, M.; Journaux, Y.; Pasán, J.; Ruiz-Pérez, C. *Chem. Eur. J.* **2011**, *17*, 2176–2188.
- (14) Chui, S. S. *Science*, 1999, *283*, 1148–1150.
- (15) Yaghi, O. M.; O’Keeffe, M.; Ockwig, N. W.; Chae, H. K.; Eddaoudi, M.; Kim, J. *Nature* **2003**, *423*, 705–714.
- (16) Tsao, C.-S.; Yu, M.-S.; Wang, C.-Y.; Liao, P.-Y.; Chen, H.-L.; Jeng, U.-S.; Tzeng, Y.-R.; Chung, T.-Y.; Wu, H.-C. *J. Am. Chem. Soc.* **2009**, *131*, 1404–1406.
- (17) Horcajada, P.; Gref, R.; Baati, T.; Allan, P. K.; Maurin, G.; Couvreur, P.; Férey, G.; Morris, R. E.; Serre, C. *Chem. Rev.* **2012**, *112*, 1232–1268.
- (18) Ferrando-Soria, J.; Ruiz-García, R.; Cano, J.; Stiriba, S.-E.; Vallejo, J.; Castro, I.; Julve, M.; Lloret, F.; Amorós, P.; Pasán, J.; Ruiz-Pérez, C.; Journaux, Y.; Pardo, E. *Chem. Eur. J.* **2012**, *18*, 1608–1617.
- (19) Kaminskaia, N. V.; Kostic, N. M. *J. Chem. Soc. Dalt. Trans.* **1996**, 3677.
- (20) Yutaka, T.; Mori, I.; Kurihara, M.; Mizutani, J.; Kubo, K.; Furusho, S.; Matsumura, K.; Tamai, N.; Nishihara, H. *Inorg. Chem.* **2001**, *40*, 4986–4995.
- (21) Cotton, F. A.; Murillo, C. A.; Wang, X.; Yu, R. *Inorg. Chem.* **2004**, *43*, 8394–8403.
- (22) Cotton, F. A.; Murillo, C. A.; Stiriba, S.-E.; Wang, X.; Yu, R. *Inorg. Chem.* **2005**, *44*, 8223–8233.

- (23) Kukushkin, V. Y.; Pombeiro, A. J. L. *Inorg. Chim. Acta* **2005**, *358*, 1–21.
- (24) Van Zutphen, S.; Reedijk, J. *Coord. Chem. Rev.*, 2005, *249*, 2845–2853.
- (25) Bock, V. D.; Hiemstra, H.; van Maarseveen, J. H. *Eur. J. Org. Chem.* **2006**, *2006*, 51–68.
- (26) Tadpetch, K.; Rychnovsky, S. D. *Org. Lett.* **2008**, *10*, 4839–4842.
- (27) Chen, X.; Engle, K. M.; Wang, D.-H.; Yu, J.-Q. *Angew. Chem. Int. Ed. Engl.* **2009**, *48*, 5094–5115.
- (28) Armelao, L.; Quici, S.; Barigelletti, F.; Accorsi, G.; Bottaro, G.; Cavazzini, M.; Tondello, E. *Coord. Chem. Rev.* **2010**, *254*, 487–505.
- (29) Murrie, M. *Chem. Soc. Rev.* **2010**, *39*, 1986–1995.
- (30) Marqués-Gallego, P.; Gamiz-Gonzalez, M. A.; Fortea-Pérez, F. R.; Lutz, M.; Spek, A. L.; Pevec, A.; Kozlevčar, B.; Reedijk, J. *Dalt. Trans.* **2010**, 5152–5158.
- (31) Powers, D. C.; Ritter, T. *Top. Organomet. Chem.* **2011**, *503*, 129–156.
- (32) McCall, A. S.; Wang, H.; Desper, J. M.; Kraft, S. *J. Am. Chem. Soc.* **2011**, *133*, 1832–1848.
- (33) Marinescu, G.; Andruh, M.; Lloret, F.; Julve, M. *Coord. Chem. Rev.* **2011**, *255*, 161–185.
- (34) Vilela, R. S.; Oliveira, T. L.; Martins, F. T.; Ellena, J. A.; Lloret, F.; Julve, M.; Cangussu, D. *Comptes Rendus Chim.* **2012**, *15*, 856–865.
- (35) Guo, X.-Q.; Wang, Y.-N.; Wang, D.; Cai, L.-H.; Chen, Z.-X.; Hou, X.-F. *Dalt. Trans.* **2012**, *41*, 14557–14567.
- (36) Ehle, A. R.; Zhou, Q.; Watson, M. P. *Org. Lett.* **2012**, *14*, 1202–1205.
- (37) Bruno, N. C.; Tudge, M. T.; Buchwald, S. L. *Chem. Sci.* **2013**, *4*, 916.
- (38) Zhang, P.; Guo, Y.-N.; Tang, J. *Coord. Chem. Rev.* **2013**, *257*, 1728–1763.
- (39) Morel, A.; Silarska, E.; Trzeciak, A. M.; Pernak, J. *Dalt. Trans.* **2013**, *42*, 1215–1222.
- (40) Lehn, J.-M. In *Supramolecular Chemistry. Concepts and Perspectives*; Wiley-VCH, Weinheim, Germany, 1995.
- (41) E. C. Constable. In *Prog. Inorg. Chem.*; 1994; Vol. 42, p. 67.
- (42) Stang, P. J.; Olenyuk, B. *Acc. Chem. Res.* **1997**, *30*, 502–518.
- (43) Albrecht, M. *Chem. Soc. Rev.*, 1998, *27*, 281.
- (44) Swiegers, G. F.; Malefetse, T. J. *Chem. Rev.* **2000**, *100*, 3483–3537.
- (45) Steel, P. J. *Acc. Chem. Res.* **2005**, *38*, 243–250.
- (46) Fujita, M. *Chem. Soc. Rev.*, 1998, *27*, 417.
- (47) Caulder, D. L.; Raymond, K. N. *Acc. Chem. Res.*, 1999, *32*, 975–982.
- (48) Leininger, S.; Olenyuk, B.; Stang, P. J. *Chem. Rev.* **2000**, *100*, 853–907.
- (49) Seidel, S. R.; Stang, P. J. *Acc. Chem. Res.* **2002**, *35*, 972–983.
- (50) Batten, S. R.; Robson, R. *Angew. Chem. Int. Ed. Int. Ed.* **1998**, *37*, 1460–1494.
- (51) Cotton, F. A.; Lin, C.; Murillo, C. A. *Proc. Natl. Acad. Sci. U. S. A.* **2002**, *99*, 4810–4813.
- (52) Férey, G.; Mellot-Draznieks, C.; Serre, C.; Millange, F. *Acc. Chem. Res.* **2005**, *38*, 217–225.
- (53) Suh, M. P.; Cheon, Y. E.; Lee, E. Y. *Coord. Chem. Rev.*, 2008, *252*, 1007–1026.

- (54) Kuppler, R. J.; Timmons, D. J.; Fang, Q.-R.; Li, J.-R.; Makal, T. A.; Young, M. D.; Yuan, D.; Zhao, D.; Zhuang, W.; Zhou, H.-C. *Coord. Chem. Rev.* **2009**, *253*, 3042–3066.
- (55) Fiedler, D.; Leung, D. H.; Bergman, R. G.; Raymond, K. N. *Acc. Chem. Res.* **2005**, *38*, 349–358.
- (56) Thompson, L. K.; Waldmann, O.; Xu, Z. *Coord. Chem. Rev.*, 2005, *249*, 2677–2690.
- (57) Ruben, M.; Rojo, J.; Romero-Salguero, F. J.; Uppadine, L. H.; Lehn, J. M. *Angew. Chem. Int. Ed.*, 2004, *43*, 3644–3662.
- (58) Macgillivray, L. R.; Papaefstathiou, G. S.; Friščić, T.; Hamilton, T. D.; Bučar, D. K.; Chu, Q.; Varshney, D. B.; Georgiev, I. G. *Acc. Chem. Res.* **2008**, *41*, 280–291.
- (59) Kahn, O. In *Molecular Magnetism: From Molecular Assemblies to the Devices*; E. Coronado, P. Delhaes, D. G. and J. S. M., Ed.; NATO ASI Series E321, Kluwer, Dordrecht, 1996; p. 243.
- (60) Kahn, O. *Acc. Chem. Res.* **2000**, *33*, 647–657.
- (61) L. K. Thompson, O. W. and Z. S. In *Magnetism: Molecules to Materials IV*; Drillon, J. S. M. and M., Ed.; Wiley-VCH Verlag, Weinheim, Germany, 2001; Vol. 0.
- (62) Doedens, R. J. *J. Am. Chem. Soc.* **2002**, *124*, 7250–7250.
- (63) Wang, X.-Y.; Avendaño, C.; Dunbar, K. R. *Chem. Soc. Rev.* **2011**, *40*, 3213–3238.
- (64) Dechambenoit, P.; Long, J. R. *Chem. Soc. Rev.* **2011**, *40*, 3249–3265.
- (65) Launay, J.-P.; Michel Verdaguer. In *Electrons in Molecules: From Basic Principles to Molecular Electronics*; Oxford University Press, United Kingdom, 2014; p. 78.
- (66) Albelda, M. T.; Frías, J. C.; García-España, E.; Schneider, H.-J. *Chem. Soc. Rev.* **2012**, *41*, 3859–3877.
- (67) Starha, P.; Trávníček, Z.; Popa, I. *J. Inorg. Biochem.* **2009**, *103*, 978–988.
- (68) Kreno, L. E.; Leong, K.; Farha, O. K.; Allendorf, M.; Van Duyne, R. P.; Hupp, J. T. *Chem. Rev.* **2012**, *112*, 1105–1125.
- (69) Amouri, H.; Gruselle, M. *Chirality in Transition Metal Chemistry: Molecules, Supramolecular Assemblies and Materials*; John Wiley & Sons, Chichester United Kingdom, 2008.
- (70) Train, C.; Gruselle, M.; Verdaguer, M. *Chem. Soc. Rev.* **2011**, *40*, 3297–3312.
- (71) Yoon, M.; Srirambalaji, R.; Kim, K. *Chem. Rev.* **2012**, *112*, 1196–1231.
- (72) Horike, S.; Umeyama, D.; Kitagawa, S. *Acc. Chem. Res.* **2013**, *46*, 2376–2384.
- (73) In *Multifunctional Molecular Materials*; Ouahab, L., Ed.; Pan Stanford Publishing, Singapore, 2013.
- (74) Miller, K. J.; Baag, J. H.; Abu-Omar, M. M. *Inorg. Chem.* **1999**, *38*, 4510–4514.
- (75) Munz, D.; Poethig, A.; Tronnier, A.; Strassner, T. *Dalt. Trans.* **2013**.
- (76) Cook, T. R.; Zheng, Y.-R.; Stang, P. J. *Chem. Rev.* **2013**, *113*, 734–777.
- (77) Andruh, M. *Chimia.* **2013**, *67*, 383–387.

- (78) Andruh, M. *Chem. Commun.* **2007**, 2565–2577.
- (79) Andruh, M. *Chem. Commun.* **2011**, 47, 3025–3042.
- (80) Gable, R. W.; Hoskins, B. F.; Robson, R. J. *Chem. Soc. Chem. Commun.* **1990**, 1677.
- (81) Hoskins, B. F.; Robson, R. J. *Am. Chem. Soc.* **1990**, 112, 1546–1554.
- (82) Lescouëzec, R.; Toma, L. M.; Vaissermann, J.; Verdaguer, M.; Delgado, F. S.; Ruiz-Pérez, C.; Lloret, F.; Julve, M. *Coord. Chem. Rev.*, 2005, 249, 2691–2729.
- (83) Wang, S.; Ding, X. H.; Li, Y. H.; Huang, W. *Coord. Chem. Rev.*, 2012, 256, 439–464.
- (84) Wang, S.; Ding, X.-H.; Zuo, J.-L.; You, X.-Z.; Huang, W. *Coord. Chem. Rev.* **2011**, 255, 1713–1732.
- (85) Li, Y.-H.; He, W.-R.; Ding, X.-H.; Wang, S.; Cui, L.-F.; Huang, W. *Coord. Chem. Rev.* **2012**, 256, 2795–2815.
- (86) Decurtins, S.; Pellaux, R.; Antorrena, G.; Palacio, F. *Coord. Chem. Rev.* **1999**, 190–192, 841–854.
- (87) Gruselle, M.; Train, C.; Boubekeur, K.; Gredin, P.; Ovanesyan, N. *Coord. Chem. Rev.* **2006**, 250, 2491–2500.
- (88) Train, C.; Gheorghe, R.; Krstic, V.; Chamoreau, L.-M.; Ovanesyan, N. S.; Rikken, G. L. J. A.; Gruselle, M.; Verdaguer, M. *Nat. Mater.* **2008**, 7, 729–734.
- (89) Coronado, E.; Galán-Mascarós, J. R.; Martí-Gastaldo, C. *Cryst. Eng. Comm.* **2009**, 11, 2143.
- (90) Train, C.; Nuida, T.; Gheorghe, R.; Gruselle, M.; Ohkoshi, S. J. *Am. Chem. Soc.* **2009**, 131, 16838–16843.
- (91) Okawa, H.; Shigematsu, A.; Sadakiyo, M.; Miyagawa, T.; Yoneda, K.; Ohba, M.; Kitagawa, H. *J. Am. Chem. Soc.* **2009**, 131, 13516–13522.
- (92) Pardo, E.; Train, C.; Lescouëzec, R.; Boubekeur, K.; Ruiz, E.; Lloret, F.; Verdaguer, M. *Dalton Trans.* **2010**, 39, 4951–4958.
- (93) Pardo, E.; Train, C.; Gontard, G.; Boubekeur, K.; Fabelo, O.; Liu, H.; Dkhil, B.; Lloret, F.; Nakagawa, K.; Tokoro, H.; Ohkoshi, S.; Verdaguer, M. *J. Am. Chem. Soc.* **2011**, 133, 15328–15331.
- (94) Pardo, E.; Train, C.; Liu, H.; Chamoreau, L.-M.; Dkhil, B.; Boubekeur, K.; Lloret, F.; Nakatani, K.; Tokoro, H.; Ohkoshi, S.; Verdaguer, M. *Angew. Chem. Int. Ed. Engl.* **2012**, 51, 8356–8360.
- (95) Julve, M.; Verdaguer, M. *Under Prep. - Chem. Rev.*
- (96) Paonessa, R. S.; Prignano, A. L.; Trogler, W. C. *Organometallics* **1985**, 4, 647–657.
- (97) Cowan, R. L.; Pourreau, D. B.; Rheingold, A. L.; Geib, S. J.; Trogler, W. C. *Inorg. Chem.* **1987**, 26, 259–265.
- (98) Pan, Y.; Mague, J. T.; Fink, M. J. *J. Am. Chem. Soc.* **1993**, 115, 3842–3843.
- (99) Blokhina, M. L.; Blokhin, A. I.; Nikulin, M. Y.; Derikova, M. G. *Powder Metallurgy and Metal Ceramics*, 1996, 35, 118–121.
- (100) Arendse, M. J.; Anderson, G. K.; Rath, N. P. *Polyhedron*, 2001, 20, 2495–2503.
- (101) Dey, S.; Banerjee, P.; Gangopadhyay, S.; Vojtišek, P. *Transit. Met. Chem.* **2003**, 28, 765–771.

- (102) Navaladian, S.; Viswanathan, B.; Varadarajan, T. K.; Viswanath, R. P. *Nanoscale Res. Lett.* **2009**, *4*, 181–186.
- (103) Ayodele, O. B.; Abbas, H. F.; Daud, W. M. A. W. *Energy & Fuels* **2014**.
- (104) Kahn, O. *Angew. Chem. Int. Ed.. Int. Ed.* **1985**, *24*, 834–850.
- (105) Charlot, M.-F.; Kahn, O.; Chaillet, M.; Larrieu, C. J. *Am. Chem. Soc.* **1986**, *108*, 2574–2581.
- (106) Nonoyama, K.; Ojima, H.; Ohki, K.; Nonoyama, M. *Inorg. Chim. Acta*, 1980, *41*, 155–159.
- (107) Bencini, A.; Benelli, C.; Gatteschi, D.; Zanchini, C.; Fabretti, A. C.; Franchini, G. C. *Inorg. Chim. Acta*, 1984, *86*, 169–172.
- (108) Verdaguer, M.; Kahn, O.; Julve, M.; Gleizes, A. *Nouv. J. Chim.* **1985**, *9*, 325.
- (109) Soto, L.; Garcia, J.; Escriva, E.; Legros, J. P.; Tuchagues, J. P.; Dahan, F.; Fuertes, A. *Inorg. Chem.* **1989**, *28*, 3378–3386.
- (110) Armendarez, P. X.; Nakamoto, K. *Inorg. Chem.* **1966**, *5*, 796–800.
- (111) Kuroda, Y.; Kato, M.; Sone, K. *Bull. Chem. Soc. Jpn.*, **1961**, *34*, 877–880.
- (112) Sletten, J.; Mønsted, O.; Stølevik, R.; Vorren, Ø.; Bastiansen, O.; Braathen, G.; Fernholt, L.; Gundersen, G.; Nielsen, C. J.; Cyvin, B. N.; Cyvin, S. J. *Acta Chem. Scand.*, **1982**, *36a*, 345–351.
- (113) Sletten, J.; Vikane, O.; Strauch, P.; Dietzsch, W.; Hoyer, E.. *Acta Chem. Scand.*, **1985**, *39a*, 475–481.
- (114) Ruiz, R.; Faus, J.; Lloret, F.; Julve, M.; Journaux, Y. *Coord. Chem. Rev.* **1999**, *193-195*, 1069–1117.
- (115) Kahn, O. In *Theoretical Approaches Structure and Bonding*; 1987; Vol. 68, pp. 89–167.
- (116) Kahn, O. *Molecular Magnetism*; Wiley-VCH, 1993.
- (117) Dul, M.-C.; Pardo, E.; Lescouëzec, R.; Journaux, Y.; Ferrando-Soria, J.; Ruiz-García, R.; Cano, J.; Julve, M.; Lloret, F.; Cangussu, D.; Pereira, C. L. M.; Stumpf, H. O.; Pasán, J.; Ruiz-Pérez, C. *Coord. Chem. Rev.* **2010**, *254*, 2281–2296.
- (118) Nonoyama, K.; Ojima, H.; Nonoyama, M. *Inorg. Chim. Acta* **1976**, *20*, 127–132.
- (119) Journaux, Y.; Ruiz, R.; Aukauloo, A.; Pei, Y. New Oxamido Bridged Molecular Based Magnets and High-Spin Molecules. *Molecular Crystals and Liquid Crystals Science and Technology. Section A. Molecular Crystals and Liquid Crystals*, 1997, *305*, 193–202.
- (120) Cano, J.; Ruiz, E.; Alemany, P.; Lloret, F.; Alvarez, S. *J. Chem. Soc. Dalton Trans.* **1999**, 1669–1676.
- (121) Kahn, O.; Pei, Y.; Verdaguer, M.; Renard, J. P.; Sletten, J. *J. Am. Chem. Soc.* **1988**, *110*, 782–789.
- (122) Stumpf, H. O.; Pei, Y.; Kahn, O.; Sletten, J.; Renard, J. P. *J. Am. Chem. Soc.* **1993**, *115*, 6738–6745.
- (123) Lloret, F.; Julve, M.; Ruiz, R.; Journaux, Y.; Nakatani, K.; Kahn, O.; Sletten, J. *Inorg. Chem.* **1993**, *32*, 27–31.

- (124) Stumpf, H. O.; Pei, Y.; Kahn, O.; Ouahab, L.; Grandjean, D. *Science* **1993**, *261*, 447–449.
- (125) Ruiz, R.; Surville-Barland, C.; Journaux, Y.; Colin, J. C.; Castro, I.; Cervera, B.; Julve, M.; Lloret, F.; Sapiña, F. *Chem. Mater.* **1997**, *9*, 201–209.
- (126) Vaz, M. G. F.; Pinheiro, L. M. M.; Stumpf, H. O.; Alcântara, A. F. C.; Golhen, S.; Ouahab, L.; Cador, O.; Mathonière, C.; Kahn, O. *Chem. Eur. J.* **1999**, *5*, 1486–1495.
- (127) Pereira, C. L. M.; Pedroso, E. F.; Stumpf, H. O.; Novak, M. A.; Ricard, L.; Ruiz-García, R.; Rivière, E.; Journaux, Y. *Angew. Chem. Int. Ed. Engl.* **2004**, *43*, 956–958.
- (128) Pei, Y.; Journaux, Y.; Kahn, O.; Dei, A.; Gatteschi, D. *J. Chem. Soc. Chem. Commun.* **1986**, 1300.
- (129) Pei, Y.; Journaux, Y.; Kahn, O. *Inorg. Chem.* **1988**, *27*, 399–404.
- (130) Ribas, J.; Diaz, C.; Costa, R.; Journaux, Y.; Mathoniere, C.; Kahn, O.; Gleizes, A. *Inorg. Chem.* **1990**, *29*, 2042–2047.
- (131) Fernández, I.; Ruiz, R.; Faus, J.; Julve, M.; Lloret, F.; Cano, J.; Ottenwaelder, X.; Journaux, Y.; Muñoz, M. C. *Angew. Chem. Int. Ed. Engl.* **2001**, *40*, 3039–3042.
- (132) Grancha, T.; Ferrando-Soria, J.; Castellano, M.; Julve, M.; Pasán, J.; Armentano, D.; Pardo, E. *Chem. Commun.* **2014**, *50*, 7569–7585.
- (133) Fortea-Pérez, F. R.; Vallejo, J.; Julve, M.; Lloret, F.; De Munno, G.; Armentano, D.; Pardo, E. *Inorg. Chem.* **2013**, *52*, 4777–4779.
- (134) Pardo, E.; Morales-Osorio, I.; Julve, M.; Lloret, F.; Cano, J.; Ruiz-García, R.; Pasán, J.; Ruiz-Pérez, C.; Ottenwaelder, X.; Journaux, Y. *Inorg. Chem.* **2004**, *43*, 7594–7596.
- (135) Pardo, E.; Burguete, P.; Ruiz-García, R.; Julve, M.; Beltrán, D.; Journaux, Y.; Amorós, P.; Lloret, F. *J. Mater. Chem.* **2006**, *16*, 2702.
- (136) Pardo, E.; Train, C.; Lescouëzec, R.; Journaux, Y.; Pasán, J.; Ruiz-Pérez, C.; Delgado, F. S.; Ruiz-García, R.; Lloret, F.; Paulsen, C. *Chem. Commun. (Camb)*. **2010**, *46*, 2322–2324.
- (137) Ferrando-Soria, J.; Cangussu, D.; Eslava, M.; Journaux, Y.; Lescouëzec, R.; Julve, M.; Lloret, F.; Pasán, J.; Ruiz-Pérez, C.; Lhotel, E.; Paulsen, C.; Pardo, E. *Chem. Eur. J.* **2011**, *17*, 12482–12494.
- (138) Ferrando-Soria, J.; Castellano, M.; Ruiz-García, R.; Cano, J.; Julve, M.; Lloret, F.; Ruiz-Pérez, C.; Pasán, J.; Cañadillas-Delgado, L.; Armentano, D.; Journaux, Y.; Pardo, E. *Chem. - A Eur. J.* **2013**, *7201*, 12124–12137.
- (139) Ferrando-Soria, J.; Khajavi, H.; Serra-Crespo, P.; Gascon, J.; Kapteijn, F.; Julve, M.; Lloret, F.; Pasán, J.; Ruiz-Pérez, C.; Journaux, Y.; Pardo, E. *Adv. Mater.* **2012**, *24*, 5625–5629.
- (140) Ferrando-Soria, J.; Serra-Crespo, P.; de Lange, M.; Gascon, J.; Kapteijn, F.; Julve, M.; Cano, J.; Lloret, F.; Pasán, J.; Ruiz-Pérez, C.; Journaux, Y.; Pardo, E. *J. Am. Chem. Soc.* **2012**, *134*, 15301–15304.

- (141) Do Pim, W. D.; Oliveira, W. X. C.; Ribeiro, M. A.; de Faria, É. N.; Teixeira, I. F.; Stumpf, H. O.; Lago, R. M.; Pereira, C. L. M.; Pinheiro, C. B.; Figueiredo, J. C. D.; Nunes, W. C.; de Souza, P. P.; Pedroso, E. F.; Castellano, M.; Cano, J.; Julve, M. *Chem. Commun.* **2013**, 49, 10778–10780.
- (142) Grancha, T.; Tourbillon, C.; Ferrando-Soria, J.; Julve, M.; Lloret, F.; Pasán, J.; Ruiz-Pérez, C.; Fabelo, O.; Pardo, E. *Cryst. Eng. Comm.* **2013**, 15, 9312.
- (143) Grancha, T.; Ferrando-Soria, J.; Zhou, H.-C.; Gascon, J.; Seoane, B.; Pasán, J.; Fabelo, O.; Julve, M.; Pardo, E. *Angew. Chem. Int. Ed. Int. Ed.* **2015**, 54, 6521–6525.
- (144) Castellano, M.; Ruiz-García, R.; Cano, J.; Ferrando-Soria, J.; Pardo, E.; Fortea-Pérez, F. R.; Stiriba, S.-E.; Julve, M.; Lloret, F. *Acc. Chem. Res.* **2015**, 48, 510–520.
- (145) Castellano, M.; Ruiz-García, R.; Cano, J.; Ferrando-Soria, J.; Pardo, E.; Fortea-Pérez, F. R.; Stiriba, S.-E.; Barros, W. P.; Stumpf, H. O.; Cañadillas-Delgado, L.; Pasán, J.; Ruiz-Pérez, C.; de Munno, G.; Armentano, D.; Journaux, Y.; Lloret, F.; Julve, M. *Coord. Chem. Rev.* **2015**, 303, 110–138.
- (146) Negishi, E. *Handbook of Organopalladium Chemistry for Organic Synthesis*; John Wiley & Sons, 2003.
- (147) Tsuji, J. *Palladium Reagents and Catalysts: New Perspectives for the 21st Century*; John Wiley & Sons, 2006.
- (148) In *Organometallic Chemistry and Catalysis*; Kirchner, K.; Weissensteiner, W., Eds.; Springer Science & Business Media, 2012; pp. 43–69.
- (149) Tsuji, J. *Organic Synthesis with Palladium Compounds*; Springer Science & Business Media, 2012.
- (150) Figueras, F.; Coq, B. *J. Mol. Catal. A Chem.* **2001**, 173, 223–230.
- (151) Urbano, F. J.; Marinas, J. M. *J. Mol. Catal. A Chem.* **2001**, 173, 329–345.
- (152) Heck, R. F. *Acc. Chem. Res.* **1979**, 12, 146–151.
- (153) Lamblin, M.; Nassar-Hardy, L.; Hierso, J.-C.; Fouquet, E.; Felpin, F.-X. *Adv. Synth. Catal.* **2010**, 352, 33–79.
- (154) Suzuki, A. *Angew. Chem. Int. Ed. Engl.* **2011**, 50, 6722–6737.
- (155) Suzuki, A.; Yamamoto, Y. *Chem. Lett.* **2011**, 40, 894–901.
- (156) Balanta, A.; Godard, C.; Claver, C. *Chem. Soc. Rev.* **2011**, 40, 4973–4985.
- (157) Molnár, Á. *Chem. Rev.* **2011**, 111, 2251–2320.
- (158) Kuwabe, S. I.; Torraca, K. E.; Buchwald, S. L. *J. Am. Chem. Soc.* **2001**, 123, 12202–12206.
- (159) Kataoka, N.; Shelby, Q.; Stambuli, J. P.; Hartwig, J. F. *J. Org. Chem.* **2002**, 67, 5553–5566.
- (160) Muci, A. R.; Buchwald, S. L. *Cross-Coupling React.* **2002**, 219, 131–209.
- (161) Li, G. Y.; Zheng, G.; Noonan, A. F. *J. Org. Chem.* **2001**, 66, 8677–8681.
- (162) Bryan, C. S.; Braunger, J. A.; Lautens, M. *Angew. Chem. Int. Ed. - Int. Ed.* **2009**, 48, 7064–7068.
- (163) Zaleskiy, S. S.; Ananikov, V. P. *Organometallics* **2012**, 31, 2302–2309.

- (164) Kivekas, R.; Pajunen, A.; Navarrete, A.; Colacio, E. *Inorg. Chim. Acta* **1999**, *284*, 292–295.
- (165) Oliveira, W. X. C.; Ribeiro, M. A.; Pinheiro, C. B.; Nunes, W. C.; Julve, M.; Journaux, Y.; Stumpf, H. O.; Pereira, C. L. M. *Eur. J. Inorg. Chem.* **2012**, *2012*, 5685–5693.
- (166) Oliveira, W. X. C.; da Costa, M. M.; Fontes, A. P. S.; Pinheiro, C. B.; de Paula, F. C. S.; Jaimes, E. H. L.; Pedroso, E. F.; de Souza, P. P.; Pereira-Maia, E. C.; Pereira, C. L. M. *Polyhedron* **2014**, *76*, 16–21.
- (167) Oliveira, W. X. C.; Ribeiro, M. A.; Pinheiro, C. B.; da Costa, M. M.; Fontes, A. P. S.; Nunes, W. C.; Cangussu, D.; Julve, M.; Stumpf, H. O.; Pereira, C. L. M. *Cryst. Growth Des.* **2015**, *15*, 1325–1335.
- (168) Fortea-Pérez, F. R.; Marino, N.; Armentano, D.; De Munno, G.; Julve, M.; Stiriba, S.-E. *Cryst. Eng. Comm.* **2014**, *16*, 6971.
- (169) Fortea-Pérez, F. R.; Schlegel, I.; Julve, M.; Armentano, D.; De Munno, G.; Stiriba, S.-E. *J. Organomet. Chem.* **2013**, *743*, 102–108.
- (170) Fortea-Pérez, F. R.; Armentano, D.; Julve, M.; De Munno, G.; Stiriba, S.-E. *J. Coord. Chem.* **2014**, *67*, 4003–4015.

II

Chapter 1

Structural versatility of bis(oxamato)palladate(II) complexes

Part I

Cis-trans isomerism in solid state of bis(oxamato)palladate(II) complexes: X-ray structures and catalytic activity

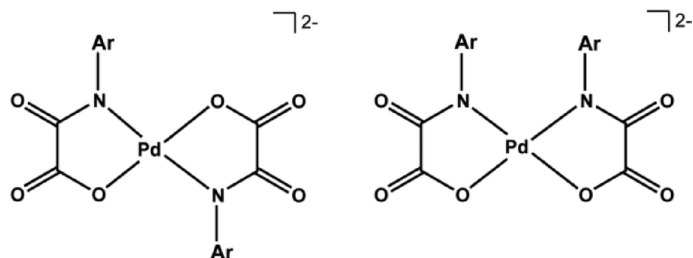
II.1. Aim

In the last decade, oxamate ligands have been used in coordination chemistry in the search for magnetic,¹⁻²² photo switching,²³ catalytic properties (first-row transition metal ions)²⁴⁻³² and gas absorption³³. However, the oxamate-containing palladium(II) complexes are really scarce in the literature,³⁴⁻³⁶ (only a few examples in the last years) and their catalytic properties were not investigated.³⁷⁻³⁹

Having in mind the possible catalytic activity of these complexes, four novel compounds with the same ligand (2,6-Me₂pma) and different counter-ions [Na(I) (**1** and **1'**), K(I) (**2**), Rb(I) (**3**) and Cs(I) (**4**)] were prepared and their crystal structures determined by X-ray diffraction. Their catalytic activity for carbon-carbon coupling Suzuki type reaction was investigated, moderate to high yields being obtained.

- 1** {[Na(H₂O)]₂*trans*-[Pd(2,6-Me₂pma)₂]}_n
1' {[Na(H₂O)]₂*cis*-[Pd(2,6-Me₂pma)₂]}_n
2 {[K₄(H₂O)₃]*cis*-[Pd(2,6-Me₂pma)₂]}_n
3 {[Rb₄(H₂O)₃]*cis*-[Pd(2,6-Me₂pma)₂]}_n
4 {[Cs₆(H₂O)₇]*trans*-[Pd(2,6-Me₂pma)₂]*cis*-[Pd(2,6-Me₂pma)₂]}_n · 3nH₂O

The present chapter focuses on their preparation, structural characterization and study of their catalytic properties concerning the carbon-carbon coupling Suzuki type in homogeneous catalysis (DMF as solvent). The possible influence of the alkaline counter-ion on this process is also analyzed. It deserves to be noted that the occurrence of *cis*- and *trans*- isomers when using monosubstituted oxamate ligands in the corresponding palladium(II) complexes (see Scheme 1) has been materialized in these series of compounds.



Scheme 1. (Left) *trans*- and (right) *cis*-isomers (Ar stands for aryl).

II.2. Synthesis and characterization

The general synthetic method for the preparation of the proligand EtH-2,6-Me₂-pma follows the reported one in previous works¹⁵ (see Appendix A for further information).

Synthesis of the complexes:

A general synthetic method for the bis(2,6-dimethylphenyloxamato)palladate(II) complexes **1/1'** and **2-4** is as follows: an aqueous solution (5mL) of MOH (3 mmol) [M = Na (**1/1'**), K (**2**), Rb (**3**) and Cs (**4**)] was poured into an aqueous suspension (5mL) of the N-2,6-dimethylphenyloxamate proligand (0.6 mmol) in a one-neck round flask under continuous stirring at 60 °C. Then, an aqueous solution (5mL) of K₂[PdCl₄] (0.30 mmol) was added dropwise to the resulting solution under continuous stirring and the reaction mixture was heated at 60 °C for 10 hours. The corresponding resulting red-yellowish solutions were filtered to remove any residual solid and they were allowed to slowly evaporate at room temperature.

Following this procedure, large, good-quality crystals of **1** (yellow prisms) were grown after one month, together with a few crystals of **1'** (light orange microcrystals). X-ray quality crystals of **2-4** as red-yellowish prisms appeared within 2-4 weeks. X-ray powder diffraction profiles for **1**, **1'** and **2-4** could be found in Appendix A.⁴⁰

Characterization of the complexes

{[Na(H₂O)]₂*trans*-[Pd(2,6-Me₂pma)₂]}_n (**1**). Yield: 83%. IR (KBr/cm⁻¹): 3399 (O-H), 2944, 2916, 2850, (C-H), 1675, 1641, 1604, 1582 (C=O). Anal. Calcd for C₂₀H₂₂N₂O₈Na₂Pd (**1**): C, 42.08; H, 3.89; N, 4.91. Found: C, 41.95; H, 4.10; N, 5.01%.

{[Na₄(H₂O)]₂*cis*-[Pd(2,6-Me₂pma)₂]}_n (**1'**). Its formula was determined by X-ray diffraction on single crystals.

$\{[\text{K}_4(\text{H}_2\text{O})_3]\text{cis-}[\text{Pd}(\text{2,6-Me}_2\text{pma})_2]_2\}_n$ (**2**). Yield: 91%. IR (KBr/cm⁻¹): 3422 (O-H), 2946, 2918, 2851 (C-H), 1676, 1646, 1605, 1583 (C=O). Anal. Calcd for C₄₀H₄₂N₄O₁₅K₄Pd₂ (**2**): C, 40.44; H, 3.56; N, 4.72. Found: C, 40.70; H, 3.88; N, 4.63%.

$\{[\text{Rb}_4(\text{H}_2\text{O})_3]\text{cis-}[\text{Pd}(\text{2,6-Me}_2\text{pma})_2]_2\}_n$ (**3**). Yield: 77%. IR (KBr/cm⁻¹): 3398 (O-H), 2958, 2939, 2915, 2850 (C-H), 1677, 1642, 1605, 1583 (C=O). Anal. Calcd for C₄₀H₄₂N₄O₁₅Pd₂Rb₄ (**3**): C, 34.98; H, 3.08; N, 4.08. Found: C, 35.01; H, 3.20; N, 4.12%.

$\{[\text{Cs}_6(\text{H}_2\text{O})_7]\text{trans-}[\text{Pd}(\text{2,6-Me}_2\text{pma})_2]_2\text{cis-}[\text{Pd}(\text{2,6-Me}_2\text{pma})_2]\}_n \cdot 3n\text{H}_2\text{O}$ (**4**). Yield: 75%. IR (KBr/cm⁻¹): 3422 (O-H), 2951, 2940, 2917, 2850 (C-H), 1670, 1638, 1602, 1580 (C=O). Anal. Calcd for C₆₀H₇₄N₆O₂₈Cs₆Pd₃ (**4**): C, 29.49; H, 3.05; N, 3.44. Found: C, 28.95; H, 3.17; N, 3.50%.

II.3. Results and discussion

Synthesis and IR Spectroscopy. The syntheses of the complexes **1/1'** and **2-4** were carried out by reacting $K_2[PdCl_4]$ with the oxamate dianion $2,6-Me_2pma^{2-}$ which was generated *in situ* by the treatment of its monoester derivative with the appropriate alkaline hydroxide MOH [M = Na (**1/1'**), K (**2**), Rb (**3**) and Cs(**4**)] in water. After gentle heating to favor the substitution of the chloride ligands by the chelating oxamate group, the resulting clear solution was allowed to concentrate by slow evaporation at room temperature. Crystals of **1/1'**, **2-4** were grown from the mother liquor within a few weeks. Their infrared spectra as KBr pellets show the characteristic bands of the oxamate ligand at 1670, 1640, 1600 and 1580 cm^{-1} (see Appendix A for the graphical information). The shift of the C=O stretching towards lower wavenumbers in the spectra of **1/1'** and **2-4** compared to the starting oxamate proligand (1727 and 1676 cm^{-1}) supports the coordination of the oxamate to the metal ions (see Appendix), as confirmed by single-crystal X-ray analysis (see below).

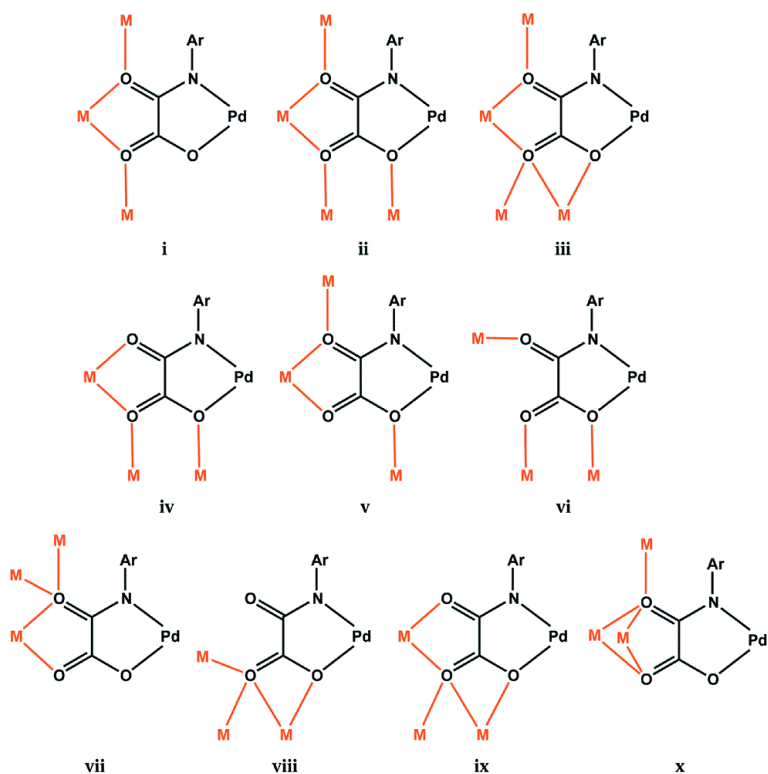
An appealing solvatochromism of the aqueous solutions of **1/1'** and **2-4** from a yellow to reddish colour corresponding to a bathochromic shift was observed when comparing them with that containing the sodium(I) as counterion (Figure 1). This positive solvatochromism observed along the series Na, K, Rb and Cs can be attributed to the external increasing solvation of the intimate ion pair [M(I), bis(oxamato)palladate(II)] in water. Bathochromic shifts in intimate ion pair maxima is a phenomenon that was already studied and found to be noticeable when the solvent polarity is increased, especially with strong complexing agents such as macrocyclic polyethers.^{41,42} In our case, the resulting positive solvatochromism of the ion pair appears to affect noticeably the coordination sphere of the bis(oxamato)palladate(II) units leading to a colour change from yellow to red of the aqueous solutions of **1/1'** and **2-4**.



Figure 1. Bathochromic effect of the alkaline metal ion [M = Na(I), K(I), Rb(I) and Cs(I) (from left to right)] in the aqueous solutions of the $[Pd(2,6-Me_2pma)_2]^{2-}$ complex.

Description of the structures. Single-crystal X-ray diffraction analyses of **1/1'** and **2-4** confirmed that all compounds are made up of monomeric bis(oxamato)palladate(II) units, a variable amount of water molecules, and the alkaline counteranion of choice, i. e. Na⁺ (**1**), K⁺ (**2**), Rb⁺ (**3**) or Cs⁺ (**4**). Both the *trans* and *cis* isomers of the [Pd^{II}(2,6-Me₂pma)₂]²⁻ complex anion (see Scheme I) were isolated in the solid state: the *trans* isomer as sodium salt (**1**), while the *cis*- form either as sodium (**1'**), potassium (**2**) or rubidium (**3**) salts (**2** and **3** are isostructural compounds). Curiously, the two isomers co-crystallize in the cesium(I) derivative (**4**).

The coordination modes adopted by the 2,6-Me₂pma ligand in **1/1'** and **2-4** is shown in Scheme 2. The structures of the complexes are described in detail hereunder.



Scheme 2. Coordination modes adopted by the 2,6-Me₂pma ligand in **1** (i), **1'** (ii-iv) **2/3** (ii, v, vi) and **4** (i, vii-x) [Ar and M represent the 2,6-dimethylphenyl fragment and the univalent alkaline cation, respectively].

Table1. Summary of the crystal data for $\{[\text{Na}(\text{H}_2\text{O})]_2\text{trans}-[\text{Pd}^{\text{II}}(2,6\text{-Me}_2\text{pma})_2]_n\}$ (**1**), $\{[\text{Na}_4(\text{H}_2\text{O})_2]\text{cis}-[\text{Pd}^{\text{II}}(2,6\text{-Me}_2\text{pma})_2]_n\}$ (**1'**), $\{[\text{K}_4(\text{H}_2\text{O})_3]\text{cis}-[\text{Pd}^{\text{II}}(2,6\text{-Me}_2\text{pma})_2]_n\}$ (**2**), $\{[\text{Rb}_4(\text{H}_2\text{O})_3]\text{cis}-[\text{Pd}^{\text{II}}(2,6\text{-Me}_2\text{pma})_2]_n\}$ (**3**) and $\{[\text{Cs}_6(\text{H}_2\text{O})_7]\text{trans}-[\text{Pd}^{\text{II}}(2,6\text{-Me}_2\text{pma})_2]_n\text{cis}-[\text{Pd}^{\text{II}}(2,6\text{-Me}_2\text{pma})_2]_n \cdot 3n\text{H}_2\text{O}\}$ (**4**)

	1	1'	2	3	4
Formula	$\text{C}_{20}\text{H}_{22}\text{N}_2\text{O}_8\text{Na}_2\text{Pd}$	$\text{C}_{40}\text{H}_{40}\text{N}_4\text{Na}_4\text{O}_{14}\text{Pd}_2$	$\text{C}_{40}\text{H}_{42}\text{N}_4\text{O}_{15}\text{K}_4\text{Pd}_2$	$\text{C}_{40}\text{H}_{42}\text{N}_4\text{O}_{15}\text{Rb}_4\text{Pd}_2$	$\text{C}_{60}\text{H}_{74}\text{N}_6\text{O}_{28}\text{Cs}_6\text{Pd}_3$
M_r	570.78	1105.52	1187.98	1373.46	2443.91
Crystal system	Monoclinic	Monoclinic	Monoclinic	Monoclinic	Orthorhombic
Space group	$I2/a$	Cc	Cc	Cc	$Pbca$
$a/\text{\AA}$	12.889(2)	16.4083(6)	16.317(2)	16.4305(10) \AA	24.874(5)
$b/\text{\AA}$	14.4316(18)	22.4457(12)	25.271(2)	25.1810(19) \AA	24.355(5)
$c/\text{\AA}$	13.6143(19)	13.4740(4)	13.9855(14)	14.1936(7) \AA	26.539(5)
$\beta/^\circ$	105.888(10)	124.4800(10)	124.893(6)	124.878(2)	(90)
$V/\text{\AA}^3$	2435.7(6)	4090.6(3)	4730.1(8)	4817.6(5)	16078(6)
Z	4	4	4	4	8
$D_c/\text{g cm}^{-3}$	1.556	1.795	1.668	1.894	2.019
T/K	100(2)	100(2)	100(2)	296(2)	296(2)
$\mu(\text{Mo-K}\alpha)/\text{mm}^{-1}$	0.843	0.998	1.182	4.830	3.420
$F(000)$	1152	2224	2392	2680	9344
Refl.collected	25193	23741	51992	76964	358776
Refl.indep. (R_{int})	2298 (0.0252)	7475 (0.0397)	10332 (0.0280)	10045 (0.0203)	17069 (0.0690)
Refl.obs. [$I > 2\sigma(I)$]	2208	7363	10191	9771	11235
Goodness-of-fit on F^2	1.332	1.080	1.045	1.063	1.075
$R_1^a [I > 2\sigma(I)]$	0.0164	0.0286	0.0199	0.0629	0.0681
R_1^a (all)	0.0189	0.0294	0.0203	0.0648	0.1011
$wR_2^b [I > 2\sigma(I)]$	0.0537	0.0747	0.0489	0.1926	0.2282
wR_2^b (all)	0.0697	0.0812	0.0492	0.1975	0.2592
Abs. struct. parameter	-	0.00(3)	-0.011(12)	0.139(9)	-
$\Delta\rho_{\text{max,min}}/e \text{\AA}^{-3}$	-	1.027, -0.588	1.277, -0.928	3.227, -3.259	3.025, -4.547

$^a R_1 = \sum(|F_o| - |F_d|) / \sum |F_o|$, $^b wR_2 = \{\sum[w(F_o^2 - F_c^2)^2] / \sum[w(F_o^2)^2]\}^{1/2}$ and $w = 1/[\sigma^2(F_o^2) + (mP)^2 + nP]$ with $P = (F_o^2 + 2F_c^2)/3$, $m = 0.0383$ (**1**), 0.0427 (**1'**), 0.0235 (**2**), 0.1687 (**3**), 0.1674 (**4**), and $n = 1.7111$ (**1**), 13.4385 (**1'**), 5.9743 (**2**), 8.7604 (**3**), 29.3263 (**4**).

$\{[\text{Na}(\text{H}_2\text{O})]_2\text{trans-}[\text{Pd}^{\text{II}}(\text{2,6-Me}_2\text{pma})_2]\}_n$ (**1**). This compound crystallizes in the monoclinic space group $I2/a$ with half a molecule in the asymmetric unit, the second half being generated by the crystallographic inversion centre. Its structure consists of *trans*- $[\text{Pd}(\text{2,6-Me}_2\text{pma})_2]^{2-}$ anions and monohydrated sodium(I) cations linked together by means of single carboxylate- and amidate-oxygen atoms (Figure 2). Selected bond lengths and angles for **1** are listed in Table 2.

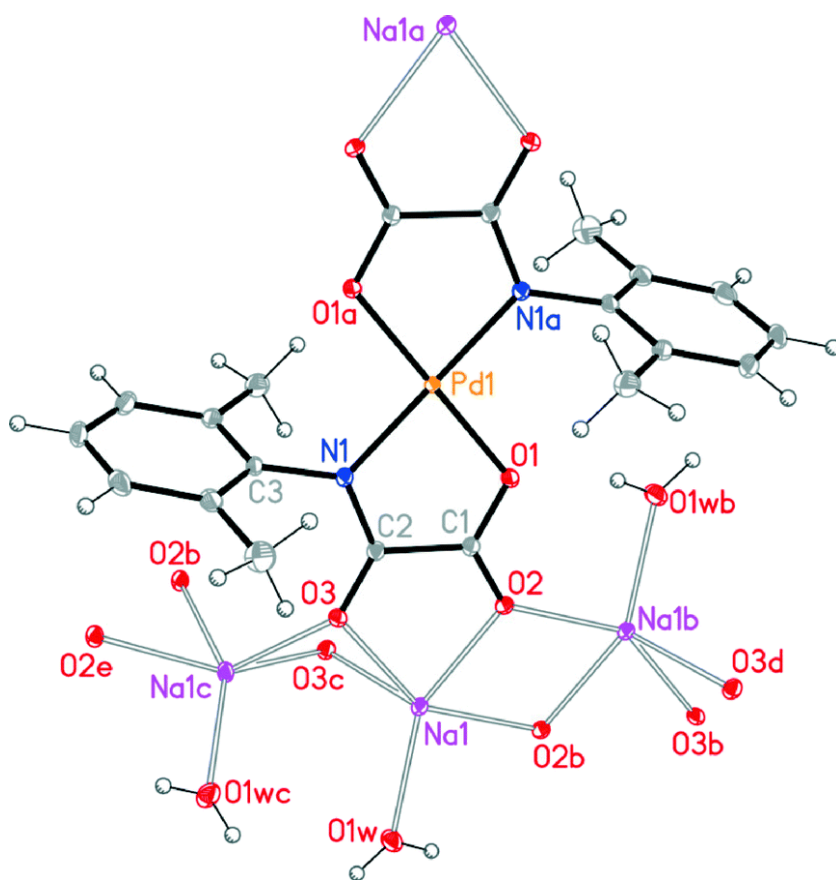


Figure 2. A perspective view of the *trans*- $[\text{Pd}^{\text{II}}(\text{Me}_2\text{pma})_2]^{2-}$ anionic entity in **1** with its vicinal sodium(I) cation surrounding and showing the atom numbering. Thermal ellipsoids are drawn at the 30% probability level [Symmetry codes: (a) = $0.5-x, 0.5-y, 0.5-z$; (b) = $1-x, 1-y, 1-z$; (c) = $0.5-x, y, 1-z$; (d) = $0.5+x, 1-y, z$; (e) = $-0.5+x, 1-y, z$].

Each palladium(II) ion is four-coordinate with two amidate-nitrogen and two carboxylate-oxygen atoms from the two *trans* oxamate ligands building as slightly distorted NOO'N' square-planar surrounding. The reduced bite angle of the chelating oxamate [82.25(5)°] accounts for the deviations from the ideal geometry. In fact, the Pd(II) ion and the atoms building its surrounding lie exactly on a plane for symmetry reasons. The Pd-N and Pd-O bond lengths are 2.020(1) and 2.009(1) Å, respectively. The plane at the Pd(II) ion and the mean plane of the oxamate group are almost coplanar [the dihedral angle between these two planes (ϕ) is 3.65(8)°]. Focusing on the phenyloxamate ligand, the dihedral angle between the 2,6- substituted phenyl ring and the mean plane of the oxamate group (ϕ) is 75.79(4)°.

Table 2. Selected bond lengths (Å) and angles (°) for **1***

Pd(1)-O(1)	2.009(1)	Pd(1)-N(1)	2.020(1)
N(1)-Pd(1)-O(1)	82.25(5)	N(1)-Pd(1)-O(1a)	97.75(5)
Na(1)-O(2)	2.335(1)	Na(1)-O(2b)	2.312(1)
Na(1)-O(3)	2.461(1)	Na(1)-O(3c)	2.296(1)
Na(1)-O(1w)	2.339(2)		
O(1w)-Na(1)-O(2)	151.45(6)	O(2)-Na(1)-O(3c)	110.55(5)
O(1w)-Na(1)-O(3)	126.00(5)	O(3)-Na(1)-O(2b)	146.64(5)
O(1w)-Na(1)-O(2b)	85.09(5)	O(3)-Na(1)-O(3c)	75.64(6)
O(1w)-Na(1)-O(3c)	97.02(5)	O(2b)-Na(1)-O(3c)	116.18(5)
O(2)-Na(1)-O(3)	70.30(4)	Na(1)-O(2)-Na(1b)	103.63(5)
O(2)-Na(1)-O(2b)	76.37(5)	Na(1)-O(3)-Na(1c)	86.75(5)

*Symmetry code: (a) = 0.5-x, 0.5-y, 0.5-z; (b) = 1-x, 1-y, 1-z; (c) = 0.5-x, y, 1-z.

The coordination mode of the oxamate ligand in **1** is shown in Scheme 2i and in Figure 3a. It adopts a bis-bidentate coordination mode connecting the Pd(1) and Na(1) atoms [through N(1) and O(1) towards the Pd(II) ion and across O(2) and O(3) towards the Na(I) cation]. The outer oxamate-oxygens [O(2) and O(3)] further link another sodium(I) cation each one [Na(1b) and Na(1c)]. Thus, each oxamate ligand interacts with three different sodium centers simultaneously (Figure 3a), while each sodium(I) cation is linked to four carboxylate oxygen atoms from three different oxamate ligands, for symmetry reasons.

As evidenced in Figure 3b, the sodium(I) ions in **1** are overall five-coordinate with a distorted square-pyramidal geometry. The Na-O distances span in the range 2.296(2)-2.461(1) Å. The sodium atom is shifted by 0.285(1) Å from the equatorial plane [(O)2]O(2b)O(3)O(1w) set of atoms towards the apical position which is occupied by a carboxylate oxygen atom [O3c].

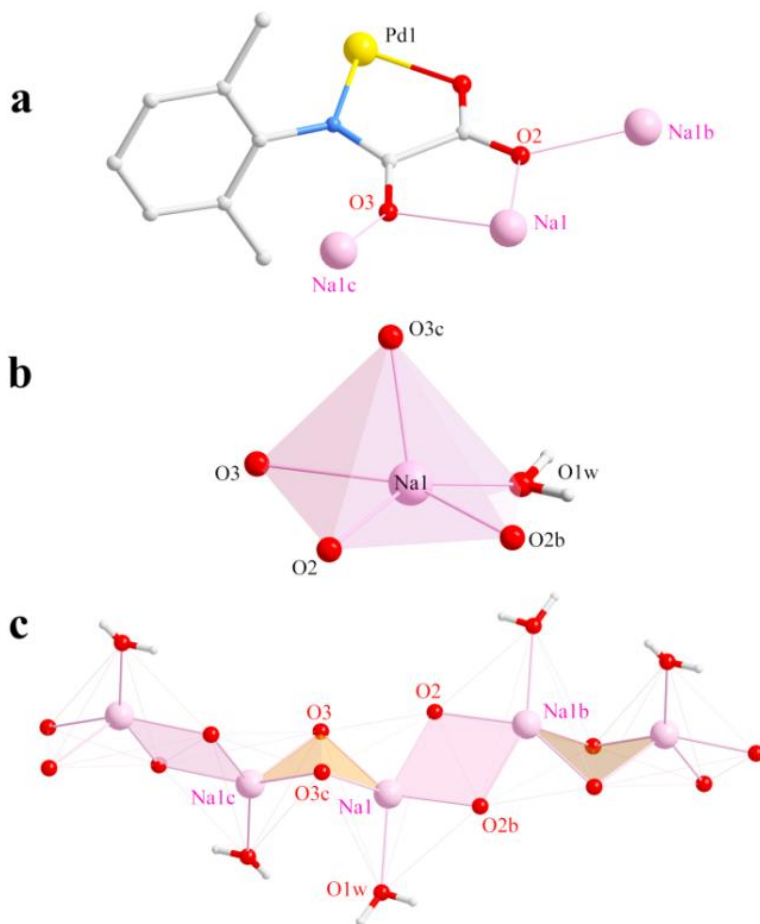


Figure 3. (a) Surrounding of the oxamate ligand in **1**. (b) View of the coordination geometry around Na(1) in **1** [the basal plane of the square pyramid is defined by O(2), O(3), O(2b) and O(1w)]. (c) A view of the alternating flat [Na(1)Na(1b)O(2)O(2b)] and bent [Na(1)Na(1c)O(3)O(3c)] di- μ -O_{oxamate} disodium units in the [Na₂O₂]_n chains running along the crystallographic *c* axis in **1**. Color codes: Pd, yellow; Na, pink; C, grey; N, blue; O, red. The symmetry codes are specified in Table 2.

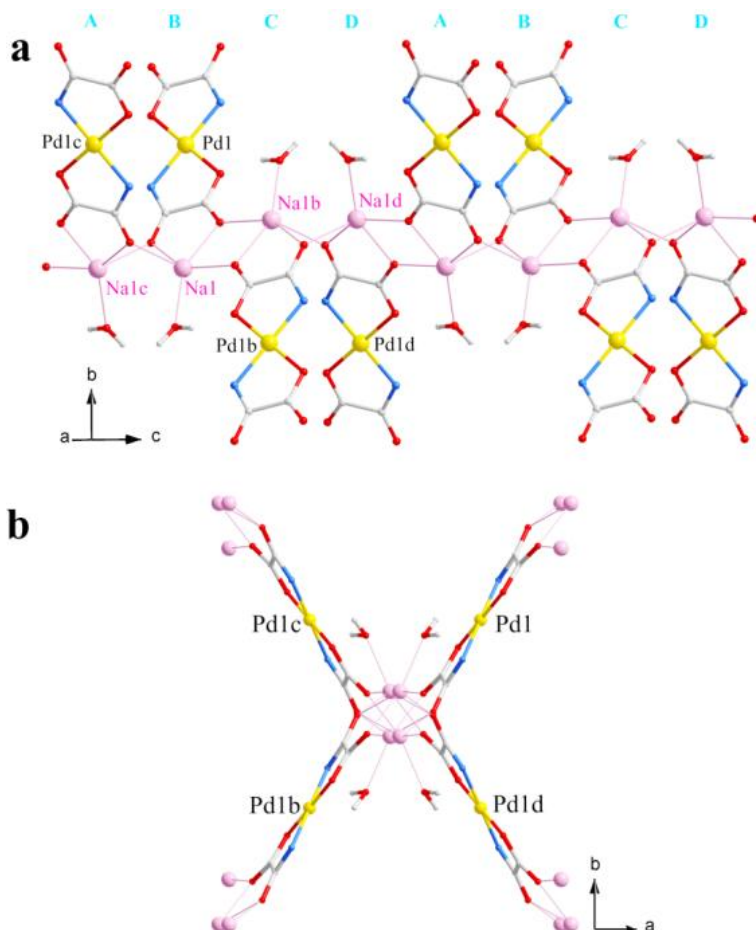


Figure 4. A fragment of the crystal packing in **1** showing the chain arrangement of the monohydrated sodium cations running along the crystallographic *c* axis together with their neighboring bis(oxamato)palladate(II) complexes [the 2,6-dimethylphenyl rings on the ligands are omitted for clarity]: (a) side view; (b) view down to the *c* axis. The whole sodium environment of each oxamate ligand is shown in (b). Color codes: Pd, yellow; Na, pink; C, grey; N, blue; O, red. The symmetry codes are as indicated in Figure 2.

Focusing on the sodium-oxamate interactions, $\{\text{Na}_2\text{O}_2\}_n$ chains running along the crystallographic *c* axis can be identified (Figures 3c and 4a), where flat and bent di- μ -O_{oxamate} disodium units sharing a vertex alternate regularly with $\text{Na}\cdots\text{Na}$ separations of 3.653(1) and 3.269(1) Å, respectively (Figure 3c). The bis(oxamato)palladate(II) units anchored to the array of the sodium atoms point approximately in the directions of the diagonals of the crystallographic *ab* plane (Figure 4b).

The dihedral angles between the Pd(II) mean plane of a Pd(II) complex and its two adjacent symmetry analogues is regularly either 180° [Pd(1) and Pd(1b) in Figure 4a] or ca. 60° [Pd(1) and Pd(1c) in Figure 4a]. This means that the trend of sodium(I) and palladium(II) cations along the crystallographic *c* axis is of the type *ABCDABCD* type (Figure 4a).

Given its centrosymmetric nature, each bis(oxamato)palladate(II) entity in **1** is involved in the formation of two different $[\text{Na}_2\text{O}_2]_n$ chains (see Figure 4b) which are set at a distance equal to the Na(1)⋯Na(1a) separation [11.392(2) Å; symmetry code: (a) = 0.5-*x*, 0.5-*y*, 0.5-*z*] (see Figure 2). This leads to a mixed Pd(II)-Na(I) three-dimensional (3D) network shown in Figure 5.

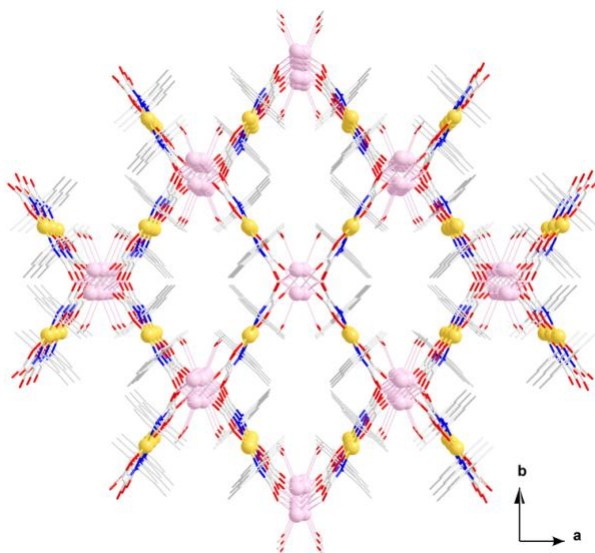


Figure 5. Perspective view of the crystal packing of **1** along the crystallographic *c* axis. Color codes: Pd, yellow; Na, pink; C, grey; N, blue; O, red.

$\{[\text{Na}_4(\text{H}_2\text{O})]_2\text{cis-}[\text{Pd}^{\text{II}}(2,6\text{-Me}_2\text{pma})_2]\}_n$ (**1'**). Compound **1'** crystallizes in the monoclinic space group *Cc*, with two bis(oxamate)palladate(II) units in the asymmetric unit, along with four, partially hydrated sodium(I) cations. Unlike **1**, its structure comprises *cis*- $[\text{Pd}(2,6\text{-Me}_2\text{pma})_2]^{2-}$ anions (see Figure 6). Selected bond lengths and angles for this species are given in Table 3.

Each Pd(II) ion in **1'** is four-coordinate with two amidate nitrogen and two carboxylate-oxygen atoms from the two *cis*-oxamate ligands building a slightly distorted square-planar [NON'O'] surrounding. The Pd-N and Pd-O bond lengths (see Table 3) compare well with those found in **1** and similar species, including compounds **2-4** presented herein (*vide infra*). The square plane at the Pd(II) and the mean plane of the chelating oxamate groups in the two crystallographically independent *cis*-[Pd(2,6-Me₂pma)₂]²⁻ units of **1'** form dihedral angles (φ) in the ranges 5.8(2)-6.6(2)^o at Pd(1) and 1.7(3)-3.4(3)^o at Pd(2).

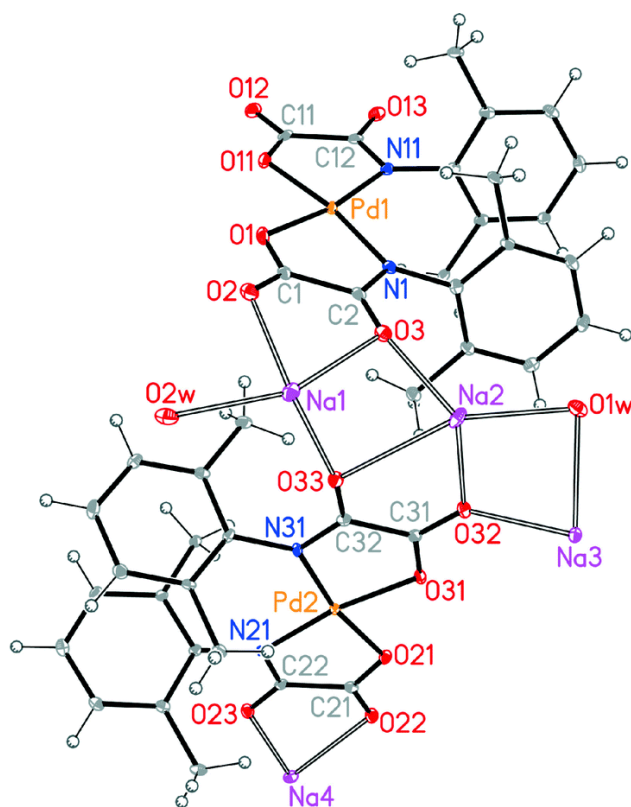


Figure 6. Perspective view of the two crystallographically independent *cis*-[Pd^{II}(2,6-Me₂pma)₂]²⁻ units in **1'**, showing the atom numbering. The sodium and water contents of the asymmetric unit are also included. Thermal ellipsoids are drawn at the 30% probability level.

Intramolecular face-to-face stacking interactions are clearly established between the phenyl rings on each chelating ligands of the *cis*-[Pd(2,6-Me₂pma)₂]²⁻ unit, the centroid-centroid distance and off-set angle having approximate values of 3.7-3.9 Å and 20-21°, respectively. The observed twist angle at Pd(1) and Pd(2) is equal to 5.6(3) and 2.5(4)°, respectively.

Table 3. Selected bond lengths (Å) and angles (°) for **1***.

Pd(1)-O(11)	2.023(4)	Pd(2)-O(21)	2.015(4)
Pd(1)-N(11)	2.029(5)	Pd(2)-N(21)	2.019(5)
Pd(1)-O(1)	2.031(4)	Pd(2)-O(31)	2.015(4)
Pd(1)-N(1)	2.039(5)	Pd(2)-N(31)	2.033(5)
O(1)-Pd(1)-N(1)	81.3(2)	O(21)-Pd(2)-N(21)	81.9(2)
O(11)-Pd(1)-N(1)	170.2(2)	O(31)-Pd(2)-N(21)	169.6(2)
N(11)-Pd(1)-N(1)	108.0(2)	N(21)-Pd(2)-N(31)	108.5(2)
N(11)-Pd(1)-O(1)	170.2(2)	O(21)-Pd(2)-N(31)	169.5(2)
O(11)-Pd(1)-O(1)	89.8(2)	O(21)-Pd(2)-O(31)	87.8(2)
O(11)-Pd(1)-N(11)	81.2(2)	O(13)-Pd(2)-N(13)	81.9(2)
Na(1)-O(3)	2.517(5)	Na(3)-O(1w)	2.474(5)
Na(1)-O(2)	2.393(5)	Na(3)-O(2wa)	2.480(5)
Na(1)-O(33)	2.273(5)	Na(3)-O(32)	2.303(5)
Na(1)-O(11a)	2.373(5)	Na(3)-O(2a)	2.473(5)
Na(1)-O(2w)	2.420(5)	Na(3)-O(12b)	2.327(5)
		Na(3)-O(22c)	2.337(5)
Na(2)-O(1w)	2.420(5)	Na(4)-O(22)	2.569(5)
Na(2)-O(1a)	2.406(5)	Na(4)-O(23)	2.334(5)
Na(2)-O(2a)	2.99(5)	Na(4)-O(13d)	2.309(4)
Na(2)-O(3)	2.302(5)	Na(4)-O(12d)	2.680(5)
Na(2)-O(32)	2.323(5)	Na(4)-O(31e)	2.408(5)
Na(2)-O(33)	2.711(5)	Na(4)-O(21e)	2.618(5)
Na(1)-O(3)-Na(2)	85.8(2)	Na(2)-O(1w)-Na(3)	85.7(2)
Na(1)-O(33)-Na(2)	82.0(2)	Na(2)-O(2a)-Na(3)	75.9(1)
Na(1)-O(2)-Na(3f)	86.4(2)	Na(2)-O(32)-Na(3)	92.0(2)
Na(1)-O(2w)-Na(3f)	85.6(2)	Na(3)-O(12b)-Na(4g)	106.0(2)
Na(1)-O(2)-Na(2f)	161.6(2)	Na(3)-O(22c)-Na(4c)	120.1(2)

* Symmetry codes: (a) $x+1/2, -y+1/2, z+1/2$; (b) $x+1, y, z+1$; (c) $x, -y+1, z+1/2$; (d) $x+1, y, z$; (e) $x, -y+1, z-1/2$; (f) $x-1/2, -y+1/2, z-1/2$; (g) $x, y, z+1$.

Focusing on the four non-equivalent phenyloxamate ligands (L1-L4 in Figure 7), their 2,6-substituted phenyl rings and the mean plane of the oxamate groups form dihedral angles (ϕ) in the ranges 73.64(2)-79.85(2) $^\circ$. They adopt overall three different coordination modes as shown in Figure 7. In particular, L2 and L3 interact with three sodium(I) cations each on (coordination mode indicated as iv in Scheme II), while L1 and L4 have four cations in their proximity (coordination modes iii and ii in Scheme II). The values of the Na-O_{oxamate} distances cover the range 2.273(5)-2.909(5) Å.

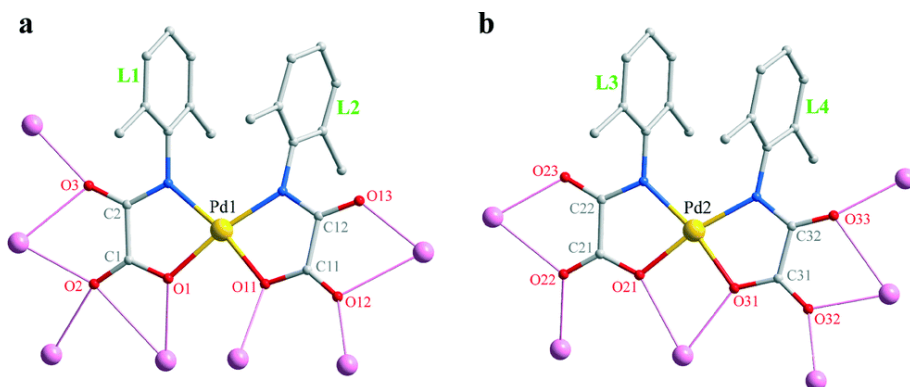


Figure 7. Views of the four crystallographically independent oxamate ligands (L1-L4) in **1'**, showing their coordination modes. O(2), O(3), O(12), O(22), O(32) and O(33) are the bridging oxygen atoms. Color codes: Pd, yellow; Na, pink; C, grey; N, blue; O, red.

The surrounding of the four crystallographically-independent sodium(I) cations in **1'** is shown in Figure 8. Na(1) is five-coordinate in a distorted trigonal bipyramidal environment which is built up by four carboxylate-oxygen atoms from three different oxamate ligands plus a water molecule. The other three cations are all six-coordinate, their geometry being either distorted octahedral [Na(3)] or closer to a distorted rectangular prism [Na(2), Na(4)].

There are two crystallographically independent water molecules per each four alkaline(I) cations and they act as bridges with Na-O_w distances in the range 2.420(5)-2.480(5) Å. Significant cation-cation separation through their respective bridges are 3.85(3) [Na(1)··Na(2), O3/O33], 5.234(3) [Na(1)··Na(2f), O2] 3.331(3) [Na(1)··Na(3f), O2/O2w], 3.327(3) [Na(2)··Na(3), O1w/O2/O32], 4.253(3) [Na(3)··Na(4c), O22c] and 4.006(3) Å [Na(3)··Na(4g), O12b].

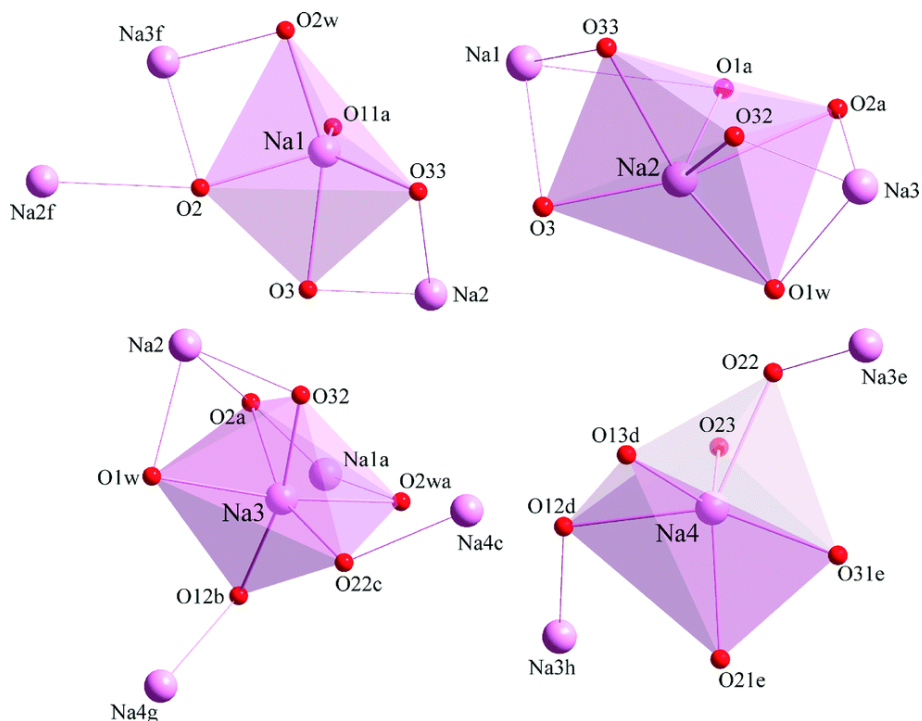


Figure 8. View of the surrounding of the four crystallographically independent sodium(I) cations in **1'** [Symmetry codes: (h) = x, y, z-1; (a)-(g) are those given in Table 3].

As far as the 3D framework of **1'** is concerned (Figure 9), it is very similar to that of the potassium (**2**) and rubidium (**3**) derivatives described in detail below. Peculiar cation- π interactions observed in **2-3** are not observed in **1'**; however, this has no substantial influence on the overall crystal packing of the three samples.

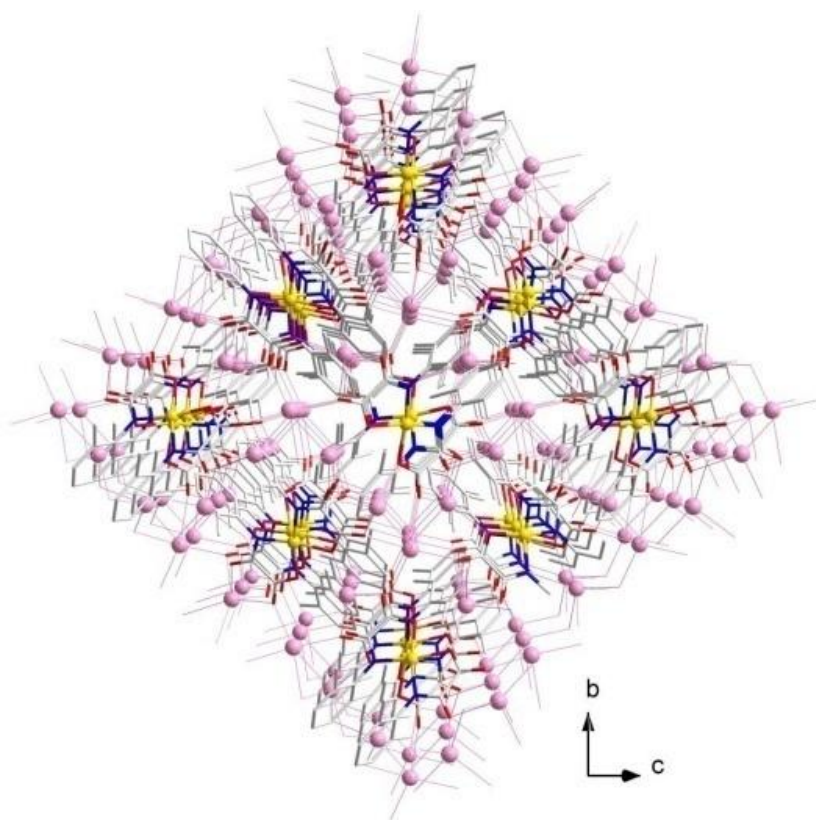


Figure 9. Perspective view of the crystal packing of **1'** along the crystallographic *a* axis.

$\{[\text{K}_4(\text{H}_2\text{O})_3]\text{cis}[\text{Pd}^{\text{II}}(2,6\text{-Me}_2\text{pma})_2]_2\}_n$ (**2**) and $\{[\text{Rb}_4(\text{H}_2\text{O})_3]\text{cis}[\text{Pd}^{\text{II}}(2,6\text{-Me}_2\text{pma})_2]_2\}_n$ (**3**). Compounds **2** and **3** are isostructural and they crystallize in the monoclinic space group *Cc* with two entire molecules in the asymmetric unit. Their structures consist of *cis*-[Pd(2,6-Me₂pma)₂]²⁻ anions and hydrated K(I) (**2**) or Rb(I) (**3**) cations linked together by means of oxamate-oxygen atoms and water molecules leading to intricate Pd(II)-K(I) (**2**) or Pd(II)-Rb(I) (**3**) 3D networks. A view of the two crystallographically independent bis(oxamato)palladate(II) units in **2** and **3** is given in Figures 10 and 11 respectively, whereas main bond lengths and angles are listed in Table 4 (**2**) and 5 (**3**).

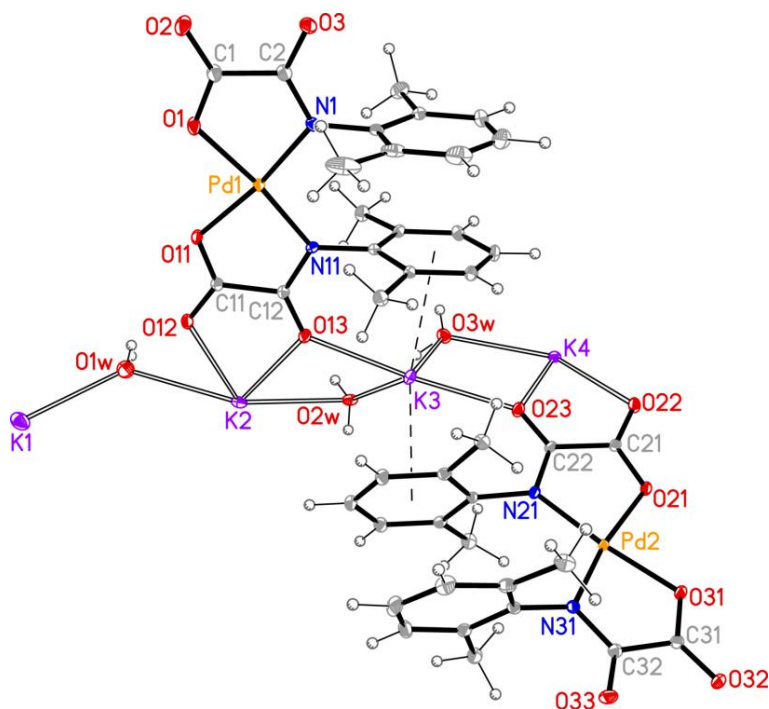


Figure 10. Perspective view of the two crystallographically independent *cis*-[Pd^{II}(2,6-Me₂pma)₂]²⁻ units in **2** showing the atom numbering. The potassium(I) cations and the water molecules of the asymmetric unit are also included. Thermal ellipsoids are drawn at the 30% probability level.

As in the previous structures, each Pd(II) ion in **2** and **3** is four-coordinate with two amidate nitrogen and two carboxylate-oxygen atoms from the two *cis*-oxamate ligands building a slightly distorted square-planar [NON'O'] surrounding. The reduced bite of the chelating oxamate [81.23(8)-81.49(8)° (**2**), 81.1(3)-81.6(3)° (**3**)] mostly accounts for the deviations from the ideal geometry. All Pd(II) ions belong practically to their square planes, being displaced by only 0.008(1)-0.011(1) Å (**2**) and 0.003(4)-0.007(4) Å (**3**).

The square plane at the Pd(II) and the mean plane of the chelating oxamate groups in the two crystallographically independent *cis*-[Pd^{II}(2,6-Me₂pma)₂]²⁻ units of **2** and **3** are not as close to coplanarity as observed in **1** [the values of the dihedral angle between these two planes (φ) being in the ranges 6.6(1)-11.4(1)° (**2**) and 5.9(4)-10.2(4)° (**3**)].

Intramolecular face-to-face stacking interactions are clearly established between the phenyl rings on each chelating ligand of the *cis*-[Pd^{II}(2,6-Me₂pma)₂]²⁻ unit. The steric hindrance between the methyl substituents at each ring precludes the ideal 100% overlap in both **2** and **3**, the centroid-centroid distance and off-set angle having approximate values of 3.7–3.9 Å and 23–27°, respectively. Steric effects are also likely responsible for the non-zero twist angle observed in this class of compounds with *cis* stereochemistry [2.4(2) (2)/2.4(6)° (3) at Pd(1) and 5.5(2) (2)/4.0(6)° (3) at Pd(2)].

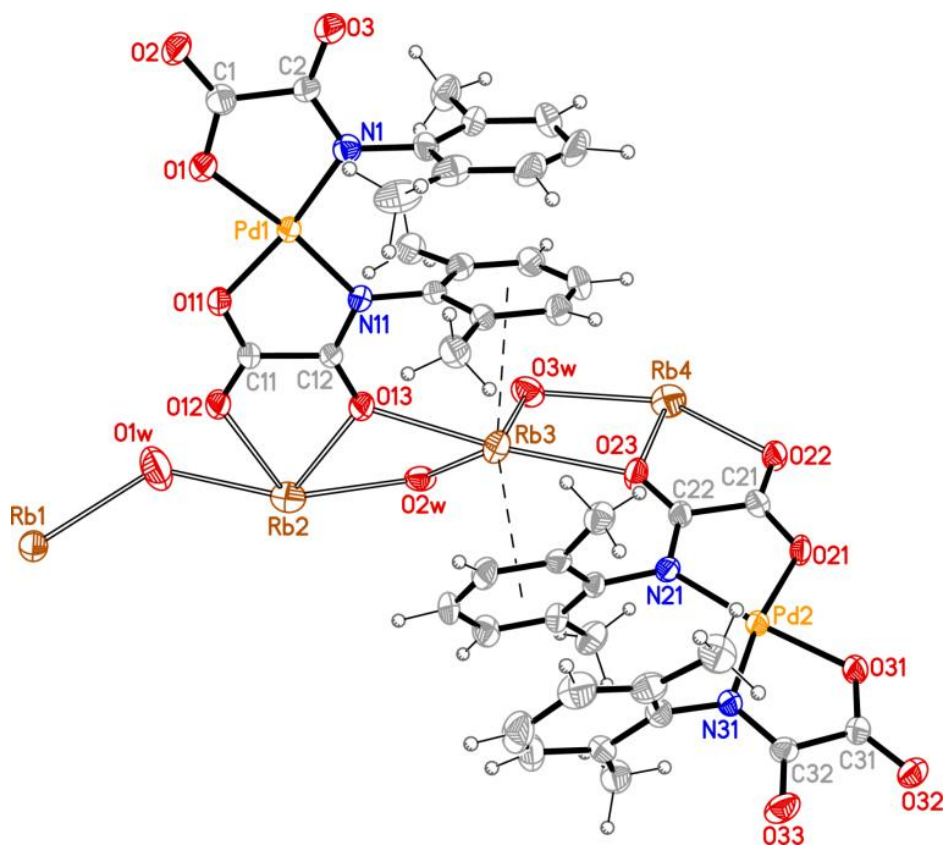


Figure 11. Perspective view of the two crystallographically independent *cis*-[Pd^{II}(2,6-Me₂pma)₂]²⁻ units in **3** showing the atom numbering. The rubidium(I) cations and water molecules of the asymmetric unit are also included. Thermal ellipsoids are drawn at the 30% probability level.

Table 4. Selected bond lengths (Å) and angles (°) for **2***

Pd(1)-N(1)	2.031(2)	Pd(2)-N(21)	2.040(2)
Pd(1)-O(1)	2.034(2)	Pd(2)-O(21)	2.039(2)
Pd(1)-N(11)	2.037(2)	Pd(2)-N(31)	2.035(2)
Pd(1)-O(11)	2.040(2)	Pd(2)-O(31)	2.023(2)
N(1)-Pd(1)-O(1)	81.49(8)	N(21)-Pd(2)-O(21)	81.23(8)
N(1)-Pd(1)-O(11)	171.71(8)	N(21)-Pd(2)-O(31)	170.20(8)
N(1)-Pd(1)-N(11)	106.95(8)	N(21)-Pd(2)-N(31)	107.74(8)
O(1)-Pd(1)-N(11)	171.32(9)	O(21)-Pd(2)-N(31)	170.27(8)
O(1)-Pd(1)-O(11)	90.29(7)	O(21)-Pd(2)-O(31)	89.59(7)
O(11)-Pd(1)-N(11)	81.31(8)	O(31)-Pd(2)-N(31)	81.67(8)
K(1)-O(1w)	2.867(3)	K(3)-O(2w)	2.807(2)
K(1)-O(2a)	3.044(3)	K(3)-O(3w)	2.785(2)
K(1)-O(3b)	2.836(2)	K(3)-O(13)	2.680(2)
K(1)-O(22c)	2.858(2)	K(3)-O(23)	2.676(2)
K(1)-O(32d)	2.842(2)		
K(2)-O(1w)	2.993(3)	K(4)-O(3w)	2.782(2)
K(2)-O(2w)	2.891(2)	K(4)-O(22)	2.835(2)
K(2)-O(12)	2.811(2)	K(4)-O(23)	2.723(2)
K(2)-O(13)	2.788(2)	K(4)-O(2g)	2.774(2)
K(2)-O(1a)	2.749(2)	K(4)-O(3g)	2.762(2)
K(2)-O(11a)	2.867(2)	K(4)-O(21h)	2.817(2)
K(2)-O(33f)	2.680(2)	K(4)-O(31h)	2.759(2)
K(1)-O(2a)-K(4e)	99.30(8)	K(2)-O(13)-K(3)	105.43(6)
K(1)-O(3b)-K(4c)	99.32(6)	K(2)-O(2w)-K(3)	99.57(6)
K(1)-O(22c)-K(4c)	97.12(6)	K(3)-O(23)-K(4)	102.85(6)
K(1)-O(1w)-K(2)	130.3(1)	K(3)-O(3w)-K(4)	98.60(6)

*Symmetry codes: (a) = $x-1/2, -y+1/2, z-1/2$; (b) = $x-1/2, y-1/2, z$; (c) = $x+1/2, y-1/2, z+1$; (d) = $x+1/2, -y+1/2, z+3/2$; (e) = $x+1/2, -y+1/2, z+1/2$; (f) = $x, y, z+1$; (g) = $x-1, y, z-1$; (h) = $x, -y+1, z+1/2$.

Concerning the four non-equivalent phenyloxamate ligands (L1-L4 in Figure 12), their 2,6-substituted phenyl rings are basically orthogonal to the mean plane of the oxamate groups with values of the dihedral angle (ϕ) in the ranges 81.26(8)-89.32(8)° (**2**) and 84.3(3)-89.00(3)° (**3**). They adopt overall three different coordination modes (Figure 12 and ii, v and vi in Scheme II).

The two outer oxygen atoms O(2) and O(3) for L1 and O(22) and O(23) for L3 exhibit a bis-monodentate bridging mode, as observed for the oxamate ligand in **1**. However, L1 and L3 here are further connected to another alkaline cation [K(I) (**2**) or Rb(I) (**3**)] *via* the Pd-bound carboxylate-oxygen atom [O(1) for L1 and O(21) for L3], giving rise to the coordination environment noted ii in Scheme II.

Table 5. Selected bond lengths (Å) and angles (°) for **3***

Pd(1)-N(1)	2.012(8)	Pd(2)-N(21)	2.030(7)
Pd(1)-O(1)	2.020(7)	Pd(2)-O(21)	2.034(6)
Pd(1)-N(11)	2.020(7)	Pd(2)-N(31)	2.015(6)
Pd(1)-O(11)	2.035(6)	Pd(2)-O(31)	1.995(6)
N(1)-Pd(1)-O(1)	81.6(3)	N(21)-Pd(2)-O(21)	81.1(2)
N(1)-Pd(1)-O(11)	171.4(3)	N(21)-Pd(2)-O(31)	170.4(3)
N(1)-Pd(1)-N(11)	107.2(3)	N(21)-Pd(2)-N(31)	108.2(3)
O(1)-Pd(1)-N(11)	171.1(3)	O(21)-Pd(2)-N(31)	170.4(2)
O(1)-Pd(1)-O(11)	89.9(3)	O(21)-Pd(2)-O(31)	89.8(2)
O(11)-Pd(1)-N(11)	81.4(3)	O(31)-Pd(2)-N(31)	81.1(3)
Rb(1)-O(1w)	2.954(12)	Rb(3)-O(2w)	2.926(7)
Rb(1)-O(2a)	3.071(8)	Rb(3)-O(3w)	2.874(9)
Rb(1)-O(3b)	2.957(7)	Rb(3)-O(13)	2.767(6)
Rb(1)-O(22c)	2.978(7)	Rb(3)-O(23)	2.769(6)
Rb(1)-O(32d)	3.027(8)		
Rb(2)-O(1w)	2.889(14)	Rb(4)-O(3w)	2.875(10)
Rb(2)-O(2w)	2.941(9)	Rb(4)-O(22)	2.883(6)
Rb(2)-O(12)	2.850(6)	Rb(4)-O(23)	2.752(7)
Rb(2)-O(13)	2.844(7)	Rb(4)-O(2g)	2.822(7)
Rb(2)-O(1a)	2.789(7)	Rb(4)-O(3g)	2.784(7)
Rb(2)-O(11a)	2.940(6)	Rb(4)-O(21h)	2.851(6)
Rb(2)-O(33f)	2.784(7)	Rb(4)-O(31h)	2.778(6)
Rb(1)-O(2a)-Rb(4e)	102.5(2)	Rb(2)-O(13)-Rb(3)	103.0(2)
Rb(1)-O(3b)-Rb(4c)	99.6(2)	Rb(2)-O(2w)-Rb(3)	96.9(2)
Rb(1)-O(22c)-Rb(4c)	96.9(2)	Rb(3)-O(23)-Rb(4)	102.1(2)
Rb(1)-O(1w)-Rb(2)	122.7(5)	Rb(3)-O(3w)-Rb(4)	96.6(3)

*Symmetry codes: (a) = $x-1/2, -y+1/2, z-1/2$; (b) = $x-1/2, y-1/2, z$; (c) = $x+1/2, y-1/2, z+1$; (d) = $x+1/2, -y+1/2, z+3/2$; (e) = $x+1/2, -y+1/2, z+1/2$; (f) = $x, y, z+1$; (g) = $x-1, y, z-1$; (h) = $x, -y+1, z+1/2$.

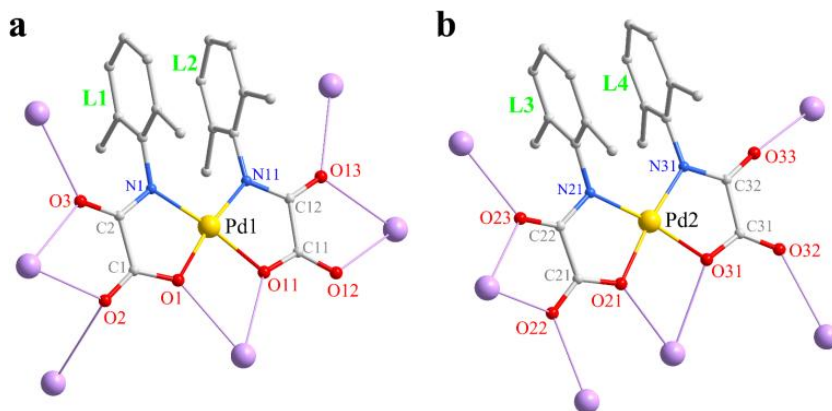


Figure 12. Views of the four crystallographically independent oxamate ligands L1-L4 in **2** (the same applies to **3**), together with their potassium linking. O(2), O(3), O(13), O(22) and O(23) are the bridging oxygen atoms. Color codes: Pd, yellow; K, violet; C, grey; N, blue; O, red.

In the case of L2, the two outer oxygen atoms are either bridging or monodentate whereas they are both just monodentate in L4. Again the involvement of the Pd-bound carboxylate-oxygen atom [O(11) for L2 and O(31) for L4] is observed in a close contact with another potassium(I) (**2**) or rubidium(I) (**3**) cation, giving rise to an overall coordination environment indicated in Scheme II as ii for L2 and iv for L4. As a consequence, each oxamate ligand in **2** and **3** interacts simultaneously with either three or four different alkaline cations, with K-O_{oxamate} (**2**) and Rb-O_{oxamate} (**3**) distances varying in the ranges 2.723(2)-3.044(3) and 2.767(6)-3.071(8) Å, respectively.

Four crystallographically-independent alkaline cations are present in **2** and **3** and they are connected to each other through single-carboxylate and/or single-water molecules as bridges (Figures 10 and 11). The surrounding of the potassium(I) cations in **2** is shown in Figure 13 [identical surrounding for the rubidium(I) cations in **3**]. Each univalent cation is bound to a variable amount of carboxylate-oxygen atoms as well as water molecules. In addition, K(1) and K(3) in **2** [Rb(1) and Rb(3) in **3**] are involved respectively in one or two cation- π type interactions³⁵ with the phenyl ring of vicinal dimethylphenyloxamate ligands.

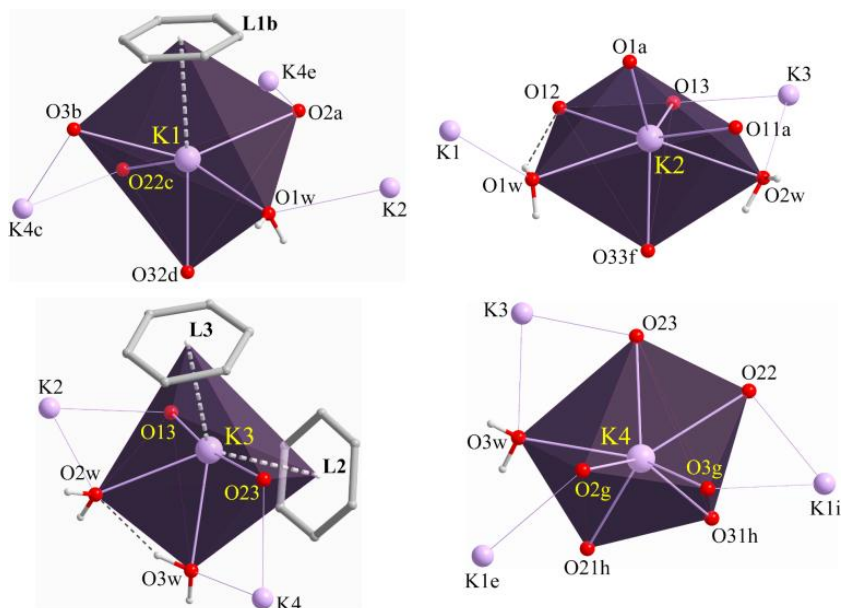


Figure 13. View of the surrounding of the four crystallographically-independent potassium(I) cations in **2**. For the sake of clarity, only the phenyl ring of the corresponding dimethylphenyloxamato ligand is shown where cation- π interactions occur. Hydrogen bonds [O(1w) \cdots O(12) and O(3w) \cdots O(2w)] and cation- π interactions are depicted as dashed lines [Symmetry codes: (i) = $x-1/2, y+1/2, z-1$; (a)-(h) are those shown in Table 4].

Four carboxylate-oxygen atoms from four different oxamate ligands, a water molecule and the ring-centroid of a phenyl ring belonging to a symmetry equivalent of L1 build a distorted octahedral geometry around K(1) in **2** [Rb(1) in **3**], while two carboxylate-oxygen atoms from two different oxamate ligands, two water molecules and the ring-centroid of the phenyl ring belonging to L2 and L3 form a rather distorted octahedron around K(3) in **2** [Rb(3) (**3**)] (Figure 13). The cation-ring centroid distances observed in **2** are 3.5 Å [K(1) \cdots L(1b)] and 3.2 Å [K(3) \cdots L2 and K(3) \cdots L3] [3.5 Å (Rb(1) \cdots L1b), 3.3 Å (Rb(3) \cdots L2) and 3.2 Å (Rb(3) \cdots L3) in **3**]. The values of the L2 \cdots K(3) \cdots L3 and L2 \cdots Rb(3) \cdots L3 centroid-cation-centroid angle in **2** and **3** are ca. 128 and 130°, respectively.

The remaining univalent cations [K(2) and K(4) (**2**) or Rb(2) and Rb(4) (**3**)] are seven-coordinate, the surrounding being defined by either five carboxylate-oxygen atoms from three different oxamate ligands plus two water molecules [at K(2) (**2**) and Rb(2) (**3**)] or six carboxylate-oxygen

atoms from three different oxamate ligands plus one water molecules [at K(4) (2) and Rb(4) (3)] (see Figure 13).

Dealing with the water molecules, three of them every four alkaline cations are crystallographically independent and they all act as bridges. The K-O_w (2) and Rb-O_w (3) distances cover the ranges 2.782(2)-2.993(3) Å and 2.87(1)-3.36(1) Å, respectively. The longest bonds are those established with the O(1w) atom which only connects two cations [K(1) and K(2) (2) and Rb(1) and Rb(2) (3)], without the support of an additional O_{carboxylate} bridge as for the K(2)/K(3) and K(3)/K(4) pairs [Rb(2)/Rb(3) and Rb(3)/Rb(4) (3)] (see Figures 10 and 11).

The cation-cation separation through the single aqua bridge [O(1w)] and the double aqua/oxo(carboxylate) bridges [O(2w)/O(13) and O(3w)/O(23)] are 5.317(1) [K(1)··K(2)], 4.351(1) [K(2)··K(3)] and 4.221(1) Å [K(3)··K(4)] (2) and 5.127(2) [Rb(1)··Rb(2)], 4.390(2) [Rb(2)··Rb(3)] and 4.292(2) Å [Rb(3)··Rb(4)] (3).

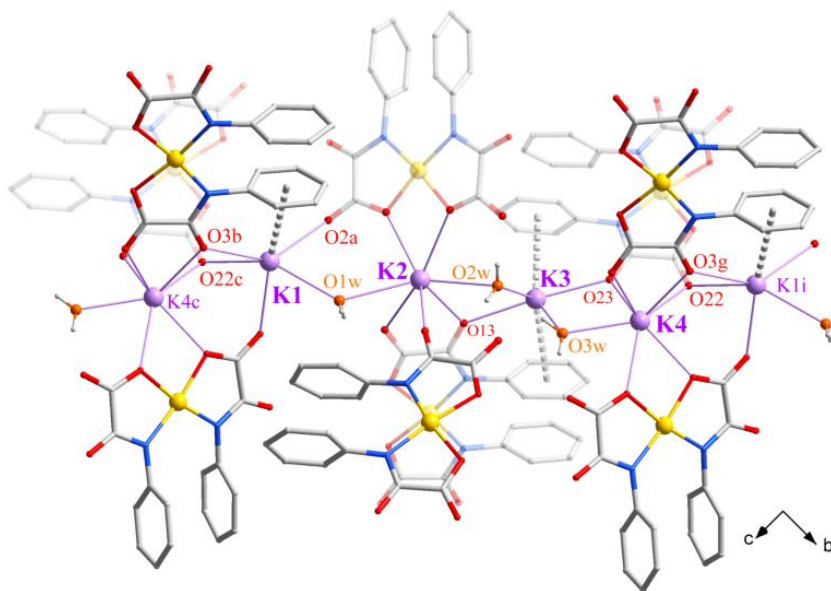


Figure 14. View of a fragment of the $\{K(1)K(2)K(3)K(4)\}_n$ chain in **2**. The methyl groups on the phenyl ring of the oxamate ligands are omitted for clarity. Cation- π type interactions are depicted as dashed lines; hydrogen bonds are not indicated. The same motif is found in the structure of **3**. Symmetry codes are those given in Table 4 and Figure 12.

The tetrameric assembly of potassium(I) (**2**) or rubidium(I) (**3**) cations in the asymmetric unit is not isolated but rather involved in the formation of linear $\{K_4O_x\}_n$ (**2**) [$\{Rb_4O_x\}_n$ (**3**)] chains where adjacent tetramers follow one another by means of a di- μ -oxo(carboxylate) bridge, according to the sequence...K(1)K(2)K(3)K(4)-K(1')K(2')K(3')K(4')...(**2**) [...Rb(1)Rb(2)Rb(3)Rb(4)-Rb(1')Rb(2')Rb(3')Rb(4')...](**3**). A view of a fragment of such chains for **2** is shown in Figure 14. The K(1) \cdots K(4c) separation through the di- μ -oxo(carboxylate) bridge O(3b)/O(22c) is 4.268(1) Å (**2**) [Rb(1) \cdots Rb(4c) = 4.386(2) Å (**3**)] [symmetry code: (b) = $x-1/2, y-1/2, z$; (c) = $x+1/2, y-1/2, z+1$].

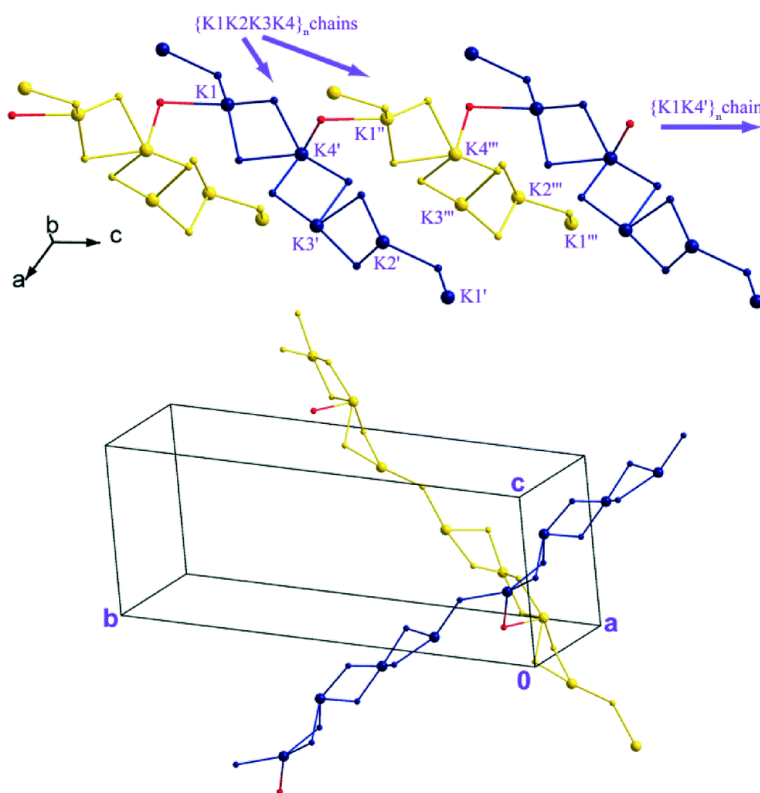


Figure 15. Schematic view of the two different one-dimensional assemblies of potassium(I) ions in **2** and their relative propagation. Note the $\{K(1)K(4')\}_n$ chain growing along the crystallographic c axis and the anchored $\{K(1)K(2)K(3)K(4)\}_n$ chains growing along two different and orthogonal directions. An identical arrangement is found in **3**.

As shown in Figure 13, the alkaline cation K(1) in **2** [Rb(1) (**3**)] is indeed connected to another symmetry-equivalent of the K(4) atom [Rb(4) (**3**)] *via* a single oxo(carboxylate) bridge O(2a), the K(1)··K(4e) separation being 4.438(1) Å [Rb(1)··Rb(4e) = 4.599(2) Å(**3**)] [symmetry code: (e) = $x+1/2, -y+1/2, z+1/2$]. As a consequence, chains formed only by the K(1) and K(4) type of atoms in **2** [or Rb(1) and Rb(4) (**3**)] can also be defined, and these run along the crystallographic *c* axis. Moreover, the {K(1)K(2)K(3)K(4)}_{*n*} (**2**) [{Rb(1)Rb(2)Rb(3)Rb(4)}_{*n*} (**3**)] chains described above, which are anchored to the latter but spaced apart by a K-O-K (**2**) or Rb-O-Rb (**3**) fragments [K(1)-O(2a)-K(4e) (**2**) and Rb(1)-O(2a)-Rb(4e) (**3**)] propagate into two non-equivalent and basically orthogonal vectors identified as the crystallographic [$1/2 \ 1/2 \ 1$] and [$1/2 \ -1/2 \ 1$] directions (Figure 15).

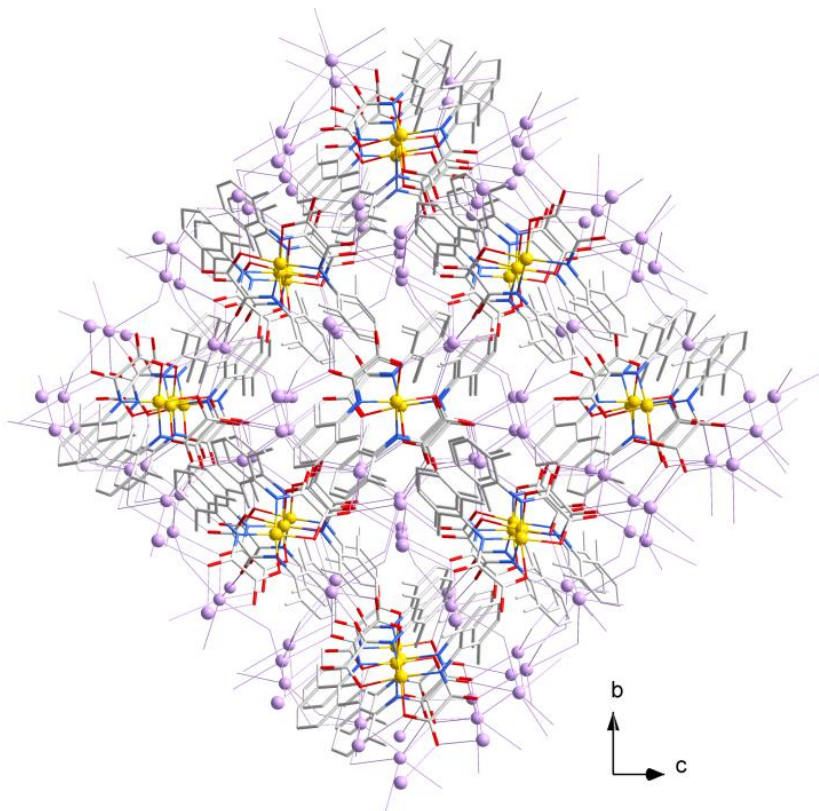


Figure 16. Perspective view of the crystal packing of **2** along the crystallographic *a* axis. The packing of **3** is identical.

From the connection between the two described types of chains growing overall in three different directions, a {K-O} or {Rb-O} 3D assembly and consequently, a rather intricate mixed Pd(II)/K(I) or Pd(II)/Rb(I) 3D network arises in **2** and **3**, respectively (Figure 16). A very similar 3D network is found in **1'** (Figure 9).

$\{[\text{Cs}_6(\text{H}_2\text{O})_7]\text{trans-}[\text{Pd}^{\text{II}}(2,6\text{-Me}_2\text{pma})_2]_2\text{cis-}[\text{Pd}^{\text{II}}(2,6\text{-Me}_2\text{pma})_2]\}_n \cdot 3n\text{H}_2\text{O}$ (**4**). Compound **4** crystallizes in the orthorhombic space group *Pbca*. One *cis*-[Pd(2,6-Me₂pma)₂]²⁻ and a *trans*-[Pd(2,6-Me₂pma)₂]²⁻ entry, plus two half motifs of the latter type are found in the asymmetric unit, together with six interconnected hydrated cesium(I) cations and additional uncoordinated water molecules. Once again, complex anions and cations are linked together mostly by means of outer oxamate-oxygen atoms, acting as bridges. A view of the crystallographically independent bis(oxamato)palladated(II) units in **4** is given in Figure 17. Main bond lengths and angles for **4** are listed in Table 6.

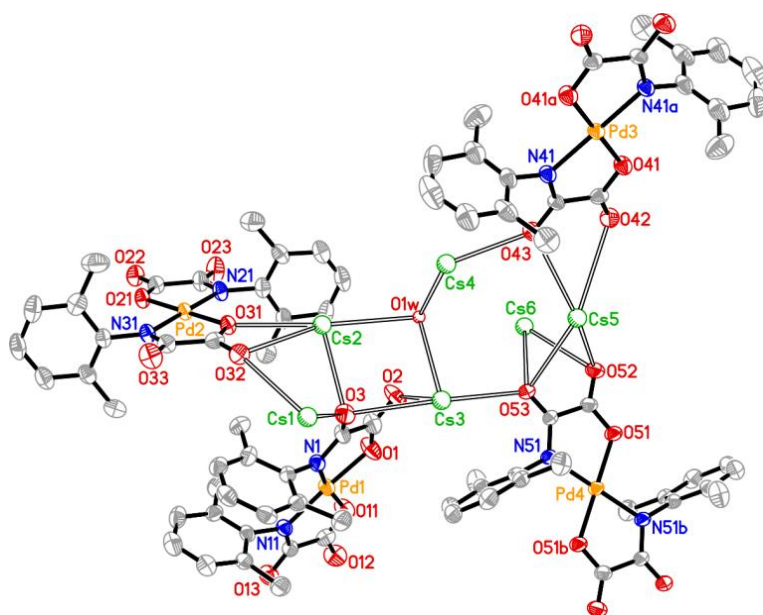


Figure 17. Molecular structure of the two non-centrosymmetric [Pd(1) (*cis*) and Pd(2) (*trans*)] and two centrosymmetric [Pd(3)(*trans*) and Pd(4)(*trans*)] crystallographically independent [Pd^{II}(2,6-Me₂pma)₂]²⁻ units in **4** showing the atom numbering. Thermal ellipsoids are drawn at the 30% probability level. The six cesium(I) cations in the asymmetric unit are also shown. Hydrogen atoms on the 2,6-Me₂pma²⁻ ligands and the water molecules [except O(1w)] are omitted for clarity.

Each Pd(II) ion in **4** is four-coordinate with two amidate- nitrogen and two carboxylate-oxygen atoms from two oxamate ligands building slightly distorted square-planar surroundings in *cis*- [NON'O'] [at Pd(1)] and *trans*- [NOO'N'] arrangements [at Pd(2), Pd(3) and Pd(4)]. The reduced bite of the chelating oxamate [81.3(3)-82.7(3) $^\circ$] mostly accounts for the deviations from the ideal geometry in **4**, as in **1**, **2-3**. Pd(1) (*cis* complex) is displaced from its square plane by 0.032(4) Å whereas the other three palladium centres belong practically to their square planes, either by symmetry reasons [Pd(3) and Pd(4)] or not [Pd(2)]. The Pd-N and Pd-O bond lengths are in the expected range (see Table 6). The values of the dihedral angle φ between the square plane at each Pd(II) and the mean plane of the chelating oxamate groups are 5.5(4) and 7.9(3) $^\circ$ [Pd(1)], 2.77(3) and 3.42(4) $^\circ$ [Pd(2)], 1.18(4) $^\circ$ [Pd(3)] and 2.1(4) $^\circ$ [Pd(4)]. The values of the twist angle for the two non-centrosymmetric molecules in the asymmetric unit are 4.9(4) $^\circ$ and 0.76(2) $^\circ$ at Pd(1) and Pd(2) respectively, clearly reflecting the influence of steric hindrance on this particular molecular feature. The values of the centroid-centroid distance and off-set angle concerning the π - π type interactions between the phenyl rings on each chelating oxamate at Pd(4) are ca. 3.6 Å and 17 $^\circ$, respectively.

Focusing on the phenyloxamate ligands (L1-L6 in Figure 18), their 2,6-substituted phenyl rings are basically orthogonal to the mean plane of the oxamate groups with values of the dihedral angle (ϕ) in the range 80.7(3)-89.4(3) $^\circ$ confirming the already observed trend. The six non-equivalent ligands adopt five different coordination modes.

Table 6. Selected bond lengths (Å) and angles ($^\circ$) for **4***

Pd(1)-N(1)	1.987(7)	Pd(2)-N(21)	2.008(7)
Pd(1)-O(1)	2.003(7)	Pd(2)-O(21)	1.997(6)
Pd(1)-N(11)	2.025(7)	Pd(2)-N(31)	2.008(7)
Pd(1)-O(11)	2.020(7)	Pd(2)-O(31)	1.988(5)
Pd(3)-N(41)	2.016(7)	Pd(4)-N(51)	2.013(7)
Pd(3)-O(41)	2.015(6)	Pd(4)-O(51)	2.005(6)
N(1)-Pd(1)-O(1)	82.1(3)	O(1)-Pd(1)-O(11)	90.2(3)
N(1)-Pd(1)-O(11)	171.0(3)	O(1)-Pd(1)-N(11)	171.5(3)
N(1)-Pd(1)-N(11)	106.4(3)	O(11)-Pd(1)-N(11)	81.3(3)
N(21)-Pd(2)-O(21)	82.7(3)	O(21)-Pd(2)-O(31)	179.2(3)
N(21)-Pd(2)-O(31)	97.9(3)	O(21)-Pd(2)-N(31)	97.5(3)

Table 6 contn.

N(21)-Pd(2)-N(31)	179.4(3)	O(31)-Pd(2)-N(31)	81.9(3)
N(41)-Pd(3)-O(41)	81.4(3)	O(41)-Pd(3)-O(41a)	179.997(1)
N(41)-Pd(3)-O(41a)	98.6(3)	O(41)-Pd(3)-N(41a)	98.6(3)
N(41)-Pd(3)-N(41a)	180.0(3)	O(41a)-Pd(3)-N(41a)	81.4(3)
N(51)-Pd(4)-O(51)	81.5(3)	O(51)-Pd(4)-O(51b)	180.0(4)
N(51)-Pd(4)-O(51b)	98.5(3)	O(51)-Pd(4)-N(51b)	98.5(3)
N(51)-Pd(4)-N(51b)	180.0(4)	O(51b)-Pd(4)-N(51b)	81.5(3)
Cs(1)-O(1w)	2.62(2)	Cs(4)-O(3w)	3.09(1)
Cs(1)-O(2w)	3.07(1)	Cs(4)-O(4w)	3.59(1)
Cs(1)-O(6wc)	3.03(1)	Cs(4)-O(5w)	3.19(2)
Cs(1)-O(3)	2.97(1)	Cs(4)-O(43)	3.00(1)
Cs(1)-O(32)	3.10(1)	Cs(4)-O(12d)	2.96(1)
Cs(1)-O(42c)	2.99(1)	Cs(4)-O(22e)	3.10(1)
Cs(2)-O(1w)	3.25(2)	Cs(5)-O(6w)	3.147(7)
Cs(2)-O(3w)	3.25(1)	Cs(5)-O(42)	3.417(7)
Cs(2)-O(3)	3.02(1)	Cs(5)-O(43)	3.237(7)
Cs(2)-O(31)	3.07(1)	Cs(5)-O(52)	3.266(7)
Cs(2)-O(32)	3.33(1)	Cs(5)-O(53)	3.194(7)
Cs(2)-O(12d)	2.94(1)	Cs(5)-O(21e)	3.081(6)
Cs(2)-O(13d)	3.41(1)	Cs(5)-O(22e)	3.271(8)
Cs(3)-O(2w)	3.28(2)	Cs(6)-O(6w)	3.31(1)
Cs(3)-O(3w)	3.18(1)	Cs(6)-O(7w)	3.07(2)
Cs(3)-O(2)	3.17(1)	Cs(6)-O(1wf)	3.66(2)
Cs(3)-O(3)	3.22(1)	Cs(6)-O(52)	3.16(1)
Cs(3)-O(53)	3.33(1)	Cs(6)-O(53)	3.59(1)
Cs(3)-O(22e)	3.06(1)	Cs(6)-O(32f)	3.08(1)
		Cs(6)-O(33f)	3.50(1)
		Cs(6)-O(13g)	3.25(1)
Cs(1)-O(3)-Cs(2)	87.3(2)	Cs(2)-O(13d)-Cs(6c)	112.2(2)
Cs(1)-O(32)-Cs(2)	79.8(2)	Cs(2)-O(32)-Cs(6c)	118.8(2)
Cs(1)-O(1w)-Cs(2)	88.7(5)	Cs(2)-O(1w)-Cs(6c)	105.9(5)
Cs(1)-O(3)-Cs(3)	99.4(2)	Cs(3)-O(22e)-Cs(4)	93.0(2)
Cs(1)-O(2w)-Cs(3)	96.0(3)	Cs(3)-O(3w)-Cs(4)	90.8(3)
Cs(1)-O(6wc)-Cs(5c)	98.2(2)	Cs(3)-O(22e)-Cs(5)	108.7(2)
Cs(1)-O(42c)-Cs(5c)	93.3(2)	Cs(3)-O(53)-Cs(5)	104.0(2)
Cs(1)-O(32)-Cs(6c)	92.6(2)	Cs(3)-O(53)-Cs(6)	118.2(2)
Cs(1)-O(6wc)-Cs(6c)	89.5(2)	Cs(4)-O(22c)-Cs(5)	96.5(2)
Cs(1)-O(1w)-Cs(6c)	89.1(7)	Cs(4)-O(43)-Cs(5)	99.3(2)
Cs(2)-O(3)-Cs(3)	96.3(2)	Cs(5)-O(52)-Cs(6)	88.5(2)

Table 6 contn.

Cs(2)-O(3w)-Cs(3)	92.7(3)	Cs(5)-O(53)-Cs(6)	82.5(2)
Cs(2)-O(12d)-Cs(4)	108.4(2)	Cs(5)-O(6w)-Cs(6)	87.9(2)
Cs(2)-O(3w)-Cs(4)	98.0(3)		

*Symmetry codes: (a) = $-x, 1-y, 1-z$; (b) = $1-x, 1-y, 1-z$; (c) = $0.5-x, -0.5+y, +z$; (d) = $0.5+x, +y, 0.5-z$; (e) = $+x, 0.5-y, 0.5+z$; (f) = $0.5-x, 0.5+y, +z$; (g) = $1-x, 0.5+y, 0.5-z$.

L2 and L5 connect three cesium(I) ions according to the same mode observed in **1** [noted i in Scheme 2]; similarly, L1, L3, L4 and L6 connect three different cesium(I) ions each as well, but in the four novel fashions noted vii, viii, ix and x in Scheme II, respectively

A Pd-bound carboxylate-oxygen atom [O(21) and O(31)] is involved in the coordination with a cesium(I) cation only in the case of L3 and L4, indicating that the oxamate outer-oxygen atoms are basically responsible for the anion-cation connections in **4**. Nine of them act as bridges toward either two [O(12), O(13), O(42), O(43) and O(52)] or three [O(3), O(22), O(32), and O(53)] alkaline cations, adopting thus either bis- or trimonodentate bridging modes, respectively. The remaining oxamate oxygens involved in the coordination with the univalent cations [O(2), O(21), O(31) and O(33)] are all just monodentate (see Figure 18).

The surrounding of the six crystallographically-independent cesium(I) ions in **4** is shown in Figure 19. They are bound to either six [Cs(1), Cs(3) and Cs(4)], seven [Cs(2) and Cs(5)] or eight [Cs(6)] atoms from oxamate ligands and water molecules, the values of the Cs-O_{oxamate} and Cs-O_w distances varying in the ranges 2.94(1)-3.59(1) and 2.62(2)-3.66(2) Å, respectively (see Table 6). Moreover, each cesium(I) cation interacts with a directly connected or anyhow vicinal bis(oxamato)palladate(II) units through single cation- π contacts, with a cation-to-ring centroid distance of about 3.4 Å in each case. This is especially interesting since cation- π interactions in the presence of cesium(I) ions are not as well documented in the literature as those involving e.g. lithium(I), sodium(I), potassium(I) or rubidium(I) ions.^{43,44}

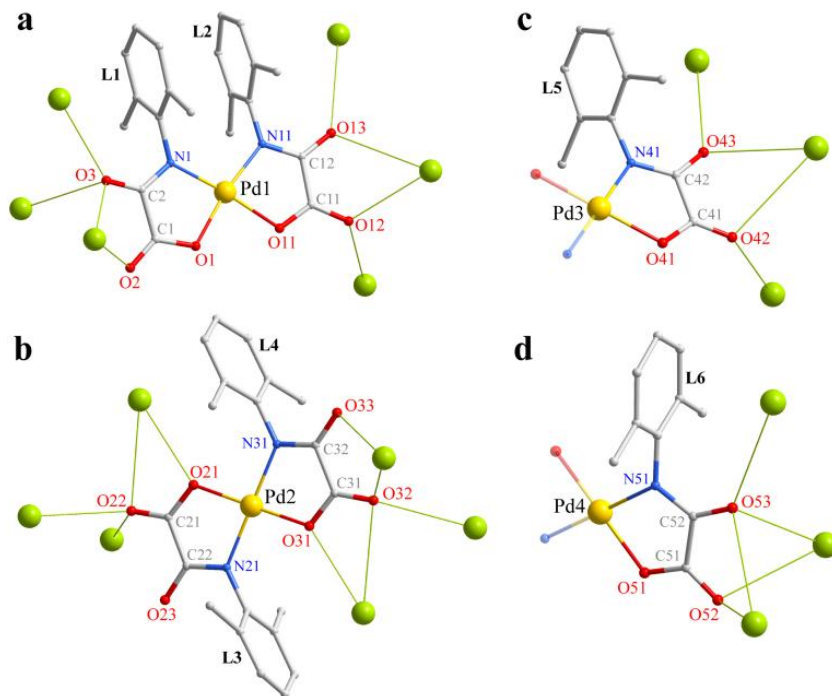


Figure 18. Views of the six crystallographically-independent oxamate ligands (L1-L6) in **4**, together with their cesium(I) linking. O(3), O(12), O(13), O(22), O(32), O(42), O(43), O(52) and O(53) are the bridging oxygen atoms. Color codes: Pd, yellow; Cs, green; C, grey; N, blue; O, red.

Taking into account the latter interaction and also the weakest Cs-O bonds [3.41(1), 3.59(1), 3.417(7), 3.59(1), 3.50(1) and 3.66(1) Å for Cs(2)-O(13d), Cs(4)-O(4w), Cs(5)-O(42), Cs(6)-O(53), Cs(6)-O(33f) and Cs(6)-O(1wf), respectively; symmetry code: (d) = $-0.5+x, +y, 0.5-z$; (f) = $0.5-x, 0.5+y, +z$], three of the six univalent cations [Cs(1), Cs(3) and Cs(4)] are seven-coordinate, their distorted surrounding being defined by either three carboxylate-oxygen atoms from three different oxamate ligands plus three water molecules and a phenyl ring centroid [at Cs(1) and Cs(4)] or four carboxylate-oxygen atoms from three different oxamate ligands plus two water molecules and a phenyl ring centroid [at Cs(3)].

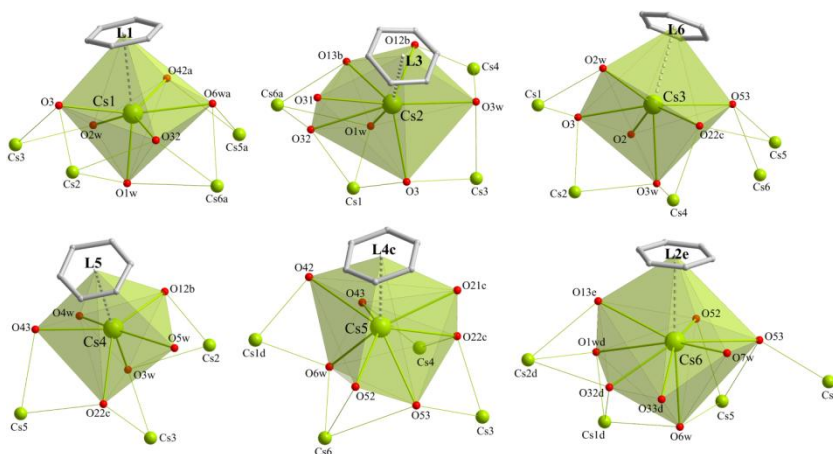


Figure 19. View of the surroundings of the six crystallographically-independent cesium(I) cations in **4**. For the sake of clarity, only the phenyl ring of the corresponding dimethylphenyloxamate ligand is shown where the cation- π type interactions occur (dashed lines) [symmetry codes (a)-(g) are those reported in Table 6].

Similarly, Cs(2) and Cs(5) are eight-coordinate in a rather distorted geometry built up by either five carboxylate-oxygen atoms from three different oxamate ligands plus two water molecules and a phenyl ring centroid [at Cs(2)], or six carboxylate-oxygen atoms from three different oxamate ligands and just one water molecule plus a phenyl ring centroid [at Cs(5)]. Finally, the Cs(6) ion is nine-coordinate and its fairly distorted coordination surrounding is defined by five carboxylate-oxygen atoms from three different oxamate ligands plus three water molecules and a phenyl ring centroid (see Figure 19).

Seven water molecules found in the asymmetric unit of **4** are coordinated to cesium(I) cations and they act either as bridges [O(1w), O(2w) and O(3w) and O(6w)] or as terminal ligands [O(4w), O(5w) and O(7w)]. O(1w), O(3w) and O(6w) connect three cations each one, while O(2w) adopts a more common bis-monodentate bridging mode (see Figure 19).

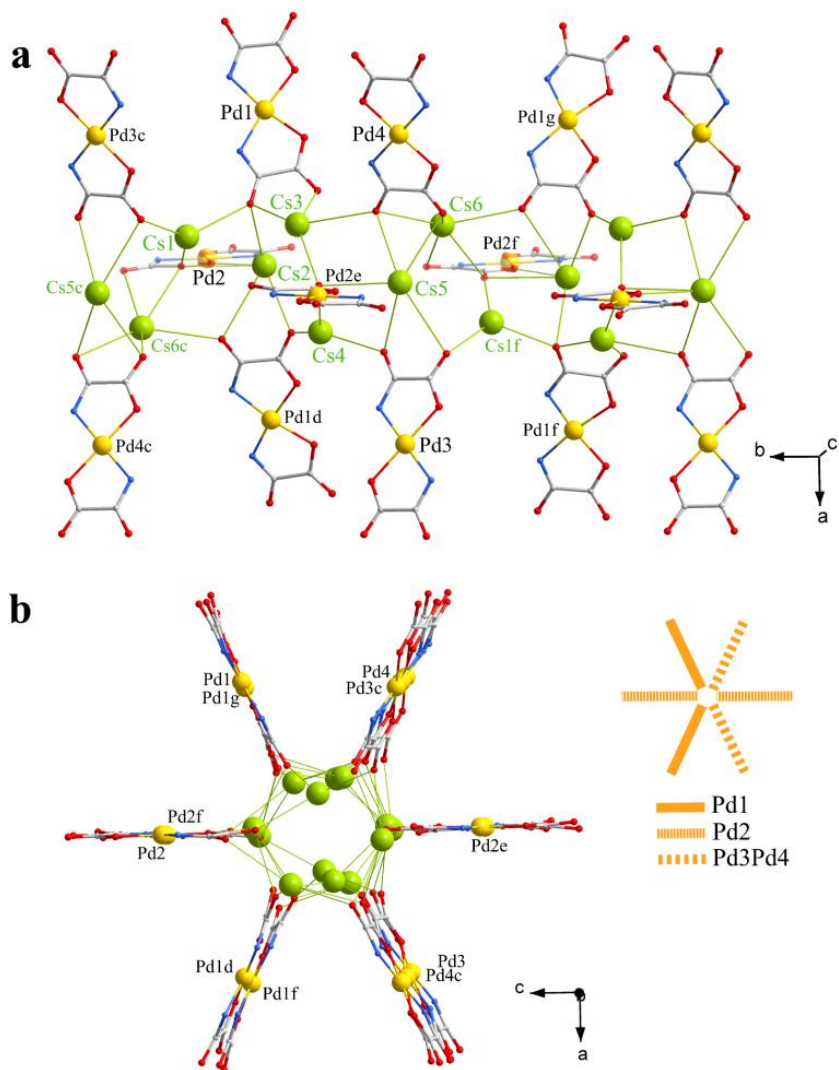


Figure 20. A fragment of the crystal packing in **4** showing the chain arrangement of the cesium(I) cations running along the crystallographic *b* axis together with their neighbouring bis(oxamato)palladate(II) complexes (the 2,6-dimethylphenyl rings on the ligands and the water molecules are omitted for clarity): (a) side view; (b) view down to the crystallographic *b* axis; the inset on the right highlights the regular disposition of just Pd(1)-, Pd(2)- or alternate Pd(3)/Pd(4)-bearing complexes along precise directions. Color codes: Pd, yellow; Cs, green; C, grey; N, blue; O, red. [Symmetry codes: (a) = $0.5-x, -0.5+y, +z$; (b) = $-0.5+x, +y, 0.5-z$; (c) = $+x, -0.5-y, 0.5+z$; (d) = $0.5-x, 0.5+y, +z$; (e) = $1-x, 0.5+y, 0.5-z$].

Pillared 1D arrays of cesium(I) ions and oxygen atoms running along the crystallographic *b* axis arise in **4** from a combination of the Cs-O_{oxamate} and Cs-O_w connections (Figure 20a). Similarly to what is observed in **1**, these are well separated from each other by means of the complex anions, which act as spacers (Figures 20a and 21), revealing that the intricate 3D array of alkaline cations-oxygen atoms observed in **2** and **3** remains a peculiarity only of that network topology. The metal-metal distances between directly interconnected cesium(I) ions within the {Cs₆O_x}_n motif along the crystallographic *b* axis in **4** are in the range 4.128(1)–5.937(1) Å [Cs(1)··Cs(2) = 4.128(1), Cs(1)··Cs(3) = 4.721(2), Cs(1)··Cs(5c) = 4.669(1), Cs(1)··Cs(6c) = 4.467(1), Cs(2)··Cs(3) = 4.647(1), Cs(2)··Cs(4) = 4.784(1), Cs(2)··Cs(6c) = 5.522(1), Cs(3)··Cs(4) = 4.465(1), Cs(3)··Cs(5c) = 5.142(1), Cs(3)··Cs(6c) = 5.937(1), Cs(4)··Cs(5) = 4.757(1) and Cs(5)··Cs(6) = 4.481(1) Å; symmetry code: (c) = 0.5-*x*, -0.5+*y*, +*z*] (see Figure 19).

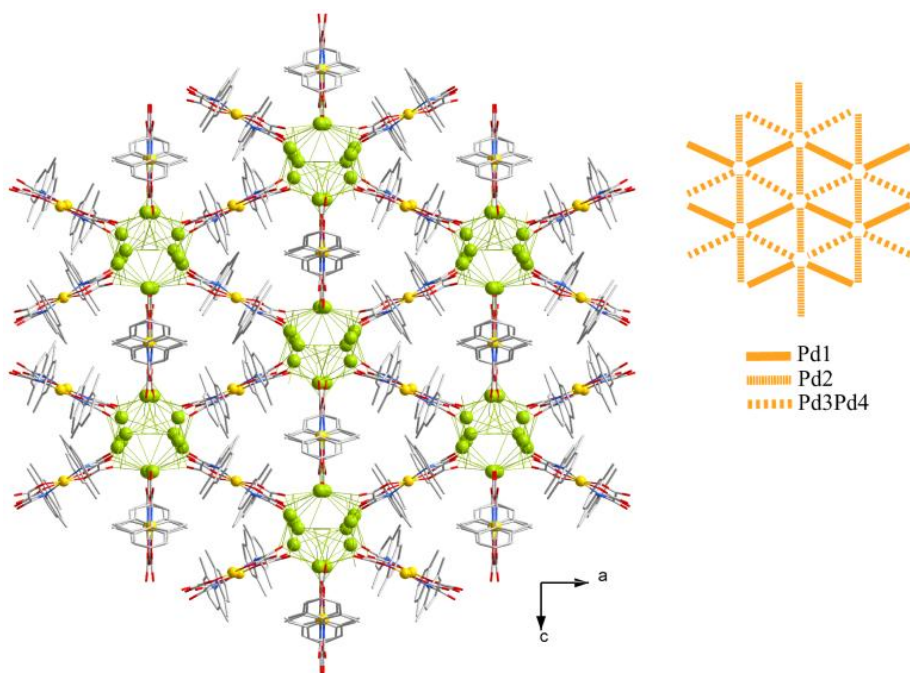


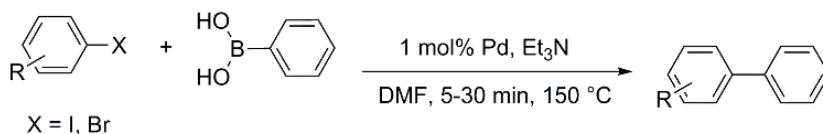
Figure 21. View of a fragment of the crystal packing of **4** along the crystallographic *b* axis and of its schematic representation after Figure 20b. The H-atoms of the ligands and water molecules are omitted for clarity. Color code: Pd, yellow; Cs, green; C, grey; N, blue; O, red.

The bis(oxamato)palladate(II) complexes anchored to the one-dimensional array of hydrated cesium(I) cations are regularly disposed along six hexagonal directions with the peculiar alternation scheme indicated in Figure 20b. As shown in Figure 21, this motif expands in the three-dimensional space defining trigonal hydrophobic and hexagonal hydrophilic cavities in the direction of the crystallographic *b* axis, the latter ones hosting the pillars of cesium(I) cations

II.4. Catalytic properties

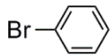






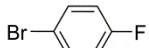
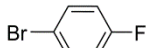
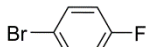
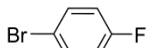
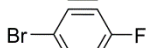
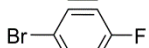
The four compounds $\{[\text{Na}(\text{H}_2\text{O})]_2\text{trans}-[\text{Pd}^{\text{II}}(2,6\text{-Me}_2\text{pma})_2]\}_n$ (**1**), $\{[\text{K}_4(\text{H}_2\text{O})_3]\text{cis}-[\text{Pd}^{\text{II}}(2,6\text{-Me}_2\text{pma})_2]_2\}_n$ (**2**), $\{[\text{Rb}_4(\text{H}_2\text{O})_3]\text{cis}-[\text{Pd}^{\text{II}}(2,6\text{-Me}_2\text{pma})_2]_2\}_n$ (**3**) and $\{[\text{Cs}_6(\text{H}_2\text{O})_7]\text{trans}-[\text{Pd}^{\text{II}}(2,6\text{-Me}_2\text{pma})_2]_2\text{cis}-[\text{Pd}^{\text{II}}(2,6\text{-Me}_2\text{pma})_2]\}_n \cdot 3n\text{H}_2\text{O}$ (**4**) are found to catalyse the arylation of phenylboronic acid with aryl halides referred to as Suzuki reaction in dimethylformamide (DMF) as solvent and in the presence of triethylamine (Et_3N) as a base at 150 °C without further promoting salt additive as performed for other palladium species that catalyze carbon-carbon cross-coupling reactions (see further information about the procedure in Appendix A).^{45–48} The formation of the biaryl coupling product, under homogenous catalytic conditions, is predominant (yields up to 99%, TON up to 99).

Table 7. Suzuki reaction of aryl halides and phenyl boronic acid in DMF^a



Entry ^a	Aryl halide	Compound	Time (min)	Yield (%) ^b	TON ^c	TOF ^d (h ⁻¹)
1		1	5	99	99	1188
2		2	5	95	95	1140
3		3	5	88	88	1056
4		4	5	94	94	1128
5		$[\text{Pd}_3(\text{OAc})_6]$	5	25	25	300
6		$[\text{PdCl}_2(\text{PPh}_3)_2]$	5	22	22	264
7		1	15	35	35	140
8		2	15	35	35	140
9		3	15	37	37	148
10		4	15	40	40	160
11		$[\text{Pd}_3(\text{OAc})_6]$	20	17	17	51

Table 7 contn.

12		$[\text{PdCl}_2(\text{PPh}_3)_2]$	20	29	29	87
13		1	30	53	53	106
14		2	30	60	60	120
15		3	30	70	70	140
16		4	30	70	70	140
17		$[\text{Pd}_3(\text{OAc})_6]$	30	45	45	90
18		$[\text{PdCl}_2(\text{PPh}_3)_2]$	30	45	33	66
19		1	15	44	44	176
20		2	15	43	43	172
21		3	15	40	40	160
22		4	15	53	53	212
23		$[\text{Pd}_3(\text{OAc})_6]$	20	23	23	69
24		$[\text{PdCl}_2(\text{PPh}_3)_2]$	20	34	34	102

^aReactions were performed using 0.5 mmol aryl halide, 0.75 mmol phenyl boronic acid, 1 mmol% Pd, 1.5 mmol Et₃N in DMF at 150 °C. ^bYields were determined by GC using perfluorotributylamine (PFTBA) as the internal standard. ^cTON = Turnover number. ^dTOF = Turnover frequency.

Well known commercially available precatalysts, namely dichloro bis(triphenylphosphine)palladium(II) $[\text{PdCl}_2(\text{PPh}_3)_2]$ and the trinuclear palladium(II) acetate $[\text{Pd}_3(\text{OAc})_6]$ were used for comparative properties. They promote the cross-coupling iodobenzene with phenylboronic acid with low yields of 22 and 25% respectively (Table 6, entry 5-6), during the same time recorded for the catalytic performance of compounds **1** and **2-4**. It deserves to be noted that the trinuclear $[\text{Pd}_3(\text{OAc})_6]$ complex was also relatively less active than **1** and **2-4** in the cross-coupling of bromobenzene with phenylboronic acid (17% yield entry 11) with the clear formation of insoluble palladium black during and after the completion of the catalytic reactions, as visually observed.

Interestingly, **1** and **2-4** proved to be efficient (pre)catalysts under the described homogeneous conditions without clear formation of inactive palladium black⁴⁹⁻⁵³ throughout the catalytic reaction (Figure 21). This observation points out the fact that the coupling reaction does not occur on the surface of inactive palladium black as found for many commercially available and phosphine-containing palladium catalysts generated *in situ*.^{54,55}

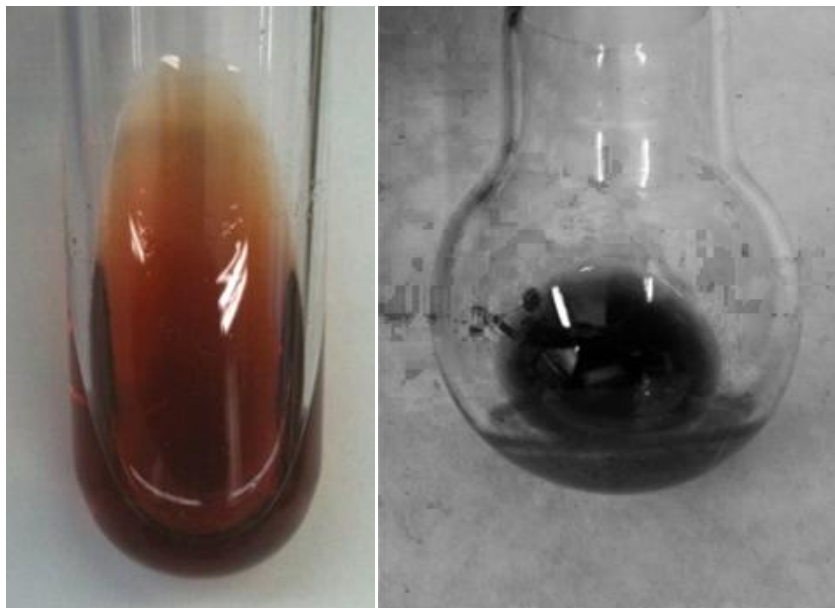


Figure 21. Samples of the Suzuki coupling reaction of iodobenzene and phenylboronic acid in DMF at 150 °C after 5 min, catalyzed by **2** (left) and by $[\text{Pd}_3(\text{OAc})_6]$ (right).

The presence of Et_3N as base was found to be crucial in the fast promotion of the catalytic reaction. Its replacement by another base such as K_2CO_3 does not help in promoting the studied catalytic reactions. Attempts to perform the arylation of aryl halides at temperatures lower than 150 °C resulted in significant reduction of the corresponding yields. It appears that under such conditions [Et_3N as a base and at 150 °C], the formation of the active catalytic palladium species from complexes **1** and **2-4** is quite favored.

The formation of the unsymmetrical coupling product was predominant with or without the formation of the homocoupling product. The only detected side product arises from deboronation reaction of phenylboronic acid.

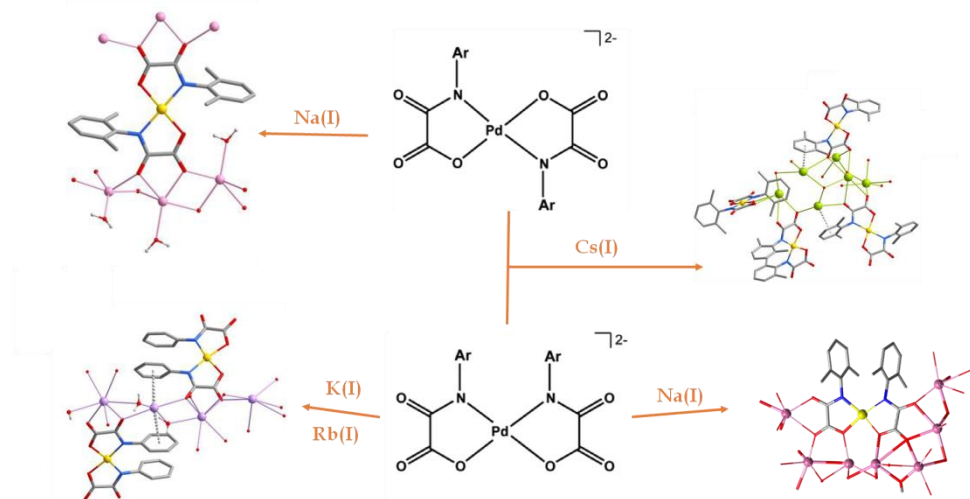
The presence of alkaline cations in **1** and **2-4** appears to be of beneficial effect on the thermal stability of the formed palladium catalytic species, which highly influences the carbon-carbon cross-coupling reaction at higher temperatures and so the achievement of higher catalytic activities.⁵⁶ Their immobilization on adequate supports could lead to their recovery and reuse for further catalytic cycles and would allow to compare them with other recyclable polymeric heterogeneous palladium(II) precatalysts, mainly those featuring metal-organic framework structures (MOFs).⁵⁷⁻⁵⁹

Regarding the catalytic palladium species involved in the catalytic cross-coupling reaction between aryl halides and phenylboronic acid, it appears that the formation of individual palladium nanoparticles takes place being stabilized by the alkaline cations present in the catalytic medium.^{49,60} The use of these well-defined palladium(II) precatalysts in very low amount (1 mol% Pd atom) is very interesting. Whether the assembly of bis(oxamato)palladate(II) species is kept or lost in solution during the catalytic process and the employment of very low loading Pd(II) precatalyst (1 mol%) together with the immobilization of complexes **1** and **2-4** on silica-support for optical monitoring (based on color changes) are issues still under investigation by us.

II.5. Conclusions

A new generation of stable functional palladium(II)-oxamate complexes has been presented herein which are active for carbon-carbon cross-coupling reaction as Suzuki.

These complexes, that can be synthesized in a straightforward manner have as added values the facts of being environmentally friendly and containing highly versatile and very cheap ligands. These have been isolated in the solid state as the alkaline salts $\{[\text{Na}(\text{H}_2\text{O})]_2\text{trans-}[\text{Pd}^{\text{II}}(2,6\text{-Me}_2\text{pma})_2]\}_n$ (**1**), $\{[\text{Na}_4(\text{H}_2\text{O})]_2\text{cis-}[\text{Pd}^{\text{II}}(2,6\text{-Me}_2\text{pma})_2]\}_n$ (**1'** traces), $\{[\text{K}_4(\text{H}_2\text{O})_3]\text{cis-}[\text{Pd}^{\text{II}}(2,6\text{-Me}_2\text{pma})_2]_2\}_n$ (**2**), $\{[\text{Rb}_4(\text{H}_2\text{O})_3]\text{cis-}[\text{Pd}^{\text{II}}(2,6\text{-Me}_2\text{pma})_2]_2\}_n$ (**3**) and $\{[\text{Cs}_6(\text{H}_2\text{O})_7]\text{trans-}[\text{Pd}^{\text{II}}(2,6\text{-Me}_2\text{pma})_2]_2\text{cis-}[\text{Pd}^{\text{II}}(2,6\text{-Me}_2\text{pma})_2]\}_n \cdot 3n\text{H}_2\text{O}$ (**4**) by using either sodium(I), potassium(I), rubidium(I) or cesium(I) as assembling cations.



Scheme 3. *Trans-cis* isomerism in the bis(oxamato)palladate(II) complexes with alkaline counterions.

A *trans-cis* isomerism was observed within the series (see Scheme 3), with sodium(I) ions affording prevalently the *trans* isomer, potassium(I) or rubidium(I) ions preferentially precipitating the *cis* isomer while the cesium(I) ions promote the co-crystallization of both stereoisomers. Various attempts to isolate the *trans* isomer with K(I) or Rb(I) cations failed, whereas the *cis* isomer could be noted (although in

traces) in the presence of Na(I) cations. The cation- π interactions^{41,42} stabilizing the peculiar crystal packing observed in the potassium (**2**) or rubidium (**3**) salts may be involved in the stereoisomer discrimination at the solid state level. Note that such interactions are not present in the *cis* form with sodium cations (**1'**), somehow supporting this hypothesis. At the moment, we do not have means to hypothesize whether or not potassium(I) and rubidium(I) cations could even exert a templating effect toward the formation of the *cis* over the *trans* stereoisomer in this type of complexes, perhaps through their capability of establishing peculiar cation- π interactions with the chosen ligands. In any case, considering the isolation of both the *trans* and *cis* isomers in the solid state when employing Na(I) as counter ion, as well as co-crystallization of the two isomers in the presence of the cesium(I) ion, the concomitant existence of both isomers in solution cannot be ruled out, whatever the precipitating cation. Concerning cation- π type interactions, they occur in the solid state of **4** as well, although devoid of the sandwich-like typology observed in **2** and **3**. It deserves to be noted that the ratio between the *cis* and *trans* stereoisomers in **4** is 1:2. This feature highlights the possibility of a true relationship between cation- π interactions and stereochemistry in such [PdL₂] systems with symmetrically substituted phenyloxamate ligands. In any case, as far as we know, complexes **1'** and **2-4** reported herein are unique examples of the *cis* stereochemistry in oxamate-based mononuclear compounds, regardless of the coordinating metal ion.

As far as the catalytic activity is concerned, it seems to be significantly influenced by neither a change in the alkaline counter cation nor the stereochemistry. The catalytic activity is moderate to high with the advantages that very small amounts of palladium precatalyst (1 mol% Pd atom) are employed and non-catalytic palladium black occurs neither throughout the reaction nor after its completion. The presence of alkaline cations appears to prevent the catalyst deactivation and it allows maintaining high activities in many instances.

Part II

Halogen derivatives of bis-(*N*-substituted oxamato)palladate(II) complexes: structural and supramolecular features

II.6. Halogen bonding as supramolecular tool in crystal engineering

Among the different areas of chemical sciences, the synthesis of tailor-made mononuclear complexes to be employed as building ligands in the so-called *metal-as-ligand strategy* has experienced a fast growth during the last decades. Two main reasons accounts for this exponential increasing interest:

(i) the large variety of supramolecular motifs that can be achieved contributing to the development of the crystal engineering

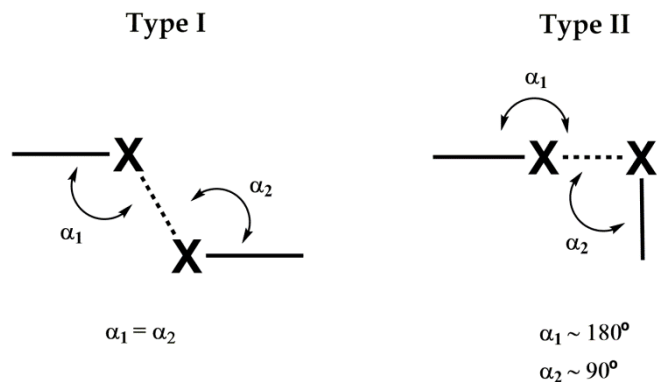
(ii) and the possibility to build molecular architectures with desired properties based on the great versatility of this strategy.⁶¹⁻⁷²

A careful selection of ligands, metal centers, spacers and reaction conditions are required in order to allow the preparative chemist to gain some control over the topology of the resulting frameworks.^{67,68} Furthermore, since the crystal packing may be defined based on the investigation of the concerted effects of the weak intermolecular interactions on the overall crystal structure, a careful inspection of the expected assembling interactions, depending on the metal-ligand features could be used as design elements in crystal engineering.^{61,73-76}

Since the late 1990s, it was evident that other than hydrogen bonds, supramolecular halogen atom interactions could be used as robust design elements in crystal engineering.⁷⁸⁻⁸⁴ The halogen bond is an attractive interaction in which an electrophilic halogen atom approaches a negatively polarized species.

As it is shown in Scheme 4, such contacts are classified into two groups, symmetrical (type I) and bent (type II), which are both influenced by geometric and chemical considerations.⁸⁵ These interactions include halogen··halogen ($X\cdots X$) and halogen··heteroatom interactions ($X\cdots B$). Many $X\cdots X$ and almost all $X\cdots B$ contacts can be classified as halogen bonds.

In terms of crystal design, halogen bonds offer a unique opportunity in the strength, atom size and interaction gradation; this may be used in the design and structural modularity in which an entire crystal structure is defined as a combination of modules formed on the basis of the intermediate strength of a halogen bond.⁸⁶



Scheme 4. Type I and Type II X...X contacts (X = halogen atom).⁷⁷

These intermolecular X...X contacts can be also highly relevant in magnetic studies. In this respect, a good number of magneto-structural studies on mononuclear $[\text{ReX}_6]^{2-}$ complexes have shown the occurrence of significant through space magnetic interactions between the paramagnetic Re(IV) ions which are mediated by Re-X...X-Re contacts (Chart 1), the halogen-halogen separation being strongly dependent on the nature of the counteraction used.⁸⁷

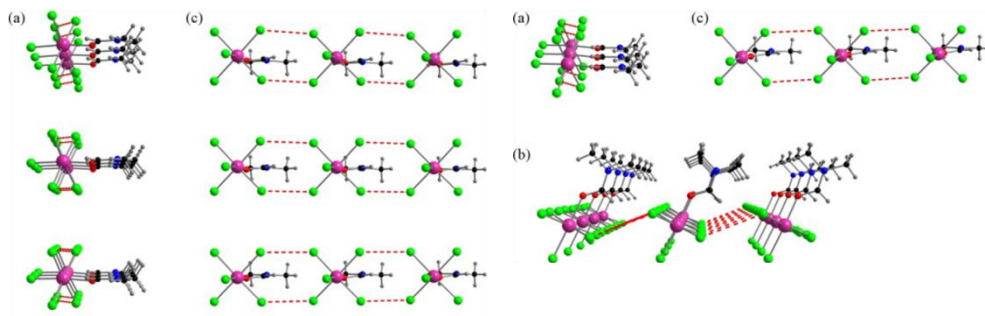


Chart 1. A projection view along the crystallographic *a* (a), *b* (b) and *c* axes (c) of the arrangements of the $[\text{ReCl}_5(\text{DMF})]^-$ anions in **B**. The shortest interionic Cl...Cl contacts between the $[\text{ReCl}_5(\text{DMF})]^-$ units are indicated by means of broken lines. The cations have been omitted for clarity.⁸⁷

II.7. Aim

The evidence of supramolecular halogen bonds has played an important role in crystal engineering and it has become a useful tool in the control of molecule assembling.

In order to check the possibilities offered by this supramolecular halogen...halogen interaction in our tailor-made bis(oxamato)palladate(II) complexes, a series of new *N*-4-phenyloxamate ligands ($X = F, Cl$ and Br) have been prepared and used to prepare the corresponding bis(oxamato)palladate(II) complexes. Their preparation, crystal growing, structural determination and deep analysis of their crystal packing are described in this Part II.

II.8. Synthesis and characterization

The general synthetic method for the preparation of proligands as ethyl esters (EtH-4-F-pma, EtH-4-Cl-pma, EtH-4-Br-pma) was carried out by following a previously reported procedure¹⁵ (see Appendix A).

Synthesis of complexes

A general synthetic method for the bis(*N*-substituted oxamate)palladate(II) complexes **5-7** is as follows: a methanolic solution of *n*-Bu₄NOH (1.0 M, 1.5 ml, 1.2 mmol) was added directly to a one-neck round flask suspension of the corresponding *N*-substituted oxamate proligand (0.6 mmol) in 10 mL of acetonitrile at 60 °C. Then, an aqueous solution of K₂[PdCl₄] (100 mg, 0.3 mmol) was added dropwise to the resulting solution and the reaction mixture was heated at 60 °C for 10 hours. The resulting mixture was filtered and the acetonitrile was removed under vacuum. Dichloromethane (5 mL) was added to extract the complex from the aqueous solution. The solution was stirred for 30 min and the organic layer was separated from the aqueous one. The solvent was removed under vacuum to afford a pale yellow solid, which was washed and dried with *n*-hexane for 24 hours under stirring, collected by filtration and dried under vacuum (**5a-7a**).

The recrystallization in water at room temperature afforded X-ray quality yellow prisms of **5-7** after 2-3 weeks.

Characterization of complexes

(*n*-Bu₄N)₂[Pd(**4-Fpma**)₂] (**5**). Yield: 92%. IR(KBr/cm⁻¹): 3423 (O-H), 2961, 2933, 2875 (C-H), 1671, 1655, 1619, 1586 (C=O). ¹H NMR (CDCl₃) δ (ppm): 0.90 – 0.94 (t, 33H, *n*-Bu₄N⁺), 1.24 – 1.46 (m, 45H, *n*-Bu₄N⁺), 2.93 – 2.99 (t, 22H, *n*-Bu₄N⁺), 6.63 – 6.66 (d, 4H, H_{aryl}), 7.27 – 7.30 (d, 4H, H_{aryl}). Anal. Calcd for C₄₈H₈₀F₂N₄O₆Pd (954 g/mol) (**5**): C 60.46, H 8.46, N 5.88. Found: C 61.24, H 9.66, N 5.96 %.

(*n*-Bu₄N)₂[Pd(4-Fpma)₂] (5a). Yield: 54%. IR(KBr/cm⁻¹): 3423 (O-H), 2961, 2933, 2875 (C-H), 1671, 1655, 1619, 1586 (C=O). ¹H NMR (CDCl₃) δ (ppm): 0.90 – 0.94 (t, 33H, *n*-Bu₄N⁺), 1.24 – 1.46 (m, 45H, *n*-Bu₄N⁺), 2.93 – 2.99 (t, 22H, *n*-Bu₄N⁺), 6.63 – 6.66 (d, 4H, H_{aryl}), 7.27 – 7.30 (d, 4H, H_{aryl}). Anal. Calcd for C₄₈H₈₀F₂N₄O₆Pd (5a): C 60.46, H 8.46, N 5.88. Found: C 61.24, H 9.66, N 5.96 %.

(*n*-Bu₄N)₂[Pd(4-Clpma)₂] · 4H₂O (6). Yield: 71%. IR(KBr/cm⁻¹): 3423 (O-H), 2961, 2930, 2874 (C-H), 1671, 1655, 1619, 1582 (C=O). ¹H NMR (CDCl₃) δ (ppm): 0.91–0.96 (t, 78H, *n*-Bu₄N⁺), 1.28 – 1.40 (m, 53H, *n*-Bu₄N⁺), 1.46 – 1.56 (m, 52H, *n*-Bu₄N⁺), 3.08 – 3.14 (t, 51H, *n*-Bu₄N⁺), 7.02 – 7.05 (d, 4H, H_{aryl}), 7.33 – 7.36 (d, 4H, H_{aryl}). Anal. calcd for C₄₈H₈₈Cl₂N₄O₁₀Pd (1058.52 g mol⁻¹) (6): C 54.46, H 8.38, N 5.29. Found: C 54.32, H 8.27, N 5.21%.

(*n*-Bu₄N)₂[Pd(4-Clpma)₂] (6a). Yield: 51%. IR(KBr/cm⁻¹): 3423 (O-H), 2961, 2930, 2874 (C-H), 1671, 1655, 1619, 1582 (C=O). ¹H NMR (CDCl₃) δ (ppm): 0.91–0.96 (t, 78H, *n*-Bu₄N⁺), 1.28 – 1.40 (m, 53H, *n*-Bu₄N⁺), 1.46 – 1.56 (m, 52H, *n*-Bu₄N⁺), 3.08 – 3.14 (t, 51H, *n*-Bu₄N⁺), 7.02 – 7.05 (d, 4H, H_{aryl}), 7.33 – 7.36 (d, 4H, H_{aryl}). Anal. Calcd for C₄₈H₈₀Cl₂N₄O₆Pd (6a): C 58.44, H 8.17, N 5.68. Found: C 58.82, H 9.09, N 5.70 %.

(*n*-Bu₄N)₂[Pd(4-Brpma)₂] · 4H₂O (7). Yield: 97%. IR(KBr/cm⁻¹): 3422 (O-H), 2961, 2933, 2874 (C-H), 1671, 1648, 1606, 1577 (C=O): ¹H NMR (CDCl₃) δ (ppm): 0.90 – 0.95 (t, 38H), 1.26 – 1.38 (m, 26H, *n*-Bu₄N⁺), 1.41 – 1.52 (m, 25H, *n*-Bu₄N⁺), 3.01 – 3.07 (t, 24H, *n*-Bu₄N⁺), 6.75 – 6.81 (t, 4H, H_{aryl}), 7.31 – 7.36 (m, 4H, H_{aryl}). Anal. calcd for C₄₈H₈₈Br₂N₄O₁₀Pd (1147.44 g mol⁻¹) (7): C 50.24, H 7.73, N 4.88. Found: C 50.11, H 7.65, N 4.79%.

(*n*-Bu₄N)₂[Pd(4-Brpma)₂] (7a). Yield: 47%. IR(KBr/cm⁻¹): 3422 (O-H), 2961, 2933, 2874 (C-H), 1671, 1648, 1606, 1577 (C=O). ¹H NMR (CDCl₃) δ (ppm): 0.90 – 0.95 (t, 38H), 1.26 – 1.38 (m, 26H, *n*-Bu₄N⁺), 1.41 – 1.52 (m, 25H, *n*-Bu₄N⁺), 3.01 – 3.07 (t, 24H, *n*-Bu₄N⁺), 6.75 – 6.81 (t, 4H, H_{aryl}), 7.31 – 7.36 (m, 4H, H_{aryl}). Anal. Calcd for C₄₈H₈₀Br₂N₄O₆Pd (7a): C 53.61, H 7.50, N 5.21. Found: C 54.43, H 8.66, N 5.39 %.

Further information about the characterization is given in Appendix A.

II.9. Results and discussion

X-ray structural determination. Single crystal X-ray diffraction data for 5-7 were collected at 296 K on a Bruker-Nonius X8-APEXII CCD area detector system using graphite-monochromated Mo-K α radiation ($\lambda = 0.71073 \text{ \AA}$), and processed through the SAINT reduction and SADABS absorption software. All the structures were solved by direct methods and subsequently completed by Fourier recycling using the SHELXTL-2013 software packages, then refined by the full-matrix least-squares refinements based on F^2 with all observed reflections. All structures, especially in **6**, show large thermal motion on chains of *n*-tetrabutylammonium as often found in other complexes containing this cation. All non-hydrogen atoms were refined anisotropically, except C38 and C48 in **6**. The hydrogen atoms on the phenyl-substituted oxamate ligand and on the tetra-*n*-butylammonium cations were included at geometrically calculated positions and refined using a riding model. The hydrogen atoms on water molecules in **6** and **7** were neither found nor calculated.

Crystal data and refinements conditions for 5-7 are summarized in Table 8, whereas selected bond lengths and angles and hydrogen bonds are listed from Tables 9 to 13, respectively.

Table 8. Crystal Data and Data Collection Parameters for 5-7

	5	6	7
Formula	C ₄₈ H ₈₀ N ₄ O ₆ F ₂ Pd	C ₄₈ H ₈₈ N ₄ O ₁₀ Cl ₂ Pd	C ₄₈ H ₈₈ N ₄ O ₁₀ Br ₂ Pd
Mr	953.56	1058.52	1147.44
Crystal	Monoclinic	Triclinic	Monoclinic
Space	<i>P</i> 2 ₁ / <i>c</i>	<i>P</i> -1	<i>P</i> 2 ₁ / <i>c</i>
<i>a</i> / Å	9.6448(7)	12.5224(9)	14.827(4)
<i>b</i> / Å	16.3141(12)	15.6996(11)	14.635(4)
<i>c</i> / Å	16.9067(13)	17.1433(13)	15.017(4)
α / °	90	65.551(3)	90
β / °	92.808(3)	69.815(4)	114.983(9)
γ / °	90	82.697(4)	90
<i>V</i> / Å ³	2657.0(3)	2830.8(4)	2953.8(13)
<i>Z</i>	2	2	2
<i>D_c</i> / g cm ⁻³	1.192	1.242	1.290
<i>T</i> / K	293(2)	293(2)	293
μ / mm ⁻¹	0.402	0.475	1.718
<i>F</i> (000)	1016	11128	1200
Reflections collected	34933	54404	27339
Independent reflections	5622	11951	5573
	[<i>R</i> (int) = 0.0507]	[<i>R</i> (int) = 0.0600]	[<i>R</i> (int) = 0.0615]
Data/restraints/parameters	5622/190 /281	11951/0/597	5573/242/309
Goodness-of-fit on <i>F</i> ²	1.094	1.000	1.045
Final <i>R</i> indices	<i>R</i> ₁ = 0.0294,	<i>R</i> ₁ = 0.0583,	<i>R</i> ₁ = 0.0433,
[<i>I</i> > 2σ(<i>I</i>)]	<i>wR</i> ₂ = 0.0855	<i>wR</i> ₂ = 0.1630	<i>wR</i> ₂ = 0.1189
<i>R</i> indices (all data)	<i>R</i> ₁ = 0.0422,	<i>R</i> ₁ = 0.0840,	<i>R</i> ₁ = 0.0554,
	<i>wR</i> ₂ = 0.1008	<i>wR</i> ₂ = 0.1878	<i>wR</i> ₂ = 0.1276
Largest diff. peak and hole / e Å ⁻³	0.390 and -0.570	0.947 and -0.438	0.867 and -0.927

$$R_1 = \sum(|F_o| - |F_d|) / \sum|F_o|. \quad wR_2 = \{\sum[w(F_o^2 - F_c^2)^2] / \sum[w(F_o^2)^2]\}^{1/2}$$

Table 9. Selected bond lengths (Å) and angles (deg) for 5*

Pd(1)-O(1)	1.9989(14)	Pd(1)-N(1)	2.0411(16)
O(1)-Pd(1)-O(1a)	180.0	O(1a)-Pd(1)-N(1)	98.33(6)
O(1)-Pd(1)-N(1)	81.67(6)		

*Symmetry transformations used to generate equivalent atoms:

(a) = -*x*+1, -*y*+1, -*z*.

Table 10. Selected bond lengths (Å) and angles (deg) for **6***

Pd(1)-O(1)	2.008(3)	O(4)-Pd(2)	2.007(3)
Pd(1)-N(1)	2.013(3)	N(2)-Pd(2)	2.013(3)
O(1a)-Pd(1)-O(1)	180.0	O(4b)-Pd(2)-N(2)	98.40(14)
O(1)-Pd(1)-N(1a)	98.97(12)	O(4)-Pd(2)-N(2)	81.60(14)
O(1)-Pd(1)-N(1)	81.03(12)	O(4)-Pd(2)-N(2b)	98.39(14)
N(1a)-Pd(1)-N(1)	180.0	N(2)-Pd(2)-N(2b)	180.0(2)
O(4b)-Pd(2)-O(4)	180.0		

*Symmetry transformations used to generate equivalent atoms:

(a) = $-x+2, -y, -z+1$. (b) = $-x+2, -y, -z+2$.

Table 11. Selected bond lengths (Å) and angles (deg) for **7***

Pd(1)-O(1)	2.008(2)	Pd(1)-N(1)	2.021(2)
O(1a)-Pd(1)-O(1)	90.30(12)	O(1)-Pd(1)-N(1)	81.52(10)
O(1a)-Pd(1)-N(1)	171.30(9)	N(1)-Pd(1)-N(1a)	106.80(14)

*Symmetry transformations used to generate equivalent atoms:

(a) = $-x+1, y, -z+1/2$.

Table 12. Hydrogen bonds (Å) for **6***

O(1W)··O(3)	2.853(4)	O(2W)··O(2)	2.915(4)
O(1W)··O(3c)	2.900(4)	O(2W)··O(3W)	2.782(4)
O(1W)··O(2W)	2.660(4)	O(3W)··O(3Wd)	2.817(4)

*Symmetry transformations used to generate equivalent atoms: (c) = $1-x, -y, 1-$

z; (d) = $1-x, 1-y, 1-z$.

Table 13. Hydrogen bonds (Å) for **7***

O(1W)···O(2)	2.840(4)	O(1W)···O(2W)	2.859(4)
O(1W)···O(1Wb)	2.893(4)	O(2W)···O(3)	2.817(4)
O(2W)···O(2Wb)	2.840(4)		

*Symmetry transformations used to generate equivalent atoms: (b) = $-x, y, -z+1/2$.

Description of the structures. Compounds **5** and **7** crystallize in the monoclinic space groups $P2_1/c$ and $P2/c$, respectively, with half a molecule in the asymmetric unit, the second half being generated by the crystallographic inversion centre, while **6** crystallizes in the triclinic $P-1$ space group with two half a molecule in the asymmetric unit. Each structure consists of $[\text{Pd}(4\text{-Xpma})_2]^{2-}$ anions and $n\text{-Bu}_4\text{N}^+$ counterions (**5-7**) plus crystallization water molecules (**6-7**) (see Figures 22 - 24). The complex anions in **5** are grouped into pairs through weak $\text{F}\cdots\text{O}$ type interactions (Figure 25), these units being well separated from each other by the bulky organic cations (Figure 26). On the contrary, the bis(oxamato)palladate(II) species in **6** are assembled into a pretty supramolecular three-dimensional structure by means of an extended network of hydrogen bonds and chloro···chloro interactions (Figures 27-30). The complex anions in the case of **7**, are interconnected through hydrogen bonds involving four membered rings of water molecules leading to supramolecular anionic chains which grow along the crystallographic a axis (Figures 31 - 33).

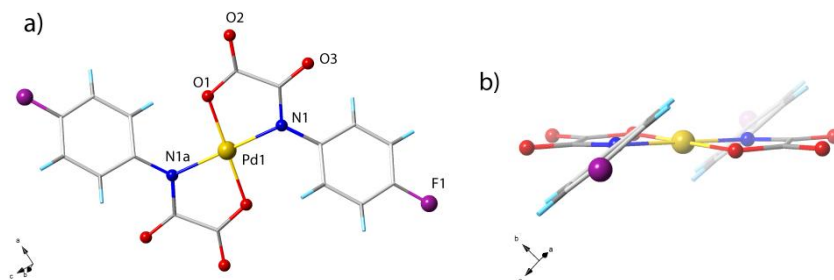


Figure 22. Top (a) and side (b) views of the anionic $\text{trans-}[\text{Pd}(4\text{-Fpma})_2]^{2-}$ complex in **5** [symmetry code: (a) = $-x+1, -y+1, -z$].

The structures of **5** and **6** have in common the presence of the *trans*-[Pd(4-Xpma)₂]²⁻ anions [X = F (**5**) or Cl (**6**)] where the palladium(II) ion is four-coordinate with two amidate-nitrogen [N1 and N1a] and two carboxylate-oxygen atoms [O1 and O1a] building a slightly distorted square-planar surrounding. The reduced bite angle of the chelating oxamate [81.67(6)° (**5**) and 81.0(1)° (**6**)] accounts for the deviations from the ideal geometry.

The Pd(II) ion and the atoms building its surrounding lie exactly on a plane for symmetry reasons. The Pd-N/Pd-O bond lengths are 2.041(2)/1.999(2) (**5**) and 2.013(3)/2.008(2) Å (**6**), values which compare well with those found in other oxamato-containing palladium(II) complexes.^{35,36,40,88–90}

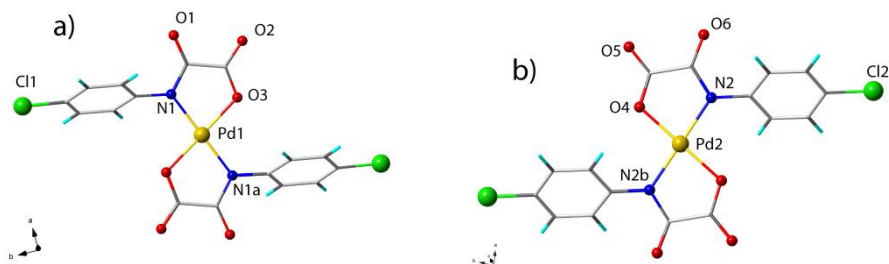


Figure 23. Perspective views of the two crystallographically independent anionic *trans*-[Pd(4-Clpma)₂]²⁻ complexes in **6** [symmetry codes: (a) = $-x+2, -y, -z+1$; (b) = $-x+2, -y, -z+2$].

The plane at the Pd(II) ion and the mean plane of the oxamate group are almost coplanar [the values of the dihedral angle between these two planes (φ) are 4.70(4)° (**5**) and 4.0(2)° and 0.5 (2)° (**6**) for Pd1 and Pd2, respectively]. Focusing on the phenyloxamate ligand, the dihedral angle between the 4-substituted phenyl ring and the mean plane of the oxamate group are 36.71(3) (**5**) and 62.3(3)° and 46.9(2) (**6a**), values which are not so close to orthogonality as those observed in $\{[\text{Na}(\text{H}_2\text{O})_2\text{trans}-[\text{Pd}(2,6\text{-Me}_2\text{pma})_2]]_n\}$ [$\varphi = 75.79(4)$],⁴⁰ but the compare well the ones found in $(n\text{-Bu}_4\text{N})_2\text{trans}-[\text{Pd}(2\text{-Mepma})_2] \cdot 4\text{H}_2\text{O}$ and $(n\text{-Bu}_4\text{N})_2\text{trans}-[\text{Pd}(4\text{-Mepma})_2] \cdot 4\text{H}_2\text{O}$ [$\varphi = 51.1(1)$ and $52.2(1)$ °, respectively].⁸⁹

The $[\text{Pd}(4\text{-Brpma})]^{2-}$ mononuclear units in the structure of **7** exhibit a *cis* conformation. However; the Pd(II) environment is practically that of **5** and **6** being four-coordinate with two amidate nitrogen and two carboxylate-oxygen atoms from the two *cis*-oxamate ligands and building a slightly distorted square-planar $[\text{NON}'\text{O}']$ surrounding. Again, the reduced bite of the chelating oxamate $[81.5(1)^\circ]$ accounts for the deviations from the ideal geometry. The Pd(II) ion lies practically in the $\text{NON}'\text{O}'$ square plane.

The Pd-N and Pd-O bond lengths $[2.021(2)/2.008(2) \text{ \AA}]$ compare well with those found in **5** and **6** and in the already mentioned literature species.^{35,36,40,88–90}

The square plane at the Pd(II) and the mean plane of the chelating oxamate group in the *cis*- $[\text{Pd}^{\text{II}}(4\text{-Brpma})_2]^{2-}$ units are very close to coplanarity as observed in **5** and **6** [the value of the dihedral angle between these two planes (φ) is $0.4(1)^\circ$ the one between the 4-substituted phenyl ring and the mean plane of the oxamate group is $57.00(2)^\circ$]. Intramolecular face-to-face stacking interactions are clearly established in **7** between the phenyl rings on each chelating ligand of the *cis*- $[\text{Pd}^{\text{II}}(4\text{-Brpma})_2]^{2-}$ unit. The steric hindrance between the Br substituents at each ring induces an evident nonparallel arrangement, and in fact the two 4-substituted phenyl ring forming a dihedral angle of $14.2(1)^\circ$.

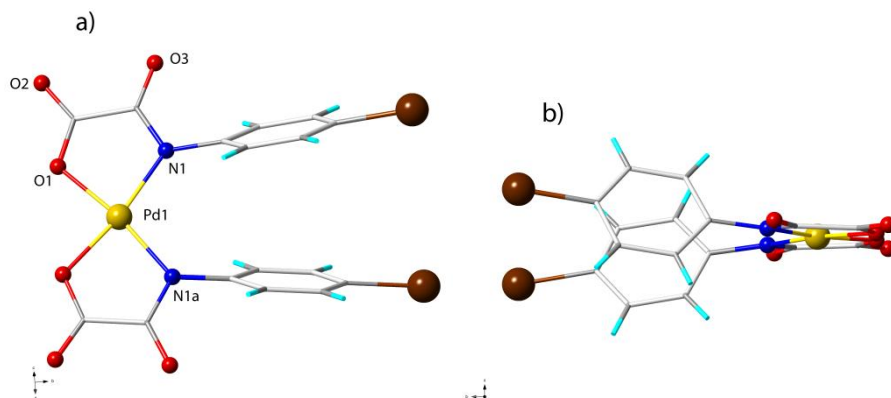


Figure 24. Top (a) and side (b) views of the anionic complex *cis*- $[\text{Pd}(4\text{-Brpma})_2]^{2-}$ in **7** [symmetry code: (a) = $-x+1, y, -z+1/2$].

A detailed description of the different crystal packing of **5-7** is given in the following section.

Crystal packing of $(n\text{-Bu}_4\text{N})_2\text{trans}[\text{Pd}(\text{4-F-pma})_2]$ (5**).** No insights of halogen bonding in the crystal packing of **5** are present, in agreement with the report from previous work.⁸⁵ The bis(oxamato)palladium(II) units are well separated from each other due to the presence of bulky $(n\text{-Bu}_4\text{N})^+$ cations and only a very weak $\text{F}\cdots\text{O}$ interaction (of 4.19 Å) related to the shortest $\text{Pd}(1)\cdots\text{Pd}(1b)$ separation of 9.645(3) Å [symmetry code: (b) = $-x, y, z$] (Figures 25 and 26a) occurs in **5**. Furthermore, very weak $\text{F}\cdots\text{H-C}$ interactions involving $(n\text{-Bu}_4\text{N})^+$ cations are present [shortest $\text{F}\cdots\text{H-C}$ and $\text{F}\cdots\text{C}$ separations of 3.381(2) and 2.468(2) Å, respectively] (Figure 26b).

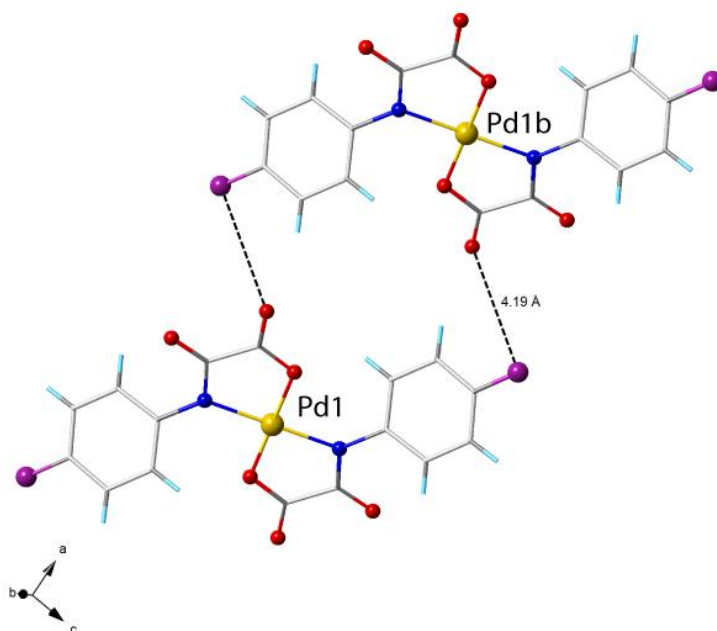


Figure 25. A view illustrating the shortest contacts between $\text{trans}[\text{Pd}(\text{4-Fpma})_2]^{2-}$ anionic moieties in **5**. $\text{Pd}1\cdots\text{Pd}1b$ separation of 9.645(3) Å [symmetry code: (b) = $-x, y, z$].

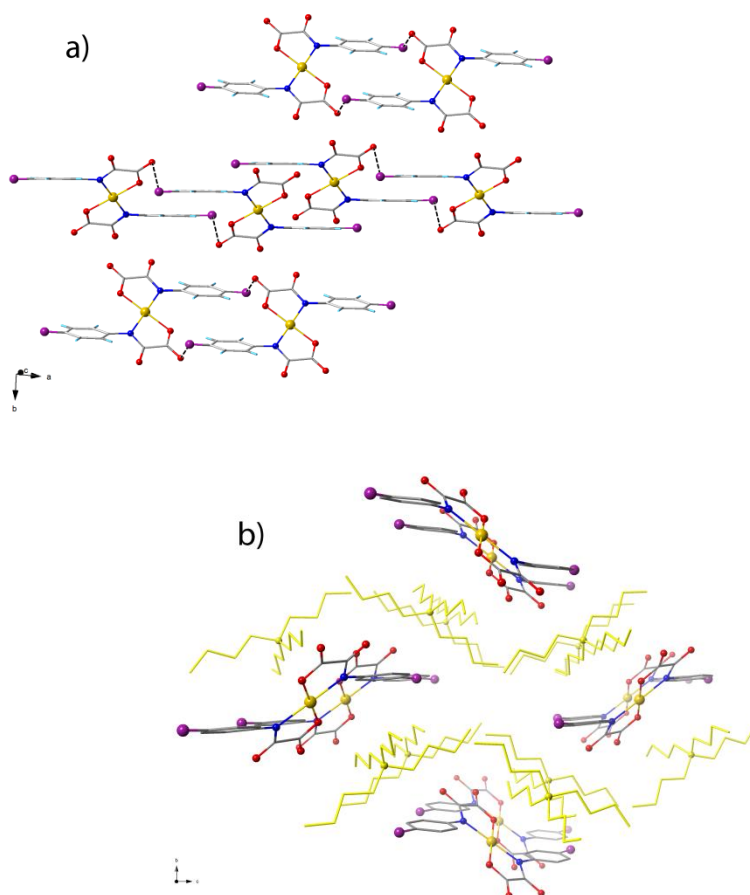


Figure 26. A fragment of the crystal packing in **5** showing a) showing only the anionic complexes and b) their distribution among the organic cations. The organic counterions have been depicted as yellow sticks. Hydrogen atoms have been omitted for clarity.

Crystal packing of $(n\text{-Bu}_4\text{N})_2\text{trans}[\text{Pd}(4\text{-Cl-pma})_2] \cdot 4\text{H}_2\text{O}$ (6**).** Compound **6** shows a fascinating crystal packing due to the cooperation of weak halogen \cdots halogen interactions involving also the co-crystallized water molecules, the whole leading to an intriguing net. One of the two independent complex anions [Pd1] is engaged in such H-bond interactions between the terminal oxygen atoms of the ligand and the lattice water molecules [$\text{O}_{\text{oxamate}}\cdots\text{O}_{\text{w}}$ distances varying in the range 2.847(3)-2.908(3) Å, see Table S5] (Figure 27).

Further strong H-bonds between water molecules [$O_w \cdots O_w$ distances in the range 2.664(1)–2.801(1) Å] and weak $Cl \cdots O_w$ interactions [$Cl \cdots O_w$ distance 3.92 Å] give rise to a 2D motif developing in the crystallographic *ab* plane, yielding a noteworthy intercalation of water chains, trapped in well-defined water ribbons (Figure 27).

The supramolecular three-dimensional packing is reached by means of weak $Cl \cdots Cl$ interactions [$Cl1 \cdots Cl2$ separation of 4.30 Å] involving the previously described layers and more isolated *trans*-[Pd(4-Clpma)₂]²⁻ moieties. These interactions are most likely responsible of the grasping of the two crystallographically-independent complex anions in **6** (Figures 28–29).

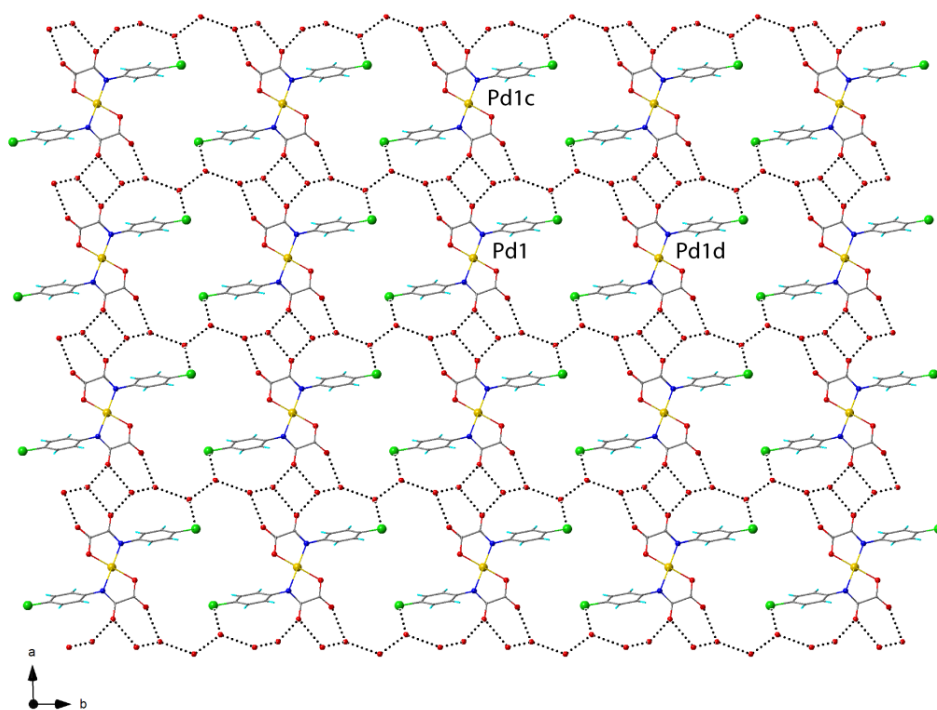


Figure 27. View along the crystallographic *c* axis of the *trans*-[Pd(4-Clpma)₂]²⁻ moieties in **6** showing intercalated water chains in a pretty sheet arrangement by mean of H-bonds and $Cl \cdots O_w$ type interactions. Pd(1)⋯Pd(1c) and Pd(1)⋯Pd(1d) distances equal to 12.522(1) and 15.700(1) Å, respectively [symmetry code: (c) = 2-*x*, *y*, *z*; (d) = *x*, 2-*y*, *z*].

In fact, one of the two independent complex anions [Pd2] is involved in H-bond interactions only with one of the terminal oxygen atoms of the ligand and a water lattice molecule [$O_{\text{oxamate}} \cdots O_{\text{w}}$ distances 2.785(3) Å] (Figure 28). As shown in Figure 29, the packing consists of sheets with water ribbons [Pd1] staggered by other independent halogen bonded anions [Pd2]. The remaining voids are filled by bulky organic counteranions (Figure 30).

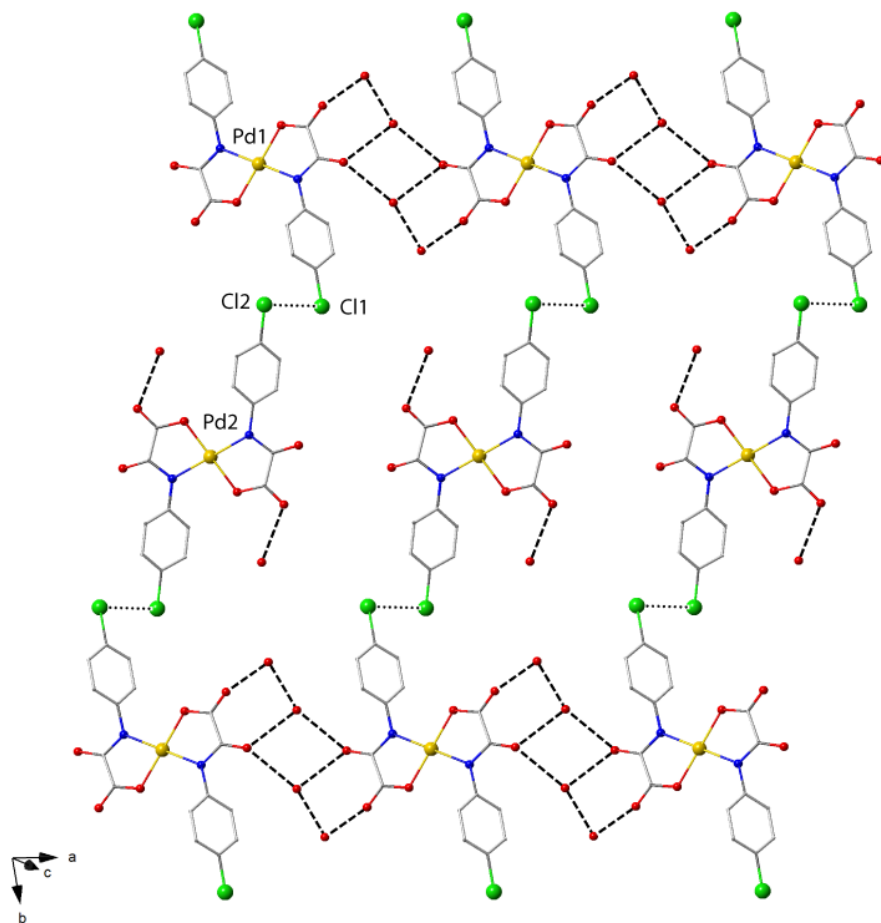


Figure 28. Details of weak Cl...Cl interactions linking the two independent *trans*-[Pd(4-Clpma)₂]²⁻ moieties in **6**.

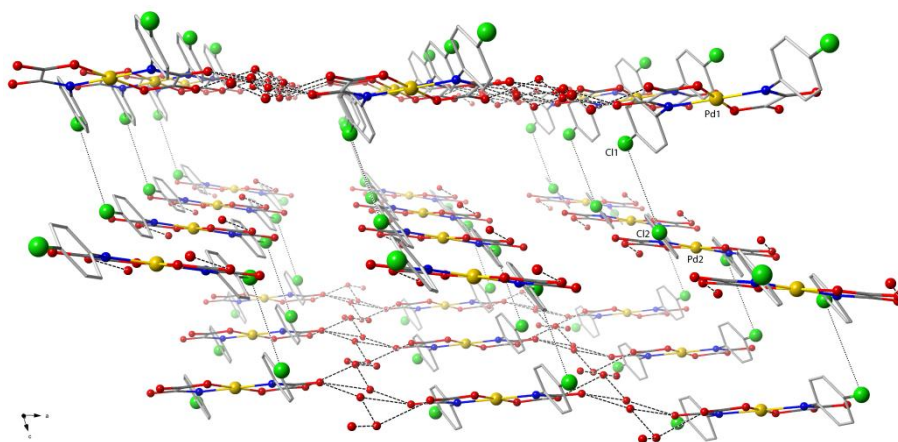


Figure 29. A view along the crystallographic *b* axis of the crystal packing of **6** showing isolated [Pd2] units interconnecting the H-bonded layers of [Pd1] units through weak Cl...Cl interactions. The Pd1...Pd2 distance is 8.572(1) Å.

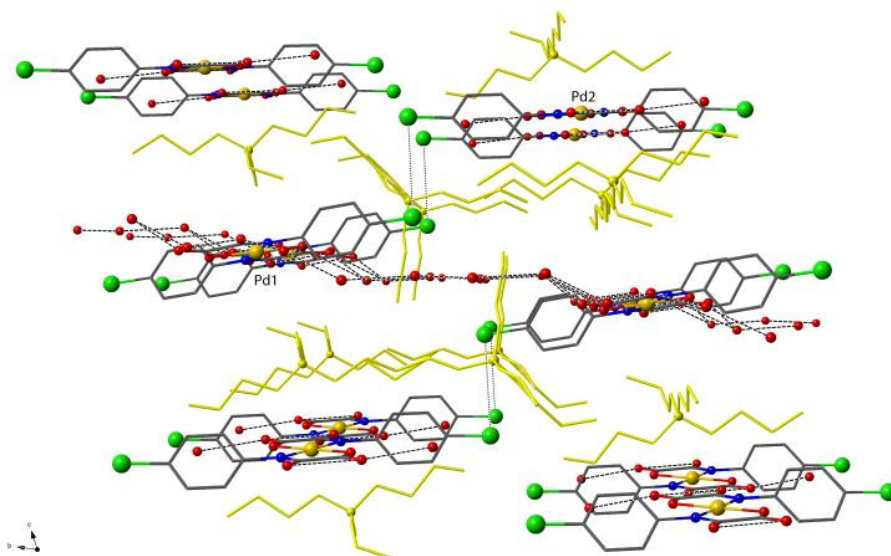


Figure 30. A view of a fragment of the crystal packing of **6** showing anionic layers and isolated *trans*-[Pd(4-Clpma)₂]²⁻ moieties, separated by the bulky *n*-Bu₄N⁺ cations. The organic counterions have been depicted as yellow sticks. Hydrogen atoms have been omitted for clarity.

Crystal packing of $(n\text{-Bu}_4\text{N})_2\text{cis-}[\text{Pd}(4\text{-Br-pma})_2] \cdot 4\text{H}_2\text{O}$ (a). Compound **7** it is the only one containing complex anions in a *cis* conformation, namely the $\text{cis-}[\text{Pd}^{\text{II}}(4\text{-Brpma})_2]^{2-}$ units. As expected for such a conformation, intramolecular face-to-face stacking interactions are clearly established between the phenyl rings on each chelating ligand of the $\text{cis-}[\text{Pd}^{\text{II}}(4\text{-Br-pma})_2]^{2-}$ unit (Figure 24). The value of the centroid-centroid distance (h) between the two facing benzene rings is 3.401(1) Å, while the value of the off-set angle (φ) between the centroid-centroid vector and the normal to the plane of the benzene rings is 19.9(1)°. Steric effects are also likely responsible for the non-zero twist angle [$\tau = 4.2(2)^\circ$] observed in **7** and related compounds with *cis* stereochemistry.³¹ Halogen interactions between Br atoms of neighboring oxamate ligands are the driving force toward the *cis*-isomers [Br...Br distances 4.28 Å] (Figure 24). These forces together with H-bonds, involving both the terminal oxygen atoms of the ligand and the lattice water molecules [$\text{O}_{\text{oxamate}} \cdots \text{O}_{\text{w}}$ and $\text{O}_{\text{w}} \cdots \text{O}_{\text{w}}$ distances of 2.817(3)-2.840(3) and 2.860(3)-2.892(3) Å, respectively; see Tables S6] give rise to a 1D supramolecular motif (Figures 31 and 32) developing along the crystallographic *a* axis. The shortest Pd...Pd separation is 8.489(1) Å and it corresponds to an interchain distance. This value is much shorter than the shortest intrachain separation [ca. 14.827(1) Å] through the network of H-bonded water molecules (Figure 32).

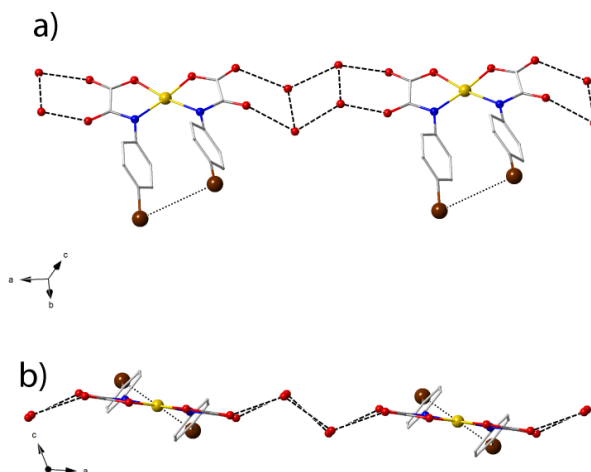


Figure 31. Top (a) and side (b) views along the crystallographic *c* axis of the supramolecular chain in **7** formed through H-bonds between the $\text{cis-}[\text{Pd}(4\text{-Brpma})_2]^{2-}$ unit and the crystallization water molecules.

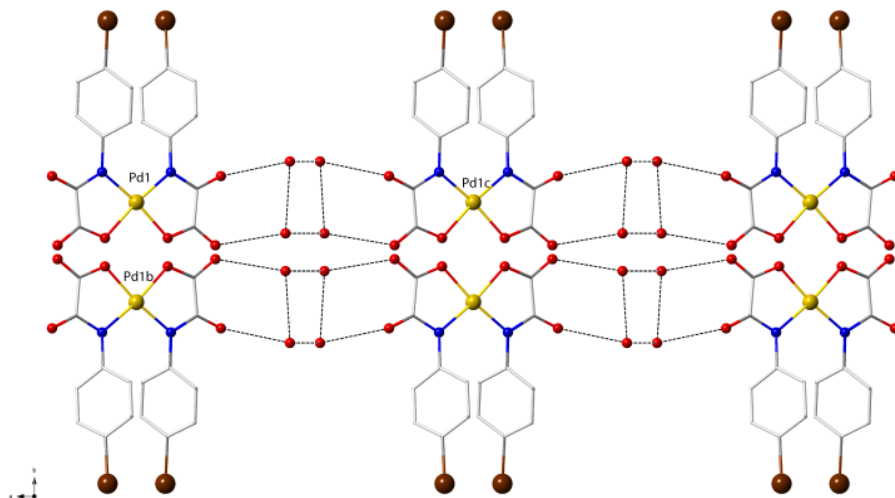


Figure 32. A view along the crystallographic *c* axis of a fragment of the supramolecular anionic chains in **7**. Pd1...Pd1b and Pd1...Pd1c distances are equal to 8.489(1) and 14.827(1) Å, respectively [symmetry codes: (b) = 1-*x*, *y*, 0.5-*z*; (c) = -1+*x*, *y*, *z*].

Adjacent 1D supramolecular motifs are disposed into a *zig-zag* arrangement leaving pseudo-hydrophobic voids which are filled by the bulky *n*-Bu₄N⁺ cations (Figure 33).

It has been found that both the *trans* and *cis* isomers of the [Pd^{II}(4-Brpma)₂]²⁻ complex anion can be isolated in the solid state. On the contrary, we have no evidence of the *cis* isomer formation when 4-Fpma⁴⁻ and 4-Clpma⁴⁻ ligands were used as ligands. This result induces us to suggest the better flexibility of bromo atoms to form halogen bonds as the factor responsible for the improved structural stability of a *cis* isomer in **7**.

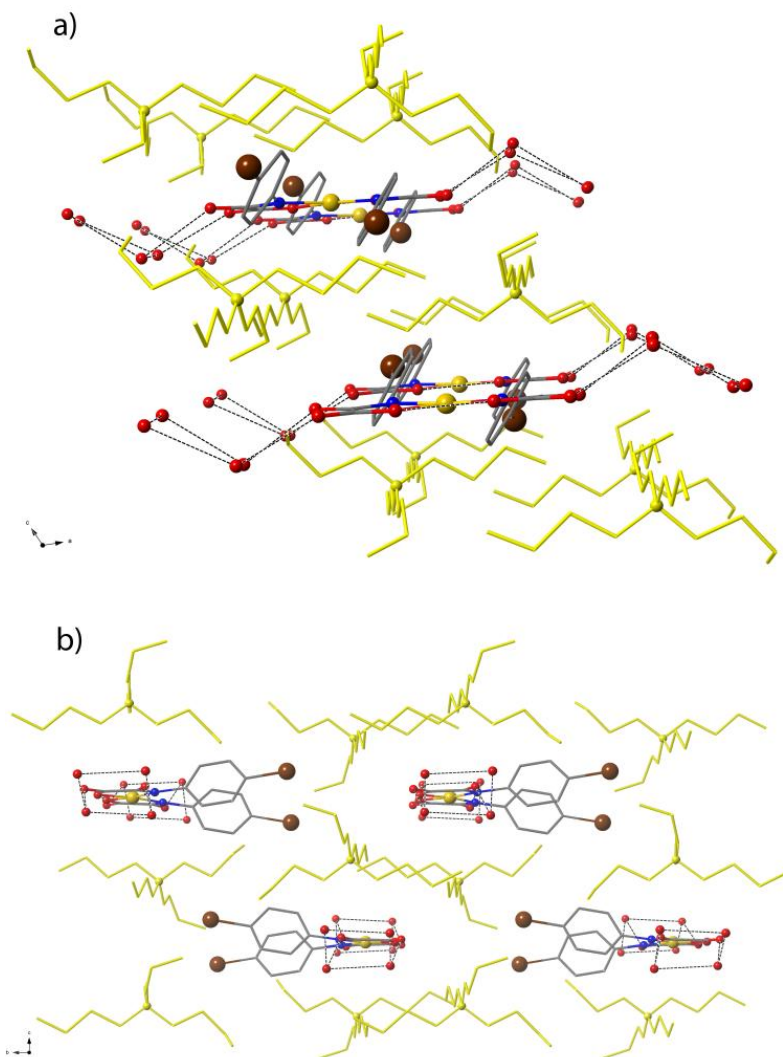
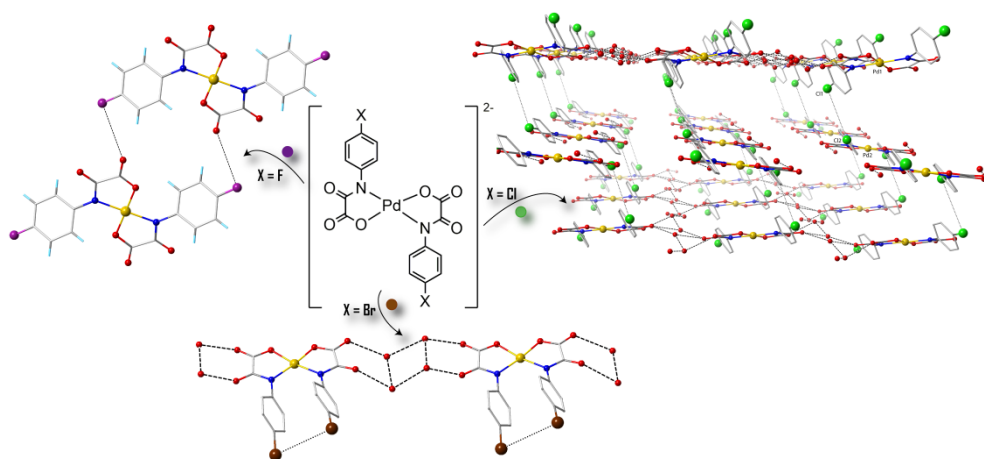


Figure 33. View of a fragment of the crystal packing in 7 along the crystallographic *b* (a) and *a* (b) axes. The whole organic counterions have been depicted in yellow. Hydrogen atoms have been omitted for clarity.

II.10. Conclusions

In summary, concerted supramolecular motifs in new fluoro-, chloro- and bromo-derivatives of the mononuclear bis(oxamato)palladate(II) complexes have been investigated. The different nature and size of the halogen atoms show a clear putative role in the supramolecular assemblies of the similar anionic complexes. These intriguing different assemblies described are undoubtedly driven by simply van der Waals and ionic forces, (5), or combined H-bonds, halogen-halogen (6-7) and/or π - π interactions (7) merely depending on the substitution on the ligand used.



Scheme 5. Supramolecular motifs of fluoro-, chloro- and bromo-derivatives of the mononuclear bis(oxamato)palladate(II) complexes.

This study is a rare report on structural modularity of the supramolecular assemblies in *complexes as ligands* for which a modulation of supramolecular features can be achieved with a judicious choice of slightly modified ligands. The supramolecular halogen-halogen interactions are not only useful in the field of crystal engineering where insights in the prediction of the crystal structures are gained but also in the design of new functional molecule-based materials exhibiting interesting physical-chemical properties as observed in the hexahalorhenate(IV) salts.⁸⁷

II.11. References

- (1) Steggerda, J. J.; Bour, J. J.; Birker, P. J. M. W. L. *Inorg. Chem.* **1971**, *10*, 1202–1205.
- (2) Lloret, F.; Julve, M.; Real, J. A.; Faus, J.; Ruiz, R.; Mollar, M.; Castro, I.; Bois, C.; Philoche-Levisalles, M. *Inorg. Chem.* **1992**, *31*, 2956–2961.
- (3) Stumpf, H. O.; Pei, Y.; Kahn, O.; Sletten, J.; Renard, J. P. *J. Am. Chem. Soc.* **1993**, *115*, 6738–6745.
- (4) Real, J. A.; Mollar, M.; Ruiz, R.; Faus, J.; Lloret, F.; Julve, M.; Philoche-Levisalles, M. *J. Chem. Soc. Dalt. Trans.* **1993**, 1483.
- (5) Stumpf, H. O.; Pei, Y.; Ouahab, L.; Le Berre, F.; Codjovi, E.; Kahn, O. *Inorg. Chem.* **1993**, *32*, 5687–5691.
- (6) Stumpf, H. O.; Pei, Y.; Kahn, O.; Ouahab, L.; Grandjean, D. *Science* **1993**, *261*, 447–449.
- (7) Cervera, B.; Sanz, J. L.; Ibáñez, M. J.; Vila, G.; Lloret, F.; Julve, M.; Ruiz, R.; Ottenwaelder, X.; Aukauloo, A.; Poussereau, S.; Journaux, Y.; Muñoz, M. C. *J. Chem. Soc. Dalt. Trans.* **1998**, 781–790.
- (8) Aukauloo, A.; Ottenwaelder, X.; Ruiz, R.; Poussereau, S.; Pei, Y.; Journaux, Y.; Fleurat, P.; Volatron, F.; Cervera, B.; Muñoz, M. C. *Eur. J. Inorg. Chem.* **1999**, *1999*, 1067–1071.
- (9) Aukauloo, A.; Ottenwaelder, X.; Ruiz, R.; Journaux, Y.; Pei, Y.; Rivière, E.; Cervera, B.; Muñoz, M. C. *Eur. J. Inorg. Chem.* **1999**, *1999*, 209–212.
- (10) Kahn, O. *Acc. Chem. Res.* **2000**, *33*, 647–657.
- (11) Berg, K. E.; Pellegrin, Y.; Blondin, G.; Ottenwaelder, X.; Journaux, Y.; Canovas, M. M.; Mallah, T.; Parsons, S.; Aukauloo, A. *Eur. J. Inorg. Chem.* **2002**, *2002*, 323–325.
- (12) Pardo, E.; Ruiz-García, R.; Lloret, F.; Faus, J.; Julve, M.; Journaux, Y.; Delgado, F.; Ruiz-Pérez, C. *Adv. Mater.* **2004**, *16*, 1597–1600.
- (13) Ottenwaelder, X.; Ruiz-García, R.; Blondin, G.; Carasco, R.; Cano, J.; Lexa, D.; Journaux, Y.; Aukauloo, A. *Chem. Commun.* **2004**, 504–505.
- (14) Pardo, E.; Ruiz-García, R.; Lloret, F.; Faus, J.; Julve, M.; Journaux, Y.; Novak, M. A.; Delgado, F. S.; Ruiz-Pérez, C. *Chem. Eur. J.* **2007**, *13*, 2054–2066.
- (15) Pardo, E.; Ruiz-García, R.; Cano, J.; Ottenwaelder, X.; Lescouëzec, R.; Journaux, Y.; Lloret, F.; Julve, M. *Dalt. Trans.* **2008**, 2780–2805.
- (16) Stroh, C.; Stuparu, A. *Tetrahedron Lett.* **2010**, *51*, 5157–5159.
- (17) Dul, M.-C.; Pardo, E.; Lescouëzec, R.; Journaux, Y.; Ferrando-Soria, J.; Ruiz-García, R.; Cano, J.; Julve, M.; Lloret, F.; Cangussu, D.; Pereira, C. L. M.; Stumpf, H. O.; Pasán, J.; Ruiz-Pérez, C. *Coord. Chem. Rev.* **2010**, *254*, 2281–2296.
- (18) Ferrando-Soria, J.; Pardo, E.; Ruiz-García, R.; Cano, J.; Lloret, F.; Julve, M.; Journaux, Y.; Pasán, J.; Ruiz-Pérez, C. *Chem. Eur. J.* **2011**, *17*, 2176–2188.
- (19) Vilela, R. S.; Oliveira, T. L.; Martins, F. T.; Ellena, J. A.; Lloret, F.; Julve, M.; Cangussu, D. *Comptes Rendus Chim.* **2012**, *15*, 856–865.

- (20) Ferrando-Soria, J.; Rood, M. T. M.; Julve, M.; Lloret, F.; Journaux, Y.; Pasán, J.; Ruiz-Pérez, C.; Fabelo, O.; Pardo, E. *Cryst.Eng.Comm* **2012**, *14*, 761.
- (21) Castellano, M.; Fortea-Pérez, F. R.; Stiriba, S.-E.; Julve, M.; Lloret, F.; Armentano, D.; De Munno, G.; Ruiz-García, R.; Cano, J. *Inorg. Chem.* **2011**, *50*, 11279–11281.
- (22) Castellano, M.; Fortea-Pérez, F. R.; Bentama, A.; Stiriba, S.-E.; Julve, M.; Lloret, F.; De Munno, G.; Armentano, D.; Li, Y.; Ruiz-García, R.; Cano, J. *Inorg. Chem.* **2013**, *52*, 7645–7657.
- (23) Castellano, M.; Ferrando-Soria, J.; Pardo, E.; Julve, M.; Lloret, F.; Mathonière, C.; Pasán, J.; Ruiz-Pérez, C.; Cañadillas-Delgado, L.; Ruiz-García, R.; Cano, J. *Chem. Commun.* **2011**, *47*, 11035–11037.
- (24) Soto, J.; Martínez-Mañez, R.; Payá, J.; Lloret, F.; Julve, M. *Transit. Met. Chem.* **1993**, *18*, 69–72.
- (25) Estrada, J.; Fernández, I.; Pedro, J.; Ottenwaelder, X.; Ruiz, R.; Journaux, Y. *Tetrahedron Lett.* **1997**, *38*, 2377–2380.
- (26) Ruiz, R.; Surville-Barland, C.; Aukauloo, A.; Anxolabehere-Mallart, E.; Journaux, Y.; Cano, J.; Muñoz, M. C. *J. Chem. Soc. Dalt. Trans.* **1997**, 745–752.
- (27) Ruiz, R.; Triannidis, M.; Aukauloo, A.; Journaux, Y.; Fernández, I.; Pedro, J. R.; Cervera, B.; Castro, I.; Carmen Muñoz, M. *Chem. Commun.* **1997**, 2283–2284.
- (28) Blay, G.; Fernández, I.; Formentin, P.; Pedro, J.; Roselló, A. L.; Ruiz, R.; Journaux, Y. *Tetrahedron Lett.* **1998**, *39*, 3327–3330.
- (29) Fernández, I.; Pedro, J.; Rosello, A. L.; Ruiz, R.; Ottenwaelder, X.; Journaux, Y. *Tetrahedron Lett.* **1998**, *39*, 2869–2872.
- (30) Ruiz, R.; Aukauloo, A.; Journaux, Y.; Fernández, I.; Pedro, J. R.; Roselló, A. L.; Cervera, B.; Castro, I.; Carmen Muñoz, M. *Chem. Commun.* **1998**, 989–990.
- (31) Blay, G.; Fernández, I.; Giménez, T.; Pedro, J. R.; Ruiz, R.; Pardo, E.; Lloret, F.; Muñoz, M. C. *Chem. Commun.* **2001**, 2102–2103.
- (32) Blay, G.; Fernández, I.; Marco-Aleixandre, A.; Monje, B.; Pedro, J. R.; Ruiz, R. *Tetrahedron* **2002**, *58*, 8565–8571.
- (33) Ferrando-Soria, J.; Serra-Crespo, P.; de Lange, M.; Gascon, J.; Kapteijn, F.; Julve, M.; Cano, J.; Lloret, F.; Pasán, J.; Ruiz-Pérez, C.; Journaux, Y.; Pardo, E. *J. Am. Chem. Soc.* **2012**, *134*, 15301–15304.
- (34) Kivekas, R.; Pajunen, A.; Navarrete, A.; Colacio, E. *Inorg. Chim. Acta* **1999**, *284*, 292–295.
- (35) Oliveira, W. X. C.; Ribeiro, M. A.; Pinheiro, C. B.; Nunes, W. C.; Julve, M.; Journaux, Y.; Stumpf, H. O.; Pereira, C. L. M. *Eur. J. Inorg. Chem.* **2012**, *2012*, 5685–5693.
- (36) Oliveira, W. X. C.; da Costa, M. M.; Fontes, A. P. S.; Pinheiro, C. B.; de Paula, F. C. S.; Jaimes, E. H. L.; Pedroso, E. F.; de Souza, P. P.; Pereira-Maia, E. C.; Pereira, C. L. M. *Polyhedron* **2014**, *76*, 16–21.
- (37) Chen, X.; Engle, K. M.; Wang, D.-H.; Yu, J.-Q. *Angew. Chem. Int. Ed.* **2009**, *48*, 5094–5115.
- (38) Sehnal, P.; Taylor, R. J. K.; Fairlamb, I. J. S. *Chem. Rev.* **2010**, *110*, 824–889.

- (39) Miyaura, N.; Suzuki, A. *Chem. Rev.* **1995**, *95*, 2457–2483.
- (40) Fortea-Pérez, F. R.; Marino, N.; Armentano, D.; De Munno, G.; Julve, M.; Stiriba, S.-E. *Cryst. Eng. Comm* **2014**, *16*, 6971.
- (41) Smid, J. *Angew. Chemie Int. Ed.* **1972**, *11*, 112–127.
- (42) Mukaiyama, T.; Tamura, Y.; Fujisawa, T. *Bull. Chem. Soc. Jpn.* **1964**, *37*, 628–634.
- (43) Ma, J. C.; Dougherty, D. A. *Chem. Rev.* **1997**, *97*, 1303–1324.
- (44) Mahadevi, A. S.; Sastry, G. N. *Chem. Rev.* **2013**, *113*, 2100–2138.
- (45) Beletskaya, I. P.; Cheprakov, A. V. *Chem. Rev.* **2000**, *100*, 3009–3066.
- (46) Yin, L.; Liebscher, J. *Chem. Rev.* **2007**, *107*, 133–173.
- (47) Hassan, J.; Sévignon, M.; Gozzi, C.; Schulz, E.; Lemaire, M. *Chem. Rev.* **2002**, *102*, 1359–1470.
- (48) Kotha, S.; Lahiri, K.; Kashinath, D. *Tetrahedron* **2002**, *58*, 9633–9695.
- (49) Biffis, A.; Zecca, M.; Basato, M. *J. Mol. Catal. A Chem.* **2001**, *173*, 249–274.
- (50) De Vries, A. H. M.; Mulders, J. M. C. a; Mommers, J. H. M.; Henderickx, H. J. W.; de Vries, J. G. *Org. Lett.* **2003**, *5*, 3285–3288.
- (51) Brasche, G.; García-Fortanet, J.; Buchwald, S. L. *Org. Lett.* **2008**, *10*, 2207–2210.
- (52) Tamami, B.; Ghasemi, S. *J. Mol. Catal. A Chem.* **2010**, *322*, 98–105.
- (53) Yeung, C. S.; Dong, V. M. *Chem. Rev.* **2011**, *111*, 1215–1292.
- (54) Amatore, C.; Jutand, A.; M'Barki, M. A. *Organometallics* **1992**, *11*, 3009–3013.
- (55) Herrmann, W. A.; Böhm, V. P. W. *J. Organomet. Chem.* **1999**, *572*, 141–145.
- (56) Bertoux, F.; Monflier, E.; Castanet, Y.; Mortreux, A. *J. Mol. Catal. A Chem.* **1999**, *143*, 23–30.
- (57) Llabresixamena, F.; Abad, A.; CORMA, A.; GARCIA, H. *J. Catal.* **2007**, *250*, 294–298.
- (58) Wang, X.; He, L.; He, Y.; Zhang, J.; Su, C.-Y. *Inorg. Chim. Acta* **2009**, *362*, 3513–3518.
- (59) Zhang, S.; Liu, Q.; Shen, M.; Hu, B.; Chen, Q.; Li, H.; Amoureux, J.-P. *Dalton Trans.* **2012**, *41*, 4692–4698.
- (60) El-Sayed, M. A. *Acc. Chem. Res.* **2001**, *34*, 257–264.
- (61) Lehn, J.-M. *Supramolecular Chemistry*; Wiley-VCH Verlag GmbH & Co. KGaA: Weinheim, FRG, 1995.
- (62) Teresa Albelda, M.; Frías, J. C.; García-España, E.; Schneider, H.-J. *Chem. Soc. Rev.* **2012**, *41*, 3859.
- (63) Štarha, P.; Trávníček, Z.; Popa, I. *J. Inorg. Biochem.* **2009**, *103*, 978–988.
- (64) Horcajada, P.; Gref, R.; Baati, T.; Allan, P. K.; Maurin, G.; Couvreur, P.; Férey, G.; Morris, R. E.; Serre, C. *Chem. Rev.* **2012**, *112*, 1232–1268.
- (65) Kreno, L. E.; Leong, K.; Farha, O. K.; Allendorf, M.; Van Duyne, R. P.; Hupp, J. T. *Chem. Rev.* **2012**, *112*, 1105–1125.
- (66) Albrecht, M. *Angew. Chemie Int. Ed.* **2009**, *48*, 3214–3214.
- (67) Train, C.; Gruselle, M.; Verdagner, M. *Chem. Soc. Rev.* **2011**, *40*, 3297.
- (68) Horike, S.; Umeyama, D.; Kitagawa, S. *Acc. Chem. Res.* **2013**, *46*, 2376–2384.
- (69) Andruh, M. *Chem. Commun.* **2007**, 2565.
- (70) Andruh, M. *Chem. Commun.* **2011**, *47*, 3025.

- (71) Gable, R. W.; Hoskins, B. F.; Robson, R. J. *Chem. Soc. Chem. Commun.* **1990**, 1677.
- (72) Hoskins, B. F.; Robson, R. J. *Am. Chem. Soc.* **1990**, *112*, 1546–1554.
- (73) Desiraju, G. R. *The Crystal as a Supramolecular Entity*; 1996.
- (74) Maginn, S. J. *J. Appl. Crystallogr.* **1991**, *24*, 265–265.
- (75) Desiraju, G. R. *Crystal Engineering: The Design of Organic Solids* <http://www.amazon.com/Crystal-Engineering-Organic-Materials-Monographs/dp/0444874577> (accessed Jul 2, 2015).
- (76) Steed, J. W.; Atwood, J. L. *Supramolecular Chemistry*; 2nd Editio.; John Wiley & Sons, Ltd: Chichester, UK, 2009.
- (77) Ding, X.; Tuikka, M.; Haukk, M. In *Recent Advances in Crystallography*; InTech, 2012.
- (78) Reddy, D. S.; Panneerselvam, K.; Pilati, T.; Desiraju, G. R. *J. Chem. Soc. Chem. Commun.* **1993**, 661.
- (79) Desiraju, G. R.; Harlow, R. L. *J. Am. Chem. Soc.* **1989**, *111*, 6757–6764.
- (80) Reddy, D. S.; Craig, D. C.; Desiraju, G. R. *J. Am. Chem. Soc.* **1996**, *118*, 4090–4093.
- (81) Thallapally, P. K.; Chakraborty, K.; Katz, A. K.; Carrell, H. L.; Kotha, S.; Desiraju, G. R. *CrystEngComm* **2001**, *3*, 134.
- (82) Metrangolo, P.; Resnati, G. *Chem. - A Eur. J.* **2001**, *7*, 2511–2519.
- (83) Metrangolo, P.; Neukirch, H.; Pilati, T.; Resnati, G. *Acc. Chem. Res.* **2005**, *38*, 386–395.
- (84) Thalladi, V. R.; Goud, B. S.; Hoy, V. J.; Allen, F. H.; Howard, J. A. K.; Desiraju, G. R. *Chem. Commun.* **1996**, 401.
- (85) Metrangolo, P.; Resnati, G. *IUCrJ* **2014**, *1*, 5–7.
- (86) Mukherjee, A.; Tothadi, S.; Desiraju, G. R. *Acc. Chem. Res.* **2014**, *47*, 2514–2524.
- (87) Martínez-Lillo, J.; Faus, J.; Lloret, F.; Julve, M. *Coord. Chem. Rev.* **2015**, *289–290*, 215–237.
- (88) Fortea-Pérez, F. R.; Armentano, D.; Julve, M.; De Munno, G.; Stiriba, S.-E. *J. Coord. Chem.* **2014**, *67*, 4003–4015.
- (89) Fortea-Pérez, F. R.; Schlegel, I.; Julve, M.; Armentano, D.; De Munno, G.; Stiriba, S.-E. *J. Organomet. Chem.* **2013**, *743*, 102–108.
- (90) Oliveira, W. X. C.; Ribeiro, M. A.; Pinheiro, C. B.; da Costa, M. M.; Fontes, A. P. S.; Nunes, W. C.; Cangussu, D.; Julve, M.; Stumpf, H. O.; Pereira, C. L. M. *Cryst. Growth Des.* **2015**, *15*, 1325–1335.

III

Chapter 2

Study of the influence of the
substituents and solvents on the
catalytic properties of
bis(oxamato)palladate(II) complexes

III.1. Carbon-carbon cross-coupling reactions

The field of the cross-coupling chemistry where the substitution of an aryl, vinyl and alkyl halide/pseudohalide by a nucleophile takes place in the presence of a transition metal catalyst has been subject of thorough investigation since the early 1970's.¹⁻¹² These impressive worldwide research efforts were rewarded with the award of the 2010 Nobel Prize in chemistry to Richard Heck, Ei-ichi Negishi and Akira Suzuki.¹³⁻¹⁵ One of the main reasons to pursue with this chemistry is its great impact on the chemical industry as well as on the ligand design, this last point revealing of outmost relevance to other research fields (supramolecular chemistry, molecular magnetism, bioinorganic chemistry, materials science, etc.).^{10,16-26}

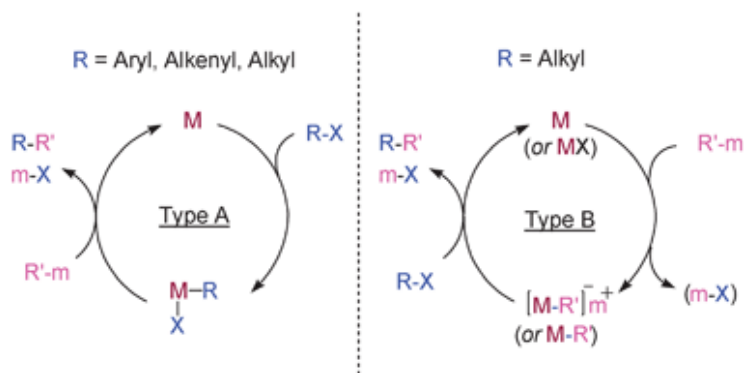


Chart I. Postulated catalytic cycles for cross-coupling reactions. Ligands are omitted.²⁷

A good number of palladium-based systems with excellent catalytic performances in carbon-carbon cross-coupling reactions have been developed during the last five decades, their efficiency being largely checked. Without being exhaustive, representative examples are those with phosphine ligands,²⁸⁻³¹ palladacycle catalysts,³²⁻³⁵ *N*-heterocyclic carbene-containing catalysts (NHCs),³⁶⁻⁴⁰ nanoparticles⁴¹⁻⁴⁴ and immobilized catalysts⁴⁵⁻⁴⁸ in both homogenous and heterogenous phases. It deserves to be noted that in most cases, the activity of homogeneous phase catalysts was found to be richer than the one for the heterogenous analogues.⁴⁹⁻⁵⁵

Nowadays, the search for new procedures concerning ecologically benign carbon-carbon cross-coupling is still a command and the conditions to be fulfilled thinking at them are the following:

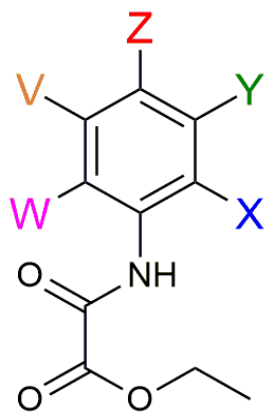
- (i) low amounts of catalyst,
- (ii) high activity and selectivity,
- (iii) mild reaction conditions in environmentally benign solvents that save energy costs
- (iv) and efficient recycling and reuse of the catalyst with regular yields over a large number of runs.

Keeping this in mind, part of our current research work has focused onto the design and use of simple, cheap, and recyclable active palladium(II)-based catalysts together with environment-friendly green solvents. In this context, we bet on ionic liquids as alternative green solvents,⁵⁶⁻⁶⁵ in particular the tetra-*n*-butylbromide (*n*-Bu₄NBr) which was widely used by other research teams.⁶⁶⁻⁷⁰ By performing cross-coupling Heck reaction in an alternative green catalysis without harmful ecological chemicals (phosphine ligands for instance) or well by using ligands easier to handle than the carbene ones, our proposal to employ low-cost versatile *N,O* ligands,^{71,72} should be advantageous as environmentally friendly organic reaction methodology and also as a suitable strategy for recycling catalysts.^{64,73,74} Noteworthy, chelating ligands containing oxygen or nitrogen as donor atoms have been shown to stabilize palladium complexes.⁷⁵⁻⁷⁷

III.2. Aim

After demonstrating in the previous *Chapter* that bis(oxamato)palladate(II) complexes are active catalysts for carbon-carbon cross-coupling reactions, it became important to check if these kind of complexes are active not only for Suzuki type reactions (*Chapter 1*) but also for the Heck ones.

Therefore having in mind the idea of checking and increasing carbon-carbon cross-coupling catalytic activities, a different group of oxamate ligands with electronic and steric effects have been prepared and characterized.



Proligand	X	Y	Z	V	W
EtHpma					
EtH-2-Mepma	Me				
EtH-4-Mepma			Me		
EtH-4-Fpma			F		
EtH-4-Clpma			Cl		
EtH-4-Brpma			Br		
EtH-4-OMepma			OMe		
EtH-4- <i>i</i> -Prpma			Iso		
EtH-2,3-Me ₂ pma	Me	Me			
EtH-2,4-Me ₂ pma	Me		Me		
EtH-2,5-Me ₂ pma	Me			Me	
EtH-2,6-Me ₂ pma	Me				Me
EtH-3,4-Me ₂ pma		Me	Me		
EtH-3,5-Me ₂ pma		Me		Me	
EtH-2,4,6-Me ₃ pma	Me		Me		Me
EtH-2,4,6-Ph ₃ pma	Ph		Ph		Ph

Scheme 1. Proligands from aniline derivatives. Hydrogen atoms are omitted for the sake of clarity.

The present *Chapter* focuses on the investigation of the catalytic activity of the palladium(II) complexes with oxamate ligands derived from the proligands of Scheme 1. The Heck and Suzuki coupling reactions both in DMF (homogeneous phase) and ionic liquids (*n*-Bu₄Br) are investigated.

III.3. Synthesis and characterization

The preparation of the proligands shown in Scheme 1 has been carried out by following previously reported procedures⁷⁸. For further information see Appendix B.

Synthesis of the complexes:

The synthesis of the bis(oxamato)palladate(II) complexes, listed hereunder, was followed as described in *Chapter 1 (Part II)* but using the corresponding proligand.

List of the novel bis(oxamato)palladate(II) complexes:

8a	$(n\text{-Bu}_4\text{N})_2[\text{Pd}(\text{pma})_2]$
9a	$(n\text{-Bu}_4\text{N})_2[\text{Pd}(2\text{-Mepma})_2]$
10a	$(n\text{-Bu}_4\text{N})_2[\text{Pd}(4\text{-Mepma})_2]$
11a	$(n\text{-Bu}_4\text{N})_2[\text{Pd}(4\text{-OMepma})_2]$
12a	$(n\text{-Bu}_4\text{N})_2[\text{Pd}(4\text{-}i\text{-Prpma})_2]$
13a	$(n\text{-Bu}_4\text{N})_2[\text{Pd}(2,3\text{-Me}_2\text{pma})_2]$
14a	$(n\text{-Bu}_4\text{N})_2[\text{Pd}(2,4\text{-Me}_2\text{pma})_2]$
15a	$(n\text{-Bu}_4\text{N})_2[\text{Pd}(2,5\text{-Me}_2\text{pma})_2]$
16a	$(n\text{-Bu}_4\text{N})_2[\text{Pd}(2,6\text{-Me}_2\text{pma})_2]$
17a	$(n\text{-Bu}_4\text{N})_2[\text{Pd}(3,4\text{-Me}_2\text{pma})_2]$
18a	$(n\text{-Bu}_4\text{N})_2[\text{Pd}(3,5\text{-Me}_2\text{pma})_2]$
19a	$(n\text{-Bu}_4\text{N})_2[\text{Pd}(2,4,6\text{-Me}_3\text{pma})_2]$
20a	$(n\text{-Bu}_4\text{N})_2[\text{Pd}(2,4,6\text{-Ph}_3\text{pma})_2]$

X-ray quality crystals (yellow prisms) were grown by recrystallization of the solid sample by two different methods: (i) in a water/acetonitrile mixture (2:1, v/v) for **11**, **16** and **19**, or (ii) by slow vapour diffusion of ether into an acetonitrile solution of the palladium(II) for **9**⁷⁹, **10**⁷⁹ and **20**. X-ray suitable crystals were grown within 2-4 weeks (i) and overnight (ii).

Characterization of complexes:

(*n*-Bu₄N)₂[Pd(pma)₂] (8a). Yield: 80%. IR(KBr/cm⁻¹): 3412 (O-H), 2999, 2961, 2933, 2875 (C-H), 1670, 1653, 1615, 1585 (C=O). ¹H NMR (DMSO-d₆) δ (ppm): 0.90-0.94 (t, 24H), 1.29-1.33 (m, 16H, *n*-Bu₄N⁺), 1.52-1.56 (m, 16H, *n*-Bu₄N⁺), 3,12-3,13 (m, 16H, *n*-Bu₄N⁺), 6,89-6,91 (m, 2H, H_{aryl}), 7,49-7,57 (m, 8H, H_{aryl}). Anal. Calcd. for C₄₈H₈₆N₄O₈Pd (8a): C 60.45 H 9.09 N 5.88. Found: C 61.26 H 10.04 N 5.51 %.

(*n*-Bu₄N)₂[Pd(2-Mepma)₂] (9a). Yield: 86%. IR(KBr/cm⁻¹): 3423 (O-H), 2961, 2930, 2874 (C-H), 1669, 1647, 1618, 1590 (C=O). ¹H NMR (CDCl₃) δ (ppm): 1.00-1.02 (t, 24H), 1.40-1.42 (m, 16H, *n*-Bu₄N⁺), 1.51-1.59 (m, 16H, *n*-Bu₄N⁺), 2.17 (s, 6H, CH₃), 3,18-3,24 (m, 16H, *n*-Bu₄N⁺), 7,16-7,19 (m, 8H, H_{aryl}). Anal. Calcd. for C₅₀H₈₆N₄O₁₀Pd (9a): C 63.50, H 9.17, N 5.92. Found: C 62.98, H 9.96, N 5.44 %.

(*n*-Bu₄N)₂[Pd(4-Mepma)₂] (10a). Yield: 95%. IR(KBr/cm⁻¹): 3422 (O-H), 2961, 2930, 2874 (C-H), 1658, 1617, 1588, 1540 (C=O). ¹H NMR (CDCl₃) δ (ppm): 0.92-0.95 (t, 24H), 1.33-1.36 (m, 16H, *n*-Bu₄N⁺), 1.48-1.52 (m, 16H, *n*-Bu₄N⁺), 1.89 (s, 6H, CH₃), 3,07-3,13 (m, 16H, *n*-Bu₄N⁺), 6,32-6,35 (d, 2H, H_{aryl}), 6,43-6,46 (d, 2H, H_{aryl}), 6,87-6,90 (d, 2H, H_{aryl}), 7,00-7,02 (d, 2H, H_{aryl}). Anal. Calcd. for C₅₀H₈₆N₄O₁₀Pd (10a): C 63.50, H 9.17, N 5.92. Found C 62.55 H 10.31 N 6.35 %.

(*n*-Bu₄N)₂[Pd(4-OMepma)₂] (11a). Yield: 50%. IR(KBr/cm⁻¹): 3422 (O-H), 2960, 2930, 2874 (C-H), 1667, 1647, 1610 (C=O). ¹H NMR (CDCl₃) δ (ppm): 0.97 - 1.02 (t, 52H, *n*-Bu₄N⁺), 1.35 - 1.47 (m, 35H, *n*-Bu₄N⁺), 1.50- 1.60 (m, 34H, *n*-Bu₄N⁺), 3.11 - 3.17 (t, 34H, *n*-Bu₄N⁺), 3.73 (s, 6H, OCH₃), 6.71 - 6.74 (d, 4H, H_{aryl}), 7.37 - 7.40 (d, 4H, H_{aryl}). Anal. Calcd. for (11a): C 61.43, H 8.87, N 5.73. Found: C 62.23, H 9.93, N 5.80 %.

(*n*-Bu₄N)₂[Pd(4-*i*-Prpma)₂] (12a). Yield: 52%. IR(KBr/cm⁻¹): 3422 (O-H), 2959, 2933, 2873 (C-H), 1669, 1648, 1619, 1597 (C=O). ¹H NMR (CDCl₃) δ (ppm): 0.97 - 1.02 (t, 52H, *n*-Bu₄N⁺), 1.19 - 1.21 (d, 12H, CH₃), 1.36 - 1.48 (m, 36H, *n*-Bu₄N⁺), 1.52 - 1.62 (m, 34H, *n*-Bu₄N⁺), 2.76 - 2.85 (m, 2H, CH), 3.15 - 3.21 (t, 33H, *n*-Bu₄N⁺), 7.02 - 7.05 (d, 4H, H_{aryl}), 7.35 - 7.38 (d, 4H, H_{aryl}). Anal. Calcd. for C₅₄H₉₄N₄O₈Pd (12a): C 64.74, H 9.46, N 5.59. Found: C 64.52, H 10.28, N 6.15 %.

(*n*-Bu₄N)₂[Pd(2,3-Me₂pma)₂] (13a). Yield: 74%. IR(KBr/cm⁻¹): 3423 (O-H), 2962, 2930, 2874 (C-H), 1670, 1638, 1606, 1577 (C=O). ¹H NMR (CDCl₃) δ (ppm): 0.99-1.01 (t, 24H), 1.38-1.40 (m, 16H, *n*-Bu₄N⁺), 1.52-1.55 (m, 16H, *n*-Bu₄N⁺), 2.23-2.26 (m, 12H, CH₃), 3,10-3,16 (m, 16H, *n*-Bu₄N⁺), 6.78-6.80 (m, 2H, H_{aryl}), 6.88-6.91 (m, 2H, H_{aryl}), 7.00-7.04 (m, 2H, H_{aryl}). Anal. Calcd. for C₅₂H₉₀N₄O₆Pd (13a): C 64.14 H 9.32 N 5.75. Found: C 63.77 H 10.12 N 5.52 %.

(*n*-Bu₄N)₂[Pd(2,4-Me₂pma)₂] (14a). Yield: 68%. IR(KBr/cm⁻¹): 3448 (O-H), 2962, 2936, 2874 (C-H), 1670, 1637, 1516, 1596 (C=O). ¹H NMR (CDCl₃) δ (ppm): 0.99-1.02 (t, 24H), 1.39-1.42 (m, 16H, *n*-Bu₄N⁺), 1.53-1.55 (m, 16H, *n*-Bu₄N⁺), 2.19 (s, 6H, CH₃), 2.34 (s, 6H, CH₃), 3,08-3,14 (m, 16H, *n*-Bu₄N⁺), 6.82-6.85 (m, 2H, H_{aryl}), 6.95-6.98 (m, 2H, H_{aryl}), 7.01-7.03 (m, 2H, H_{aryl}). Anal. Calcd. for C₅₂H₉₀N₄O₆Pd (14a): C 64.14 H 9.32 N 5.75. Found: C 64.60 H 10.05 N 5.40 %.

(*n*-Bu₄N)₂[Pd(2,5-Me₂pma)₂] (15a). Yield: 87%. IR(KBr/cm⁻¹): 3447 (O-H), 2961, 2926, 2874 (C-H), 1670, 1654, 1638, 1600 (C=O). ¹H NMR (CDCl₃) δ (ppm): 0.97-1.02 (t, 24H), 1.36-1.39 (m, 16H, *n*-Bu₄N⁺), 1.53-1.55 (m, 16H, *n*-Bu₄N⁺), 1.94 (s, 6H, CH₃), 2.01 (s, 6H, CH₃), 3,07-3,13 (m, 16H, *n*-Bu₄N⁺), 6.71-6.72 (m, 2H, H_{aryl}), 6.90-6.93 (m, 2H, H_{aryl}), 6.98-6.99 (m, 2H, H_{aryl}). Anal. Calcd. for C₅₂H₉₀N₄O₆Pd (15): C 64.14 H 9.32 N 5.75. Found: C 63.55 H 10.20 N 5.64 %.

(*n*-Bu₄N)₂[Pd(2,6-Me₂pma)₂] (16a). Yield: 89%. IR(KBr/cm⁻¹): 3433 (O-H), 2961, 2936, 2873 (C-H), 1670, 1638, 1604, 1582 (C=O). ¹H NMR (DMSO-d₆) δ (ppm): 0.90-0.94 (t, 24H), 1.30-1.32 (m, 16H, *n*-Bu₄N⁺), 1.55-1.58 (m, 16H, *n*-Bu₄N⁺), 2,24 (s, 12H, CH₃), 3,13-3,16 (m, 16H, *n*-Bu₄N⁺), 6,80-6,87 (m, 6H, H_{aryl}). Anal. Calcd. for C₅₈H₉₄N₄O₆Pd (16a): C 64.14 H 9.32 N 5.75. Found: C 63.45 H 10.13 N 5.61 %.

(*n*-Bu₄N)₂[Pd(3,4-Me₂pma)₂] (17a). Yield: 60%. IR(KBr/cm⁻¹): 3414 (O-H), 2961, 2935, 2874 (C-H), 1670, 1647, 1615, 1591 (C=O). ¹H NMR (CDCl₃) δ (ppm): 0.99-1.01 (t, 24H), 1.39-1.44 (m, 16H, *n*-Bu₄N⁺), 1.48-1.54 (m, 16H, *n*-Bu₄N⁺), 1.85 (s, 6H, CH₃), 1.95 (s, 6H, CH₃), 3,09-3,14 (m, 16H, *n*-Bu₄N⁺), 6,32-6,33 (d, 2H, H_{aryl}), 6,44-6,47 (d, 2H, H_{aryl}), 6,52-6,55 (q, 2H, H_{aryl}). Anal. Calcd. for C₅₂H₉₀N₄O₆Pd (17a): C 64.14 H 9.32 N 5.75. Found: C 63.67 H 10.01 N 5.38 %.

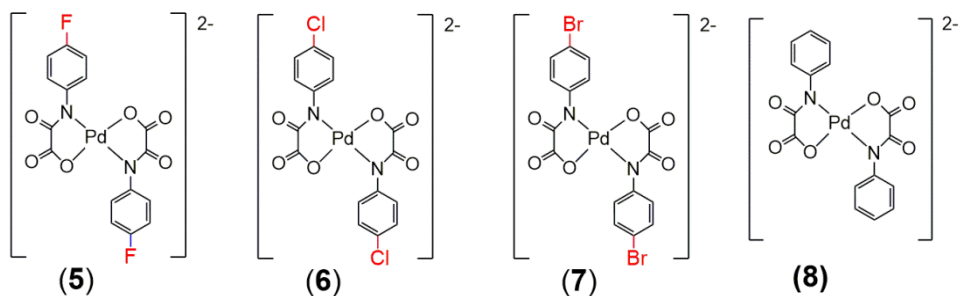
(*n*-Bu₄N)₂[Pd(3,5-Me₂pma)₂] (18a). Yield: 75%. IR(KBr/cm⁻¹): 3423 (O-H), 2960, 2930, 2874 (C-H), 1673, 1647, 1617, 1581 (C=O). ¹H NMR (CDCl₃) δ (ppm): 1.00-1.02 (t, 24H), 1.39-1.42 (m, 16H, *n*-Bu₄N⁺), 1.51-1.54 (m, 16H, *n*-Bu₄N⁺), 2.29 (m, 12H, CH₃), 3.07-3.13 (m, 16H, *n*-Bu₄N⁺), 6.58-6.60 (m, 2H, H_{aryl}), 6.99-7.01 (m, 4H, H_{aryl}). Anal. Calcd. for C₅₂H₉₀N₄O₆Pd (**18a**): C 64.14 H 9.32 N 5.75. Found: C 64.38 H 8.98 N 6.05 %.

(*n*-Bu₄N)₂[Pd(2,4,6-Me₃pma)₂] (19a). Yield: 90%. IR(KBr/cm⁻¹): 3439 (O-H), 2962, 2926, 2873 (C-H), 1670, 1627, 1595, 1560 (C=O). ¹H NMR (DMSO-*d*₆) δ (ppm): 0.91-0.96 (t, 24H), 1.27-1.34 (m, 16H, *n*-Bu₄N⁺), 1.54-1.56 (m, 16H, *n*-Bu₄N⁺), 2.07 (s, 6H, CH₃), 2.14-2.18 (d, 18H, CH₃), 3.13-3.18 (m, 16H, *n*-Bu₄N⁺), 6.63-6.69 (m, 4H, H_{aryl}). Anal. Calcd. for C₅₄H₉₄N₄O₆Pd (**19a**): C 64.74 H 9.46 N 5.59. Found: C 62.28 H 9.86 N 5.30 %.

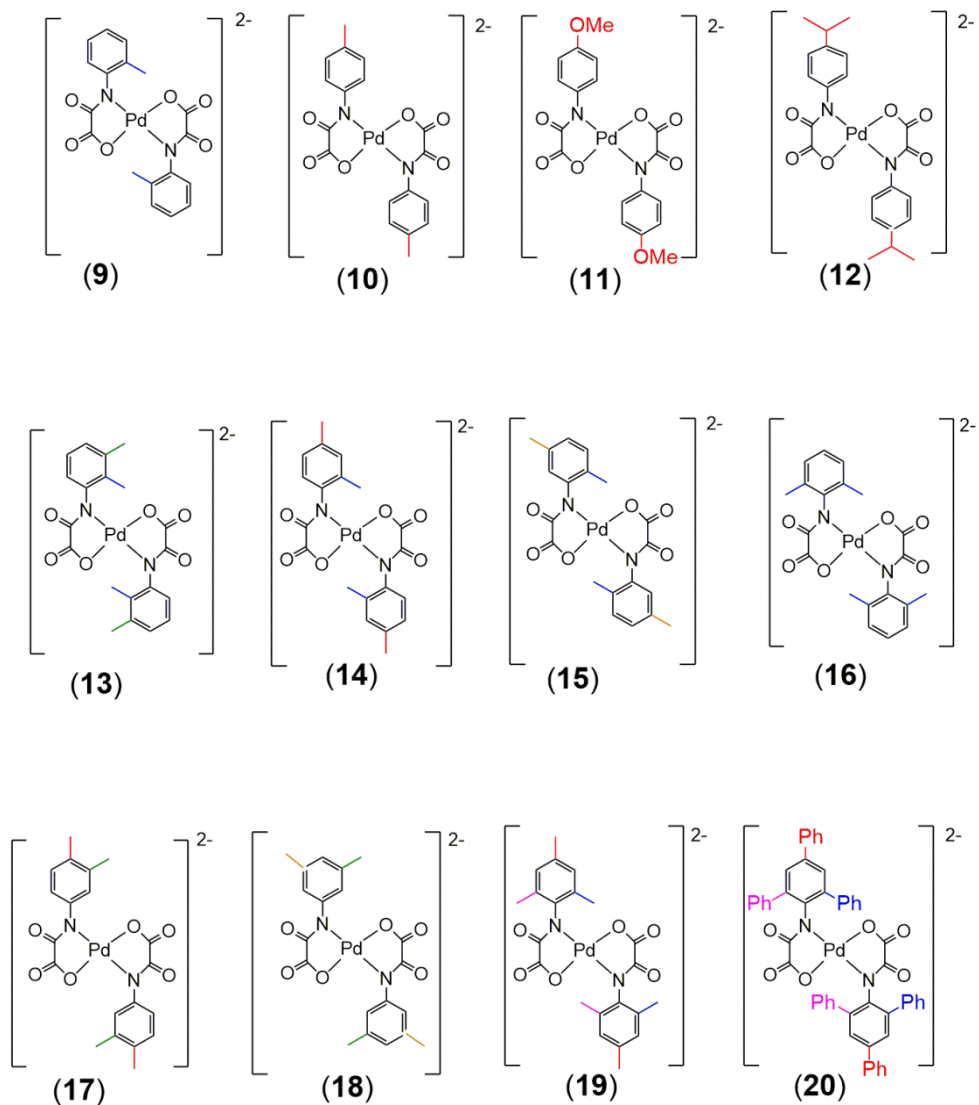
(*n*-Bu₄N)₂[Pd(2,4,6-Ph₃pma)₂] (20a). Yield: 15%. IR(KBr/cm⁻¹): 3422 (O-H), 3057, 3028 (C-H_{aryl}) 2962, 2930, 2873 (*n*-Bu₄N⁺), 1665, 1641, 1614, 1587 (C=O). Anal. Calcd. for C₉₀H₁₁₈N₄O₆Pd (**20a**): C 74.12 H 8.16 N 3.84. Found: C 74.28 H 8.86 N 3.98 %.

III.4. Results and discussion

Synthesis and IR Spectroscopy. The *N*-substituted oxamate ligands in **5-20** (Scheme 2 and 3) were easily prepared as the respective ethyl ester proligands by the straightforward condensation of the ethyl chlorooxoacetate with the corresponding aniline derivative in THF, in presence of Et₃N as a base at room temperature. They were isolated in very good yields (ca. 80–96%). Their IR spectra exhibit a typical absorption peak at ca. 3000 – 3300 cm⁻¹ for the N-H stretching vibration and two intense bands at ca. 1727 and 1677 cm⁻¹ which clearly correspond to the stretching modes of the ester and amide groups, respectively. ¹H and ¹³C NMR spectra provide additional support for the signal of the N-H amide hydrogen as well as those of the ethyl (CH₂CH₃) group of the ester. The lack of the N-H vibration band at ca. 3240 cm⁻¹ and the occurrence of two intense bands shifting to lower energies (ca. 1638 and 1600 cm⁻¹) in infrared spectra of **5-20** supports the deprotonation of the amide group and the hydrolysis of the ester group upon the coordination to the palladium(II) ion. The other hydrogen atoms of the oxamate ligands exhibited only slight changes in their chemical shifts compared with those of the corresponding free proligand. Finally, the crystal structure of **5-10**, **16**, **19** and **20** confirmed these spectroscopic features.



Scheme 2. Complexes **5-8** of formula [Pd(*N*-substituted oxamate ligand)₂]²⁻ with *n*-Bu₄N⁺ as counter ion.



Scheme 3. Complexes 9-20 of formula $[\text{Pd}(\text{N}$ -substituted oxamate ligand) $_{2}]^{2-}$ with $n\text{-Bu}_{4}\text{N}^{+}$ as counter ion.

X-ray structural determination for $(n\text{-Bu}_4\text{N})_2[\text{Pd}(2\text{-Mepma})_2] \cdot 4\text{H}_2\text{O}$ (**9**), $(n\text{-Bu}_4\text{N})_2[\text{Pd}(4\text{-Mepma})_2] \cdot 2\text{H}_2\text{O} \cdot \text{MeCN}$ (**10**), $(n\text{-Bu}_4\text{N})_2[\text{Pd}(4\text{-OMepma})_2]$ (**11**), $(n\text{-Bu}_4\text{N})_2[\text{Pd}(2,4,6\text{-Me}_3\text{pma})_2] \cdot 2 \text{ MeCN}$ (**19**) and $(n\text{-Bu}_4\text{N})_2[\text{Pd}(2,4,6\text{-Ph}_3\text{pma})_2] \cdot \text{CH}_3\text{CH}_2\text{OCH}_2\text{CH}_3$ (**20**)

Single crystal of **9-11**, **19** and **20** were mounted on a Bruker-Nonius X8-APEXII CCD area detector system and the data collection was performed at 100 K (**9**, **10**, **11** and **20**) and 296 K (**19**) by using graphite-monochromated Mo-K α radiation ($\lambda = 0.71073 \text{ \AA}$). The collected data were processed through the SAINT reduction and SADABS absorption software. The structures were solved by direct methods and subsequently completed by Fourier recycling by means of the SHELXTL-2013 software packages, then refined by the full-matrix least-squares refinements based on F^2 with all observed reflections.

Table 1. Selected bond lengths (\AA) and angles ($^\circ$) for **5-7**, **9-11**, **19** and **20**

Complex	Pd-N	Pd-O	C(1)-O(2)	C(2)-O(3)	C(1)-O(3)	N(1)-Pd-O(1)
5	2.0411(16)	1.9984(14)	1.226(3)	1.240(3)	1.297(3)	81.67(6)
6	2.014(4)	2.011(4)	1.214(7)	1.243(7)	1.292(7)	81.14(16)
7	2.0439(19)	2.0033(16)	1.225(3)	1.240(3)	1.302(3)	81.61(7)
9	2.0209(11)	2.0384(13)	1.2413(18)	1.2543(19)	1.309(2)	82.14(5)
10	2.0207(13)	2.0214(14)	1.217(2)	1.241(2)	1.300(2)	81.89(6)
11	2.0425(18)	2.0033(15)	1.227(3)	1.238(3)	1.303(3)	81.69(7)
19	1.996(13)	2.0170(19)	1.227(4)	1.218(4)	1.263(4)	81.78(10)
20	2.0225(10)	2.0258(11)	1.2345(15)	1.2463(16)	1.3013(17)	81.65(4)

*Crystal structures of 5-7 were described in *Chapter 1 – Part II*

The description of the structures is carried out for each by family of compounds: firstly complexes **5-7** described in *Chapter 1 – Part II*, secondly **9** and **10**, thirdly **11** and finally, complexes **19** and **20**.

Summary of the selected bond lengths (\AA) and angles ($^\circ$) of the complexes are compiled in Table 1. For crystallographic tables are grounded in Tables 2-3.

Table 2. Crystal data and structure refinement **9-11.**

	9	10	11
Formula	C ₂₇ H ₄₆ N ₃ O ₃ Pd _{0.50}	C ₂₇ H ₄₆ N ₃ O ₃ Pd _{0.50}	C ₂₅ H ₄₃ N ₂ O ₄ Pd
Mr	513.87	513.87	542.01
Crystal	Triclinic	Triclinic	Monoclinic
Space	<i>P</i> (-1)	<i>P</i> (-1)	<i>P</i> 2 ₁ / <i>c</i>
<i>a</i> / Å	10.8293(16)	11.8546(9)	9.7934(5)
<i>b</i> / Å	11.8316(17)	12.5442(9)	16.3308(8)
<i>c</i> / Å	12.5466(19)	12.9348(9)	16.0994(8)
α / °	78.025(6)	104.059(3)	90
β / °	79.152(6)	115.455(3)	95.392(3)
γ / °	66.646(6)	104.241(3)	90
<i>V</i> / Å ³	1433.7(4)	1544.04(19)	2563.4(2)
<i>Z</i>	2	2	4
<i>D</i> _c / g cm ⁻³	1.190	1.105	1.404
<i>T</i> / K	100(2)	293(2)	100(2)
μ / mm ⁻¹	0.373	0.347	0.756
<i>F</i> (000)	552	552	1140
Theta range for data collection (°)	1.67 to 35.29	1.90 to 29.04	1.780 to 26.359
Index ranges	-17 ≤ <i>h</i> ≤ 17, -11 ≤ <i>k</i> ≤ 18, -18 ≤ <i>l</i> ≤ 19	-14 ≤ <i>h</i> ≤ 15, -17 ≤ <i>k</i> ≤ 16, -17 ≤ <i>l</i> ≤ 16	-11 ≤ <i>h</i> ≤ 12, -20 ≤ <i>k</i> ≤ 20, -20 ≤ <i>l</i> ≤ 20
Reflections collected	20008	37311	60762
Refinement method	Full-matrix least-squares on <i>F</i> ²		
Independent reflections	10679 [<i>R</i> (int) = 0.0221]	7208 [<i>R</i> (int) = 0.0251]	5215 [<i>R</i> (int) = 0.0862]
Data/restraints parameters	10679/0/316	7208/0/310	5215/0/292
Goodness-of-fit on <i>F</i> ²	1.121	0.966	1.209
Final <i>R</i> indices [<i>I</i> > 2σ(<i>I</i>)]	<i>R</i> ₁ = 0.0412, <i>wR</i> ₂ = 0.1280	<i>R</i> ₁ = 0.0334, <i>wR</i> ₂ = 0.1026	<i>R</i> ₁ = 0.0330, <i>wR</i> ₂ = 0.0828
<i>R</i> indices (all data)	<i>R</i> ₁ = 0.0438, <i>wR</i> ₂ = 0.1342	<i>R</i> ₁ = 0.0388, <i>wR</i> ₂ = 0.1116	<i>R</i> ₁ = 0.0478, <i>wR</i> ₂ = 0.0939
Largest diff. peak and hole (e Å ⁻³)	2.423 and -0.871	0.560 and -0.504	0.482 and -0.481

$$R_1 = \frac{\sum(|F_o| - |F_d|)}{\sum|F_o|}, wR_2 = \left\{ \frac{\sum[w(F_o^2 - F_c^2)^2]}{\sum[w(F_o^2)^2]} \right\}^{1/2}$$

Table 3. Crystal data and structure refinement 19-20.

	19	20
Formula	C ₂₉ H ₄₉ N ₃ O ₃ Pd _{0.50}	C ₉₂ H ₁₂₄ N ₄ O ₈ Pd
Mr	540.91	1520.35
Crystal	Triclinic	Monoclinic
Space	<i>P</i> (-1)	<i>P</i> 2 ₁ / <i>c</i>
<i>a</i> / Å	11.769(4)	14.9124(10)
<i>b</i> / Å	11.933(5)	14.4942(11)
<i>c</i> / Å	12.808(5)	19.9007(16)
α / °	73.962(16)	90
β / °	78.670(16)	97.128(4)
γ / °	65.665(14)	90
<i>V</i> / Å ³	1568.1(11)	4268.2(6)
<i>Z</i>	2	2
<i>D</i> _c / g cm ⁻³	1.146	1.183
<i>T</i> / K	293(2)	100(2)
μ / mm ⁻¹	0.344	0.273
<i>F</i> (000)	582	1628
Theta range for data collection (°)	1.662 to 31.632	1.38 to 33.91
Index ranges	-15 ≤ <i>h</i> ≤ 9, -16 ≤ <i>k</i> ≤ 16, -14 ≤ <i>l</i> ≤ 16	-23 ≤ <i>h</i> ≤ 20, -21 ≤ <i>k</i> ≤ 22, -31 ≤ <i>l</i> ≤ 29
Reflections collected	12639	102691
Refinement method	Full-matrix least-squares on <i>F</i> ²	
Independent reflections	6564 [<i>R</i> (int) = 0.0340]	17060 [<i>R</i> (int) = 0.0327]
Data/restraints parameters	6564/0/329	17060/0/487
Goodness-of-fit on <i>F</i> ²	1.090	1.208
Final <i>R</i> indices [<i>I</i> > 2σ(<i>I</i>)]	<i>R</i> ₁ = 0.0495, <i>wR</i> ₂ = 0.1417	<i>R</i> ₁ = 0.0422, <i>wR</i> ₂ = 0.1447
<i>R</i> indices (all data)	<i>R</i> ₁ = 0.0614, <i>wR</i> ₂ = 0.1571	<i>R</i> ₁ = 0.0554, <i>wR</i> ₂ = 0.1566
Largest diff. peak and hole (e Å ⁻³)	1.239 and -0.731	1.390 and -1.043

$$R_1 = \sum(|F_o| - |F_d|) / \sum|F_o|. \quad wR_2 = \{\sum[w(F_o^2 - F_c^2)^2] / \sum[w(F_o^2)^2]\}^{1/2}$$

Description of the structures. Compounds **9** and **10** which crystallize in the triclinic space group *P*-1 show the occurrence of centrosymmetric mononuclear $[\text{Pd}(\text{L})_2]^{2-}$ units (Figure 1) and $n\text{-Bu}_4\text{N}^+$ as counter cations. Each palladium(II) ion is four-coordinate with two amidate-nitrogen and two carboxylate-oxygen atoms from the two oxamate ligands in a *trans* arrangement building a distorted square-planar surrounding. The reduced bite of the bidentate oxamate [82.14(5) $^\circ$ (**9**) and 81.89(6) $^\circ$ (**10**)] accounts for the deviations of the ideal value of 90 $^\circ$ for the square planar surrounding.

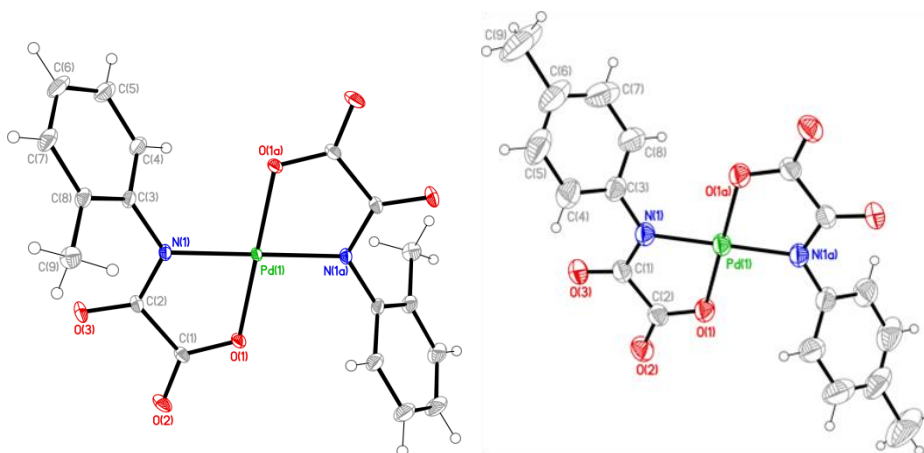


Figure 1. Anionic complexes **9** ($[\text{Pd}(2\text{-Mepma})_2]^{2-}$, left) and **10** ($[\text{Pd}(4\text{-Mepma})_2]^{2-}$, right) with $n\text{-Bu}_4\text{N}^+$ as counter ion.

The average Pd–N/Pd–O bond lengths for **9/10** are 2.0209(11)/2.0207(13) Å and 2.0384(13)/2.0214(14) Å, respectively (see Appendix B). These values agree with those found in the mononuclear species $\text{Na}[\text{Pd}(\text{Hpba})] \cdot 2\text{H}_2\text{O}$ [H_4pba = 1,3-propylenebis(oxamic acid)] [1.97/2.04 Å] and $(\text{PPh}_4)_2[\text{Pd}(\text{opba})] \cdot 2\text{H}_2\text{O}$ [H_4opba = 1,2-phenylenebis(oxamic acid)] [1.93/2.05 Å].^{80,81} The values of the dihedral angle between the basal plane at the palladium(II) ion and the mean plane of the oxamate groups for **9/10** are 7.4(1)/3.9(1) $^\circ$, whereas those between the square plane and the phenyl ring are 51.1(1)/52.2(1) $^\circ$.

The values of the peripheral C(1)-O(2)/C(2)-O(3) bond distances [1.2413(18)/1.2543(19) Å (**9**) and 1.217(2)/1.241(2) Å (**10**)] are somewhat shorter than the inner C(1)-O(1) bond [1.309(2) Å (**9**)/1.300(2) Å (**10**)] in agreement with the greater double bond character of the former carbonyl groups.

The distances and angles of each tetrahedral *n*-Bu₄N⁺ cations in **9** and **10** are as expected. The little discrepancy in the N-C and C-C distances and in the N-C-C and C-C-C angles arises from crystallographic disorder, which is quite a common feature observed in most of the crystals containing this organic cation.

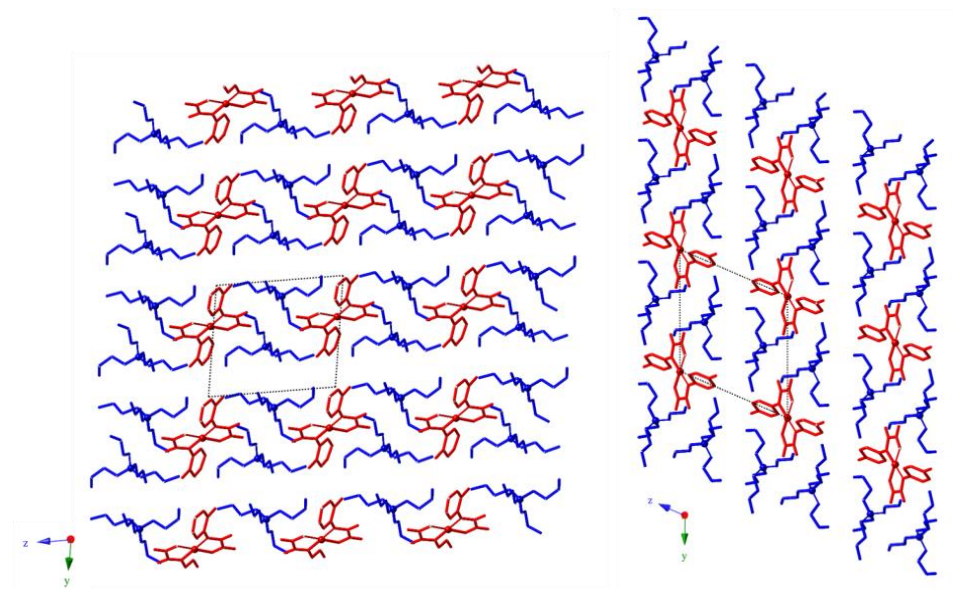


Figure 2. Crystal packing of **9** (right) and **10** (left) showing the relative positions of the anionic complexes (red) and tetra-*n*-butylammonium cations (blue). The solvent molecules have been omitted for clarity.

The complex anions of **9** and **10** are well separated from each other by the bulky *n*-Bu₄N⁺ cations in the resulting three-dimensional ionic lattices (Figure 2) and no π - π stacking interactions are present. The values of the shortest Pd \cdots Pd distances are 10.829(1) Å (**9**) and 11.855(1) Å (**10**) [Pd(1) \cdots Pd(1b); (b) = -1+x, y, z]. Very weak but non-negligible C-H \cdots O type interactions [C \cdots O = 3.5-3.6 Å] involving the methyl groups from the aceto-

nitrile molecules and the $n\text{-Bu}_4\text{N}^+$ cations with the peripheral oxygen atoms of the oxamate groups contribute to the stabilization of the structure. Furthermore very weak $\text{C-H}\cdots\text{N}$ interactions [$\text{C}\cdots\text{N} = 3.6\text{-}3.8 \text{ \AA}$] take place between the acetonitrile molecules and the methyl groups from the $n\text{-Bu}_4\text{N}^+$ cations.

Compound **11** which crystallizes in the monoclinic space group $P2_1/c$ shows the occurrence of centrosymmetric mononuclear $[\text{Pd}(4\text{-MeOpma})_2]^{2-}$ units (Figure 3, left) and $n\text{-Bu}_4\text{N}^+$ as counter cations. Each palladium center is four-coordinate with two amidate-nitrogen [N(1) and N(1a)] and two carboxylate-oxygen atoms [O(1) and O(1a)] building a slightly distorted square-planar surrounding. The reduced bite angle of the chelating oxamate is $81.69(7)^\circ$ accounts for the deviations from the ideal geometry; in fact, the Pd(II) ion and the atoms building its surrounding lie exactly on a plane for symmetry reasons.

The Pd-N/Pd-O bond lengths in **11** are $2.0425(18)/2.0033(15) \text{ \AA}$ value which compare well with those found in the oxamato-containing palladium(II) complexes **1**, **9**, **10** in previous works and literature⁷⁹⁻⁸².

The values of the peripheral C(1)-O(2)/C(2)-O(3) bond distances [$1.227(3)/1.238(3) \text{ \AA}$] are somewhat shorter than the inner C(1)-O(1) bond [$1.303(3) \text{ \AA}$] in agreement with the greater double bond character of the former carbonyl groups. The plane at the Pd(II) ion and the mean plane of the oxamate group are almost coplanar [the value of the dihedral angle between these two planes (φ) is $7.8(3)^\circ$, whereas the one between the square plane at the metal center and the phenyl ring is $31.8(3)^\circ$].

The anionic entities in the crystal packing of **11** are well separated from each other because of the presence of the bulky $n\text{-Bu}_4\text{N}^+$ cations, the shortest intermetallic Pd(1) \cdots Pd(1b) separation being 9.793 \AA . This value is shorter than those in the **9** and **10**. The crystal packing of **11** is shown in Figure S1 (Appendix B).

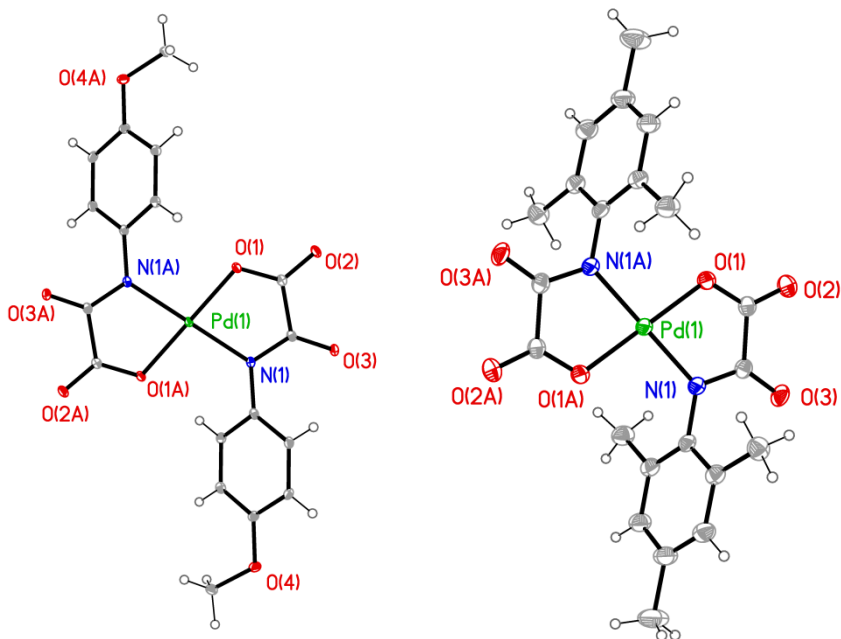


Figure 3. Perspective drawing of the anionic complexes **11** ($[\text{Pd}(4\text{-MeOpma})_2]^{2-}$, left) and **19** ($[\text{Pd}(2,4,6\text{-Me}_3\text{pma})_2]^{2-}$, right) with $n\text{-Bu}_4\text{N}^+$ as counter ion.

Compounds **19** and **20** crystallize in the triclinic $P\bar{1}$ and the monoclinic $P2_1/c$ space groups, respectively. Their structures consist of centrosymmetric mononuclear $[\text{Pd}(\text{L})_2]^{2-}$ units and $n\text{-Bu}_4\text{N}^+$ as counter cations [Figure 3, right (**19**) and 4 (**20**)]. Each palladium(II) ion is four-coordinate with two amidate-nitrogen and two carboxylate-oxygen atoms from the two oxamate ligands in a *trans* arrangement building a distorted square-planar surrounding. The reduced bite of the bidentate oxamate [$81.78(10)^\circ$ (**19**) and $81.65(4)^\circ$ (**20**)] accounts for the deviations of the ideal value of 90° for the square planar surrounding.

The average Pd–N/Pd–O bond lengths for **19** and **20** are $1.996(3)/2.0170(19)$ Å and $2.0225(10)/2.0258(11)$ Å, respectively. These values agree with those found in the mononuclear oxamato-containing palladium(II) complexes **1**, **9**, **10**, $\text{Na}[\text{Pd}(\text{Hpba})] \cdot 2\text{H}_2\text{O}$ and $\text{K}_2[\text{Pd}(\text{opba})] \cdot 2\text{H}_2\text{O}$, **5**, **6**, **7** and **11** [average Pd–N/Pd–O distances of $2.020(1)/2.009(1)$, $2.0209(11)/2.0384(13)$, $2.0207(13)/2.0214(14)$, $1.970/2.040$,

1.928/2.055, 2.0411(16)/1.9989(14), 2.014(4)/2.011(4), 2.0439(19)/2.0033(16) and 2.0425(18)/2.0033(15) Å, respectively]⁷⁹⁻⁸².

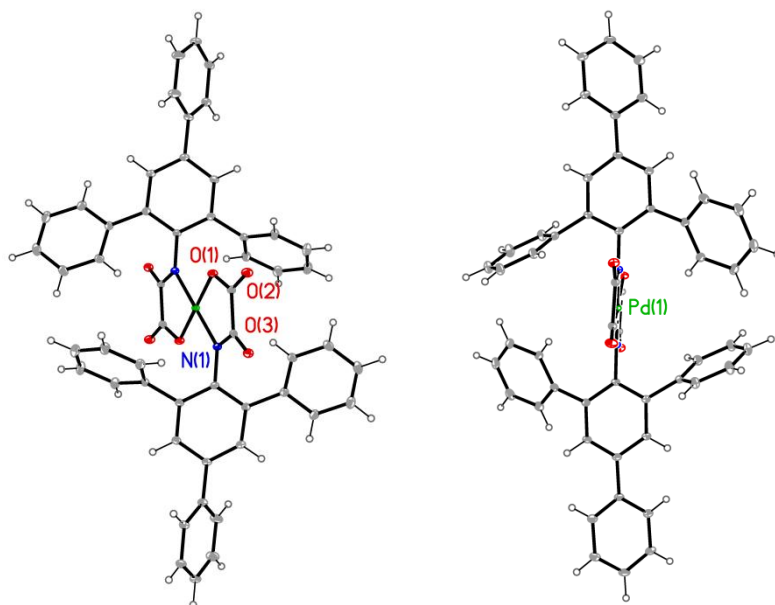


Figure 4. Views of the structure of the anionic entity $[\text{Pd}(\text{2,4,6-Ph}_3\text{pma})_2]^{2-}$ of **20**.

The values of the dihedral angle between the basal plane at the palladium(II) ion and the mean plane of the oxamate groups for **19/20** are (φ) 1.9(1)/3.2(1) $^\circ$, whereas those between the square plane and the phenyl ring are (Φ) 109.5(1)/69.5(1) $^\circ$. As in the previous structures, the values of the peripheral C(1)-O(2) and C(2)-O(3) bond distances [1.227(4) and 1.218(4) Å (**19a**) and 1.2345(15) and 1.2463(16) Å (**20**)] are somewhat shorter than the inner C(1)-O(1) bonds [1.263(4) (**19**) and 1.3013(17) Å (**20**)] in agreement with the greater double bond character of the former carbonyl groups.

As observed in the preceding structures, the crystal packing of **19-20** show that the anionic species are well separated from each other due to the presence of the bulky $n\text{-Bu}_4\text{N}^+$ organic cations, the shortest intermetallic Pd(1) \cdots Pd(1b) separation being 11.769(3) (**19**) and 12.310(3) (**20**) Å. These values are the largest distances compared with those in **5-7** and **9-11**.

III.5. Catalytic properties

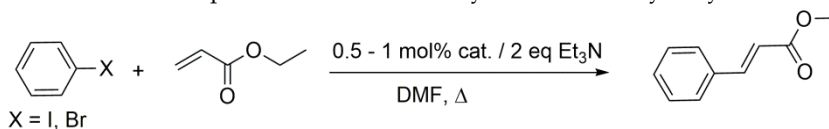
Compounds **5-19** are found to catalyze carbon-carbon cross-coupling reactions, specifically Heck and Suzuki reactions.

Firstly, we have explored the Heck reaction type using homogeneous catalysis (DMF) with complexes **5a-15a** and **17a-19a**. Secondly, we have extended this study to the same Heck reaction type with complexes **7a** to **12a** but using an ionic liquid as medium. Furthermore, complexes **5a-7a** and **13a-19a** were tested in homogeneous catalysis for the Suzuki reaction type whereas **6a-12a** were checked in ionic liquid media for the same reaction.

III. 5.1. Heck reaction – Homogeneous catalysis

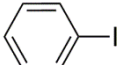
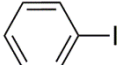
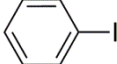
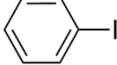
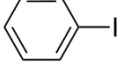
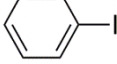
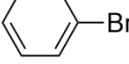
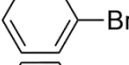
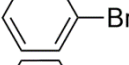
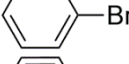
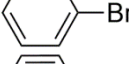
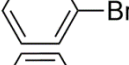
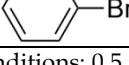
The Heck reaction was studied by using different aryl halides and olefins with complexes **5a-15a** and **17a-19a** in DMF as solvent. Et₃N is the base which provided better results. The temperature was either 80 or 120 °C and inert atmosphere was not needed to carry out these reactions. All catalysts were very active under such conditions and with iodobenzene as aryl halide (Table 4). However, electron-withdrawing and electron-donating groups as substituents at the oxamate ligand, aimed at influencing their activity with the less reactive aryl halides like bromobenzene, in homogeneous catalysis (DMF) did not work out.

Table 4. Scope of Heck reaction of aryl halide and ethyl acrylate



Entry ^a	Aryl halide	Catalyst	Time (h)	Temp (°C)	Yield ^b	TON	TOF (h ⁻¹)
1		8a	3	80	84	84	28
2		9a	3	80	90	90	30
3		10a	3	80	92	92	31

Table 4 contn.

4		14a	3	80	96	96	32
5		15a	3	80	99	99	33
6		17a	3	80	86	86	29
7		18a	3	80	93	93	31
8		19a	3	80	74	74	25
9		[Pd₃(OAc)₆]	3	120	88	88	30
10		5a	3	120	-	-	-
11		6a	3	120	-	-	-
12		7a	3	120	-	-	-
13		11a	3	120	10	2	-
14		12a	3	120	-	-	-
15		[PdCl₂]	3	120	-	-	-
16		[Pd₃(OAc)₆]	3	120	1	-	-

^aReaction conditions: 0.5 mmol iodobenzene, 0.75 mmol ethyl acrylate, 0.5 – 1 mmol% cat., 1 mmol Et₃N, 3 h, 120 °C in DMF. ^bDetermined by GC-MS analysis using perfluorotributylamine (PFTBA) as internal standard.

As illustrated in Table 5, three olefins bearing electron-donating and electron-withdrawing groups coupled with iodobenzene afforded the olefin product in excellent yields. The complexes exhibited higher activity with electron-withdrawing groups relative to electron-donating groups on the olefin in the Heck reaction.

Table 5. Scope of Heck reaction of iodobenzene with olefins.

Entry ^a	Olefin	Catalyst	Time (h)	Temp (°C)	Yield ^b	TON	TOF (h ⁻¹)
1		9a	3	80	90	90	30
2		9a	3	80	99	99	33
3		9a	3	80	99	99	33
4		10a	3	80	92	92	31
5		10a	3	80	96	96	32
6		10a	3	80	100	100	33

^a Reaction conditions: 0.5 mmol iodobenzene, 0.75 mmol acrylate, 1 mmol% cat., 1 mmol Et₃N, 3 h, 80 °C in DMF. ^bDetermined by GC-MS analysis using PFTBA as internal standard.

Interestingly, working in the open air and as in *Chapter 1*, under the described homogeneous conditions, **8a-10a** and **14a-19a** proved to be efficient (pre)catalysts without clear formation of inactive palladium black which stop the catalytic reactions^{46,83-86} (Figure 5).

Formation of palladium black was observed for a commercial palladium catalyst trying to carry out the Heck reaction with bromobenzene and ethyl acrylate, using our conditions in DMF as shown in Figure 5. However, when the reaction was performed with the oxamate-containing palladium(II) complexes **5a-7a** and **11a-12a**, no inactive palladium(0) black occurred (Figure 6).

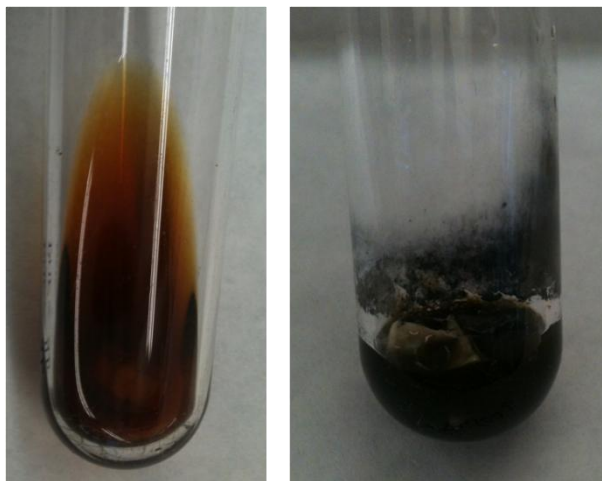


Figure 5. Samples of Heck coupling reaction of iodobenzene and ethyl acrylate in DMF at 80-120 °C after 3 hours, catalyzed by **19a** (left) and $[\text{Pd}_3(\text{OAc})_6]$ (right).

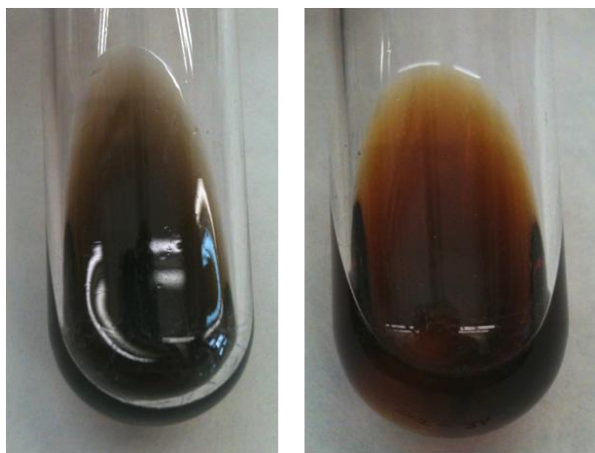


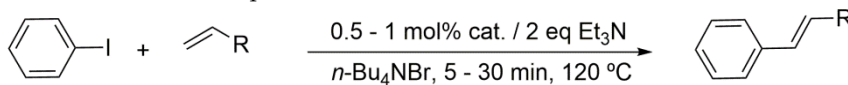
Figure 6. From left to right: $[\text{Pd}_3(\text{OAc})_6]$ and **11a** after Heck reaction between bromobenzene and ethyl acrylate in DMF at 120 °C, during 3 hours.

III. 5.2. Heck reaction – Ionic liquid medium

Once demonstrated that these kind of anionic complexes of *N*-substituted oxamate are catalytically active for Heck reaction in an organic solvent as DMF, it seemed appropriated to move towards greener solvents, as ionic liquids for instance. These type of solvents, i.e. molten salts with low melting points, seemed to be promising over conventional reaction conditions, making easier the separation of the product by simple extraction or distillation from the ionic “solvent”, a feature which allows recycling the whole catalyst-solvent system. The family of bis(*N*-substituted oxamate)palladate(II) precatalysts **5a-7a**, **11a** and **12a** which present different electron and steric effects have been tested using *n*-Bu₄NBr as solvent. In this respect, it deserves to be noted that this ionic liquid has been used as an additive for this type of reactions, its role being qualified as essential.^{70,87-94} In our case, the catalyst and solvent recovery and recycling is achieved by working with anionic bis(*N*-substituted oxamate)palladate(II) complexes in *n*-tetrabutylammonium bromide as a green solvent.

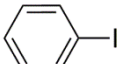
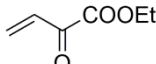
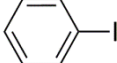
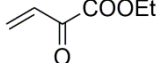
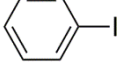
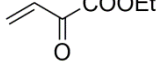
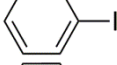
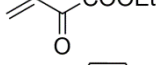
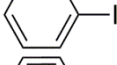
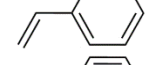
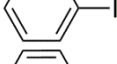
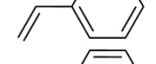
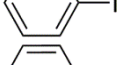
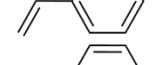
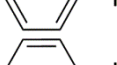
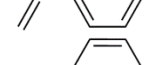
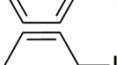
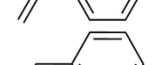
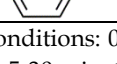
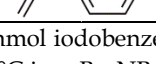
So, having in mind the idea of recycling, high yields were obtained for the Heck reaction between iodobenzene and ethyl acrylate or styrene using 0.5 – 1 mol% cat, without inert atmosphere and with very short reactions times. Interestingly, small variations of the electron-withdrawing or electron-donating groups or the steric effects of the *para*- substituent of the oxamate ligand, allowed to increase the catalytic reactivity by using less quantity of catalyst and decreasing the reaction times but without differences between them (Table 6, see entries 8-12).

Table 6. Scope of Heck reaction of iodobenzene and olefin



Entry ^a	Aryl halide	Olefin	Catalyst	Time (min)	Yield ^b	TON	TOF (h ⁻¹)
1			10a	30	99	99	198
2			5a	5	99	198	2376

Table 6 contn.

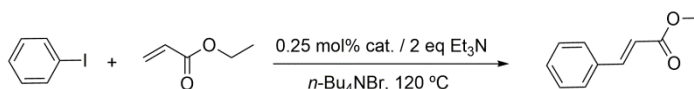
3			6a	5	99	198	2376
4			7a	5	99	198	2376
5			11a	5	99	198	2376
6			12a	5	99	198	2376
7			10a	30	69	69	138
8			5a	30	99	198	396
9			6a	30	99	198	396
10			7a	30	99	198	396
11			11a	30	99	198	396
12			12a	30	99	198	396

^aReaction conditions: 0.5 mmol iodobenzene, 0.75 mmol ethyl acrylate, 0.5 – 1 mmol% cat., 1 mmol Et₃N, 5-30 min, 120 °C in *n*-Bu₄NBr. ^bDetermined by GC-MS analysis using PFTBA as internal standard.

As shown in Table S1, high efficiency in recovery and recycling (at last 8 catalytic runs) is observed by using complexes **5a-7a**, **11a** and **12a** for a Heck coupling of aryl iodides (0.5 mmol) and ethyl acrylate (0.75 mmol, entries 1-5) or styrene (0.75 mmol, entries 6-10) and Et₃N (1 mmol). An homogenous yield value of 99% is achieved in each run for **5a-7a**, **11a** and **12a** with very short reaction times (5 minutes, entries 1-5 in Table S1; TOF ca. 2376 h⁻¹, see Table 6). Yields about 99% are also obtained by using a less activate olefin as stilbene although the reaction time is increased (30 minutes, entries 6-10 in Table S1; TOF ca. 396 h⁻¹, see Table 6). These short reaction times and the green solvent used allow not only to work in mild reaction conditions but also to save energy costs.

When the amount of catalyst is decreased until 0.25 mol%, the homogeneity of the yield in the iodobenzene and ethyl acrylate reaction is lost, but in general it is improved with the successive runs attaining values in the range 83-99% for the eight run [see Table 7 (top)]. These features demonstrates that **5a-7a**, **11a** and **12a** allow the recovery and recycling of the anionic bis(*N*-substituted oxamate)palladate(II) complexes without leaching. It deserves to be noted that reaction times of 5 min are kept with high TOF values [ca. 4800 h⁻¹, Table 7 (bottom)].

Table 7. (Top) Yields and (bottom) TON and TOF (h⁻¹) values of the Heck reaction of iodobenzene and ethyl acrylate in *n*-Bu₄NBr

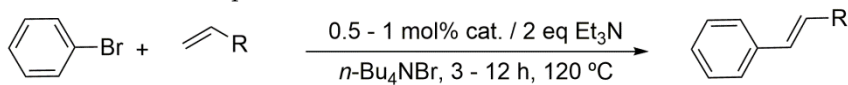


Entry ^a	Catalyst	Run - Yield (%) ^b							
		1	2	3	4	5	6	7	8
1	5a	6	94	99	99	97	98	99	99
2	6a	63	79	94	93	94	96	97	97
3	7a	69	12	53	77	81	86	88	83
4	11a	67	85	94	99	96	99	97	98
5	12a	85	99	99	99	99	80	84	84

Entry/ cat. ^a	Run - TON ^b / TOF (h ⁻¹)							
	1	2	3	4	5	6	7	8
1/ 5a	24/293	377/4525	400/4800	400/4800	388/4662	393/4719	400/4800	394/4732
2/ 6a	253/3036	316/3789	374/4491	374/4487	378/4533	386/4732	388/4758	386/4735
3/ 7a	277/3323	78/576	213/2561	307/2685	322/3869	345/4136	354/4242	333/3990
4/ 11a	266/3193	339/4068	376/4516	400/4800	383/4598	400/4800	387/4645	391/4690
5/ 12a	342/4100	400/4800	400/4800	400/4800	400/4800	319/3828	336/4035	338/4053

^a Reaction conditions: 0.5 mmol iodobenzene, 0.75 mmol ethyl acrylate, 0.25 mmol% cat., 1 mmol of Et₃N, 5 min, 120 °C in *n*-Bu₄NBr. ^bDetermined by GC-MS analysis using PFTBA as internal standard.

Table 8. Scope of Heck reaction of bromobenzene and olefins



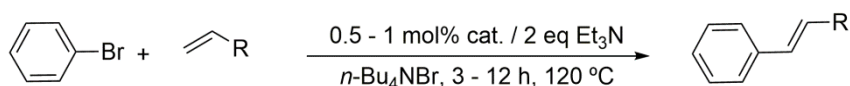
Entry	Aryl halide	Olefin	Catalyst	Time (h)	Yield	TON	TOF (h ⁻¹)
1			10a	12	99	99	8
2			5a	3	99	198	66
3			6a	3	90	180	60
4			7a	3	91	182	61
5			11a	3	82	163	54
6			12a	3	89	177	59
7			[PdCl₂]	3	0	0	0
8			[Pd₃(OAc)₆]	3	0	0	0
9			[Pd(dba)₂]	3	74	148	37
10			10a	12	97	97	8
11			5a	4	92	184	46
12			6a	4	76	152	38
13			7a	4	77	155	39
14			11a	4	92	184	46
15			12a	4	90	179	45

^a Reaction conditions: 0.5 mmol bromobenzene, 0.75 mmol ethyl acrylate, 0.5 - 1 mmol% cat., 1 mmol Et₃N, 3-12 h, 120 °C in *n*-Bu₄NBr. (Yield) Determined by GC-MS analysis using PFTBA as internal standard.

Although iodobenzene derivatives are the most common and reactive chemicals for carbon-carbon cross-coupling reactions,^{18,20,21,24,95-98} good yields were obtained by introducing bromobenzene as aryl halide (Table 8) in *n*-Bu₄NBr as ionic liquid medium.

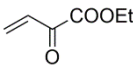
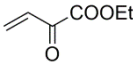
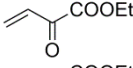
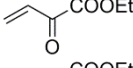
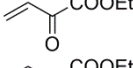
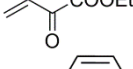
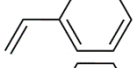
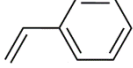
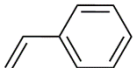
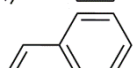
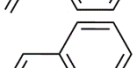
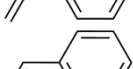
Once more, the variation of the substituent in *para*- position of the oxamate ligand greatly modifies the catalytic activity. The behavior of these complexes (**5a-7a**, **11a** and **12a**) when working with a less reactive aryl halide, such as bromobenzene, is shown in Tables 8 and 9. One can see therein the increase of the reactions times from 5 min (entries 1-5 in Table 6) to 3 hours (entries 1-5 in Table 8) when using ethyl acrylate or from 30 minutes (entries 6-10 in Table 6) to 4 hours (entries 1-5 in Table 8) by using styrene. Moreover, complexes **5a-7a**, **11a** and **12a** are more efficient than the commercial catalysts [PdCl₂] and [Pd₃(OAc)₆] and even [Pd(*dba*)₂]⁴² under our reaction conditions (entries 6-8 in Table 8). The fact that the catalytic activity using bromobenzene (Tables 8 and 9) is somewhat lower and more variable than using iodobenzene (Table 6) is due to their different bond dissociation energies (81 and 65 kcal/mol for C-Br and C-I, respectively).⁹⁹ The increase of the yield in the reaction of the bromobenzene could be achieved by working at higher temperatures but we are limited to ca. 130 °C which corresponds to the temperature of decomposition of *n*-Bu₄NBr.⁶⁷ Having reached this point, one may consider if it is worth the effort, thinking at energy costs (green chemistry), to carry out the reaction with less expensive chemicals during 4 hours (bromobenzene and styrene; entries 6-10 in Table 8) *vs.* more expensive materials during 30 minutes (iodobenzene and styrene; entries 9-13 in Table 6).

Table 9. Heck reaction of bromobenzene and olefins after different runs



Entry ^a	Olefine	Catalyst	Time (h)	Runs - Yield ^b (%)							
				1	2	3	4	5	6	7	8
1		10a	12	99	60	28	14	7	4	-	-
2		5a	3	99	99	92	86	84	79	78	61
3		6a	3	72	87	90	84	87	80	78	70

Table 9 contn

4		7a	3	84	91	91	87	88	83	80	72
5		11a	3	18	64	80	77	82	77	76	71
6		12a	3	75	89	85	84	82	82	76	69
7		[PdCl ₂]	3	0	0	0	0	0	0	- ^c	- ^c
8		[Pd ₃ (OAc) ₆]	3	0	0	0	0	0	0	- ^c	- ^c
9		[Pd(dba) ₂]	3	62	68	74	73	70	60	- ^c	- ^c
10		7a	12	69	68	41	28	12	-	-	-
11		5a	4	92	86	66	56	62	83	73	67
12		6a	4	66	76	75	72	70	74	67	68
13		7a	4	0	58	65	75	68	73	69	77
14		11a	4	36	92	72	61	70	70	70	68
15		12a	4	80	90	82	77	74	72	72	65

^a Reaction conditions: 0.5 mmol bromobenzene, 0.75 mmol ethyl acrylate, 0.5 - 1 mmol% cat., 1 mmol of Et₃N, 3-12 h, 120 °C in *n*-Bu₄NBr. ^bDetermined by GC-MS analysis using PFTBA as internal standard. ^c not tested.

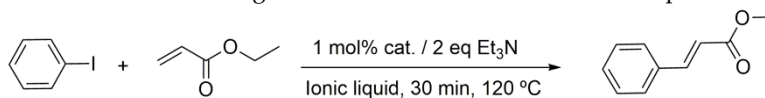
The characteristic step to stop a carbon-carbon coupling reaction is the formation of inactive metallic palladium,^{84,85,100} as occurs in our catalytic conditions working with commercially available palladium catalysts such as [PdCl₂] and [Pd₃(OAc)₆] (first two pictures in Figure 6). However, if the reaction is performed with the oxamate-containing palladium(II) complexes, the formation of the inactive palladium black does not occur (last two pictures in Figure 6).



Figure 6. From left to right: $[\text{PdCl}_2]$, $[\text{Pd}_3(\text{OAc})_6]$, **6a** and **11a**, after Heck reaction between bromobenzene and ethyl acrylate in *n*-Bu₄NBr at 120 °C and 3h.

It is important to outline that *n*-Bu₄NBr provided the best results as compared to other tested salts such as *n*-Bu₄NCl the imidazolium ones BMIMBr and BIMIMPF₆ (Table 10). Contrary to the tetrahedral shape of the tetraalkylammonium, the imidazolium cation has a planar structure, a feature that makes easier its aggregation with the planar complex anions. This would decrease the anion availability for the stabilization of the catalytically active Pd(0) species, which may be formed in the reaction mixture either by thermal reduction of the Pd(II) precatalyst or by an excess of the olefin itself as well as the Et₃N used as base, during the catalytic process.^{101,102} *n*-Bu₄NBr was described as an excellent reaction medium for the stabilization of catalytically active palladium and copper species for carbon-carbon coupling reactions via electrostatic interactions.^{103,104}

Table 10. Screening of Heck reactions in different ionic liquids

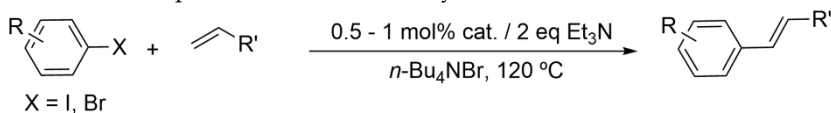


Entry ^a	Ionic Liquid	Catalyst	Time (min)	Temp (°C)	Yield ^b	TON	TOF (h ⁻¹)
1	<i>n</i> -Bu ₄ NBr	10a	30	120	99	99	198
2	<i>n</i> -Bu ₄ NCl	10a	30	120	88	88	176
3	BMIMBr	10a	30	120	85	85	170
4	BIMIMPF ₆	10a	30	120	66	66	132

^aReaction conditions: 0.5 mmol iodobenzene, 0.75 mmol acrylate, 1 mmol% cat., 1 mmol Et₃N, 30 min, 120 °C in ionic liquids. ^bDetermined by GC-MS analysis using PFTBA as internal standard.

Similar results have been obtained with the use of different aryl halides and olefins as shown in Tables 11 and S5. Very short reaction times (5 minutes) and high yields (ca. 90%) are observed when working with aryl iodide derivatives (entries 1-5 in Table 11). An increase of the reaction times to achieve the same good yields is required for the bromo derivatives (entries 5 and 7 in Table 10), as observed above. Finally, it deserves to be noted that this type of palladium(II) complexes are unable to activate less active aryl halides such as chlorobenzenes (entry 9 in Table 11) which need higher temperatures to react ($T > 120\text{ }^{\circ}\text{C}$),¹⁰⁵⁻¹⁰⁸ a feature that precludes the use of the *n*-Bu₄NBr as solvent.

Table 11. Scope de Heck reaction of aryl halides and ofefins in *n*-Bu₄NBr

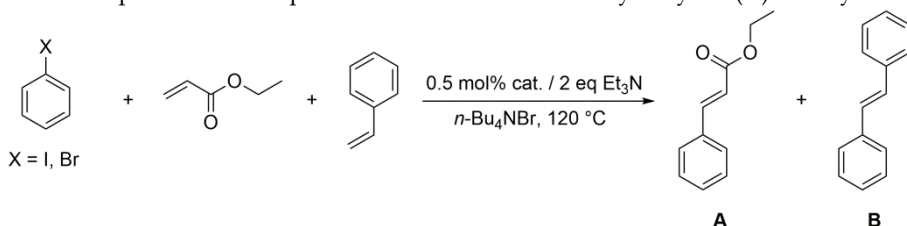


Entry ^a	Aryl Halide	Olefin	Time	Catalyst Yield ^b (%)					
				10a	5a	6a	7a	11a	12a
1			5 min	64 ^d	75	88	97	90	92
2			5 min	99 ^d	89	99	99	89	88
3			5 min	99 ^d	90	85	96	99	99
4			5 min	99 ^d	93	93	98	99	99
5			5 min	99 ^d	93	92	99	99	99
6			15 min	99 ^d	99	99	95	99	99
7			1.5 h	c	99	99	99	99	99
8			4 h	c	92	94	93	91	94
9			72 h	c	c	13	c	c	c

^a Reaction conditions: 0.5 mmol aryl halide, 0.75 mmol acrylate, 0.5 - 1 mmol% cat., 1 mmol Et₃N, 120 °C in *n*-Bu₄NBr. ^bDetermined by GC-MS analysis using PFTBA as internal standard. ^cNot tested. ^d30 min reaction time and 1 mol% cat.

Finally, the competing reactions between aryl halides and two different olefins (ethyl acrylate and styrene) was investigated. These reactions were carried out at two different times, because of the reaction with ethyl acrylate runs faster than that with styrene (Table 12). These results clearly show a higher activity for ethyl acrylate compared to styrene in the Heck reaction by using oxamate-containing palladium(II) complexes in *n*-Bu₄NBr, just the opposite trend to that reported by Böhm and Herrmann in 2001 by using a phosphapalladacycle as catalyst.¹⁰⁹

Table 12. Scope of olefin competition in Heck reaction of ethyl acrylate (A) and styrene (B)

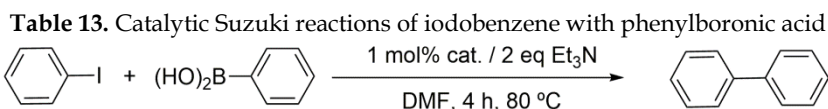


Entry ^a	Aryl halide	Catalyst	Time (min)	A ^b (%)	B ^b (%)	K _o = B/A
1		6a	6	95	5	0.05
2		11a	6	99	0	0
3		6a	30	91	9	0.10
4		11a	30	88	12	0.14
5		6a	3	99	0	0
6		11a	3	80	0	0
7		6a	4	60	0	0
8		11a	4	60	0	0

^a Reaction conditions: 1 mmol iodobenzene, 5 mmol ethyl acrylate, 5 mmol styrene, 0.5 mmol% cat., 2 mmol Et₃N, 120 °C in *n*-Bu₄NBr. ^bDetermined by GC-MS analysis using PFTBA as internal standard.

III. 5.3. Suzuki reaction – Homogeneous catalysis

The Suzuki reaction was studied with different aryl halides and phenylboronic acid for complexes **8a-10a** and **13a- 19a**, using DMF as reaction medium. The base with better results is Et₃N at a temperature of 80 °C. It deserves be pointed out that no inert atmosphere is required to carry out these reactions. All catalysts were very active under such conditions and using iodobenzene as aryl halide, although it is important to underline that complex **10a** (which has a methyl substituent in *para*- position) is the best one (89% yield, entry 3) relative to the others (Table 13).



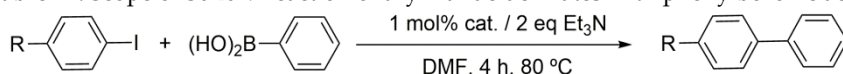
Entry ^a	Catalyst	Time (h)	Yield ^b	TON	TOF (h ⁻¹)
1	8a	4	75	75	19
2	9a	4	52	52	13
3	10a	4	91	91	23
4	13a	4	15	15	4
5	14a	4	40	40	10
6	15a	4	37	37	9
7	16a	4	57	57	14
8	17a	4	51	51	13
9	18a	4	41	41	10
10	19a	4	70	70	18

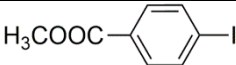

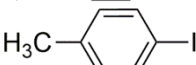
^a Reaction conditions: 1 mmol iodobenzene, 0.75 mmol phenylboronic acid, 1 mmol% cat., 2 mmol Et₃N, 4 h at 80 °C in DMF. ^bDetermined by GC-MS analysis using PFTBA as internal standard.

As specified above, complex **10a** (substituent in *para*- position) afforded the highest catalytic activity, meanwhile complexes with substituent in *ortho*-position (**9a**, Table 13, entry 2), *meta*- position or a combination of both positions (**13a**, Table 13, entry 4) yielded the lowest results, even lower than the complex without any substituent (**8a**, Table 13 entry 1). These results exhibit the opposite trend to that reported by Bedford and Cazin in 2003 by using ortho-metallated catalysts with alkylphosphine ligands in homogeneous catalysis (toluene or dioxane as solvents).¹¹⁰

In order to assess the scope of these kind of reactions, in the presence of oxamate-containing palladium(II) complexes, different halides bearing electron-donating and electron-withdrawing groups were coupled with phenylboronic acid, affording the biphenylic product in high yields (Table 14).

Table 14. Scope of Suzuki reaction of aryl halide derivates with phenylboronic acid



Entry	Aryl halide	Catalyst	Time	Temp	Yield	TON	TOF (h ⁻¹)
1		10a	4 h	80 °C	98	98	25
2		10a	4 h	80 °C	60	60	15
3		10a	4 h	80 °C	56	56	14

^aReaction conditions: 1 mmol aryl halide, 0.75 mmol phenylboronic acid, 1 mmol% cat., 2 mmol Et₃N, 4 h at 80 °C in DMF. ^bDetermined by GC-MS analysis using PFTBA as internal standard.

Good results were obtained working in the open air and when the reaction was performed with bis(oxamate)palladate(II) complexes in contrast to what occurs with commercial catalyst such as [Pd₃(OAc)₆] where formation of inactive palladium black occurs (Figure 7).

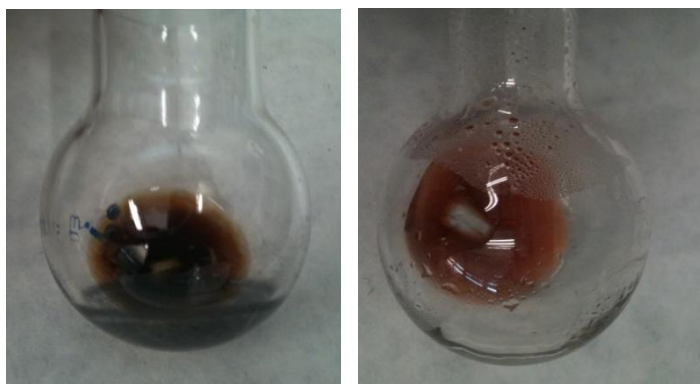
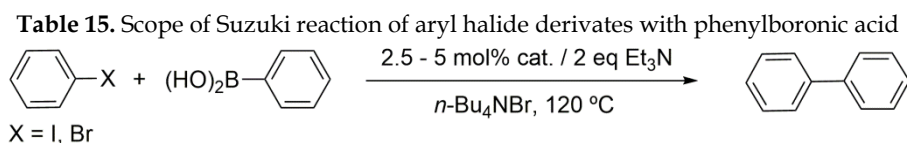


Figure 7: From left to right: [Pd₃(OAc)₆] and **10a**, after Suzuki reaction between iodobenzene and phenylboronic acid at 80 °C in DMF during 4 h.

III. 5.4. Suzuki reaction – Ionic liquid medium

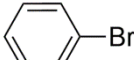
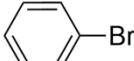
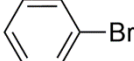
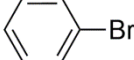
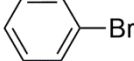
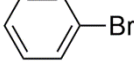
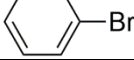
Given that these kind of anionic complexes of *N*-substituted oxamate are also catalytically active for the Suzuki reaction in an organic solvent such as DMF, we tried to use greener media such as ionic liquids. Complexes **5a-7a** and **9a-12a** were tested for Suzuki carbon-carbon cross-coupling reaction in this type of media.

High to moderate yields were obtained for the Suzuki reaction between iodobenzene and phenylboronic acid using 2.5 – 5 mol% cat. in the open air. Interestingly, small changes of electron-withdrawing or electron-donating groups or increasing the steric effects of the *para*- substituent of the oxamate ligand did not increase significantly the catalytic role but even weakened it (Table 15).



Entry ^a	Aryl halide	Catalyst	Time	Temp (°C)	Yield ^b	TON	TOF (h ⁻¹)
1		9a	2 h	120	78	16	8
2		10a	2 h	120	20	4	2
3		5a	45 min	120	89	36	48
4		6a	45 min	120	39	16	21
5		7a	45 min	120	41	16	21
6		11a	45 min	120	32	13	16
7		12a	45 min	120	30	12	16
8		9a	2 h	120	65	13	7

Table 15 contn.

9		5a	1 h	120	27	10	10
10		6a	1 h	120	30	12	12
11		7a	1 h	120	42	17	17
12		11a	1 h	120	34	14	14
13		12a	1 h	120	35	14	14
14		[Pd(dba)₂]	2 h	120	60	12	6
15		[Pd₃(OAc)₆]	2 h	120	65	13	6

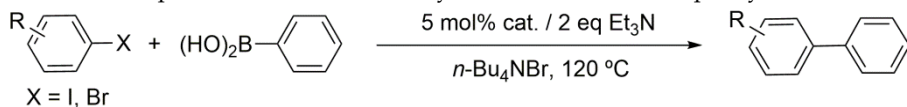
^a Reaction conditions: 1 mmol aryl halide, 0.75 mmol phenylboronic acid, 2.5-5 mmol% cat., 2 mmol Et₃N, 120 °C in *n*-Bu₄NBr. ^bDetermined by GC-MS analysis using PFTBA as internal standard.

Interestingly, working in the ionic liquid *n*-Bu₄NBr as solvent (Table 15, entries 1 and 2 with yields of 78 and 20%, respectively), we observe an opposite trend to working in homogeneous DMF medium (Table 13, entries 2 and 3 with yields of 52 and 91%, respectively). These features show that the methyl substituent in *para*- position (**10a**) does not favour the catalytic activity in the Suzuki reaction when carried out in ionic liquids.

Our results in *n*-Bu₄NBr as solvent show a similar trend to that reported by Bedford and Cazin in 2003¹¹⁰ who working with ortho-palladated amine and imine complexes, pointed out that the ortho-metalated ligands play a sacrificial role in the activation of the catalysts as in our complex **9a**.

Additionally to the reactions mentioned above, the reactions of various aryl halides derivatives with phenylboronic acid were investigated (Table 16) and we found that those with electron-withdrawing groups are more efficient.

Table 16. Scope of Suzuki reaction of aryl halide derivates with phenylboronic acid

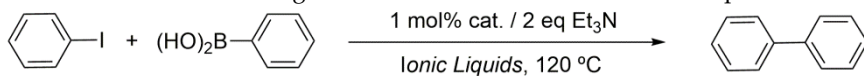


Entry	Aryl halide	Catalyst	Time (min)	Temp (°C)	Yield	TON	TOF (h ⁻¹)
1		9a	120	120	99	20	10
2		9a	120	120	99	20	10
3		9a	120	120	47	10	5
4		9a	120	120	78	16	8
5		9a	120	120	99	20	10
6		9a	120	120	60	12	6

^aReaction conditions: 1 mmol aryl halide, 0.75 mmol phenylboronic acid, 5 mmol% cat., 2 mmol Et₃N, 120 °C in *n*-Bu₄NBr. ^bDetermined by GC-MS analysis using PFTBA as internal standard.

As occurred in the Heck reaction, it is important to point out that *n*-Bu₄NBr provided the best results compared to *n*-Bu₄NCl and the imidazolium salts BMIMBr and BIMIMPF₆ (Table 17).

Table 17. Screening of Suzuki reactions in different ionic liquids



Entry	Ionic Liquid	Catalyst	Time (min)	Temp (°C)	Yield	TON	TOF (h ⁻¹)
1	<i>n</i> -Bu ₄ NBr	6a	120	120	78	16	8
2	<i>n</i> -Bu ₄ NCl	6a	120	120	46	9	5
3	BMIMBr	6a	120	120	23	5	3
4	BIMIMPF ₆	6a	120	120	33	7	4

^a Reaction conditions: 0.5 mmol iodobenzene, 0.75 mmol phenylboronic acid, 5 mmol% cat., 1 mmol Et₃N, 120 min, 120 °C in ionic liquids. ^bDetermined by GC-MS analysis using PFTBA as internal standard

III.6. Conclusions

A series of new functional palladium(II)-oxamate complexes with well-defined structures were synthesized and characterized exhibiting superior catalytic activity on carbon-carbon cross-coupling reactions over commercially available palladium(0) or palladium(II) catalysts.

The main advantages of our bis(oxamato)palladate(II) complexes as catalyst in Heck and Suzuki cross-coupling reactions are underlined hereunder: (i) they are environment friendly chemicals (in contrast to phosphines); (ii) in contrast to most of carbenes, their preparation is easier and cheaper; (iii) they are highly robust in carbon-carbon cross-coupling reactions (even working without an inert atmosphere like N₂ or Ar which is commonly used in these kind of reactions)^{5,73} specifically for Heck and Suzuki type reactions, this property being at the origin of the non formation of inactive palladium species; (iv) they are very soluble in water without decomposition and neither dissociation nor formation of black palladium species being observed during several months.



Figure 8. Stability of the palladium(II) oxamate-containing complexes after 90 days in water.

From a general point of view, the change of their electronic or steric effects modifies the catalytic activity in two different ways: a) the amount of catalyst which is required to carry out the reaction with high yields (for DMF medium from TON ca. 15 to TON ca. 99); b) the required time reactions (for DMF medium from TOF ca. 4 to TOF ca. 33 h⁻¹).

Dealing with the Heck carbon-carbon cross-coupling reactions with *n*-Bu₄NBr as ionic liquid medium, two features deserve to be outlined: i) the increase of the steric effects in *para*- position (**5-7**, **11** and **12**) of the ligand increase noteworthy their catalytic behavior permitting to use 0.5-0.25 mol% cat. (from TON ca. 69 to TON ca. 400); ii) the reaction times decreases from 30 min to 5 min and less reactive aryl halides is used (from TOF ca. 138 to TOF ca. 4800 h⁻¹).

Furthermore, the competition reactions showed that only the higher activated alkenes have the capability to govern the reaction (Table 10) and therefore, one product is favored when we use oxamate-containing palladium(II) catalysts.

In general, the almost entire series of the obtained catalysts (**5-19**) appears to be more efficient for the Heck reaction than for the Suzuki one. Moreover, it appears that changes of the steric effects in *para*- position of the oxamate ligand downward also the catalytic activity in the Suzuki reaction, the electronic and steric effect in *ortho*- position being more important.

To address upcoming environmental concerns, *n*-Bu₄NBr serve as an alternative greener medium to perform the Heck and Suzuki reactions at least for bis(oxamato)palladate(II) complexes. In addition, ionic liquids enable an easy work-up procedure and allow carrying out various consecutive runs without any loss of catalyst in the unloading and recharge of products and starting chemicals. Also, they increase the catalytic behavior of these anionic palladium(II) oxamate-containing complexes with *n*-Bu₄N⁺ as counter anion in comparison to carry out these reactions in homogeneous catalysis with DMF as medium.

To sum up, the novel palladium(II)-oxamate complexes in combination with ionic liquids, open a new pathway for the Heck and Suzuki reactions under greener conditions without reduction of the catalytic activity. Furthermore, one may consider if it is worth the effort, thinking at energy costs (green chemistry), to carry out the reaction with less expensive chemicals during long reactions times at high temperatures (bromobenzene and chlorobenzene) *vs.* more expensive materials during short times at mild temperatures (iodobenzene).

III.7. References

- (1) Heck, R. F.; Nolley, J. P. *J. Org. Chem.* **1972**, *37*, 2320–2322.
- (2) Tamao, K.; Sumitani, K.; Kumada, M. *J. Am. Chem. Soc.* **1972**, *94*, 4374–4376.
- (3) Corriu, R. J. P.; Masse, J. P. *Journal of the Chemical Society, Chemical Communications*, 1972, 144a.
- (4) Heck, R. F. *Acc. Chem. Res.* **1979**, *12*, 146–151.
- (5) Miyaura, N.; Yanagi, T.; Suzuki, A. *Synth. Commun.* **1981**, *11*, 513–519.
- (6) Shibasaki, M.; Boden, C. D. J.; Kojima, A. *Tetrahedron* **1997**, *53*, 7371–7395.
- (7) Suzuki, A. *J. Organomet. Chem.* **1999**, *576*, 147–168.
- (8) Beletskaya, I. P.; Cheprakov, A. V. *Chem. Rev.* **2000**, *100*, 3009–3066.
- (9) Herrmann, W. A.; Böhm, V. P. W.; Reisinger, C.-P. *J. Chem. Educ.* **2000**, *77*, 92.
- (10) Corbet, J.-P.; Mignani, G. *Chem. Rev.* **2006**, *106*, 2651–2710.
- (11) Hartwig, J. F. *Nature* **2008**, *455*, 314–322.
- (12) Martin, R.; Buchwald, S. L. *Acc. Chem. Res.* **2008**, *41*, 1461–1473.
- (13) Negishi, E. I. *Angew. Chem. Int. Ed.* **2011**, *50*, 6738–6764.
- (14) Suzuki, A. *Angew. Chem. Int. Ed.* **2011**, *50*, 6722–6737.
- (15) Astruc, D. *Anal. Bioanal. Chem.* **2011**, *399*, 1811–1814.
- (16) Nicolaou, K. C.; Bulger, P. G.; Sarlah, D. *Angew. Chem. Int. Ed.* **2005**, *44*, 4442–4489.
- (17) Steel, P. J. *Acc. Chem. Res.* **2005**, *38*, 243–250.
- (18) Jiang, J.-X.; Su, F.; Trewin, A.; Wood, C. D.; Campbell, N. L.; Niu, H.; Dickinson, C.; Ganin, A. Y.; Rosseinsky, M. J.; Khimiyak, Y. Z.; Cooper, A. I. *Angew. Chem. Int. Ed.* **2007**, *46*, 8574–8578.
- (19) Gadzikwa, T.; Zeng, B.-S.; Hupp, J. T.; Nguyen, T. S. *Chem. Commun.* **2008**, 3672–3674.
- (20) Lipton-Duffin, J. A.; Ivasenko, O.; Perepichka, D. F.; Rosei, F. *Small* **2009**, *5*, 592–597.
- (21) Meng, Q.; Gao, J.; Li, R.; Jiang, L.; Wang, C.; Zhao, H.; Liu, C.; Li, H.; Hu, W. *J. Mater. Chem.* **2009**, *19*, 1477.
- (22) Alyapyshev, M.; Babain, V.; Borisova, N.; Eliseev, I.; Kirsanov, D.; Kostin, A.; Legin, A.; Reshetova, M.; Smirnova, Z. *Polyhedron* **2010**, *29*, 1998–2005.
- (23) Budarin, V. L.; Shuttleworth, P. S.; Clark, J. H.; Luque, R. *Industrial Applications of C-C Coupling Reactions*; Bentham Science Publishers, 2010.
- (24) Rattanatraicharoen, P.; Yamabuki, K.; Oishi, T.; Onimura, K. *Polym. J.* **2011**, *44*, 224–231.
- (25) Juriček, M.; Barnes, J. C.; Dale, E. J.; Liu, W.-G.; Strutt, N. L.; Bruns, C. J.; Vermeulen, N. A.; Ghooray, K. C.; Sarjeant, A. A.; Stern, C. L.; Botros, Y. Y.; Goddard, W. A.; Stoddart, J. F. *J. Am. Chem. Soc.* **2013**, *135*, 12736–12746.
- (26) Castellano, M.; Ruiz-García, R.; Cano, J.; Ferrando-Soria, J.; Pardo, E.; Fortea-Pérez, F. R.; Stiriba, S.-E.; Julve, M.; Lloret, F. *Acc. Chem. Res.* **2015**, *48*, 510–520.

- (27) Kambe, N.; Iwasaki, T.; Terao, J. Pd-catalyzed cross-coupling reactions of alkyl halides. *Chem. Soc. Rev.* **2011**, *40*, 4937.
- (28) Shylesh, S.; Wang, L.; Thiel, W. R. *Adv. Synth. Catal.* **2010**, *352*, 425–432.
- (29) Fleckenstein, C. A.; Plenio, H. *Chem. Soc. Rev.* **2010**, *39*, 694–711.
- (30) Lundgren, R. J.; Stradiotto, M. *Chem. Eur. J.* **2012**, *18*, 9758–9769.
- (31) Bruno, N. C.; Tudge, M. T.; Buchwald, S. L. *Chem. Sci.* **2013**, *4*, 916.
- (32) Ge, G. C.; Mo, D. L.; Ding, C. H.; Dai, L. X.; Hou, X. L. *Org. Lett.* **2012**, *14*, 5756–5759.
- (33) Rosa, G. R.; Rosa, D. S. *RSC Advances*, **2012**, *2*, 5080.
- (34) Karami, K.; Rahimi, N.; Shehni, M. B. *Tetrahedron Lett.* **2012**, *53*, 2428–2431.
- (35) Sabounchei, S. J.; Ahmadi, M. *Inorg. Chim. Acta* **2013**, *405*, 15–23.
- (36) Fortman, G. C.; Nolan, S. P. *Chem. Soc. Rev.* **2011**, *40*, 5151–5169.
- (37) Godoy, F.; Segarra, C.; Poyatos, M.; Peris, E. *Organometallics* **2011**, *30*, 684–688.
- (38) Dunsford, J. J.; Cavell, K. J. *Dalton Trans.* **2011**, *40*, 9131–9135.
- (39) Liu, Y.-M.; Lin, Y.-C.; Chen, W.-C.; Cheng, J.-H.; Chen, Y.-L.; Yap, G. P. A.; Sun, S.-S.; Ong, T.-G. *Dalton Trans.* **2012**, *41*, 7382.
- (40) Valente, C.; Çalimsiz, S.; Hoi, K. H.; Mallik, D.; Sayah, M.; Organ, M. G. *Angew. Chem. Int. Ed.* **2012**, *51*, 3314–3332.
- (41) Costa, N. J. S.; Kiyohara, P. K.; Monteiro, A. L.; Coppel, Y.; Philippot, K.; Rossi, L. M. *J. Catal.* **2010**, *276*, 382–389.
- (42) Zalesskiy, S. S.; Ananikov, V. P. *Organometallics* **2012**, *31*, 2302–2309.
- (43) Firouzabadi, H.; Iranpoor, N.; Kazemi, F.; Gholinejad, M. *J. Mol. Catal. A Chem.* **2012**, *357*, 154–161.
- (44) Pérez-Lorenzo, M. J. *Phys. Chem. Lett.* **2012**, *3*, 167–174.
- (45) Karimi, B.; Elhamifar, D.; Clark, J. H.; Hunt, A. J. *Chem. Eur. J.* **2010**, *16*, 8047–8053.
- (46) Tamami, B.; Ghasemi, S. *J. Mol. Catal. A Chem.* **2010**, *322*, 98–105.
- (47) Prechtel, M. H. G.; Scholten, J. D.; Dupont, J. *Molecules* **2010**, *15*, 3441–3461.
- (48) Singh, A. S.; Patil, U. B.; Nagarkar, J. M. *Catal. Commun.* **2013**, *35*, 11–16.
- (49) Blaser, H.-U.; Indolese, A.; Schnyder, A.; Steiner, H.; Studer, M. *J. Mol. Catal. A Chem.* **2001**, *173*, 3–18.
- (50) Rosner, T.; Pfaltz, A.; Blackmond, D. G. *O J. Am. Chem. Soc.*, **2001**, *123*, 4621–4622.
- (51) Rocaboy, C.; Gladysz, J. A. *Org. Lett.* **2002**, *4*, 1993–1996.
- (52) Rocaboy, C.; Gladysz, J. A. *New J. Chem.*, **2002**, *27*, 39–49.
- (53) Paul, S.; Clark, J. H. *J. Mol. Catal. A Chem.* **2004**, *215*, 107–111.
- (54) Yu, K.; Sommer, W.; Richardson, J. M.; Weck, M.; Jones, C. W. *Adv. Synth. Catal.* **2005**, *347*, 161–171.
- (55) Phan, N. T. S.; Van Der Sluys, M.; Jones, C. W. *Adv. Synth. Catal.* **2006**, *348*, 609–679.
- (56) Sheldon, R. *Chem. Commun.* **2001**, 2399–2407.
- (57) Gordon, C. M. *Appl. Catal. A Gen.* **2001**, *222*, 101–117.

- (58) Zhao, D.; Wu, M.; Kou, Y.; Min, E. *Catal. Today* **2002**, *74*, 157–189.
- (59) Rogers, R. D.; Seddon, K. R. *Science* **2003**, *302*, 792–793.
- (60) Holbrey John D.; Turner Megan B.; Rogers Robin D. *Ionic Liquids as Green Solvents*; Rogers, R. D.; Seddon, K. R., Eds.; ACS Symposium Series; American Chemical Society: Washington, DC, 2003; Vol. 856.
- (61) Welton, T. *Coord. Chem. Rev.* **2004**, *248*, 2459–2477.
- (62) Imperato, G.; König, B.; Chiappe, C. *Eur. J. Org. Chem.* **2007**, *2007*, 1049–1058.
- (63) Pârvulescu, V. I.; Hardacre, C. *Chem. Rev.* **2007**, *107*, 2615–2665.
- (64) Olivier-Bourbigou, H.; Magna, L.; Morvan, D. *Appl. Catal. A Gen.* **2010**, *373*, 1–56.
- (65) Mastrorilli, P.; Monopoli, A.; Dell’Anna, M. M.; Latronico, M.; Cotugno, P.; Nacci, A. In *Topics in Organometallic Chemistry*; 2013.
- (66) Böhm, V. P. W.; Herrmann, W. A. W.; Bohm, V.; Herrmann, W. A. W. *Chem. Eur. J.* **2000**, *6*, 1017–1025.
- (67) Bellina, F.; Chiappe, C. *Molecules* **2010**, *15*, 2211–2245.
- (68) Hajipour, A. R.; Rafiee, F. *Appl. Organomet. Chem.* **2011**, *25*, 542–551.
- (69) Hornillos, V.; van Zijl, A. W.; Feringa, B. L. *Chemical Communications*, 2012, *48*, 3712.
- (70) Ataei, A.; Nadri, S.; Rafiee, E.; Jamali, S.; Joshaghani, M. *J. Mol. Catal. A Chem.* **2013**, *366*, 30–35.
- (71) Zhou, C.; Wang, J.; Li, L.; Wang, R.; Hong, M. *Green Chemistry*, 2011, *13*, 2100.
- (72) Bagherzadeh, M.; Amini, M.; Ellern, A.; Keith Woo, L. *Inorg. Chim. Acta* **2012**, *383*, 46–51.
- (73) Molnár, Á. *Chem. Rev.* **2011**, *111*, 2251–2320.
- (74) Steinrück, H.-P.; Wasserscheid, P. *Catal. Letters* **2014**, *145*, 380–397.
- (75) Guerrero, M.; García-Antón, J.; Tristany, M.; Pons, J.; Ros, J.; Philippot, K.; Lecante, P.; Chaudret, B. *Langmuir* **2010**, *26*, 15532–15540.
- (76) Sánchez, G.; García, J.; Martínez, M.; Kapdi, A. R.; Pérez, J.; García, L.; Luis Serrano, J. Bis(imidate)palladium(ii) complexes with labile ligands. Mimics of classical precursors? *Dalton Trans.* 2011, *40*, 12676.
- (77) Penno, D.; Estevan, F.; Fernández, E.; Hirva, P.; Lahuerta, P.; Sanaú, M.; Úbeda, M. A. *Organometallics* **2011**, *30*, 2083–2094.
- (78) Pardo, E.; Ruiz-García, R.; Cano, J.; Ottenwaelder, X.; Lescouëzec, R.; Journaux, Y.; Lloret, F.; Julve, M. *Dalton Trans.* **2008**, 2780–2805.
- (79) Fortea-Pérez, F. R.; Schlegel, I.; Julve, M.; Armentano, D.; De Munno, G.; Stiriba, S.-E. *J. Organomet. Chem.* **2013**, *743*, 102–108.
- (80) Kivekas, R.; Pajunen, A.; Navarrete, A.; Colacio, E. *Inorg. Chim. Acta* **1999**, *284*, 292–295.
- (81) Oliveira, W. X. C.; Ribeiro, M. A.; Pinheiro, C. B.; Nunes, W. C.; Julve, M.; Journaux, Y.; Stumpf, H. O.; Pereira, C. L. M. *Eur. J. Inorg. Chem.* **2012**, *2012*, 5685–5693.

- (82) Fortea-Pérez, F. R.; Marino, N.; Armentano, D.; De Munno, G.; Julve, M.; Stiriba, S.-E. *Cryst.Eng.Comm* **2014**, *16*, 6971.
- (83) Biffis, A.; Zecca, M.; Basato, M. *J. Mol. Catal. A Chem.* **2001**, *173*, 249–274.
- (84) De Vries, A. H. M.; Mulders, J. M. C. a; Mommers, J. H. M.; Henderickx, H. J. W.; de Vries, J. G. *Org. Lett.* **2003**, *5*, 3285–3288.
- (85) Brasche, G.; García-Fortanet, J.; Buchwald, S. L. *Org. Lett.* **2008**, *10*, 2207–2210.
- (86) Yeung, C. S.; Dong, V. M. *Chem. Rev.* **2011**, *111*, 1215–1292.
- (87) Bedford, R. B.; Blake, M. E.; Butts, C. P.; Holder, D. *Chem. Commun.* **2003**, 466–467.
- (88) Nájera, C.; Gil-Moltó, J.; Karlström, S.; Falvello, L. R. *Org. Lett.* **2003**, *5*, 1451–1454.
- (89) Wolf, C.; Lerebours, R. *Org. Biomol. Chem.* **2004**, *2*, 2161–2164.
- (90) Yao, Q.; Kinney, E. P.; Zheng, C. *Org. Lett.* **2004**, *6*, 2997–2999.
- (91) Alonso, F.; Beletskaya, I. P.; Yus, M. *Tetrahedron* **2005**, *61*, 11771–11835.
- (92) Alonso, F.; Beletskaya, I. P.; Yus, M. *Tetrahedron* **2008**, *64*, 3047–3101.
- (93) Islam, S. M.; Mondal, P.; Roy, A. S.; Mondal, S.; Hossain, D. *Tetrahedron Lett.* **2010**, *51*, 2067–2070.
- (94) Susanto, W.; Chu, C.-Y.; Ang, W. J.; Chou, T.-C.; Lo, L.-C.; Lam, Y. Development of a fluorous, oxime-based palladacycle for microwave-promoted carbon–carbon coupling reactions in aqueous media. *Green Chemistry*, 2012, *14*, 77.
- (95) Champness, N. R.; Khlobystov, A. N.; Majuga, A. G.; Schröder, M.; Zyk, N. V. *Tetrahedron Lett.* **1999**, *40*, 5413–5416.
- (96) Deeming, A. J.; Hogarth, G.; Lee, M. (Venus); Saha, M.; Redmond, S. P.; Phetmung, H. (Taya); Orpen, A. G. *Inorg. Chim. Acta* **2000**, *309*, 109–122.
- (97) Fasina, T. M.; Collings, J. C.; Burke, J. M.; Batsanov, A. S.; Ward, R. M.; Albesa-Jové, D.; Porres, L.; Beeby, A.; Howard, J. a. K.; Scott, A. J.; Clegg, W.; W., S.; Christopher; Marder, T. B. *J. Mater. Chem* 2005, *15*, 690.
- (98) Pan, H.; Yen, C. H.; Yoon, B.; Sato, M.; Wai, C. M. *Synth. Commun.* **2006**, *36*, 3473–3478.
- (99) Grushin, V. V.; Alper, H. *Chem. Rev.* **1994**, *94*, 1047–1062.
- (100) Consorti, C. S.; Zanini, M. L.; Leal, S.; Ebeling, G.; Dupont, J. *Org. Lett.* **2003**, *5*, 983–986.
- (101) Gannon, T. J.; Law, G.; Watson, P. R.; Carmichael, A. J.; Seddon, K. R. *Langmuir* **1999**, *15*, 8429–8434.
- (102) Fry, A. J. *J. Electroanal. Chem.* **2003**, *546*, 35–39.
- (103) Herrmann, W. A.; Böhm, V. P. W. *J. Organomet. Chem.* **1999**, *572*, 141–145.
- (104) Calò, V.; Nacci, A.; Monopoli, A.; Ieva, E.; Cioffi, N. *Org. Lett.* **2005**, *7*, 617–620.
- (105) Pröckl, S. S.; Kleist, W.; Köhler, K. *Tetrahedron* **2005**, *61*, 9855–9859.
- (106) Campeau, L. C.; Parisien, M.; Jean, A.; Fagnou, K. *J. Am. Chem. Soc.* **2006**, *128*, 581–590.

- (107) Kleist, W.; Pröckl, S. S.; Köhler, K. *Catal. Letters* **2008**, *125*, 197–200.
- (108) Srinivas, P.; Likhar, P. R.; Maheswaran, H.; Sridhar, B.; Ravikumar, K.; Kantam, M. L. *Chem. Eur. J.* **2009**, *15*, 1578–1581.
- (109) Böhm, V. P.; Herrmann, W. A. *Chem. Eur. J.* **2001**, *7*, 4191–4197.
- (110) Bedford, R. B.; Cazin, C. S. J.; Coles, S. J.; Gelbrich, T.; Horton, P. N.; Hursthouse, M. B.; Light, M. E. *Organometallics* **2003**, *22*, 987–999.

IV

Chapter 3

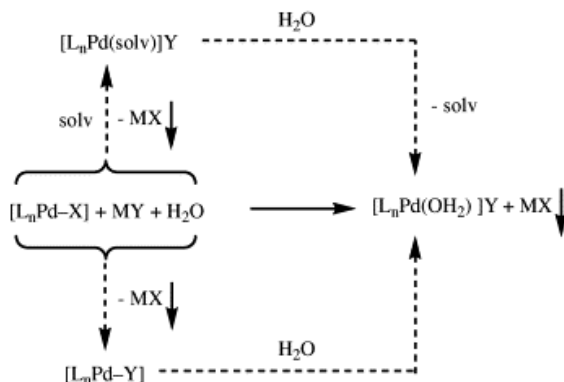
From serendipity to rational design

Part I

X-ray characterization of the $[\text{Pd}(\text{H}_2\text{O})_4]^{2+}$ cation

IV.1. Aquapalladium(II) complexes

The aquapalladium(II) species is assumed to be a key intermediate in many palladium(II)-catalyzed organic reactions which are carried out in aqueous solution.¹ However, the formation of such species is problematic by the low affinity of a soft acid [Pd(II)] *versus* a hard base (H₂O) [see Scheme 1].²



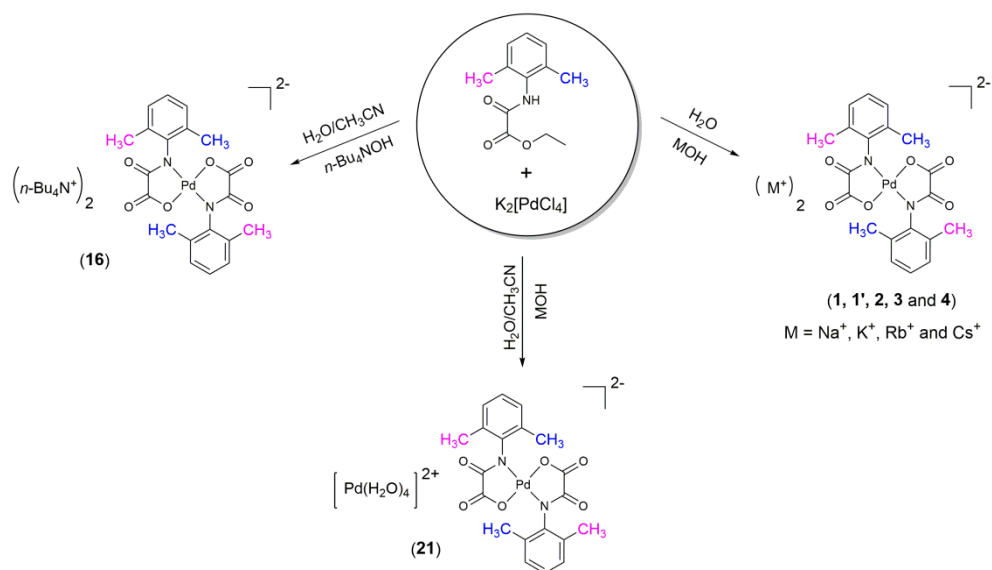
Scheme 1. Different routes to formation of aquapalladium(II) complexes.

Despite the importance in catalysis/organic,³ bio,⁴ and inorganic⁵ chemistry, aquapalladium(II) complexes have been underestimated over the years. This underestimation contrast with the fact that many aquapalladium(II) complexes of formula $[Pd(L)(H_2O)_{n<3}]^m$ have been isolated and characterized (more than one hundred) being summarized in a review by Vicente and Arcas.¹

In this respect, although the $[Pd(H_2O)_4]^{2+}$ has been extendedly studied in solution by Elding *et. al.*,⁶⁻¹⁰ it has been neither isolated nor its crystal structure elucidated by X-ray diffraction. By the way, this species has been poorly named in inorganic chemistry^{11,12} or outlined as "oxygen-containing solvents such as water, alcohol or ethers are such poor donors that few complexes with palladium(II) have been isolated".¹³ All the efforts devoted to isolate and structurally characterized the elusive and reactive $[Pd(H_2O)_4]^{2+}$ species would be welcome given its relevance in different research fields of both inorganic and organic chemistry.

IV.2. Aim

Serendipity, that is making desirable discoveries by accident is at the origin of most of the results grouped in this *chapter*. These results turned around the palladium(II) complexes with the oxamato proligand EtH-2,6-Me₂-pma (see Scheme 2). With the same synthetic method but changing the solvent we could prepare wittingly complexes like the novel compound $\{[\text{Pd}(\text{H}_2\text{O})_4][\text{Pd}(2,6\text{-Me}_2\text{-pma})_2] \cdot 2\text{H}_2\text{O}\}$ (**21**).



Scheme 2. Preparative route of the palladium(II) complexes with the EtH-2,6-Me₂-pma proligand.

The preparation of complex **21** and $(n\text{-Bu}_4\text{N})_2[\text{Pd}(2,6\text{-Me}_2\text{pma})_2] \cdot 2\text{CHCl}_3$ (**16**), their structural characterization as well as the investigation of their catalytic activity (in particular the role of the elusive $[\text{Pd}(\text{H}_2\text{O})_4]^{2+}$ species) constitute the aims of this *Part I* of Chapter II.

IV.3. Synthesis and characterization

The preparative route for the EtH-2,6-Me₂-pma proligand follows that described in previous works¹⁴. For further information see Appendix A, section A2. The synthetic method for the complex (*n*-Bu₄N)₂[Pd(2,6-Me₂pma)₂] (**16a**) was given in *Chapter 1 - part II*. X-ray suitable crystals of this compound as a chloroform solvate were grown by recrystallization of **16a** in CHCl₃.

Synthesis of the complex [Pd(H₂O)₄][Pd(2,6-Me₂-pma)₂] · 2H₂O (**21**)

Compound **21** was synthesized following a similar procedure to that described in *Chapter 1 - Part I*. An aqueous solution of KOH (15 mL, 1.2 mmol) was poured into a one-neck flask containing a suspension of EtH-2,6-Me₂-pma (1.2 mmol) in 10 mL of CH₃CN. Then, an aqueous solution of K₂[PdCl₄] (0.2g, 0.6 mmol) was added dropwise under continuous stirring and the mixture was heated at 60 °C overnight. The resulting yellow solution afforded yellow parallelepipeds upon very slow evaporation at room temperature within 2-3 days. Yield: 88%. IR (KBr/cm⁻¹): 3423 3327, 3246, 3155 (O-H), 2911 (C-H), 1670, 1638, 1630, 1577 (C=O). Anal. Calcd for C₂₀H₃₀N₂O₁₂Pd₂ (**21**): C, 34.16; H, 4.30; N, 3.98. Found: C, 34.01; H, 4.22; N, 4.05%.

IV.4. Results and discussion

Synthesis and IR Spectroscopy: The most interesting issue of this *Chapter* is how the reaction of $\text{K}_2[\text{PdCl}_4]$ (1 equivalent) with the EtH-2,6-Me₂-pma proligand (2 equivalent) and MOH (M = Li, Na, K, Cs or Rb) in a mixture of water/acetonitrile (1:1 v/v) at 60 °C overnight led to the formation of the complex $[\text{Pd}(\text{H}_2\text{O})_4][\text{Pd}(2,6\text{-Me}_2\text{-pma})_2] \cdot 2\text{H}_2\text{O}$ (**21**). The crystals of **21** were grown from the mother liquor within a couple of days at room temperature. It deserves to be noted that the same reaction in water as solvent afforded complexes **1**, **1'**, **2-4** after several weeks.

The high-frequency region of the IR spectrum of **21** exhibits a strong band at 3422 cm⁻¹ due to the O-H stretching together with the characteristic C-H vibrations (2961, 2933 and 2873 cm⁻¹) of the phenyl ring of the *N*-2,6-dimethylphenyloxamate ligand. Additionally, two strong absorption peaks appear at 1616 and 1641 cm⁻¹ (C=O vibrations) support the coordination of the 2,6-Me₂-pma dianion to palladium(II). Identical peaks concerning the aromatic C-H and C=O stretching vibrations are observed in the IR spectrum of $(n\text{-Bu}_4\text{N})_2[\text{Pd}(2,6\text{-Me}_2\text{pma})_2] \cdot 2\text{CHCl}_3$ (**16**) supporting also the occurrence of coordinated 2,6-Me₂pma in such compound.

X-ray structural determination: Single crystal X-ray diffraction data for **21** and **16** were collected at 296 K on a Bruker-Nonius X8-APEXII CCD area detector system using graphite-monochromated Mo-K α radiation ($\lambda = 0.71073 \text{ \AA}$), and processed through the SAINT¹⁵ reduction and SADABS¹⁶ absorption software. Due to the poor crystal quality, a low θ_{max} of diffraction was achieved for **16**, even if all possible steps were undertaken to ensure that the experiment was able to extract the best diffracting power from the sample. However, since the solution and refinement parameters for **16** are reasonable, we are confident about the consistency of the crystal structure found. The structures of **16** and **21** were solved by direct methods and subsequently completed by Fourier recycling using the SHELXTL-2013¹⁷ software packages, then refined by the full-matrix least-squares refinements based on F^2 with all observed reflections. All non-hydrogen atoms were refined anisotropically in the case of **21** while they were refined isotropically for **16** in order to reduce the number of parameters.

The hydrogen atoms from the 2,6-dimethylphenyl substituent on the oxamate ligand (**21** and **16**) and those from the tetra-*n*-butylammonium

cations and chloroform lattice molecules (**16**) were included at geometrically calculated positions and refined using a riding model. The hydrogen atoms of the water molecules in **21** were located on the ΔF map and refined with restraints on O-H distances and H-O-H angles. The high residual maxima and minima in the final Fourier-difference maps in **21** (3.137 and -2.201 e Å⁻³, respectively) were near the Pd(2) atoms. Crystal data and refinements conditions and selected bond lengths and angles for **16** and **21** are grouped in Tables 1, 2 and 3, respectively, whereas the hydrogen bonds for **21** are given in Table 4.

Table 1. Crystal data and structure refinement **16** and **21**.

	16	21
Formula	C ₅₄ H ₉₂ Cl ₆ N ₄ O ₆ Pd	C ₂₀ H ₃₀ N ₂ O ₁₂ Pd ₂
Mr / g mol ⁻¹	1212.42	703.26
Crystal system	Monoclinic	Monoclinic
Space group	<i>P</i> 2 ₁ / <i>n</i>	<i>C</i> 2/ <i>c</i>
<i>a</i> / Å	11.940(4)	22.620(2)
<i>b</i> / Å	18.197(7)	7.7498(7)
<i>c</i> / Å	14.892(5)	15.5036(15)
α / °	90	90
β / °	92.922(10)	108.005(7)
γ / °	90	90
<i>V</i> / Å ³	3231(2)	2584.7(4)
<i>Z</i>	2	4
<i>D_c</i> / g · cm ⁻³	1.246	1.807
<i>T</i> / K	296(2)	296(2)
μ / mm ⁻¹	0.580	1.454
<i>F</i> (000)	1268	1408
Theta range for data collection	2.134 to 12.995°	1.893 to 27.000°
Reflections collected	10301	21312
Refinement method	Full-matrix least-squares on <i>F</i> ²	
Independent reflections	846	2820
	[<i>R</i> (int) = 0.0633]	[<i>R</i> (int) = 0.0252]
Data / restraints / parameters	846/0/136	2820/9/185
Goodness-of-fit on <i>F</i> ²	1.185	1.108
Final <i>R</i> indices	<i>R</i> ₁ = 0.0799	<i>R</i> ₁ = 0.0449
[<i>I</i> > 2 σ (<i>I</i>)]	<i>wR</i> ₂ = 0.2094	<i>wR</i> ₂ = 0.0929
<i>R</i> indices (all data)	<i>R</i> ₁ = 0.0841	<i>R</i> ₁ = 0.0519
	<i>wR</i> ₂ = 0.2128	<i>wR</i> ₂ = 0.0977
Largest diff. peak / hole, eÅ ⁻³	0.434 / -0.312	3.137 / -2.201

$${}^a R_1 = \sum(|F_o| - |F_c|) / \sum|F_o|, {}^b wR_2 = [\sum w(F_o^2 - F_c^2)^2 / \sum w(F_o^2)^2]^{1/2}, {}^c S = [\sum w(|F_o| - |F_c|)^2 / (N_o - N_p)]^{1/2}.$$

Table 1. Selected bond lengths (Å) and angles (deg) for **16***

Pd(1)-N(1)	2.020(3)
Pd(1)-O(1)	1.97(2)
N(1a)-Pd(1)-N(1)	180.0
N(1)-Pd(1)-O(1a)	99.36(11)
N(1)-Pd(1)-O(1)	80.9(9)
O(1a)-Pd(1)-O(1)	180.0

*Symmetry transformations used to generate equivalent atoms:

(a) = -x, -y, -z.

Table 2. Selected bond lengths (Å) and angles (deg) for **21***

Pd(1)-N(1)	2.023(2)	Pd(2)-O(1W)	2.051(5)
Pd(1)-O(1)	2.04(2)	Pd(2)-O(2W)	2.040(5)
N(1a)-Pd(1)-N(1)	180.0	O(1W)-Pd(2)-O(2W)	177.3(2)
N(1)-Pd(1)-O(1a)	98.46(10)	O(1W)-Pd(2)-O(1Wa)	88.6(3)
N(1)-Pd(1)-O(1)	81.54(1)	O(1W)-Pd(2)-O(2Wa)	91.5(3)
O(1a)-Pd(1)-O(1)	180.0		

*Symmetry transformations used to generate equivalent atoms:

(a) = -x+1, y-1, -z+1/2

Description of the structures 16 and 21: Compounds **21** and **16** crystallize in the monoclinic space groups $C2/c$ and $P2_1/n$, respectively, with half a molecule in the asymmetric unit, the second half being generated by the crystallographic inversion centre. Each structure consists of *trans*-[Pd(2,6-Me₂-pma)₂]²⁻ anions (**16** and **21**) and [Pd(H₂O)₄]²⁺ (**21**) or *n*-Bu₄N⁺ (**16**) counter ions plus crystallization water (**21**) and chloroform (**16**) molecules (Figures 1 and 2 for **21** and Figure 3 for **16**).

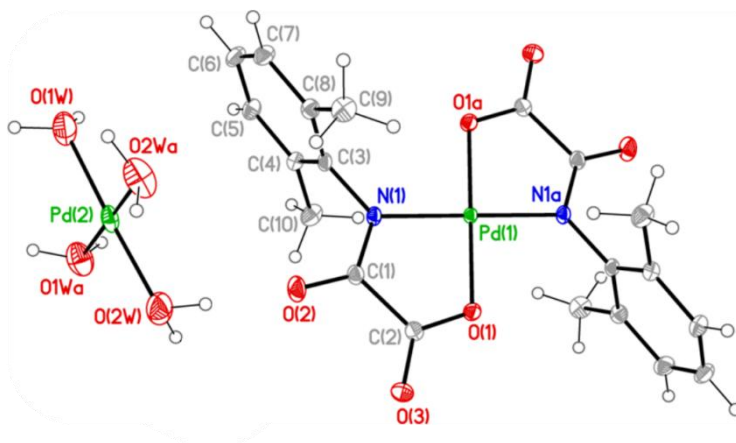


Figure 1. ORTEP drawing of the structure of **21**. The crystallization water molecules are omitted for the sake of clarity.

Anions and cations in **21** are assembled by an extended network of hydrogen bonds into a pretty 3D supramolecular structure (Figures 2 and 4), while the bis(oxamato)palladate(II) species in **16** are well separated from each other by the bulky $n\text{-Bu}_4\text{N}^+$ cations (Figure 5).

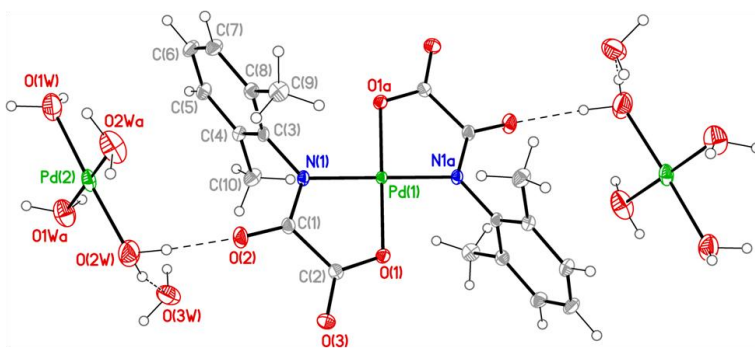


Figure 2. ORTEP drawing of the structure of **21** showing the hydrogen bonds (broken lines) involving the coordinated and lattice water molecules and the bis(oxamato)palladate(II) units.

The structures of **21** and **16** have in common the presence of the *trans*-[Pd(2,6-Me₂-pma)]²⁻ mononuclear unit where the palladium(II) ion is four-coordinate with two amidate-nitrogen [N(1) and N(1a)] and two carboxylate-oxygen atoms [O(1) and O(1a)] building a slightly distorted square-planar surrounding. The reduced bite angle of the chelating oxamate [81.6(1)° (**21**) and 80.9(9)° (**16**)] accounts for the deviations from

the ideal geometry; in fact, the Pd(II) ion and the atoms building its surrounding lie exactly on a plane for symmetry reasons. The Pd-N/Pd-O bond lengths are 2.023(3)/2.04(2) (**26**) and 2.020(3)/1.97(2) Å (**16**), values which compare well with those found in the oxamato-containing palladium(II) complexes $\{[\text{Na}(\text{H}_2\text{O})]_2\text{trans-}[\text{Pd}(\text{2,6-Me}_2\text{pma})_2]\}_n \cdot (n\text{-Bu}_4\text{N})_2\text{trans-}[\text{Pd}(\text{2-Mepma})_2] \cdot 4\text{H}_2\text{O}$ [2-Mepma = *N*-2-methylphenyloxamate], $(n\text{-Bu}_4\text{N})_2\text{trans-}[\text{Pd}(\text{4-Mepma})_2] \cdot 4\text{H}_2\text{O}$ [4-Mepma = *N*-4-methylphenyloxamate], $\text{Na}[\text{Pd}(\text{Hpba})] \cdot 2\text{H}_2\text{O}$ [H_4pba = 1,3-propylenebis(oxamic acid)] and $\text{K}_2[\text{Pd}(\text{opba})] \cdot 2\text{H}_2\text{O}$ [H_4opba = *N,N'*-1,2-phenylenebis(oxamic acid) [average Pd-N/Pd-O distances of 2.020(1)-2.009(1), 2.0209(11)/2.0384(13), 2.0207(13)/2.0214(14), 1.970/2.040 and 1.928/2.055 Å, respectively].¹⁸⁻²¹

The plane at the Pd(II) ion and the mean plane of the oxamate group are almost coplanar [the values of the dihedral angle between them (ϕ) are 2.20(4) (**21**) and 1.3(4)° (**16**)].

Focusing on the phenyloxamate ligand, the values of dihedral angle between the 2,6-substituted phenyl ring and the mean plane of the oxamate group (ϕ) are 81.52(3) (**21**) and 80.0(4)° (**16**). They are much closer to orthogonality than those observed in $\{[\text{Na}(\text{H}_2\text{O})]_2\text{trans-}[\text{Pd}(\text{2,6-Me}_2\text{pma})_2]\}_n$, $(n\text{-Bu}_4\text{N})_2\text{trans-}[\text{Pd}(\text{2-Mepma})_2] \cdot 4\text{H}_2\text{O}$ and $(n\text{-Bu}_4\text{N})_2\text{trans-}[\text{Pd}(\text{4-Mepma})_2] \cdot 4\text{H}_2\text{O}$ [ϕ = 75.79(4), 51.1(1) and 52.2(1)°, respectively].^{18,19}

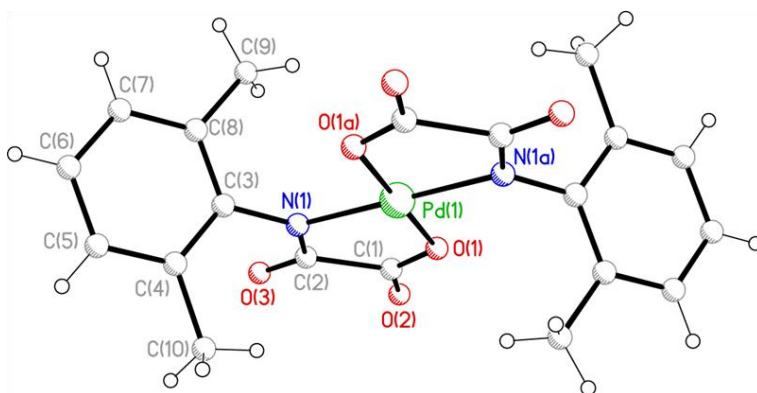


Figure 3. Perspective view of the anionic complex of **16** showing the atom numbering scheme.

A tetraaquapalladium(II) cation is present in **21**, this structural feature being reminiscent of the situation found in the double salt of formula $[\text{Pd}(\text{NH}_3)_4][\text{Pd}(\text{opba})]$ where the tetramminpalladium(II) acts as counterion of the oxamato dianion $[\text{Pd}(\text{opba})]^{2-}$.²² The palladium(II) ion in this tetraqua complex is also four-coordinate in a slightly distorted $\text{O}(1\text{w})\text{O}(2\text{w})\text{O}(1\text{wa})\text{O}(2\text{wa})$ square-planar surrounding. The values of the $\text{O}(1\text{w})\text{-Pd}(2)\text{-O}(2\text{w})$, $\text{O}(1\text{w})\text{-Pd}(2)\text{-O}(1\text{wa})$ and $\text{O}(1\text{w})\text{-Pd}(2)\text{-O}(2\text{wa})$ bond angles are $177.3(2)$, $88.6(3)$ and $91.5(3)^\circ$ respectively, and the average Pd-O_w length is $2.048(5)$ Å.

Table 4. Hydrogen bonds in **21***

D-H...A	d(D-H) [#]	d(H...A) [#]	d(D...A) [#]	<(D-H...A) ^{&}
$\text{O}(1\text{w})\text{-H}(1\text{w}1)\cdots\text{O}(2\text{c})$	0.96(3)	2.31(4)	3.095(6)	139(4)
$\text{O}(1\text{w})\text{-H}(1\text{w}1)\cdots\text{O}(3\text{c})$	0.96(3)	2.24(3)	3.083(6)	146(4)
$\text{O}(2\text{w})\text{-H}(2\text{w}2)\cdots\text{O}(2)$	0.99(3)	1.97(3)	2.958(7)	175(4)
$\text{O}(3\text{w})\text{-H}(3\text{w}1)\cdots\text{O}(3)$	0.95(3)	2.17(4)	3.005(6)	146(5)
$\text{O}(3\text{w})\text{-H}(3\text{w}2)\cdots\text{O}(3\text{d})$	0.96(3)	2.02(3)	2.945(6)	163(5)

* Symmetry transformation used to generate equivalent atoms: (c) = $-x + 1, y - 1, -z + 1/2$; (d) = $-x + 1, -y + 4, -z + 1$. [#]Values in Å. [&]Values in degrees.

Focusing on the crystal packing of **21**, hydrogen bond interactions involving coordinated and crystallization water molecules give rise to layers of *hiper*-hydrated Pd(2) ions extending on the crystallographic *bc* plane (Figure 4). The outer oxamate oxygens [O(2) and O(3)] of the anionic complex are anchored to these sheets through further hydrogen bonds, leading to an overall supramolecular 3D motif (see Table 4). The values of the shortest interionic metal-metal separations are $7.750(3)$ and $6.922(3)$ Å [Pd(1)··Pd(1e) and Pd(2)··Pd(1e), respectively; symmetry code: (e) = $x, -y + 1, z$].

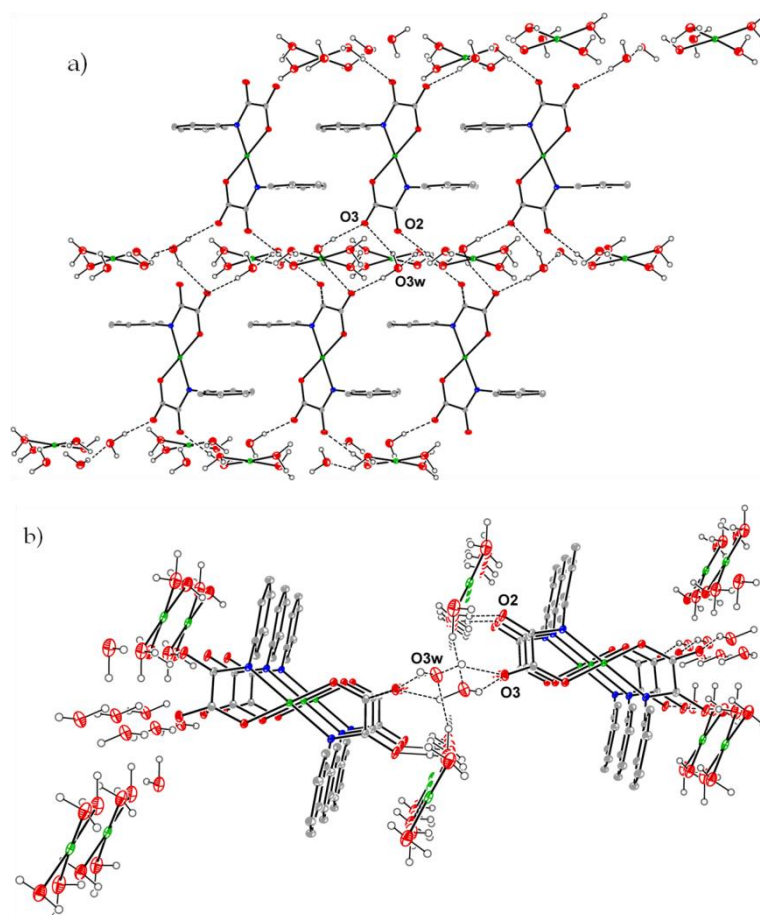


Figure 4. Views of the crystal packing of **21** along the crystallographic *c* axis (a) and *b* axis (b).

The oxamate complex anions in the crystal packing of **16** are well separated from each other most likely because the presence of bulky *n*-Bu₄N⁺ cations, the shortest intermetallic Pd(1)··Pd(1b) separation being 11.94(3) Å [symmetry code: (b) = -*x*, *y*, *z*] (Figure 5). The chloroform molecules crystallization molecules are pretty intercalated in the free voids and they contribute to the stability of the structure by means of very weak C-H··Cl type interactions.

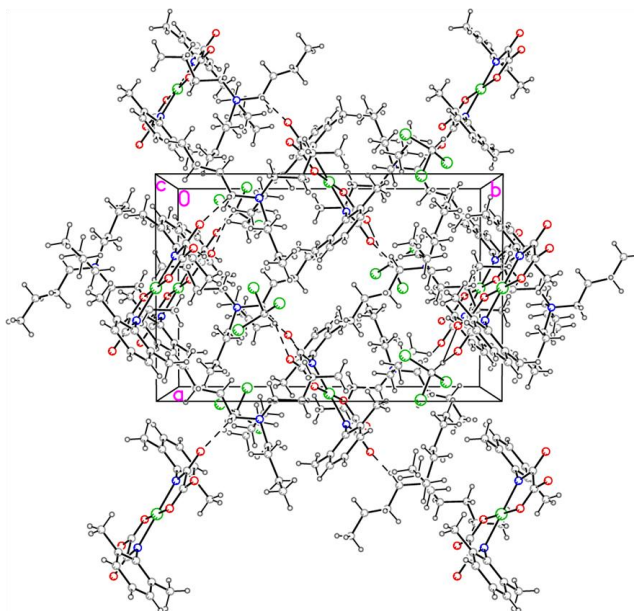
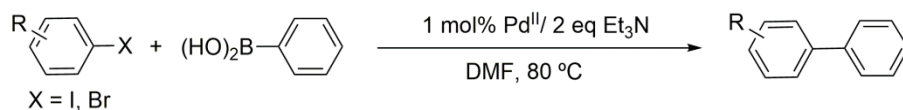


Figure 5. View of the crystal packing of **16** along *c* axis showing the isolation of the bis(oxmato)palladate(II) anions by the bulky *n*-Bu₄N⁺ cations.

IV.5. Catalytic properties

The catalytic activity of **16** and **21** has been tested in the Suzuki cross coupling of phenylboronic acid as the standard substrate and different aryl halides as the coupling partners. The catalytic reactions were carried out using two different palladium(II) precatalysts and the obtained results are listed in Table 5.

Table 5. Scope of Suzuki reaction of aryl halide derivatives with phenylboronic acid



Entry ^a	Aryl halide	Catalyst	Time	Yield ^b /%	TON	TOF/h ⁻¹
1		16a	30 min	35	35	70
		21		30	35 ^c /70 ^d	70 ^c /140 ^d
2		16a	3 h	56	56	18
		21		55	55 ^c /110 ^d	18 ^c /23 ^d
3		16a	3 h	30	30	10
		21		28	28 ^c /56 ^d	10 ^c /18 ^d
4		16a	18 h	48	48	3
		21		39	39 ^c /78 ^d	2/4 ^d
5		16a	18 h	60	60	3
		21		50	50 ^c /100 ^d	3 ^c /6 ^d
6		16a	30 min	26	26	52
		21		23	23 ^c /46 ^d	46 ^c /92 ^d
7		16a	30 min	30	30	60
		21		35	35 ^c /70 ^d	70 ^c /140 ^d
8		16a	3 h	29	29	10
		21		29	29 ^c /58 ^d	10 ^c /19 ^d

^a Reaction conditions: 0.5 mmol aryl halide, 0.75 mmol phenylboronic acid, 1 mmol% cat., 2 mmol Et₃N at 80 °C in DMF. ^bDetermined by GC-MS analysis using PFTBA as internal standard. ^cConsidering in TON by %mol of active Pd(II) (0.005 mmol). ^dConsidering in TON %mol complex (0.00025 mmol).

The comparative catalytic study of **16** and **21** with the purpose to evaluate the catalytic influence of the $[\text{Pd}(\text{H}_2\text{O})_4]^{2+}$ counter cation was carried out by using 1.0 equivalent of aryl halide, 1.2 equivalent phenylboronic acid and 2.0 equivalent Et_3N as reagents in DMF at 80 °C. Moderate yields were obtained in both cases [25-60 (**16**) and 17-55% (**21**)]. Only 1 mol% of Pd was used in the two experiments. This means that

(i) in the case of **21** which is composed by the anionic bis(oxamato)palladate(II) and the cationic tetraaquapalladate(II) entities 1 mol% of Pd corresponds to 0.0025 mmol of formula weight,

(ii) and for **16** [mononuclear bis(oxamato)palladate(II) complex] which has only one palladium metal center *per* molecular unit, 1 mol% of Pd is equal to 0.005 mmol of formula weight.

As the same catalytic results were obtained under this circumstances, it is clear that the $[\text{Pd}(\text{H}_2\text{O})_4]^{2+}$ counter cation is also an active species for the Suzuki cross coupling reaction. However, the fact that formation of inactive palladium black occurs in the experiment using **21** as precatalyst but not in that with **16**, reveals the importance of the choice of a suitable ligand as shell protection in order to avoid this decomposition.²³⁻²⁷

Finally, in order to understand the difference of the TON values in Table 2, it is important to keep in mind the definition of the turnover number,²⁸

$$\text{TON} = \frac{\text{mol}_{\text{Aryl halide}} \times \frac{\text{yield} (\%)}{100}}{\text{mol}_{\text{cat}}},$$

a dilemma is exposed when one divide *per* mol_{cat} . May one divide *per* mol of complex obtaining better and higher TON results or may one divide *per* mol of active Pd(II) resulting in lower TON values? ‡

‡*Author note: This is one of the big problems in the reports on catalytic studies with polymeric palladium compounds, because it is unclear if the authors use the TON by mol of palladium center or by mol of the polynuclear unit.*

IV.6. Conclusions

Compound **21** is the first structurally characterized example containing the elusive discrete $[(\text{Pd}(\text{H}_2\text{O})_4)]^{2+}$ species^{1,29,30} and its knowledge opens a new gate for functional palladium(II)-oxamate complexes to be used as precatalyst in carbon-carbon cross coupling reactions.

This type of complex that can be synthesized in a straightforward manner has as added value not only the fact of being environmentally friendly but also having highly versatile and very cheap ligands. Interestingly, the use of different reaction media (water or water/acetonitrile solvent mixtures) and bases for the deprotonation of the monooxamate proligands strongly influence the formation, stability and crystal structures of the oxamate-containing palladium(II) compounds.

Complexes **16** and **21** catalyze the Suzuki cross-coupling of aryl halides and phenylboronic acid into asymmetric biaryl products in moderate yields, in contrast to complexes **1-4** with alkaline counter ions which showed moderate to high yields. On the other hand, the presence of the tetraaquapalladium(II) cation appears to be catalytically active [equal %mol of active Pd(II) for the same Suzuki cross coupling reactions give practically identical yields].

Unfortunately, the observed downward of the catalytic activity in **21** may be due to the decomposition of $[(\text{Pd}(\text{H}_2\text{O})_4)]^{2+}$ into inactive palladium(0) black, a feature that shows the relevance of the coordinating ligand or protecting shell for the formation of active and stable palladium species during the catalytic cycle of palladium-catalyzed carbon-carbon coupling reactions.³¹⁻³⁴ In other catalytic reports concerning carbon-carbon coupling reactions using 'free-ligand palladium(II)', it is specified that a protecting shell of the active palladium by polymers,³⁵⁻³⁸ additives,^{39,40} inert atmosphere⁴¹ or polar co-solvents⁴² is required.

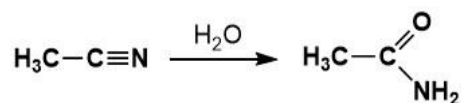
Part II

Trapping the catalyst

$[\text{Pd}(\text{H}_2\text{O})_4]^{2+}$ cation

IV.7. The nitrile hydration reaction

Hydration of nitriles to amides (Scheme 3) is a significant functional group transformation which plays an important role in organic synthesis, environment and industrial applications,⁴³⁻⁴⁷ being a sustainable method for the preparation of primary amides.⁴⁸ The hydrolysis of acetonitrile carried out in the absence of metal ions is a very old and well known reaction⁴⁹ and it has been the subject of excellent reviews in the last years.^{48,50} Nevertheless, this classical hydration with H₂SO₄ and NaOH often affords unwanted carboxylic acids as byproducts.⁵¹ Moreover, stoichiometric amounts of salts are formed in the neutralization step with inconvenient product contamination. These difficulties can be avoided by using metal ions as powerful activators of the nitrile group towards the nucleophilic attack by OH⁻/H₂O.⁵²



Scheme 3. Nitrile hydration reaction.

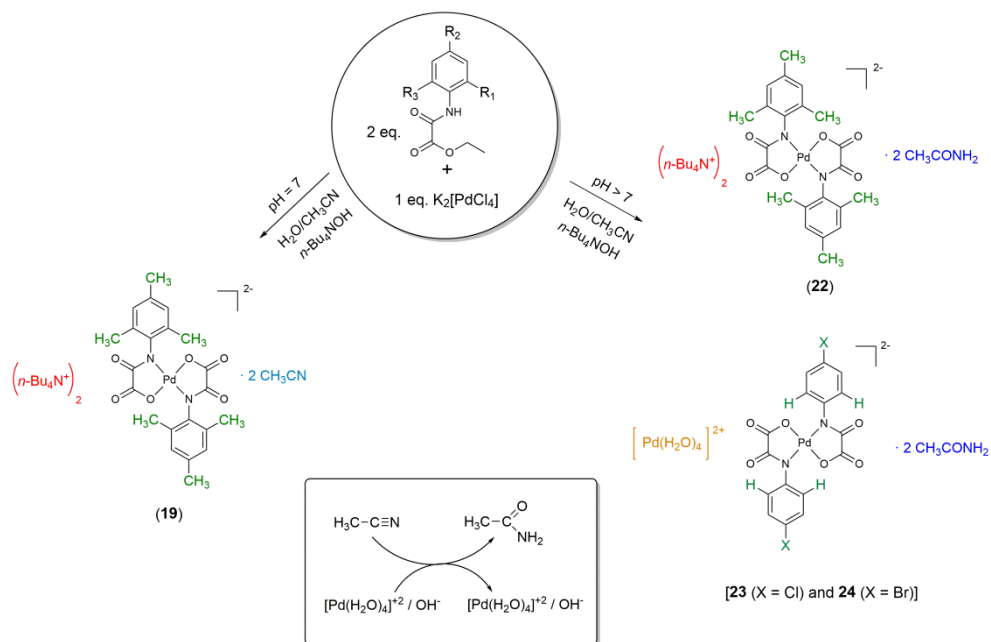
Several catalytic systems working under neutral conditions have been developed to overcome these problems.⁵³⁻⁵⁶ Furthermore, the reactions involving enzyme catalysts⁵⁷ and metal complexes such as of Co,⁵⁸ Ni,⁵⁹ Cu,⁶⁰ Ru,^{61,62} Pd,^{63,64} and Pt⁶⁵ are also well documented as those in the lack of metal ions.⁶⁶ Focusing on the Pd-catalyzed hydrolysis reaction, many aqua complexes of formula [PdL_n(H₂O)_m]^{(n-l-2)-} (l = charge of the L ligand) have been synthesized and their reactions studied during the last four decades.¹ In particular, the kinetically labile tetraaquapalladium(II) species, [Pd(H₂O)₄]²⁺, is known to be an effective catalyst even with less activated nitriles.⁵⁵

IV.8. Aim

As Suzuki stated in his Nobel Prize lecture,⁶⁷ some amount of luck matters for good researches, but what can be said with certainty is that little will come from a half-hearted effort.

This statement can be applied to the contents of the *Part II* of this Thesis where our interest in the $[\text{Pd}(\text{H}_2\text{O}_4)]^{2+}$ led us to investigate the possibility to materialize it in the bis(oxamato)palladate(II) complexes and to investigate the possibility of using the aquapalladium(II) species in the palladium(II)-catalyzed nitrile hydration.

Our synthetic attempts in this respect constitute the main goals of this *Part II* where the preparation and X-ray structure of a family of new bis(oxamato)palladate(II) compounds are reported (**19**, **22-24** in Scheme 4).



Scheme 4. Simplified reaction pathway with $\text{R} = \text{R}' = \text{R}'' = \text{CH}_3$ for **19** and **22** and $\text{R} = \text{R}'' = \text{H}$; $\text{R}' = \text{Cl}, \text{Br}$ for **23** and **24**.

IV.9. Synthesis and characterization

The preparation of the EtH-2,4,6-Me₃pma, EtH-4-Clpma and EtH-4-Brpma proligands was carried out by following previously reported procedures¹⁴. For further information see Appendixes A and B.

In this *Part II* of *Chapter 3*, the synthesis of the oxamato complexes of formula [(*n*-Bu₄N)₂[Pd(2,4,6-Me₃pma)₂] · 2CH₃CN (**19**), (*n*-Bu₄N)₂[Pd(2,4,6-Me₃pma)₂] · 2CH₃CONH₂ (**22**), (*n*-Bu₄N)₄[Pd(H₂O)₄][Pd(4-Clpma)₂]₃ · 2CH₃CONH₂ (**23**) and (*n*-Bu₄N)₄[Pd(H₂O)₄][Pd(4-Brpma)₂]₃ · 2CH₃CONH₂ (**24**) has been carried out through two different synthetic routes.

Synthesis of [(*n*-Bu₄N)₂[Pd(2,4,6-Me₃pma)₂] · 2CH₃CN (**19**)

A methanolic solution of *n*-Bu₄NOH (1.0 M, 1.2 mmol) was poured into a one-neck round flask containing a suspension of the EtH-2,4,6-Me₃pma proligand (0.6 mmol) in 10 mL of acetonitrile at 60 °C. Then, an aqueous solution of K₂[PdCl₄] (100 mg, 0.3 mmol) was added dropwise to the resulting solution and the reaction mixture was heated at 60 °C for 10 hours under continuous stirring. The neutral solution was allowed to evaporate at room temperature and X-ray quality yellow prisms of **19** were grown up after three weeks. Their stoichiometry was established by X-ray diffraction on single crystals. Yield: 92%; IR(KBr/cm⁻¹): 3437 (O-H), 2962, 2927, 2874 (C-H), 1670, 1627, 1595 (C=O).

Synthesis of (*n*-Bu₄N)₂[Pd(2,4,6-Me₃pma)₂] · 2CH₃CONH₂ (22**), (*n*-Bu₄N)₄[Pd(H₂O)₄][Pd(4-Clpma)₂]₃ · 2CH₃CONH₂ (**23**) and (*n*-Bu₄N)₄[Pd(H₂O)₄][Pd(4-Brpma)₂]₃ · 2CH₃CONH₂ (**24**)**

A methanolic solution of *n*-Bu₄NOH (1.0 M, 2.4 mmol) was added directly to a one-neck round flask suspension of the corresponding *N*-substituted oxamate proligand (0.6 mmol) in 10 mL of acetonitrile at 60 °C. Then, an aqueous solution of K₂[PdCl₄] (100 mg, 0.3 mmol) was added dropwise to the reaction mixture and resulting basic solution was heated at 60 °C for 10 hours under continuous stirring. The solution was allowed to evaporate at room temperature. X-ray quality yellow prisms were grown up after two weeks (**22**) and a couple of days (**23** and **24**). Their formulas were determined by X-ray diffraction on single crystals.

(**22**). Yield: 90%; IR(KBr/cm⁻¹): 3436-3309 (O··H-N and N-H), 2965, 2936, 2873 (C-H), 1664, 1654, 1616, 1596, (C=O_{amide/oxamato}). (**23**). Yield: 95%; IR (KBr/cm⁻¹): 3464-3148 (O··H-N, O··H-O, N-H), 2958, 2933, 2872 (C-H), 1670, 1644, 1604, 1576, 1563 (C=O_{amide/oxamato}). (**24**). Yield: 96%; IR (KBr/cm⁻¹): 3464-3148 (O··H-N, O··H-O, N-H), 2958, 2933, 2872 (C-H), 1670, 1644, 1604, 1576, 1563 (C=O_{amide/oxamato}).

IV.10. Results and discussion

Synthesis and IR Spectroscopy. Compound **19** was synthesized in neutral conditions using the stoichiometric amount of *n*-Bu₄NOH required to generate the fully deprotonated 2,4,6-Me₃pma²⁻ ligand in an acetonitrile solution and adding an aqueous solution of K₂[PdCl₄] in a 2:1 ligand-to-metal molar ratio. Instead, **22**, **23** and **24** were synthesized as **19** but using the base in a two-fold excess of that required to afford the deprotonated 2,4,6-Me₃pma²⁻, 4-Clpma²⁻ and 4-Brpma²⁻ ligands, respectively.

The *N*-substituted oxamate ligands were easily prepared as the respective ethyl ester proligands by the straightforward condensation of the ethyl chlorooxoacetate with the corresponding aniline derivative in THF, in presence of Et₃N as a base at room temperature. They were isolated in very good yields (ca. 80–96 %). Their IR spectra exhibit a typical absorption peak at ca. 3000 – 3300 cm⁻¹ for the N-H stretching vibration and two intense bands at ca. 1727 and 1677 cm⁻¹ which clearly correspond to the stretching from the ester and amide groups, respectively. ¹H and ¹³C NMR spectra provide additional support for the signal of the N-H amide hydrogen as well as those corresponding to the ethyl (CH₂CH₃) group of the ester.

The lack of the N-H vibration band at ca. 3240 cm⁻¹ and the occurrence of two intense bands shifting to lower energies (ca. 1638 and 1600 cm⁻¹) in infrared spectrum of **19** supports the deprotonation of the amide group and the hydrolysis of the ester group upon the coordination to the palladium(II) ion. These spectroscopy features are confirmed by X-ray structure of **19**.

In the case of **21**, the lack of the typical sharp N-H vibration band at ca. 3240 cm⁻¹ and the occurrence of two intense bands shifting to lower energies (ca. 1638 and 1600 cm⁻¹) in its infrared spectrum supports the deprotonation of the amide group and the hydrolysis of the ester group upon the coordination to the palladium(II) ion. New N-H···O and N-H and C=O vibrations appear at ca. 3400 cm⁻¹ and ca. 1600 cm⁻¹ respectively, which are due to the presence of amide group. All these spectroscopy features were confirmed by the X-ray structure of **21**, the presence of non coordinated CH₃CONH₂ molecule accounting for the N-H and C=O vibrations in the FT-IR spectrum.

The lack of the typical sharp N-H vibration band at ca. 3240 cm⁻¹ and the occurrence of two intense bands shifting to lower energies (ca. 1638 and 1600 cm⁻¹) in infrared spectra of **23** and **24** supports the deprotonation of the amide group and the hydrolysis of the ester group upon the coordination to the palladium(II) ion. Moreover, new broad O··H-N, O··H-O and N-H vibrations appear at ca. 3400 cm⁻¹ by the presence of [Pd(H₂O)₄]⁺² and CH₃CONH₂. The X-ray structures of **23** and **24** confirm the presence of this structures.

X-ray structural determination. Single crystal X-ray diffraction data for **19** and **22-24** were collected at 296 K on a Bruker-Nonius X8-APEXII CCD area detector system using graphite-monochromated Mo-K α radiation ($\lambda = 0.71073$ Å), and processed through the SAINT¹⁵ reduction and SADABS¹⁶ absorption software. Due to the poor crystal quality, low θ_{\max} of diffraction (completeness to theta 25 only 79.3 %) were achieved for **19** and **22**, even if all possible steps were undertaken to ensure that the experiment was able to extract the best diffracting power from the samples.

Their structures were solved by direct methods and subsequently completed by Fourier recycling using the SHELXTL-2013¹⁷ software packages, then refined by the full-matrix least-squares refinements based on F^2 with all observed reflections. All non-hydrogen atoms were refined anisotropically. The hydrogen atoms on the phenyl-substituted oxamate ligand and on the tetra-*n*-butylammonium cations and acetonitrile (**19**) and acetamide (**22**, **23** and **24**) lattice molecules were included at geometrically calculated positions and refined using a riding model. The hydrogen atoms of the water molecules in **23** and **24** were neither found nor calculated.

Crystal data and refinements conditions and selected bond lengths and angles for **19** and **22-23** are grouped in Tables 6-8, respectively; where as the hydrogen bonds for **23** and **24** are given in Table 9. Given that complexes **23** and **24** are isostructural, we will focus on the structure of **23** for brevity reasons, crystallographic tables (Tables S1-S2) and the graphic information of **23** being moved to Appendix C.

Table 6. Crystal data and structure refinement **19** and **22-24**.

	19	22	23	24
Formula	C ₅₈ H ₉₈ PdN ₆ O ₆	C ₅₈ H ₁₀₄ PdN ₆ O ₈	C ₁₁₆ H ₁₈₆ Br ₆ Pd ₄ N ₁₂ O ₂₄	C ₁₁₆ H ₁₈₆ Cl ₆ Pd ₄ N ₁₂ O ₂₄
<i>M</i> / g mol ⁻¹	1081.82	1119.87	3037.82	2771.06
Crystal system	triclinic	triclinic	triclinic	triclinic
Space group	<i>P</i> (-1)	<i>P</i> (-1)	<i>P</i> (-1)	<i>P</i> (-1)
<i>a</i> / Å	11.769(4)	11.925(5)	11.904(5)	11.8946(5)
<i>b</i> / Å	11.933(5)	12.160(5)	16.053(5)	15.9309(6)
<i>c</i> / Å	12.808(5)	13.231(5)	18.394(5)	18.2950(8)
<i>α</i> / °	73.962(16)°	70.576(5)°	90.695(5)°	90.296(2)°
<i>β</i> / °	78.670(16)°	74.155(5)°	96.350(5)°	96.290(2)°
<i>γ</i> / °	65.665(14)°	63.881(5)°	90.926(5)°	90.985(2)°
<i>V</i> / Å ³	1568.1(11)	1606.4(11)	3493(2)	3445.3(2)
<i>Z</i>	1	1	1	1
<i>ρ</i> _{calc} / g cm ⁻³	1.146	1.158	1.444	1.336
<i>μ</i> / mm ⁻¹	0.344	0.340	2.288	0.696
<i>T</i> / K	293(2)	293(2)	293	293
<i>F</i> (000)	582	604	1552	1444
Reflect. collcd.	9400	15142	95701	57484
Indep. reflections [<i>R</i> (int)]	4505 [0.0326]	4617 [0.0300]	13734 [0.0515]	14083 [0.0452]
Data / restraints / parameters	4505/2/ 329	4617/0/331	13734/4/714	14083/0/724
<i>R</i> 1 ^a [<i>I</i> > 2σ(<i>I</i>)] (all data)	0.0456 (0.0484)	0.0397 (0.0426)	0.0508 (0.0961)	0.0536 (0.0898)
<i>wR</i> 2 ^b [<i>I</i> > 2σ(<i>I</i>)] (all data)	0.1355 (0.1410)	0.1064 (0.1130)	0.1414 (0.1810)	0.1574 (0.1913)
Goodness-of-fit ^c	1.122	1.075	1.014	1.035

^a $R_1 = \sum(|F_o| - |F_c|) / \sum |F_o|$. ^b $wR_2 = [\sum w(F_o^2 - F_c^2)^2 / \sum w(F_o^2)^2]^{1/2}$. ^c $S = [\sum w(|F_o| - |F_c|)^2 / (N_o - N_p)]^{1/2}$.

Table 7. Selected bond lengths (Å) and angles (deg) for **19** and **22***

	19	22
Pd(1)-N(1)	1.998(3)	2.037(2)
Pd(1)-O(1)	2.019(2)	2.025(2)
N(1a)-Pd(1)-N(1)	180.0	180.0
N(1)-Pd(1)-O(1a)	98.30(11)	98.46(10)
N(1)-Pd(1)-O(1)	81.70(11)	81.54(10)
O(1a)-Pd(1)-O(1)	180.0	180

*Symmetry transformations used to generate equivalent atoms:

(a) = -x+1, -y, -z.

Table 8. Selected bond lengths (Å) and angles (deg) for **24***

Pd(2)-N(1)	2.004(4)	Pd(1)-O(7)	2.004(4)
Pd(2)-N(2)	1.998(4)	Pd(1)-N(3)	2.024(5)
Pd(2)-O(1)	2.009(4)	Pd(3)-O(1W)	2.071(5)
Pd(2)-O(4)	2.007(4)	Pd(3)-O(2W)	2.088(5)
N(2)-Pd(2)-N(1)	176.92(18)	O(7)-Pd(1)-N(3)	81.48(19)
N(2)-Pd(2)-O(4)	81.85(17)	O(7a)-Pd(1)-N(3)	98.52(19)
N(1)-Pd(2)-O(4)	97.88(16)	N(3a)-Pd(1)-N(3)	180.0
N(2)-Pd(2)-O(1)	97.94(17)	O(1Wb)-Pd(3)-O(1W)	180.0
N(1)-Pd(2)-O(1)	82.25(16)	O(1Wb)-Pd(3)-O(2W)	92.51(19)
O(4)-Pd(2)-O(1)	178.50(16)	O(1W)-Pd(3)-O(2W)	87.49(19)
O(7)-Pd(1)-O(7a)	180.0	O(2W)-Pd(3)-O(2Wb)	180.0
O(7)-Pd(1)-N(3a)	98.52(19)		

*Symmetry transformations used to generate equivalent atoms:

(a) = -x, -y+1, -z+3; (b) = -x, -y+2, -z+2.

Description of the structures. The structures of **19** and **22** consist of *trans*-[Pd(2,4,6-Me₂pma)₂]²⁻ anions, tetra-*n*-butylammonium cations, and either free acetonitrile (**19**) or acetamide (**22**) co-crystallized molecules as shown in Figures 6a and 6b, respectively [crystal packing in Figures S2 (**19**) and S3 (**22**)].

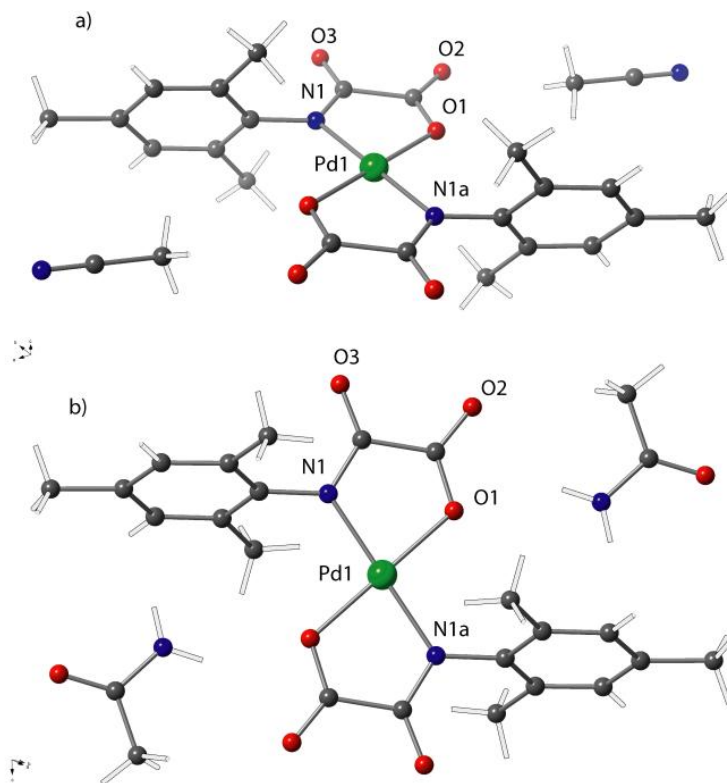


Figure 6: Perspective views of (a) $(n\text{-Bu}_4\text{N})_2[\text{Pd}(2,4,6\text{-Me}_3\text{pma})_2] \cdot 2\text{CH}_3\text{CN}$ (**19**) and (b) $(n\text{-Bu}_4\text{N})_2[\text{Pd}(2,4,6\text{-Me}_3\text{pma})_2] \cdot 2\text{CH}_3\text{CONH}_2$ (**22**) showing the acetonitrile and acetamide molecules of crystallization. Counteranions are omitted for clarity [symmetry code: (a) = $-x+1, -y, -z$].

On the contrary, **23** and **24** contains not only bis(4-Brpma)palladate(II) or bis(4-Clpma)palladate(II) anions [Pd(1) and Pd(2)] but also tetraaquapalladium(II) cations [Pd(3)] plus acetamide molecules (Figures 7-10 for **24** and Figures S3 and S6 for **23**), the electroneutrality being achieved by tetra-*n*-butylammonium cations.

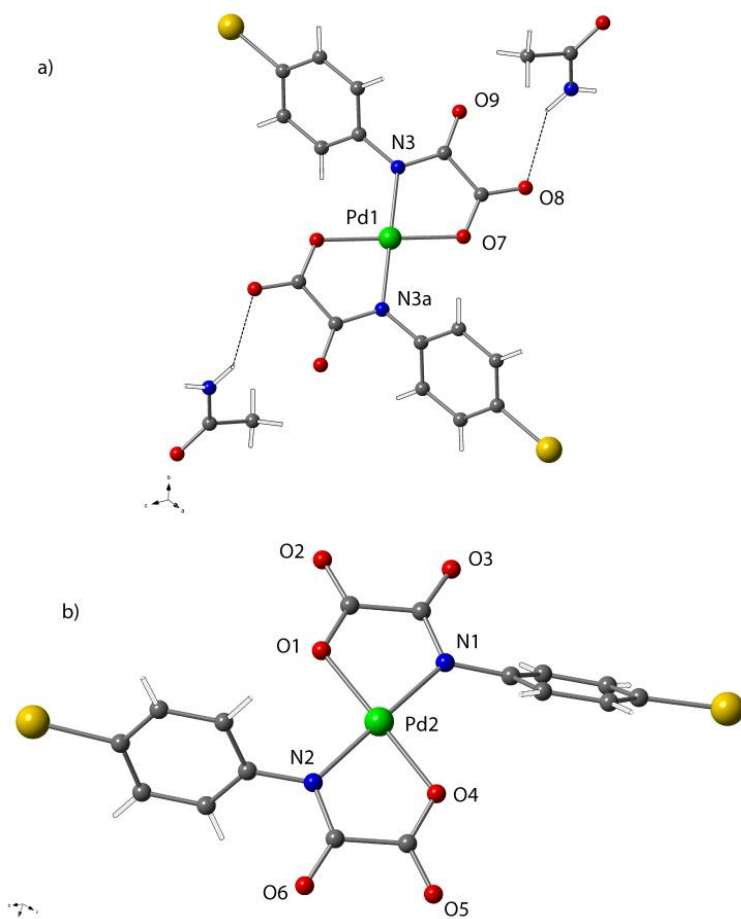


Figure 7. Perspective views of the (a) centro- [Pd(1)] and (b) non-centrosymmetric [Pd(2)] oxamate units of $(n\text{-Bu}_4\text{N})_4[\text{Pd}(\text{H}_2\text{O})_4][\text{Pd}(4\text{-Brpma})_2] \cdot 2\text{CH}_3\text{CONH}_2$ (**24**) [Symmetry code: (a) = $-x, -y+1, -z+3$].

The Pd(II) ions of the bis(oxamato)palladate(II) units in **19** and **22-24** are all four-coordinate with two amidate-nitrogen and two carboxylate-oxygen atoms from the two oxamate ligands in a *trans* square-planar arrangement, their conformation being centrosymmetric [Pd(1) in Figures 6 (**19** and **22**), 7a (**24**) and S3a (**23**)] and non-centrosymmetric [Pd(2) in Figures 7b (**24**) and S3b (**23**)]. The coexistence of the centro- and the non-centrosymmetric bis(oxamato)palladate(II) units is quite surprising.

Concerning the non-centrosymmetric unit in **24** and **23**, the dihedral angle between N(1)O(1)O(2)O(3) and N(2)O(4)O(5)O(6) oxamate planes in the Pd(2) units being ca. 13.6(1)° (Figures 7b and S3b).

Noteworthy, the phenyl rings at the Pd(1) unit of **24** and **23** are parallel (as in **19** and **22**), whereas they form an angle of 58.1° at the Pd(2) unit. The values of the dihedral angles between the square plane and the phenyl ring are 51.3(2)-122.7° (non-centrosymmetric), 51.2(2)° (centrosymmetric) (**24**). All these values are more distant from the orthogonality than those observed in **19** and **22**, probably due to steric reasons that occur in these last cases. Besides the different oxamate ligand, the main structural difference between **24** and **22** is due to the presence of the tetraaquapalladium(II) cation in **24**.

Each Pd(3) atom from the [Pd(H₂O)₄]²⁺ is four-coordinate in a slightly distorted O(1w)O(2w)O(1wa)O(2wa) square-planar geometry (Figure 8). In this regard, the structure of this cation is very similar to that of its Pt(II) analogue.⁶⁸ The O(1w)-Pd(3)-O(2w) and O(1w)-Pd(3)-O(2wa) bond angles are 87.3(2) and 92.7(2)° respectively, and the Pd-Ow lengths at 2.071(5) and 2.088(5) Å are in good agreement with theoretical and experimental values found in the literature.^{8,69-71}

Table 9. Hydrogen bonds (Å) for **24***

O(1w)··O(3)	2.919(4)	O(2w)··O(3)	3.064(4)
O(1w)··O(5b)	3.145(4)	O(2w)··O(6a)	2.895(4)
O(1w)··O(6b)	3.035(4)	O(2w)··O(1Ha)	2.998(4)
O(1w)··O(1H)	3.023(4)	N(1H)··O(8)	2.979(5)
O(2w)··O(2)	3.306(4)	N(1H)··O(9)	3.120(5)

* Symmetry transformation used to generate equivalent atoms:

(a) = -x, y + 1, -z + 3; (b) = -x, -y + 2, -z + 2.

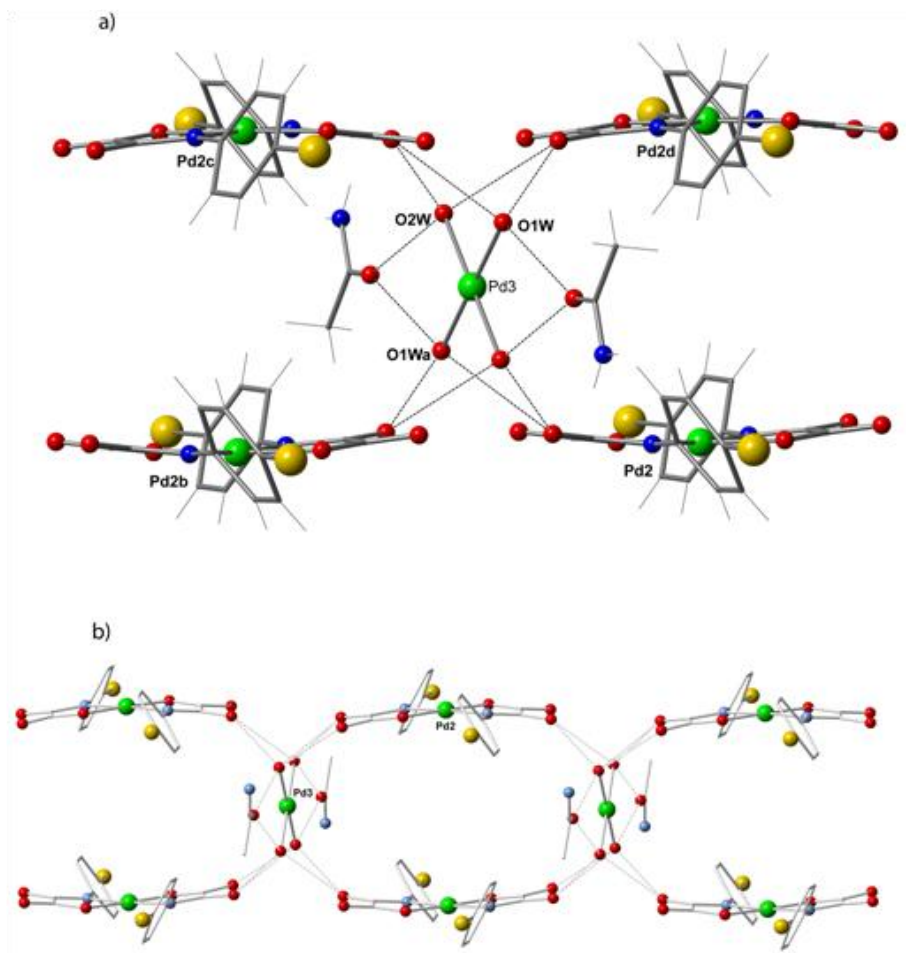


Figure 8. (a) Perspective view of the $[\text{Pd}(\text{H}_2\text{O})_4]^{2+}$ linked by H-bonds to the amide molecules and $[\text{Pd}(\text{oxamato})_2]^{2-}$ species. The organic counter cations have been omitted for clarity. Pd(3)⋯Pd(2) and Pd(3)⋯Pd(2e) distances are: 12.280(1) and 12.133(1) Å, respectively. (b) View of the supramolecular chains in **24** generated by hydrogen bonds (broken lines) involving $[\text{Pd}(\text{H}_2\text{O})_4]^{2+}$ cations, acetamide molecules and distorted bis(oxamato)palladate(II) units [symmetry code: (b) = $-x, -y+2, -z+2$; (c) = $x, 1+y, 1+z$; (d) = $x, y, 1+z$; (e) = $x, 1+y, z$].

Interestingly, this $[\text{Pd}(\text{H}_2\text{O})_4]^{2+}$ cation in **24** interacts with the distorted $[\text{Pd}(4\text{-Brpma})_2]^{2-}$ anions and with the acetamide molecules by hydrogen bonds leading to a supramolecular chain (Figures 8b and S4).

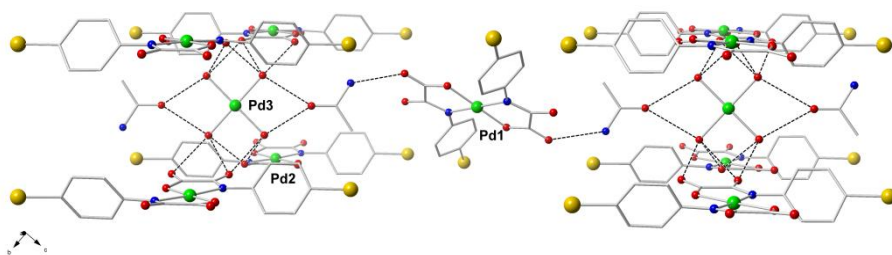


Figure 9. Perspective views of adjacent supramolecular chains in **24** joined by acetamide H-bonds involving bis(oxamato)palladate(II) units. The organic counter cations and hydrogen atoms have been omitted for clarity.

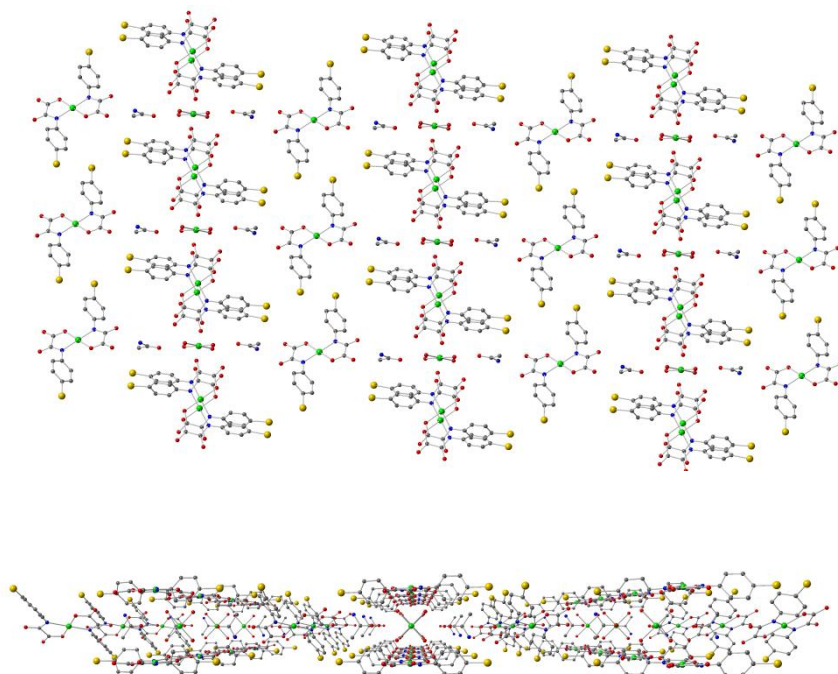
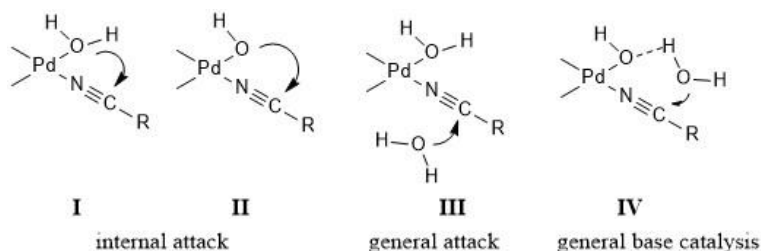


Figure 10. Perspective view (top) and view along the crystallographic *a* axis (bottom) of the packing in **24**, which consists of layers developing in the (1 -1 1) plane, which are built by centrosymmetric bis(oxamato)palladate(II) anions as spacers for different chains (Figure S4) connected to acetamide molecules [Pd(3) \cdots Pd(1) distance equal to 12.280(1) Å].

The $[\text{Pd}(\text{H}_2\text{O})_4]^{2+}$ species in this chain is connected to four non-centrosymmetric bis(oxamato)palladate(II) anions $[\text{Pd}(2)]$ by hydrogen bonds involving its four water molecules and the O(3) and O(6) oxamate-oxygen atoms $[\text{Pd}(2)\cdots\text{Pd}(3)$ distances: 6.917(1) Å] to afford a ladder-like supramolecular motif with two acetamide molecules hydrogen bonded to the tetraaquapalladate(II) unit (see Figure 9). On the whole, supramolecular layers developing in the (1 -1 1) plane arise (see Figures 9-10 and Table 5). Regarding these interactions one can speculate that the tetraaquapalladate(II) species is likely stabilized by a process of *molecular recognition*, through the anionic oxamate complex, appearing thus a suitable choice to grasp the $[\text{Pd}(\text{H}_2\text{O})_4]^{2+}$ in this singular double salt species.

Recently, density functional type DFT calculations taking into account the solvent effects were carried out to investigate the $[\text{Pd}(\text{H}_2\text{O})_4]^{2+}$ -catalyzed acrylonitrile hydration affording the important chemical acrylamide (see Scheme 5).⁷² As a result, it was found that the external water attack on the bound nitrile (**III** in Scheme 5) becomes the only viable mechanism in acidic conditions.



Scheme 5: Alternative mechanisms for Pd-catalyzed nitrile hydration.⁷²

The fact that the hydration of acetonitrile occurs only in basic medium in our system, provides experimental support to a reaction mechanism for the nitrile hydration catalyzed by $[\text{Pd}(\text{H}_2\text{O})_4]^{2+}$ *via* the participation of the hydroxide ligand akin to that proposed by Tílvez *et al.* in 2013 on the basis of DFT type calculations.⁷² The $[\text{Pd}(\text{H}_2\text{O})_3(\text{OH})]^+$ and *cis*- $[\text{Pd}(\text{H}_2\text{O})_2(\text{OH})(\text{RCN})]^+$ entities are the starting complexes that they propose for this reaction pathway, the most favorable mechanism corresponding to an intramolecular nucleophilic hydroxide attack to the coordinated nitrile in the latter species (**II** in Scheme 5).

While the hydroxide-assisted external attack by nucleophilic water leading to acetonitrile hydration (**IV** in Scheme 5) cannot be fully discarded, the presence of the stable $[\text{Pd}(\text{H}_2\text{O})_4]^{2+}$ in the final product (**24**) deserves a further comment. The aqua-Pd(II) ion, easily prepared as perchlorate solution,⁶ is known to have an acidic character (experimental value for $\text{p}K_{\text{a}}$ ca. 3 at 25 °C),⁹ and its maximum stability is achieved at low pH values.¹⁰ In the presence of additional ligands, other factors must concur to stabilize the $[\text{Pd}(\text{H}_2\text{O})_4]^{2+}$ species in solution with respect to substitution of the coordinated water. Bidentate oxamate ligands do prefer to bind in the chelating *N,O* mode usually ending up in the $[\text{Pd}(\text{oxamato})_2]^{2-}$ form. Apparently, while the basic medium is required to promote the catalytic conversion of acetonitrile to acetamide, the stabilization of the aqua-Pd(II) ion (and its incorporation in the final solid product) under our experimental conditions proceeds only through the formation of $[\text{Pd}(\text{oxamato})_2]^{2-}$ in a non-exclusive way. In turn, the bis(oxamato)palladate(II) species seems to be responsible for the extra stabilization needed to keep the $[\text{Pd}(\text{H}_2\text{O})_4]^{2+}$ cation.

IV.11. Conclusions

In the framework of our current studies with oxamato-containing metal complexes envisaging the rational design of multifunctional materials,⁷³⁻⁷⁵ we have isolated novel palladium(II) complexes with *N*-substituted oxamate ligands and proved their activity in the sustainable carbon-carbon coupling reactions.^{18,19,69} Their easy and cheap preparation, environmentally friendly character and cytotoxic activity against leukemia cells²² make them very appealing systems.

Otherwise, changing the reaction conditions and working in basic conditions in H₂O-MeCN solvent mixtures (1:2 v/v) containing [PdCl₄]²⁻ and *N*-substituted oxamic acids, we have observed the serendipitous hydration of acetonitrile to acetamide, without over-hydrolysis of the acetamide to acetic acid. Both the acetamide and the elusive [Pd(H₂O)₄]²⁺ species (likely the precatalyst) form part of the reaction products and they were identified herein by single crystal X-ray diffraction.

Our results show that the hydration of the acetonitrile can be stopped at the amide stage in the presence of oxamato complexes of Pd(II) when the reaction medium is slightly basic (**22-24**) whereas such a hydration does not occur in neutral conditions (**19**). As far as we are aware, the coexistence of the elusive [Pd(H₂O)₄]²⁺ entity and the free acetamide in **24** is unprecedented and the lack of the tetraaquapalladate(II) ion in **22** is most likely due to a different crystallization kinetics. Further studies will be required to draw a full rational for this proposed mechanism for the Pd(II) oxamate-catalyzed nitrile hydration.

IV.12. References

- (1) Vicente, J.; Arcas, A. *Coord. Chem. Rev.* **2005**, *249*, 1135–1154.
- (2) Pearson, R. G. *J. Am. Chem. Soc.* **1963**, *85*, 3533–3539.
- (3) Kettemann, F.; Wuithschick, M.; Caputo, G.; Kraehnert, R.; Pinna, N.; Rademann, K.; Polte, J. *Cryst.Eng.Comm* **2015**, *17*, 1865–1870.
- (4) Yeguas, V.; Campomanes, P.; López, R.; Díaz, N.; Suárez, D. *J. Phys. Chem. B* **2010**, *114*, 8525–8535.
- (5) Boily, J. F.; Seward, T. M. *Geochim. Cosmochim. Acta*, 2005, *69*, 3773–3789.
- (6) Elding, L. I. *Inorg. Chim. Acta*, 1972, *6*, 683–688.
- (7) Elding, L. I. *Inorg. Chim. Acta*, 1976, *20*, 65–69.
- (8) Deeth, R. J.; Elding, L. I. *Inorg. Chem.* **1996**, *35*, 5019–5026.
- (9) Shi, T.; Elding, L. I.; Meľnikov, M. Y.; Feldman, V. I.; Kristjánssdóttir, Á. G.; Matsson, O.; Mikkelsen, K. V.; Senning, A. *Acta Chem. Scand.* **1998**, *52*, 897–902.
- (10) Torapava, N.; Elding, L. I.; Mändar, H.; Roosalu, K.; Persson, I. *Dalton Trans.* **2013**, *42*, 7755–7760.
- (11) Livinghouse, S. E. *Compr. Inorg. Chem.* **1973**, *3*, 1284.
- (12) Maitlis, P.; Espinet, P.; Russel, M. J. H. *Compr. Organomet. Chem.* **1982**, *6*, 236.
- (13) Mehrotra, R. C. *Compr. Coord. Chem.* **1987**, *2*, 1112.
- (14) Pardo, E.; Ruiz-García, R.; Cano, J.; Ottenwaelder, X.; Lescouëzec, R.; Journaux, Y.; Lloret, F.; Julve, M. *Dalt. Trans.* **2008**, 2780–2805.
- (15) SAINT. Version 6.45; Bruker Analytical X-ray Systems: Madison, WI; 2003.
- (16) SADABS, version 2.03, Bruker AXS Inc., Madison, WI, 2000.
- (17) Sheldrick, G. M. *Acta Crystallogr. A.* **2008**, *64*, 112–122.
- (18) Fortea-Pérez, F. R.; Marino, N.; Armentano, D.; De Munno, G.; Julve, M.; Stiriba, S.-E. *Cryst.Eng.Comm* **2014**, *16*, 6971.
- (19) Fortea-Pérez, F. R.; Schlegel, I.; Julve, M.; Armentano, D.; De Munno, G.; Stiriba, S.-E. *J. Organomet. Chem.* **2013**, *743*, 102–108.
- (20) Kivekas, R.; Pajunen, A.; Navarrete, A.; Colacio, E. *Inorg. Chim. Acta*, **1999**, *284*, 292–295.
- (21) Oliveira, W. X. C.; Ribeiro, M. A.; Pinheiro, C. B.; Nunes, W. C.; Julve, M.; Journaux, Y.; Stumpf, H. O.; Pereira, C. L. M. *Eur. J. Inorg. Chem.* **2012**, *2012*, 5685–5693.
- (22) Oliveira, W. X. C.; da Costa, M. M.; Fontes, A. P. S.; Pinheiro, C. B.; de Paula, F. C. S.; Jaimes, E. H. L.; Pedroso, E. F.; de Souza, P. P.; Pereira-Maia, E. C.; Pereira, C. L. M. *Polyhedron* **2014**, *76*, 16–21.
- (23) Biffis, A.; Zecca, M.; Basato, M. *J. Mol. Catal. A Chem.* **2001**, *173*, 249–274.
- (24) De Vries, A. H. M.; Mulders, J. M. C. a; Mommers, J. H. M.; Henderickx, H. J. W.; de Vries, J. G. *Org. Lett.* **2003**, *5*, 3285–3288.
- (25) Brasche, G.; García-Fortanet, J.; Buchwald, S. L. *Org. Lett.* **2008**, *10*, 2207–2210.
- (26) Tamami, B.; Ghasemi, S. *J. Mol. Catal. A Chem.* **2010**, *322*, 98–105.
- (27) Yeung, C. S.; Dong, V. M. *Chem. Rev.* **2011**, *111*, 1215–1292.

- (28) Behr, A.; Neubert, P. In *Applied Homogeneous Catalysis*; John Wiley & Sons, 2012; pp. 716, pag.41.
- (29) Hao, L.; Mu, C.; Wang, R. *Acta Crystallogr. Sect. E. Struct. Rep. Online* **2008**, *64*, m896.
- (30) Salomon, C.; Fortin, D.; Darcel, C.; Jugé, S.; Harvey, P. D. *J. Clust. Sci.* **2009**, *20*, 267–280.
- (31) Caldò, V.; Nacci, A.; Monopoli, A.; Montingelli, F. *J. Org. Chem.* **2005**, *70*, 6040–6044.
- (32) Tatumi, R.; Akita, T.; Fujihara, H. *Chem. Commun.* **2006**, 3349–3351.
- (33) Marion, N.; Nolan, S. P. *Acc. Chem. Res.* **2008**, *41*, 1440–1449.
- (34) Molnár, Á. *Chem. Rev.* **2011**, *111*, 2251–2320.
- (35) Han, W.; Liu, C.; Jin, Z.-L. *Org. Lett.* **2007**, *9*, 4005–4007.
- (36) Han, W.; Liu, C.; Jin, Z. *Adv. Synth. Catal.* **2008**, *350*, 501–508.
- (37) Ogasawara, S.; Kato, S. *J. Am. Chem. Soc.* **2010**, *132*, 4608–4613.
- (38) Liu, L.; Dong, Y.; Tang, N. *Green Chem.* **2014**, *16*, 2185.
- (39) Jeffery, T. *Tetrahedron Lett.* **1985**, *26*, 2667–2670.
- (40) Leadbeater, N. E.; Marco, M. *Org. Lett.* **2002**, *4*, 2973–2976.
- (41) Bandgar, B. P.; Bettigeri, S. V.; Phopase, J. *Tetrahedron Lett.* **2004**, *45*, 6959–6962.
- (42) Liu, L.; Zhang, Y.; Xin, B. *J. Org. Chem.* **2006**, *71*, 3994–3997.
- (43) Knowles, C. J.; Wyatt, J. W. In *In Microbial Control of Pollution*; Fry, J. C.; Gadd, G. M.; Herbert, R. A.; Jones, C. W.; Watson-Craik, I. A., Eds.; Cambridge University Press, 1992; pp. 113–128.
- (44) Greenberg, A.; Breneman, C. M.; Liebman, J. F. *The Amide Linkage: Structural Significance in Chemistry, Biochemistry, and Materials Science*; John Wiley & Sons, 2000.
- (45) Gross, R. A.; Kalra, B. *Science*, **2002**, *297*, 803–807.
- (46) Vishweshwar, P.; McMahon, J. A.; Peterson, M. L.; Hickey, M. B.; Shattock, T. R.; Zaworotko, M. J. *Chem. Commun.* **2005**, 4601–4603.
- (47) Allen, C. L.; Williams, J. M. J. *Chem. Soc. Rev.* **2011**, *40*, 3405–3415.
- (48) Cadierno, V.; Crochet, P.; García-Álvarez, R.; Crochet, P.; Cadierno, V. *Green Chem.* **2013**, *15*, 46.
- (49) Kaminskaia, N. V.; Kostic, N. M. *J. Chem. Soc. Dalt. Trans.* **1996**, 3677.
- (50) Kukushkin, V. Y.; Pombeiro, A. J. L. *Inorg. Chim. Acta* **2005**, *358*, 1–21.
- (51) Bruckner, R. In *In Organic Mechanisms: Reactions, Stereochemistry and Synthesis*; Springer Science & Business Media, 2010; p. 856.
- (52) Yamaguchi, K.; Matsushita, M.; Mizuno, N. *Angew. Chem. Int. Ed.* **2004**, *43*, 1576–1580.
- (53) Kukushkin, V. Y.; Pombeiro, A. J. L. *Chem. Rev.* **2002**, *102*, 1771–1802.
- (54) McMahon, J. A.; Bis, J. A.; Vishweshwar, P.; Shattock, T. R.; McLaughlin, O. L.; Zaworotko, M. J. *Zeitschrift für Krist.* **2005**, *220*, 340–350.
- (55) Mitsudome, T.; Mikami, Y.; Mori, H.; Arita, S.; Mizugaki, T.; Jitsukawa, K.; Kaneda, K. *Chem. Commun.* **2009**, 3258–3260.

- (56) Ahmed, T. J.; Knapp, S. M. M.; Tyler, D. R. *Coord. Chem. Rev.* **2011**, *255*, 949–974.
- (57) Kumar, S.; Mohan, U.; Kamble, A. L.; Pawar, S.; Banerjee, U. C. *Bioresour. Technol.* **2010**, *101*, 6856–6858.
- (58) Swartz, R. D.; Coggins, M. K.; Kaminsky, W.; Kovacs, J. A. *J. Am. Chem. Soc.* **2011**, *133*, 3954–3963.
- (59) Crestani, M. G.; Arévalo, A.; García, J. J. *Adv. Synth. Catal.* **2006**, *348*, 732–742.
- (60) Li, Z.; Wang, L.; Zhou, X. *Adv. Synth. Catal.* **2012**, *354*, 584–588.
- (61) Cadierno, V.; Francos, J.; Gimeno, J. *Chem. Eur. J.* **2008**, *14*, 6601–6605.
- (62) Cadierno, V.; Díez, J.; Francos, J.; Gimeno, J. *Chem. - A Eur. J.* **2010**, *16*, 9808–9817.
- (63) Villain, G.; Gaset, A.; Kalck, P. *J. Mol. Catal.* **1981**, *12*, 103–111.
- (64) Hirano, T.; Uehara, K.; Kamata, K.; Mizuno, N. *J. Am. Chem. Soc.* **2012**, *134*, 6425–6433.
- (65) Ghaffar, T.; Parkins, A. W. *J. Mol. Catal. A Chem.* **2000**, *160*, 249–261.
- (66) Lignier, P.; Estager, J.; Kardos, N.; Gravouil, L.; Gazza, J.; Naffrechoux, E.; Draye, M. *Ultrasound. Sonochem.* **2011**, *18*, 28–31.
- (67) Suzuki, A. *Angew. Chem. Int. Ed.* **2011**, *50*, 6722–6737.
- (68) Seppelt, K. *Z. Anorg. Allg. Chem.* **2010**, *636*, 2391–2393.
- (69) Fortea-Pérez, F. R.; Armentano, D.; Julve, M.; De Munno, G.; Stiriba, S.-E. *J. Coord. Chem.* **2014**, *67*, 4003–4015.
- (70) Purans, J.; Fourest, B.; Cannes, C.; Sladkov, V.; David, F.; Venault, L.; Lecomte, M. *J. Phys. Chem. B* **2005**, *109*, 11074–11082.
- (71) Bowron, D. T.; Beret, E. C.; Martin-Zamora, E.; Soper, A. K.; Sánchez Marcos, E. *J. Am. Chem. Soc.* **2012**, *134*, 962–967.
- (72) Tílvez, E.; Menéndez, M. I.; López, R. *Inorg. Chem.* **2013**, *52*, 7541–7549.
- (73) Dul, M.-C.; Pardo, E.; Lescouëzec, R.; Journaux, Y.; Ferrando-Soria, J.; Ruiz-García, R.; Cano, J.; Julve, M.; Lloret, F.; Cangussu, D.; Pereira, C. L. M.; Stumpf, H. O.; Pasán, J.; Ruiz-Pérez, C. *Coord. Chem. Rev.* **2010**, *254*, 2281–2296.
- (74) Grancha, T.; Ferrando-Soria, J.; Castellano, M.; Julve, M.; Pasán, J.; Armentano, D.; Pardo, E. *Chem. Commun.* **2014**, *50*, 7569–7585.
- (75) Castellano, M.; Ruiz-García, R.; Cano, J.; Ferrando-Soria, J.; Pardo, E.; Fortea-Pérez, F. R.; Stiriba, S.-E.; Julve, M.; Lloret, F. *Acc. Chem. Res.* **2015**, *48*, 510–520.

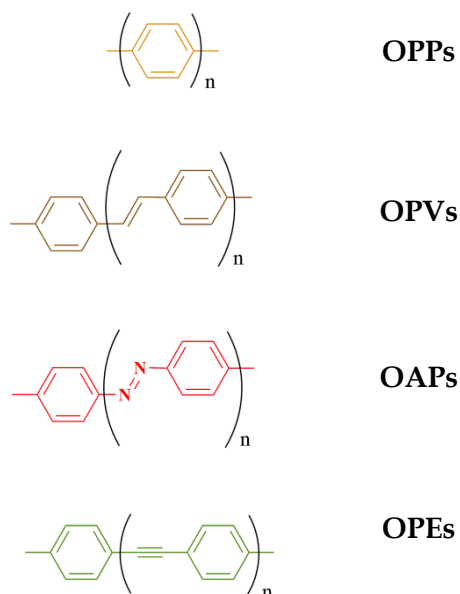
V

Chapter 4

Dipalladium(II) -oxamate metallacyclophanes

V.1. Searching new functionalities

Supramolecular coordination chemistry, referred to as metallosupramolecular chemistry, is an outstanding research area that offers convenient tools to deal with the ligand design¹⁻⁴ of new frameworks (Scheme 1) and the preparation of multi-functional complexes.⁵⁻⁸ The strategy developed by our group in this area is based on the use of dinucleating ligands having two oxamato donor groups separated by more or less rigid noninnocent, extended π -conjugated aromatic spacers that self-assemble with palladium(II) ions to form double-stranded dipalladium(II) metallacyclic complexes of the cyclophane type.



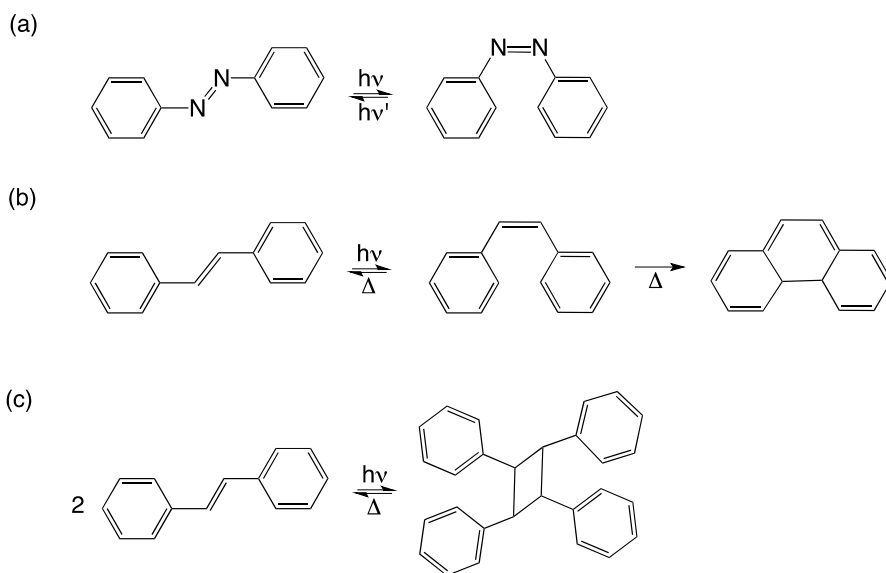
Scheme 1. New framework ligands as spacer for dinuclear metallacyclophane complexes: oligo(*p*-phenyl) (OPPs), oligo(*p*-phenylene vinylenes) (OPVs), oligo(*p*-azophenylenes) (OAPs), oligo(*p*-phenylene ethynylene) (OPEs).

This kind of proligands could be used for the design and synthesis of novel types of electro- and photoactive noninnocent aromatic bridging ligands which constitute thus a major goal in the field of metallosupramolecular chemistry.

Having this idea in mind, oligo(*p*-phenylene vinylenes) (OPVs) and oligo(*p*-azophenylenes) (OAPs) such as 4,4'-stilbene and 4,4'-azobenzene respectively, seem excellent candidates, which possess a well-recognized and rich photochemical reactivity that includes both uni- (*trans/cis* geometric isomerization or intramolecular cyclization) and bimolecular reactions (intermolecular cycloaddition), either in solution or in the solid state (Scheme 2)⁹⁻¹¹.

This means that the stable *trans* isomer of azobenzene can be converted into the unstable *cis* isomer and *vice versa* after irradiation with UV and visible light, respectively (Scheme 2a)¹².

In contrast, the stable *trans* isomer of stilbene turns into the unstable *cis* isomer after UV light irradiation, which can thermally relax to the more stable *trans* isomer or eventually lead to the closed isomer after subsequent intramolecular cyclization (Scheme 2b)¹³.



Scheme 2. Photochemical reactions of azobenzene (a) and stilbene (b) and (c).

On the other hand, stilbene may undergo a [2+2] photocycloaddition reaction through the carbon atoms of the central vinylene group to afford the corresponding photodimer (Scheme 2c)¹³⁻¹⁶.

Although the photodimerization of stilbene was also known since the beginning of the last century, relatively few investigations have focused on stilbene itself and its derivatives, probably due to the poor efficiency of the [2+2] photocycloaddition reaction. MacGillivray and co-workers have recently investigated the template photodimerization of coordinating-group substituted stilbene derivatives such as 4,4'-dipyridylethene in the solid state.^{17,18} Such studies show that ligand coordination within a metallacyclic entity direct the exclusive formation of the corresponding [2+2] photocycloaddition product in a stereospecific manner and in an almost quantitative yield.¹⁸

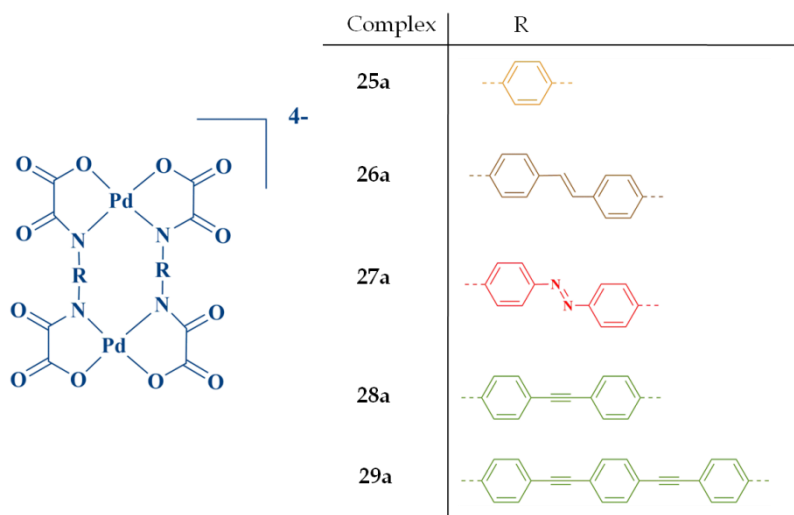
Our research interest in this type of proligands also focuses on their medical activity, specifically in cytotoxicity studies to fight leukemia cancer.¹⁹ Given that the cisplatin {*cis*-diamminedichloroplatinum(II), *cis*-[PtCl₂(NH₃)₂]}^{20,21} was found to be one of the most powerful chemotherapeutic agents against ovarian and testicular cancer,²² the finding out of new noble metal-based drugs has become a subject of outmost interest for researchers.²³ In this search, platinum(II) was the elected metal over the years²⁴⁻²⁷ but with the discover of the first non-platinum compound, the *cis*-[Ti(VI)(bzac)₂(OEt)₂],^{28,29} new metal-based drugs have been investigated as alternatives.^{30,31} Seeking out these new choices, a good candidate to compare with platinum(II) is palladium(II), which has a similar coordination chemistry and a greater solubility in water of its complexes compared to the analogous ones of platinum(II).³² It is worth noting that the first studies of Pd(II)-based anticancer activity date from 15 years ago.²³

Apart from the metal-based drugs, special attention has been paid to the replacement of one or both NH₃ ligands of *cisplatin* by other *N*-donor ligand(s) in order to avoid toxicity and development of resistance to further drug treatment.³³ In this search, the oxamate group as ligand seems a suitable choice with a strong electron-donating capability of its deprotonate nitrogen-amide atom together with the good donor properties of the carboxylate-oxygen atom which accounts for the greater stability of its metal complexes when comparing to those with the oxalate ligands.

V.2. Aim

In previous chapters it was shown that mononuclear bis(*N*-substituted oxamate)palladate(II) complexes are active catalysts for carbon-carbon cross-coupling reactions with an oxamate ligand as protecting sphere.

In an attempt to get new framework systems with more than one function, we have synthesized and characterized the *N*-phenyl(oxamic acid ethyl ester) spacer ligands (Scheme 1) the corresponding oxamate-bridge dipalladate(II) complexes of formula $(n\text{-Bu}_4\text{N})_4[\text{Pd}_2(\text{ppba})_2]$ (**25a**), $(n\text{-Bu}_4\text{N})_4[\text{Pd}_2(\text{dpvba})_2]$ (**26a**), $(n\text{-Bu}_4\text{N})_4[\text{Pd}_2(\text{dpazba})_2]$ (**27a**), $(n\text{-Bu}_4\text{N})_4[\text{Pd}_2(\text{dpeba})_2]$ (**28a**), $(n\text{-Bu}_4\text{N})_4[\text{Pd}_2(\text{tpeba})_2]$ (**29a**). One could expect that the variation of the aromatic spacer in this family of oxamate-containing dipalladium(II) metallacyclophanes might control their overall structure and properties.

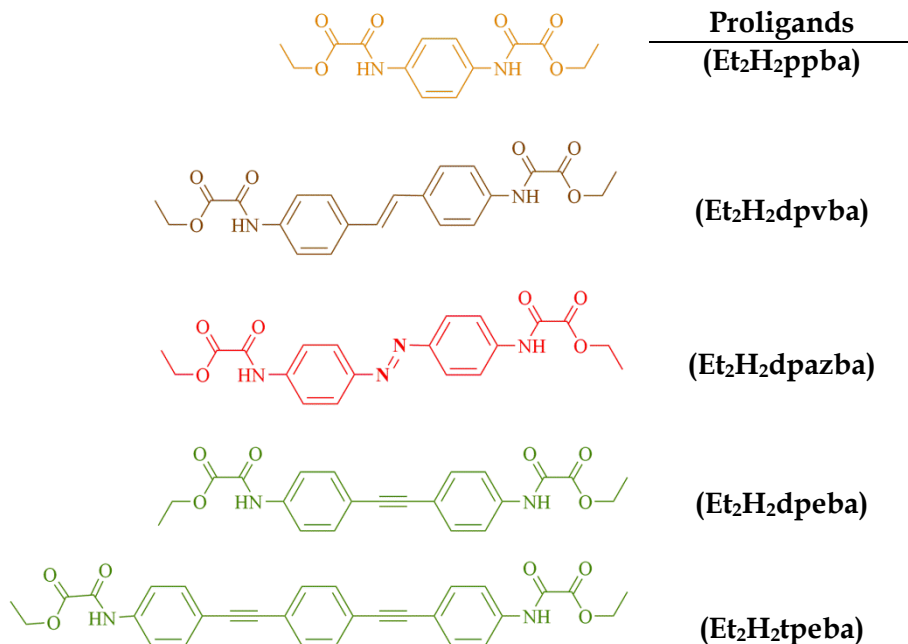


Scheme 3. Dinuclear palladium(II) metallacyclophane complexes of general formula $[\text{Pd}_2\text{L}_2]^{4-}$.

The contents of this Chapter is as follows: (i) the preparation, spectroscopy and structural characterization of these dinuclear complexes; (ii) the study of their catalytic activity for Heck and Suzuki reactions under homogeneous regime and in ionic liquid media; (iii) a preliminary study of the coordination-driven self-assembly for the supramolecular control of photochemical reactivity and photophysical properties;³⁴ (iv) and finally, a preliminary investigation of the cytotoxicity on leukemia cells.

V.3. Synthesis and characterization

The general synthetic method for the preparation of the aniline derivatives and proligands (Scheme 4) follows the procedure used in previous works^{3,35-39}. For further information see summary, Appendix C.



Scheme 4. Spacer proligands obtained from aniline derivatives.

Synthesis of complexes

The synthetic method for the dipalladium(II) metallacyclophane complexes (**21a-25a**) with *n*-Bu₄N⁺ as counter ion was detailed in *Chapter 1 - part II*.

X-ray quality crystals as yellow prisms (Ph₄As)₄[Pd₂(ppba)₂] · 23H₂O (**25**) and (*n*-Bu₄N)₄[Pd₂(dpeba)₂] · 4CH₃OH (**28**) as brown needles (*n*-Bu₄N)₄[Pd₂(dpvba)₂] · 6CH₃OH · CH₃CH₂OCH₂CH₃ (**26**) and as orange needles (*n*-Bu₄N)₄[Pd₂(dpazba)₂] · 5CH₃OH (**27**) were grown by two different methods:

(i) an aqueous solution of the solid complex was added to Ph_4AsCl to help the crystallization for **25**, suitable crystals being formed within 4-8 weeks.

(ii) vapour diffusion of ether into a methanol or acetonitrile solution of the solid sample was used for **26-28** and the single crystals appeared in hours.

Characterization of complexes:

(*n*-Bu₄N)₄[Pd₂(ppba)₂] (25a). Yield: 85%. IR (KBr/cm⁻¹): 3422 (O-H), 2961, 2931, 2874 (C-H), 1670, 1641, 1605, 1578 (C=O). ¹H NMR (CDCl₃) δ(ppm): 0.98-1.02 (t, 24H, *n*-Bu₄N⁺), 1.36-1.43 (q, 16H, *n*-Bu₄N⁺), 1.53-1.56 (m, 16H, *n*-Bu₄N⁺), 3.09-3.15 (m, 16H, *n*-Bu₄N⁺), 7.20-7.25 (m, 8H, H_{aryl}). Anal. Calcd. for C₈₄H₁₅₂N₈O₁₂Pd₂ (**25a**): C 60.09, H 9.13, N 6.67. Found: C 58.02, H 8.59, N 6.50%.

(*n*-Bu₄N)₄[Pd₂(dpvba)₂] (26a). Yield: 78%. IR (KBr/cm⁻¹): 3423 (O-H), 2962, 2936, 2875 (C-H), 1670, 1646, 1609, 1585 (C=O). ¹H NMR (CDCl₃) δ(ppm): 0.97-1.01 (t, 24H, *n*-Bu₄N), 1.39-1.44 (q, 16H, *n*-Bu₄N), 1.50-1.57 (m, 16H, *n*-Bu₄N), 3.13-3.19 (m, 16H, *n*-Bu₄N), 6.58-6.59 (d, 4H, CH), 6.61-6.71 (m, 16H, H_{aryl}). Anal. Calcd. for C₁₀₀H₁₆₄N₈O₁₂Pd₂ (**26a**): C 63.78, H 8.78, N 6.67. Found: C 64.30, H 8.84, N 6.86%.

(*n*-Bu₄N)₄[Pd₂(dpazba)₂] (27a). Yield: 84%. IR (KBr/cm⁻¹): 3422 (O-H), 2960, 2933, 2874, 2847 (C-H), 1671, 1642, 1609, 1585 (C=O). ¹H NMR (CDCl₃) δ(ppm): 0.93-0.98 (t, 24H, *n*-Bu₄N⁺), 1.35-1.37 (q, 16H, *n*-Bu₄N⁺), 1.49-1.51 (m, 16H, *n*-Bu₄N⁺), 3.06-3.12 (m, 16H, *n*-Bu₄N⁺), 6.78-6.81 (m, 8H, H_{aryl}), 7.13-7.16 (m, 8H, H_{aryl}). Anal. Calcd. for C₉₆H₁₆₀N₁₂O₁₂Pd₂ (**27a**): C 61.18, H 8.55, N 8.91. Found: C 62.82, H 9.48, N 9.65%.

(*n*-Bu₄N)₄[Pd₂(dpeba)₂] (28a). Yield: 91%. IR (KBr/cm⁻¹): 3423 (O-H), 2962, 2936, 2876 (C-H), 1671, 1643, 1609, 1583 (C=O). ¹H NMR (CDCl₃) δ(ppm): 0.97-1.02 (t, 24H, *n*-Bu₄N⁺), 1.40-1.43 (q, 16H, *n*-Bu₄N⁺), 1.56-1.59 (m, 16H, *n*-Bu₄N⁺), 3.15-3.21 (m, 16H, *n*-Bu₄N⁺), 6.60-6.63 (d, 8H, H_{aryl}), 6.82-6.85 (d, 8H, H_{aryl}). Anal. Calcd. for C₁₀₀H₁₆₀N₈O₁₂Pd₂ (28a): C 63.91, H 8.58, N 5.96. Found: C 64.07, H 9.52, N 5.85%.

(*n*-Bu₄N)₄[Pd₂(tpeba)₂] (29a). Yield: 74%. IR (KBr/cm⁻¹): 3424 (O-H), 2962, 2933, 2875 (C-H), 1676, 1655, 1634, 1583 (C=O). ¹H NMR (CDCl₃) δ(ppm): 0.96-1.02 (t, 24H, *n*-Bu₄N⁺), 1.40-1.77 (q, 16H, *n*-Bu₄N⁺), 1.61-1.67 (m, 16H, *n*-Bu₄N⁺), 3.26-3.32 (m, 16H, *n*-Bu₄N⁺), 7.44-7.48 (m, 16H, H_{aryl}), 7.65-7.69 (m, 8H, H_{aryl}). Anal. Calcd. for C₁₁₆H₁₆₈N₈O₁₂Pd₂ (29a): C 67.00, H 8.14, N 5.39. Found: C 67.90, H 4.40, N 5.02%.

V.4. Results and discussion

Synthesis and IR Spectroscopy. The *N*-substituted oxamate ligands (Scheme 4) were easily prepared as the respective ethyl ester proligands by the straightforward condensation of the ethyl chlorooxacetate with the corresponding aniline derivative in THF, in presence of Et₃N as a base at room temperature. They were isolated in very good yields (ca. 80–96 %). The IR spectra of the proligands exhibit a typical absorption peak at ca. 3300 cm⁻¹ for the N-H stretching vibration and two intense bands at ca. 1727 and 1677 cm⁻¹ which clearly correspond to the stretching from the ester and amide groups, respectively. ¹H and ¹³C NMR spectra provide additional support for the signal of the N-H amide hydrogen as well as those corresponding to the ethyl group of the ester.

The lack of the signals of the N-H amide and ethyl groups together with the occurrence of two intense bands shifting to lower energies (ca. 1638 and 1600 cm⁻¹) in infrared spectra of **25a-29a** supports the deprotonation of the amide group and the hydrolysis of the ester and suggests that these hydrogen atoms are not present after the deprotonation and hydrolysis of the proligands with the subsequent coordination of the amide-nitrogen and one carboxylate-oxygen to the palladium(II) ion. All these spectroscopic features were supported by the determination of the X-ray structures of complexes **25-28**.

X-ray structural determination: Single crystal X-ray diffraction data for **25-28** were collected at 100 K on a Bruker-Nonius X8-APEXII CCD area detector system using graphite-monochromated Mo-K α radiation ($\lambda = 0.71073 \text{ \AA}$), and processed through the SAINT reduction and SADABS absorption software. Their structures were solved by direct methods and subsequently completed by Fourier recycling using the SHELXTL-2013 software packages, then refined by the full-matrix least-squares refinements based on F^2 with all observed reflections. Crystal data and refinements conditions, selected bond lengths and angles and Pd···Pd separation for **25-28** are grouped in Tables 1 to 5, respectively.

Table 1. Crystal data and structure refinement for **25-28**

	25	26	27	28
Formula	C ₈₀ H ₈₀ N ₄ O ₁₀ As ₂ Pd ₂	C ₁₁₂ H ₂₀₄ N ₈ O ₂₁ Pd ₂	C ₁₀₂ H ₁₈₄ N ₁₂ O ₁₈ Pd ₂	C ₅₄ H ₉₇ N ₄ O ₁₀ Pd
Mr	1620.12	2211.63	2079.41	1068.75
Crystal	Triclinic	Triclinic	Triclinic	Triclinic
Space	<i>P</i> -1	<i>P</i> 1	<i>P</i> -1	<i>P</i> -1
<i>a</i> / Å	13.3025(9)	12.0326(5)	11.9627(13)	10.4534(7)
<i>b</i> / Å	18.2238(13)	14.1370(6)	14.2598(16)	14.7803(10)
<i>c</i> / Å	18.7065(12)	20.7121(9)	20.435(2)	20.3003(13)
α / °	109.375(3)	70.239(2)	69.618(5)	102.903(2)
β / °	103.060(3)	76.719(2)	89.594(5)	102.983(2)
γ / °	99.967(3)	70.278(2)	69.736(5)	105.397(2)
<i>V</i> / Å ³	4012.7(5)	3094.6(2)	3039.8(6)	2809.8(3)
<i>Z</i>	2	1	1	2
<i>D_c</i> / g cm ⁻³	1.341	1.187	1.136	1.263
<i>T</i> / K	100(2)	100(2)	100(2)	100(2)
μ / mm ⁻¹	1.322	0.355	0.356	0.388
<i>F</i> (000)	1652	1192	1116	1150
Theta range for data collection	1.21 to 23.92°	1.05 to 21.75°	1.07 to 24.45°	1.079 to 28.185°
Index ranges	-15 ≤ <i>h</i> ≤ 15, -20 ≤ <i>k</i> ≤ 20, -21 ≤ <i>l</i> ≤ 21	-12 ≤ <i>h</i> ≤ 11, -14 ≤ <i>k</i> ≤ 14, -21 ≤ <i>l</i> ≤ 21	-13 ≤ <i>h</i> ≤ 13, -16 ≤ <i>k</i> ≤ 16, -23 ≤ <i>l</i> ≤ 23	-13 ≤ <i>h</i> ≤ 13, -18 ≤ <i>k</i> ≤ 19, -26 ≤ <i>l</i> ≤ 26
Reflec. collected	72220	25272	50944	40964
Ref. method		Full-matrix least-squares on <i>F</i> ²		
Indep. reflections	12395	13532	9814	12043
[<i>R</i> (int)]	[0.0421]	[0.0420]	[0.0446]	[0.0251]
Data / restraints / parameters	12395 / 0 / 972	13532 / 4 / 1120	9814 / 6 / 636	12043 / 0 / 631
Goodness-of-fit ^c	1.024	1.606	1.092	0.898
Final <i>R</i> indices	<i>R</i> ₁ = 0.0777, [<i>I</i> > 2 σ (<i>I</i>)] <i>wR</i> ₂ = 0.1993	<i>R</i> ₁ = 0.0762, <i>wR</i> ₂ = 0.1953	<i>R</i> ₁ = 0.0967, <i>wR</i> ₂ = 0.2658	<i>R</i> ₁ = 0.0323, <i>wR</i> ₂ = 0.0920
<i>R</i> indices (all data)	<i>R</i> ₁ = 0.0943, <i>wR</i> ₂ = 0.2169	<i>R</i> ₁ = 0.0929, <i>wR</i> ₂ = 0.2185	<i>R</i> ₁ = 0.1074, <i>wR</i> ₂ = 0.2783	<i>R</i> ₁ = 0.0391, <i>wR</i> ₂ = 0.1064
Largest diff. peak / hole, e Å ⁻³	3.686 / -2.372	2.286 / -1.673	5.265 / -0.906	0.810 / -0.936

$$^a R_1 = \sum(|F_o| - |F_c|) / \sum |F_o|, \quad ^b wR_2 = [\sum w(F_o^2 - F_c^2)^2 / \sum w(F_o^2)^2]^{1/2}, \quad ^c S = [\sum w(|F_o| - |F_c|)^2 / (N_o - N_p)]^{1/2}.$$

Table 2. Selected bond lengths (Å) and angles (deg) for **25**

Pd(1)-N(1)	2.030(7)	Pd(1)-O(1)	2.034(6)
Pd(1)-N(2)	2.029(8)	Pd(1)-O(4)	2.036(6)
Pd(2)-N(3)	2.034(11)	Pd(2)-O(7)	2.043(10)
Pd(2)-N(4)	2.021(11)	Pd(2)-O(10)	2.031(10)
As(1)-C(21)	1.931(8)	As(2)-C(45)	1.932(8)
As(1)-C(27)	1.927(8)	As(2)-C(51)	1.918(8)
As(1)-C(33)	1.920(7)	As(2)-C(57)	1.917(8)
As(1)-C(39)	1.929(8)	As(2)-C(63)	1.924(8)
N(1) -Pd(1)-O(1)	81.0(3)	N(3) -Pd(2)-O(7)	81.1(4)
N(1)-Pd(1)-O(4)	172.0(3)	N(4)-Pd(2)-O(7)	173.0(4)
N(2)-Pd(1)-O(1)	173.2(3)	N(3)-Pd(2)-O(10)	172.6(4)
N(2)-Pd(1)-O(4)	81.6(3)	N(4)-Pd(2)-O(10)	82.0(4)
N(2)-Pd(1)-N(1)	105.8(3)	N(3)-Pd(2)-N(4)	105.4(4)
O(1)-Pd(1)-O(4)	91.6(3)	O(7)-Pd(2)-O(10)	91.5(4)

Table 3. Selected bond lengths (Å) and angles (deg) for **26**

Pd(1)-N(1)	1.96(2)	Pd(1)-O(1)	1.920(19)
Pd(1)-N(2)	2.067(17)	Pd(1)-O(4)	2.069(18)
Pd(2)-N(3)	1.96(2)	Pd(2)-O(7)	1.968(17)
Pd(2)-N(4)	2.14(2)	Pd(2)-O(10)	2.055(16)
N(1) -Pd(1)-O(1)	80.3(8)	N(3) -Pd(2)-O(7)	81.7(8)
N(1)-Pd(1)-O(4)	169.6(8)	N(4)-Pd(2)-O(7)	173.6(9)
N(2)-Pd(1)-O(1)	171.8(8)	N(3)-Pd(2)-O(10)	172.1(8)
N(2)-Pd(1)-O(4)	82.9(7)	N(4)-Pd(2)-O(10)	83.2(8)
N(2)-Pd(1)-N(1)	107.5(8)	N(3)-Pd(2)-N(4)	104.7(8)
O(1)-Pd(1)-O(4)	89.3(6)	O(7)-Pd(2)-O(10)	90.4(7)

Table 4. Selected bond lengths (Å) and angles (deg) for **27*** and **28†**

	27	28
Pd(1)-N(1)	2.030(6)	2.0237(19)
Pd(1)-N(2)	2.028(6)	2.0237(18)
Pd(1)-O(1)	2.010(5)	2.0064(16)
Pd(1)-O(4)	2.014(5)	2.0149(15)
N(1)-Pd(1)-O(1)	81.3(2)	81.56(7)
N(1)-Pd(1)-O(4)	171.7(2)	171.35(7)
N(2)-Pd(1)-O(1)	171.6(2)	171.46(7)
N(2)-Pd(1)-O(4)	81.4(2)	81.59(7)
N(2)-Pd(1)-N(1)	106.9(2)	106.96(7)
O(1)-Pd(1)-O(4)	90.5(2)	89.91(6)

Symmetry transformations used to generate equivalent atoms:

**(a)* = -*x*, -*y* + 1, -*z* + 1; *(b)* = -*x* + 1, -*y*, -*z* + 1

†*(a)* = -*x*, -*y*, -*z*.

Table 5. Pd ⋯ Pd separation (Å) across the dinucleating oxamate for **25-28**

	25	26	27	28
Pd(1) ⋯ Pd(2)	8.114(4)	14.706(4)		
Pd(1) ⋯ Pd(1a)			14.332(3)	14.920(3)

Symmetry transformations used to generate equivalent atoms:

(a) = -*x*, -*y* + 1, -*z* + 1 (**27**) and *(a)* = -*x*, -*y*, -*z* (**28**).

Description of the structures

(Ph₄As)₄[Pd₂(ppba)₂] · 23H₂O (25). This compound crystallizes in the triclinic space group *P*-1 and its structure consists of non-centrosymmetric binuclear [Pd₂(ppba)₂]⁴⁺ units (Figure 1) and Ph₄As⁺ counter cations. Each palladium(II) ion is four-coordinate with two amidate-nitrogen and two carboxylate-oxygen atoms from the bis(oxamate) ligand building a distorted square-planar surrounding. The reduced bite of the bidentate oxamate {81.0(3)/81.6(3) at Pd(1) and 81.1(4)/82.0(4)^o at Pd(2)} accounts for the deviations of the ideal value of 90^o for the square planar surrounding.

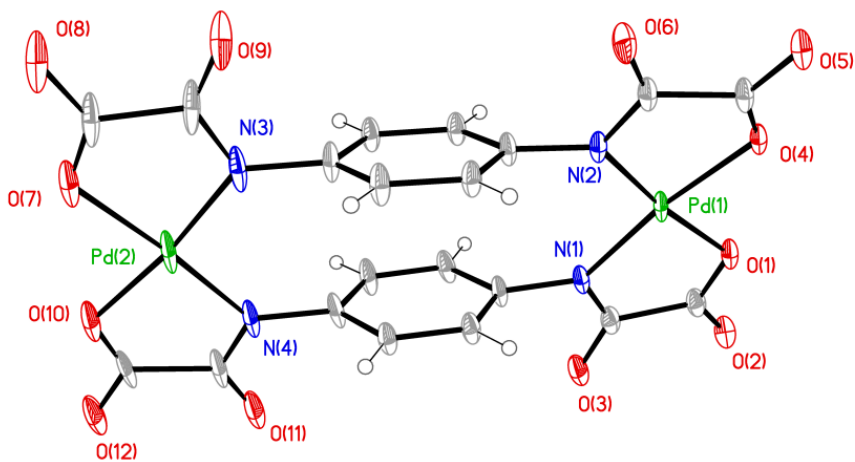


Figure 1. Perspective view of the anionic complex $[\text{Pd}_2(\text{ppba})_2]^+$ of **25**.

The average Pd(1)–N/Pd(2)–N and Pd(1)–O/Pd(2)–O bond lengths for **25** are 2.029(8)/2.0275(11) and 2.035(6)/2.037(10) Å, respectively. These values agree with those found in the oxamato-containing palladium(II) mononuclear complexes **1**, **9**, **10**, $\text{Na}[\text{Pd}(\text{Hpba})] \cdot 2\text{H}_2\text{O}$ [H_4pba = 1,3-propylenebis(oxamic acid)] and $\text{K}_2[\text{Pd}(\text{opba})] \cdot 2\text{H}_2\text{O}$ [H_4opba = N,N' -1,2-phenylenebis(oxamic acid), **5**, **6**, **7**, **11**, **19** and **20** [average Pd–N/Pd–O distances of 2.020(1)–2.009(1), 2.0209(11)/2.0384(13), 2.0207(13)/2.0214(14), 1.970/2.040, 1.928/2.055, 2.0411(16)/1.9989(14), 2.014(4)/2.011(4), 2.0439(19)/2.0033(16), 2.0425(18)/2.0033(15), 1.996(3)/2.0170(19) and 2.0225(10)/2.0258(11) Å, respectively]^{40–43}.

The values of the dihedral angle (φ) between the basal plane at the palladium(II) ion and the mean plane of the oxamate groups for **25** are very distorted 4.7(3)/5.6(3)° [Pd(1)] and 4.6(3)/2.3(3)° [Pd(2)], whereas those between the square plane and the phenyl ring (Φ) are 68.6(3)/58.2(3)° [Pd(1)] and 72.3(3)/75.9(3)° [Pd(2)], respectively. The values of the torsion angle between the palladium equatorial planes and the mean planes of the lateral benzene rings from the ligand are (ζ) 61.6(2)° [Pd(1)] and 62.35(2)° [Pd(2)], respectively.⁴⁴

The values of the peripheral C(1)-O(2), C(2)-O(3), C(3)-O(5) and C(4)-O(6) bond distances [1.226(12), 1.275(12), 1.238(12) and 1.233(12) Å, respectively] are somewhat shorter than the inner C(1)-O(1) and C(3)-O(4) bonds [1.289(12) and 1.276(12) Å] at the Pd(1) in agreement with the greater double bond character of the former carbonyl groups. This situation is also found at Pd(2) (the peripheral C(6)-O(8), C(5)-O(9), C(7)-O(11) and C(8)-O(12) bond distances [1.253(19), 1.252(18), 1.261(18) and 1.250(18) Å, respectively] being somewhat shorter than the inner C(6)-O(7) and C(8)-O(10) bonds [1.262(19) and 1.260(19) Å]).

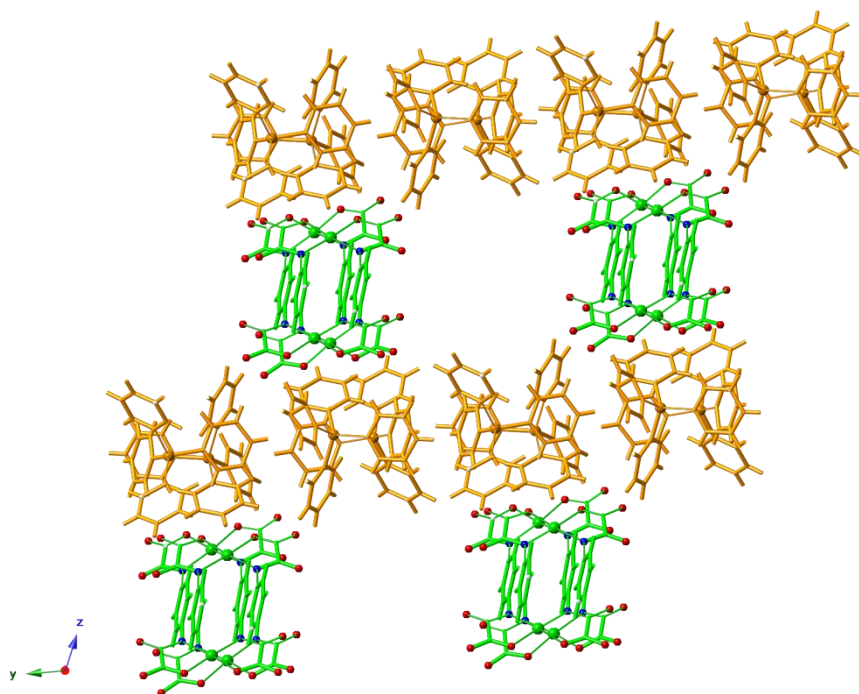


Figure 2. Crystal packing of **25** showing the relative positions of the anionic complexes (green) and tetraphenylarsonium cations (orange). The solvent molecules have been omitted for clarity.

The oxamate anionic dipalladate(II) motif in the crystal packing of **25** is separated from each other by the bulky Ph_4As^+ cations which exhibit the typical tetrahedral shape and their bond lengths and angles do not show any unusual feature. AsPh_4^+ cations are arranged into supramolecular motifs based on multiple phenyl embraces named LIT4PE^{45,46} with $\text{As} \cdots \text{As}$ separation of 6.930 Å (see Figure 3).



Figure 3. Representation of two non-equivalent tetraphenylarsonium cations in LIT4PE embrace.

The ppba dinucleating oxamate allows to form a $\text{Pd}(1) \cdots \text{Pd}(2)$ separation of 8.114(4) Å, a value which is longer than the shorter intermetallic distance [6.156(4)/5.667(4) Å for $\text{Pd}(1) \cdots \text{Pd}(1a)/\text{Pd}(2) \cdots \text{Pd}(2a)$].

$(n\text{-Bu}_4\text{N})_4[\text{Pd}_2(\text{dpvba})_2] \cdot 6\text{CH}_3\text{OH} \cdot \text{CH}_3\text{CH}_2\text{OCH}_2\text{CH}_3$ (**26**). This complex crystallizes in the triclinic space group $P1$ showing the occurrence of non-centrosymmetric $[\text{Pd}_2\text{L}_2]^+$ binuclear units (Figure 4) and $n\text{-Bu}_4\text{N}^+$ counter cations. Each palladium(II) ion is four-coordinate with two amidate-nitrogen and two carboxylate-oxygen atoms from the bis(oxamate) ligand in a *syn* (*trans, trans*) arrangement building a distorted square-planar surrounding. The reduced bite of the bidentate oxamate (80.3(8)/82.9(7) [at Pd(1)] and 81.7(8)/83.2(8) $^\circ$ [at Pd(2)] accounts for the deviations of the ideal value of 90° for the square planar surrounding.

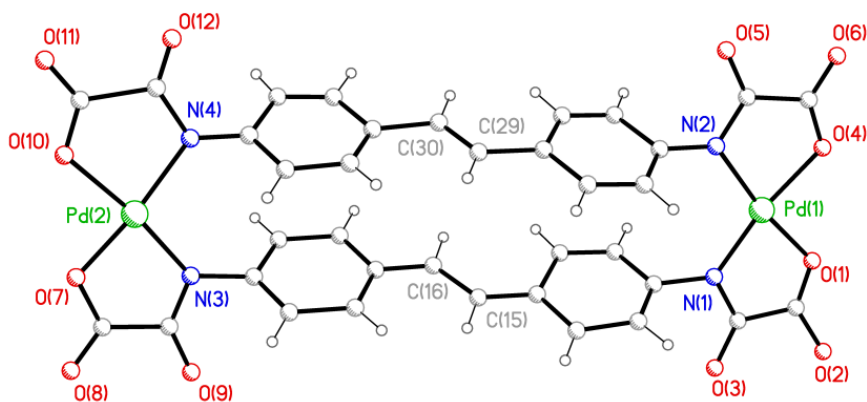


Figure 4. Perspective view of the anionic complex $[\text{Pd}_2(\text{dpvba})_2]^{4-}$ of **26**.

The average Pd(1)–N/Pd(2)–N and Pd(1)–O/Pd(2)–O bond lengths in **26** are 2.0135(17)/ 2.05(2) and 1.9945(18)/2.0115(16) Å, respectively. These values agree with those found in **25** and other oxamate-containing palladium mononuclear complexes.^{40–43}

The C(15)–C(16) and C(29)–C(30) bond lengths are 1.38(3) and 1.26(3) Å respectively, values which correspond well to the double character of the carbon-carbon bond of the stilbene molecule.

The values of the dihedral angle between the basal plane at the palladium(II) ion and the mean plane of the oxamate groups (φ) for **26** are 3.7(2)/0.2(2) $^\circ$ [Pd(1)] and 1.2(2)/2.7(2) $^\circ$ [Pd(2)].

On the other hand the average values between the square plane and the phenyl ring are (Φ) $60.4(2)^\circ$ and 61.7° for Pd(1) and Pd(2) respectively, whereas those between the torsion dihedral angle between the palladium equatorial planes and the mean planes of the lateral benzene rings from the ligand are (ζ) $61.6(2)^\circ$ [Pd(1)] and $62.35(2)^\circ$ [Pd(2)].⁴⁴

The values of the peripheral C(5)-O(8), C(6)-O(9), C(7)-O(11) and C(8)-O(12) bond distances [$1.27(3)$, $1.27(3)$, $1.15(3)$ and $1.16(3)$ Å] are somewhat shorter than the inner C(5)-O(7) and C(7)-O(10) bonds [$1.34(3)$ and $1.28(3)$ Å] at Pd(2) as expected due to the greater double bond character of the former carbonyl groups. Some of the values of the peripheral C(2)-O(2), C(1)-O(3), C(3)-O(5) and C(4)-O(6) bond distances [$1.37(3)$, $1.29(3)$, $1.26(3)$ and $1.21(4)$ Å respectively] the inner C(2)-O(1) and C(3)-O(4) bonds [$1.22(4)$ and $1.26(4)$ Å] at the Pd(1) suggesting the weakening of the double bond character of the carbonyl groups.

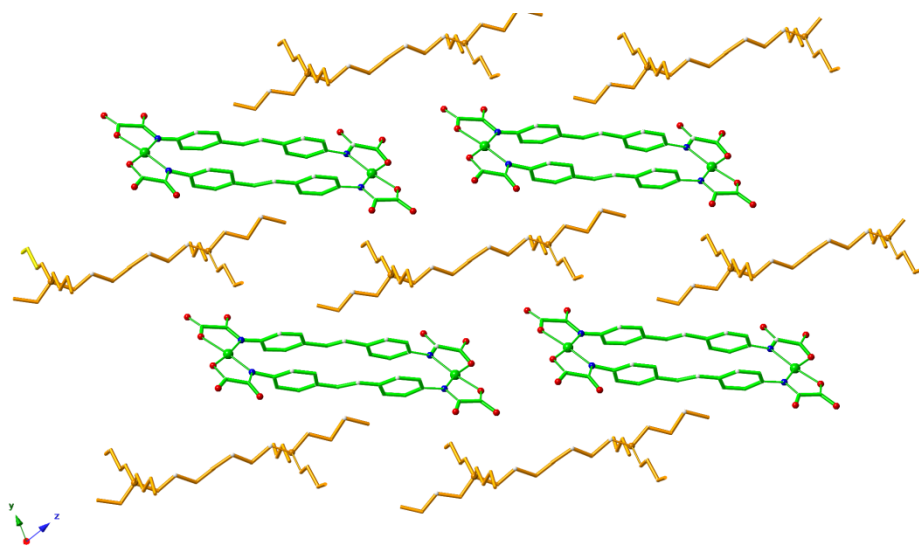


Figure 5. Crystal packing of **26** showing the relative positions of the anionic complexes (green) and tetrabutylammonium cations (orange). The solvent molecules have been omitted for clarity.

The complex anion in the crystal packing of **26** is well separated from each other because of the presence of the bulky $n\text{-Bu}_4\text{N}^+$ cations. Pd(1)··Pd(2) separation is 14.706(4) Å, a value much greater than that of complex **25** (6.6 Å), whereas the shortest intermetallic Pd(2)··Pd(1a) separation is 10.147(3) Å.

$(n\text{-Bu}_4\text{N})_4[\text{Pd}_2(\text{dpazba})_2] \cdot 5\text{CH}_3\text{OH}$ (**27**). This compound crystallizes in the triclinic space group $P\bar{1}$ and its structure is made up by centrosymmetric dinuclear $[\text{Pd}_2\text{L}_2]^{4-}$ units (Figure 6) and $n\text{-Bu}_4\text{N}^+$ counter cations. Each palladium(II) ion is four-coordinate with two amidate-nitrogen and two carboxylate-oxygen atoms from the bis(oxamate) ligand in a *syn* (*trans*, *trans*) arrangement building a distorted square-planar surrounding. The reduced bite of the bidentate oxamate [81.3(2)°] accounts for the deviations of the ideal value of 90° for the square planar surrounding.

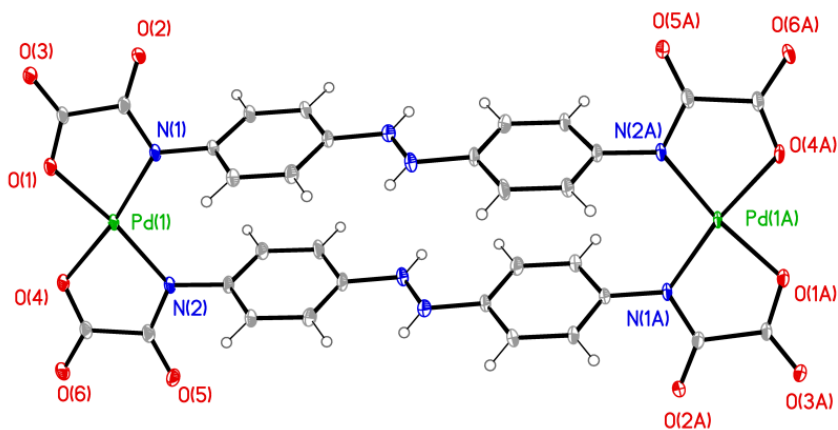


Figure 6. Perspective view of the anionic complex $[\text{Pd}_2(\text{dpazba})_2]^{4-}$ in **27**.

The average values of the Pd(1)—N and Pd(1)—O bond lengths for **27** is 2.029(6) and 2.012(5) Å, respectively. These values agree with those found in **25**, **26** and other oxamato-containing palladium(II) mononuclear complexes^{40–43}.

N(3)-N(4) bond length is 1.251(10) Å, a value which is as expected for a N=N bond for a nitrogen-nitrogen double bond of the azobenzene framework.

The values of the dihedral angle between the basal plane at the Pd(1) ion and the mean plane of the oxamate groups for **27** are (φ) 4.0(2)/1.4(2)°. On the other hand values between the square plane and the phenyl ring (Φ) are 58.2(2)/60.7(2)° [Pd(1)] whereas those between the torsion angle between the palladium equatorial planes and the mean planes of the lateral benzene rings from the ligand (ζ) is 61.6(2)° Pd(1).⁴⁴

The values of the peripheral C(1)-O(2), C(2)-O(3), C(3)-O(5) and C(4)-O(6) bond distances [1.247(9), 1.226(9), 1.242(10) and 1.239(9) Å] are somewhat shorter than the inner C(1)-O(1) and C(3)-O(4) bonds [1.284(9) and 1.287(9) Å] for Pd(1) in agreement with the greater double bond character of the former carbonyl groups.

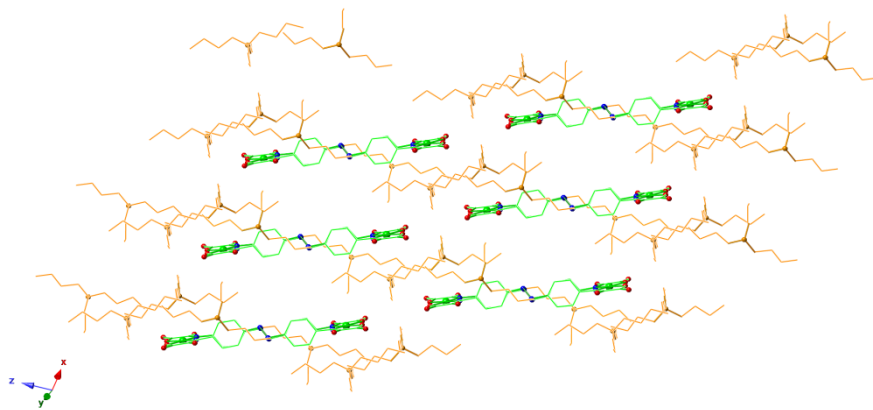


Figure 7. Crystal packing of **27** showing the relative positions of the anionic complexes (green) and tetrabutylammonium cations (orange). The solvent molecules have been omitted for clarity.

The bulky $n\text{-Bu}_4\text{N}^+$ cations in **27** ensures the isolation of the complex anions from each other in the crystal packing.

The Pd(1) \cdots Pd(1a) separation is 14.332(3) Å, a value close to that for **26** [14.406 Å] whereas the shortest intermetallic Pd(1) \cdots Pd(1b) separation is 8.612(3) Å.

$(n\text{-Bu}_4\text{N})_4[\text{Pd}_2(\text{dpeba})_2] \cdot 4\text{CH}_3\text{OH}$ (**28**). This complex crystallizes in the triclinic space group $P\bar{1}$ and its structure is made up by centrosymmetric $[\text{Pd}_2\text{L}_2]^{4-}$ binuclear units (Figure 4) and $n\text{-Bu}_4\text{N}^+$ counter cations. Each palladium(II) ion is four-coordinate with two amidate-nitrogen and two carboxylate-oxygen atoms from the bis(oxamate) ligand in a *syn* (*trans*, *trans*) arrangement building a distorted square-planar surrounding. The reduced bite of the bidentate oxamate [$81.58(7)^\circ$] accounts for the deviations of the ideal value of 90° for the square planar surrounding.

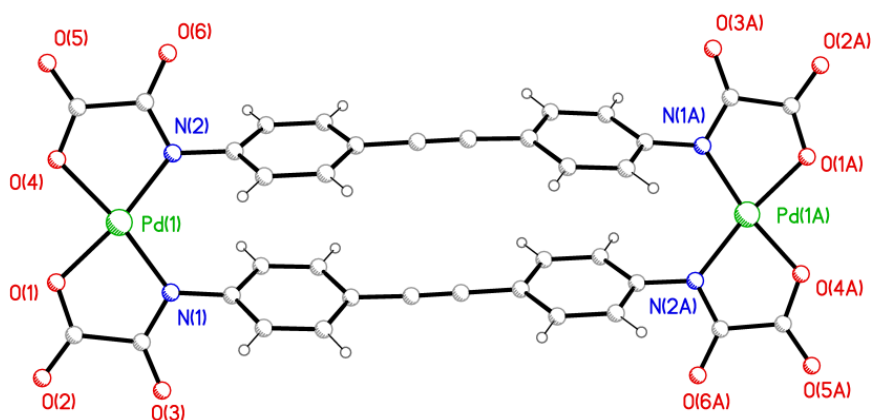


Figure 9. Perspective view of the anionic complex $[\text{Pd}_2(\text{dpeba})_2]^{4-}$ in **28**.

The average values of Pd(1)—N, Pd(1)—O bond lengths for **28** are 2.0237(18) and 2.01065(15) Å, respectively. These values agree with those found in **25-27** and other oxamato-containing palladium(II) mononuclear complexes⁴⁰⁻⁴³.

The C(9)—C(18) bond length is 1.196(3) Å, a value which is as expected for triple character of the carbon-carbon bond.⁴⁷

The values of the dihedral angle between the basal plane at the Pd(1) ion and the mean plane of the oxamate groups (φ) for **28** are 4.5(2)/7.1(2) $^\circ$. On the other hand the average value between the square plane and the phenyl ring (Φ) is 58.6(2) $^\circ$ whereas that between the torsion angle between the palladium equatorial planes and the mean planes of the lateral benzene rings from the ligand (ζ) is 61.6(2) $^\circ$.

The values of the peripheral C(1)-O(3), C(2)-O(2), C(10)-O(6) and C(11)-O(5) bond distances [1.225(3), 1.242(3), 1.227(3) and 1.244(3) Å, respectively] are somewhat shorter than the inner C(1)-O(1) and C(10)-O(4) bonds [1.284(3) and 1.292(3) Å] in agreement with the greater double bond character of the former carbonyl groups.

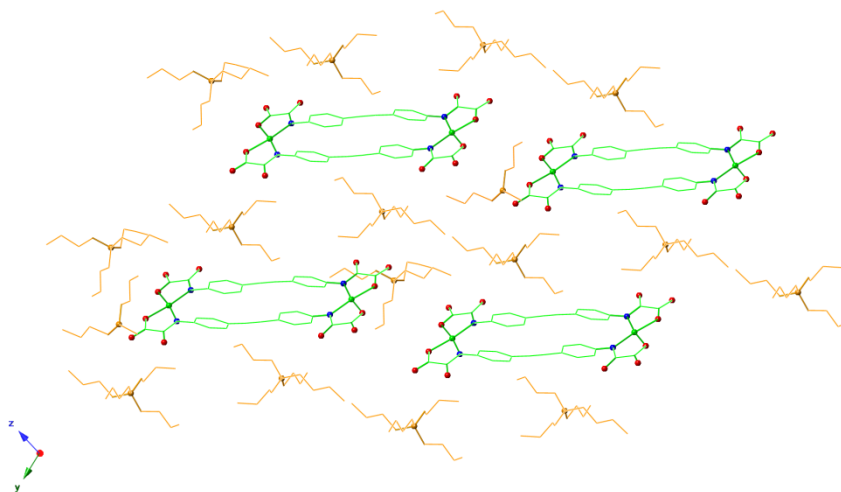


Figure 10. Crystal packing of **28** showing the relative positions of the anionic complexes (green) and tetrabutylammonium cations (orange). The solvent molecules have been omitted for clarity.

The bulky $n\text{-Bu}_4\text{N}^+$ cations exhibit their expected tetrahedral square, and ensure the isolation of the complex anions from each other in the crystal packing.

The Pd(1)··Pd(1a) separation is 14.920(3) Å, a value which is the longest one of the dinuclear palladium(II) oxamate metallacyclophanes series **25-27** [8.114(4)/ 14.706(4)/14.332(3) Å respectively], but smaller than the shortest intermetallic Pd(1)··Pd(1b) separation [8.209(3) Å].

V.5. Catalytic properties

The five novel dinuclear palladium(II) metallacyclophanes (**25a-29a**) are found to catalyze carbon-carbon cross-coupling reactions, specifically Heck and Suzuki reactions.

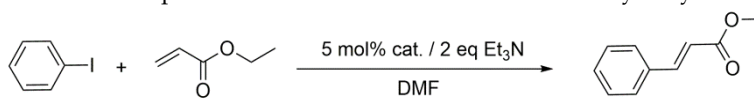
There are two active catalytic centers, when working with dinuclear palladium(II) metallacyclophanes and then, any calculation of %mol cat. hereunder is done by catalytic center.

Heck Reaction - Homogeneous catalysis

The Heck reaction was studied by the use of iodo aryl and ethyl acrylate for complexes **25a-29a** (5% mol of cat. or 10% mol of Pd), using DMF as solvent. Et₃N is the base giving the best results. The temperature used was 80 °C. It is important to point out that no inert atmosphere is needed to carry out these reactions and also that our catalysts are very active under such conditions as shown in Table 1.

Dipalladium(II) metallacyclophanes achieve high yields (Table 1, entry 1, ca. 78%) and they are better than the tested commercial complex [Pd₃(OAc)₆] tested (Table 1, entry 9): the same reaction is catalyzed in 45 minutes by the precatalysts **25a-29a** where 3 hour are required by [Pd₃(OAc)₆].

Table 1. Scope of Heck reaction of iodobenzene and ethyl acrylate



Entry ^a	Catalyst	Time (min)	Temp (°C)	Yield ^b	TON
1	25a	45	80	78	16
2	26a	45	80	76	15
3	27a	45	80	70	14
4	28a	90	80	62	13
5	29a	45	80	77	15
9	[Pd ₃ (OAc) ₆]	3 h	120	88	88

^a Reaction conditions: 0.5 mmol iodobenzene, 0.75 mmol ethyl acrylate, 5 mmol% cat (10 mmol% Pd), 1 mmol Et₃N, 45-90 min, 80 °C in DMF.

^b Determined by GC-MS analysis using PFTBA as internal standard.

A comparison of the data listed in Table 1 with those obtained with mononuclear oxamate-palladate(II) catalyst **8a-10a** and **14a-19a** (Chapter 2, Table 1, entries 1-9) shows that the yields are almost equal (Table 2, ca. 80%) although the reaction times are shorter with dinuclear oxamate-palladate metallacyclophanes precatalysts (45 min instead of 3 hours under the same catalytic conditions).

Once again working in the open air and in agreement with the results detailed in *Chapters 1* and *2*, **25a-29a** proved to be efficient (pre)catalyst, under the described homogeneous conditions, without clear formation of palladium black throughout the catalytic reactions (Figure 11).

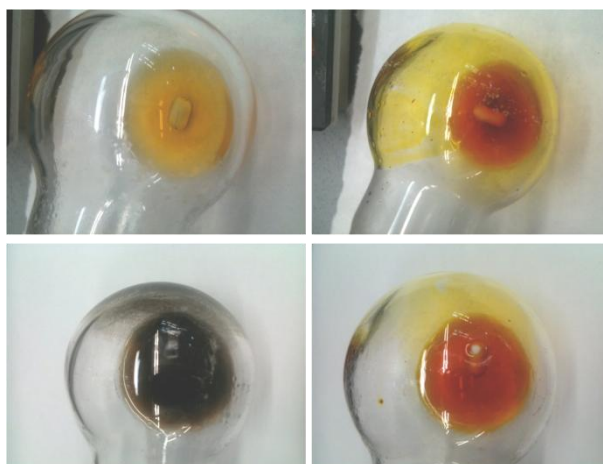


Figure 11. Pictures of the starting (top) / final (bottom) samples of Heck coupling reaction of iodobenzene and ethyl acrylate in DMF at 80 °C, catalyzed by $[\text{Pd}_3(\text{OAc})_6]$ (left) and compound **27a** (right).

Heck Reaction - Ionic liquid medium

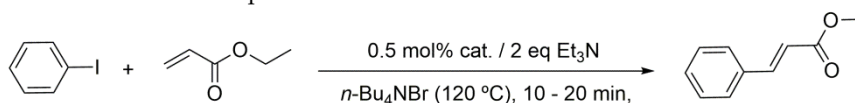
Once these kind of anionic complexes of Pd(II) with *N*-substituted oxamate ligands have been demonstrated to be catalytically active for Heck reaction under homogeneous fashion in an organic solvent such as DMF, we tried with greener media as solvents, such as ionic liquids.⁴⁸⁻⁵⁸

Anionic dipalladium(II) metallacyclophanes improve their catalytic activity working in ionic liquids: **25a-29a** achieve high yields (ca. 99% with low amounts of catalyst (0.5% mol cat. / 1% mol Pd) in very short times (10 min, 1164 h⁻¹ TOF) as shown in Table 2.

A comparison with the catalytic results in *Chapter 2* shows that the complexes **25a-29a** (Table 2) provide better results than mononuclear complexes with non electronic or steric effects in *para*- position [(**10**), 0.5 mol% cat. / 1 mol% of Pd), ca. 99% for 30 min], shorter reaction time and equal amount of catalyst [Table 2, 0.5 mol% of cat. (1 mol% of Pd), entry 1 and 2, ca. 99% for 10 min]. Instead, if the catalytic results of these complexes are compared with **5-7** and **11-12** which have an electronic and steric effects in *para*- position [*Chapter 2*, 0.5 mol% cat., ca. 99% for 5 min], **25-29** achieve the same yields but increasing a bit the reaction times (Table 2, 0.5 mol% cat. / 1 mmol% of Pd, entry 1 and 2, ca. 99% for 10 min).

Looking at the results obtained, it is impossible to state if there are some kind of cooperation between both Pd(II) ions from the same metallacyclophane. However, some kind of cooperation may be involved because even with steric/geometric effects caused by these spacer ligands, the results are as good as those from complexes **5-7** and **11-12**.

Table 2. Scope of Heck reaction of iodobenzene and olefins



Entry ^a	Aryl halide	Olefin	Catalyst	Time (min)	Yield	TON	TOF (h ⁻¹)
1			25a	10	97	194	1164
2			26a	10	99	198	1188
3			27a	10	99	198	1188
4			28a	20	98	198	594
5			29a	10	99	198	1188

^a Reaction conditions: 0.5 mmol iodobenzene, 0.75 mmol ethyl acrylate, 0.5 mmol% cat. (1 mmol% of Pd), 1 mmol Et₃N, 10-20 min, 120 °C in *n*-Bu₄NBr. (Yield) Determined by GC-MS analysis using perfluorotributylamine (PFTBA) as internal standard

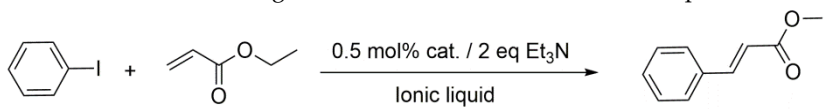
Formation of palladium black was observed when the Heck reactions between iodobenzene and ethyl acrylate were carried out with commercial palladium precatalysts such as $[\text{Pd}_3(\text{OAc})_6]$.

However, non inactive palladium black was observed if the reaction was performed with palladium(II) oxamate complexes (**25a-29a**).

The tests that we carried out with dinuclear oxamate-palladium(II) complexes in different ionic liquid media show that *n*-Bu₄NBr provides the best results in comparison to *n*-Bu₄NCl and other imidazolium salts (Tables 3, and S2).

The tetrahedral shape of the tetraalkylammonium cation, in particular the tetra-*n*-butyl bromide (*n*-Bu₄NBr) which was widely used by other research teams as the ideal ionic liquid.⁵⁹⁻⁶³ It is due to the *n*-Bu₄NBr has a temperature of decomposition (near to 130 °C)⁵⁹ more superior than *n*-Bu₄NCl, which allows working at higher temperatures (near to the C-X activation).

Table 3. Screening of Heck reactions in different ionic liquids



Entry ^a	Ionic Liquid	Catalyst	Time (min)	Temp (°C)	Yield ^b	TON	TOF (h ⁻¹)
1	<i>n</i> -Bu ₄ NBr	28a	20	120	98	196	588
2	<i>n</i> -Bu ₄ NCl	28a	20	80	40	80	240
3	BMIMBr	28a	20	80	7	14	42
4	BIMIMPF ₆	28a	20	80	7	14	42

^a Reaction conditions: 0.5 mmol iodobenzene, 0.75 mmol acrylate, 0.5 mmol% cat., 1 mmol Et₃N, 20 min, 120 °C in ionic liquids. ^bDetermined by GC-MS analysis using perfluorotributylamine (PFTBA) as internal standard

The fact that the imidazolium unit has a planar structure, makes easier its aggregation with the planar complex anions. This would decrease the anion availability for the stabilization of the catalytically active Pd(0) species, which may be formed in the reaction mixture either by thermal reduction of Pd(II) precatalyst or by an excess of the olefin itself as well as by the triethylamine employed as base, during the catalytic process.^{64,65}

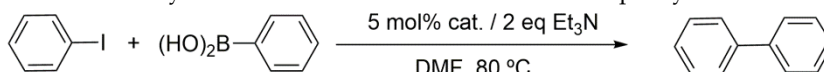
n-Bu₄NBr was described as an excellent reaction medium for the stabilization of catalytically active palladium and copper species for carbon-carbon coupling reactions via electrostatic interactions.^{66,67}

Suzuki Reaction - Homogeneous catalysis

The Suzuki reaction was tried by using iodobenzene and phenylboronic acid for complexes **25a** to **29a** (5 mol% of cat. or 10 mol% Pd) in DMF as solvent. The base providing better results is Et₃N at 80 °C and in the open air (Table 4).

A correspondence between the intramolecular separation of the Pd(II) ions and their catalytic activity can be seen through an inspection of the data listed in Table 4. Low yields are achieved for complexes **25** (Table 4, entry 1), **26** (Table 4, entry 2) and **27** (Table 4, entry 3) where the values of Pd··Pd distance are shorter than those for complexes **28** (Table 4, entry 4) and **29** (Table 4, entry 5). This could mean that each palladium(II) may work without any cooperation. However, this relationship is not observed in the Heck reaction with DMF as solvent.

Table 4. Catalytic Suzuki reactions of iodobenzene with phenylboronic acid



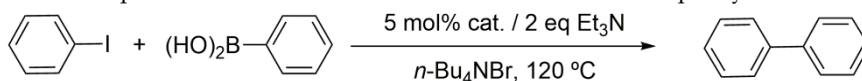
Entry ^a	Catalyst	Time (min)	Temp (°C)	Yield ^b	TON	TOF (h ⁻¹)
1	25a	145	80	47	9	4
2	26a	145	80	51	10	4
3	27a	145	80	50	10	4
4	28a	145	80	86	17	7
5	29a	145	80	74	15	6

^a Reaction conditions: 1 mmol iodobenzene, 0.75 mmol phenylboronic acid, 5 mmol% cat., 2 mmol Et₃N, 4h at 80 °C in DMF. ^bDetermined by GC-MS analysis using PFTBA as internal standard.

Suzuki Reaction – Ionic liquid medium

High yields were obtained for the Suzuki reaction between iodobenzene and phenylboronic acid using between 5 mol% cat. (10 mol% Pd), in the open air (see Table 5). But in contraposition to Heck reaction, greater amounts of catalyst were required in order to obtain ca. 99% yields with 5 mol% cat. As occurs in the Heck reaction, the catalytic activity in the Suzuki reaction is improved when working in molten *n*-Bu₄NBr.^{63,68-75}

Table 5. Scope of Suzuki reaction of iodobenzene derivates with phenylboronic acid



Entry ^a	Catalyst	Time (min)	Temp (°C)	Yield ^b	TON	TOF (h ⁻¹)
1	25a	120	120	99	20	10
2	26a	120	120	99	20	10
3	27a	120	120	99	20	10
4	28a	120	120	99	20	10
5	29a	120	120	92	19	10

^a Reaction conditions: 1 mmol iodobenzene, 0.75 mmol phenylboronic acid, 5 mmol% cat., 2 mmol Et₃N, 120 °C in *n*-Bu₄NBr. ^bDetermined by GC-MS analysis using PFTBA as internal standard.

Recovery and recycling

The stability of the catalysts **25a-29a** in molten *n*-Bu₄NBr driven by their immobilization in the ionic liquid via ionic interactions suggested the recycling procedure and indeed, the catalyst is active after at least 6 runs in our experimental conditions [Figure 12 and Figure S1-S4 (**26a-29a**)].

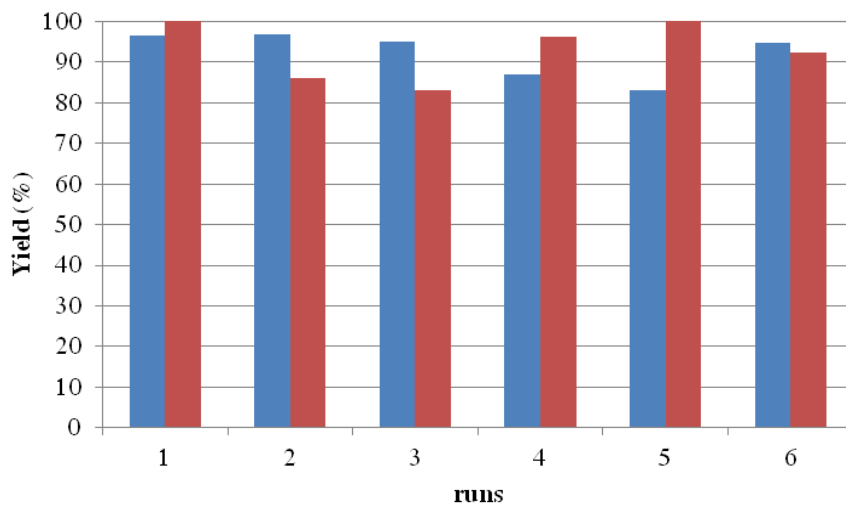


Figure 12. Histogram of the recycling experiment for the Heck reaction of iodoaryl and ethyl acrylate with 0.5 mmol% **25** (blue) and for the Suzuki reaction of iodoaryl and phenylboronic with 5 mmol% **25** (red).

V.6. Photochemical studies

Envisaging the multi-functionality as photo-chemical⁷⁶⁻⁸⁶ and photo-switchphysical⁸⁷⁻⁹⁸ studies in solution. Bis(oxamate) ligands with “non-innocent” aromatic spacers such as 4,4'-stilbene (**Et₂H₂dpvba**) and 4,4'-azobenzene (**Et₂H₂dpazba**) were isolated and their photo-chemical activity was investigated.

Photo-chemistry of the $(n\text{-Bu}_4\text{N})_4[\text{Pd}_2(\text{dpvba})_2]$ (**26a**) dinuclear complex

The aforesaid dinuclear $(n\text{-Bu}_4\text{N})_4[\text{Pd}_2(\text{dpvba})_2]$ (**26a**) complex containing the stilbene spacer can adopt two possible conformations in solution, either *syn* (*trans, trans*) or *anti* (*trans, trans*) (E and F in Scheme 5). However, only the *syn* (*trans, trans*) conformation has been observed for **26** in the solid state whereas the *anti* (*trans, trans*) is the only one for the analogous dicopper(II) complex (Figure 13).

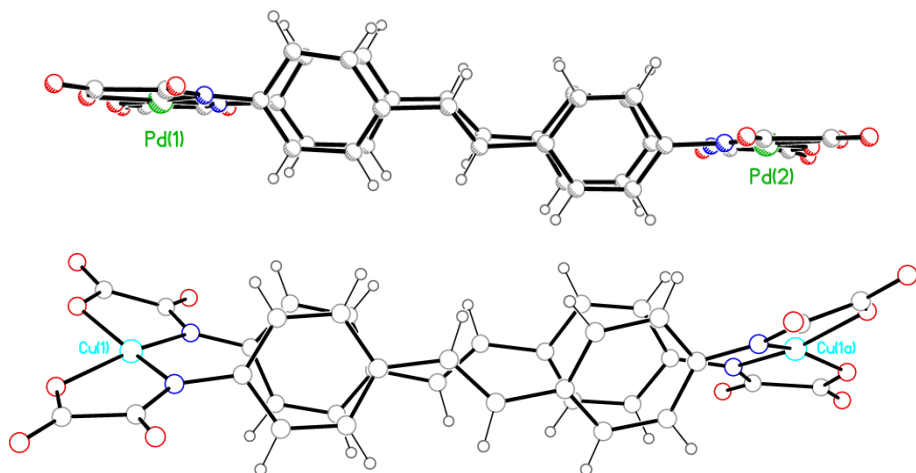
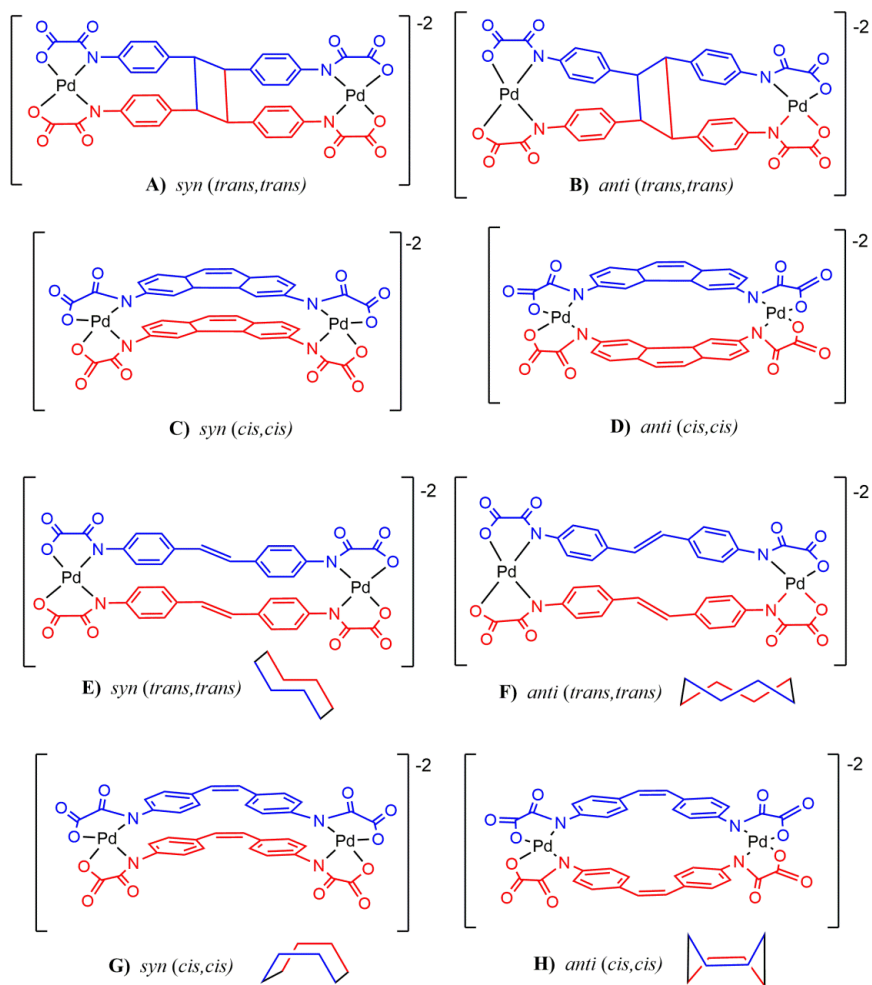


Figure 13. Perspective views of $[\text{Pd}_2(\text{dpvba})_2]^{4+}$ (**26**) (top) / $[\text{Cu}_2(\text{dpvba})_2]^{4+}$ (bottom). Single crystals of **26** were grown at low temperature and in the darkness, whereas those of the $(n\text{-Bu}_4\text{N})_4[\text{Cu}_2(\text{dpvba})_2]$ were grown at room temperature and in the daylight.†

†The structure of $(n\text{-Bu}_4\text{N})_4[\text{Cu}_2(\text{dpvba})_2]$ complex was ceded to another PhD Thesis of our group which is underway.

Upon irradiation, it is expected that each conformer of **26** can undergo an intramolecular (“pseudo-bimolecular”) [2+2] photocycloaddition to afford the corresponding *syn* or *anti* cyclodimers (**A** and **B** in Scheme 5) and/or geometric *trans/cis* photoisomerization followed by intramolecular cyclization to afford the unstable *syn* (*cis, cis*) or *anti* (*cis, cis*) isomers (**G** and **H** in Scheme 5) that in turn would transform into the resulting *syn* or *anti* dihydrophenanthrene derivatives (**C** and **D** in scheme 5)⁹⁹⁻¹⁰¹. The occurrence of all these types of conformations was investigated by us by irradiation of the products in solution using electronic spectroscopy.



Scheme 5. Possible conformations of the anionic entity $[\text{Pd}_2(\text{dpvba})_2]^{4-}$ (**26**).

A solution of **26a** in acetonitrile [5×10^{-6} M] was purged with argon for 30 min and the electronic spectrum of the degassed solution was measured (*grey line in Figure 8*). Afterwards, the sample was irradiated with UV light ($\lambda_{\text{max}} = 350$ nm) until no change was observed in the electronic spectrum (*blue line in Figure 14*), and then it was allowed to relax by thermal relaxation (*red line in Figure 14*) or by further irradiation with visible light ($\lambda_{\text{max}} = 420$ nm) (*green line in Figure 14*).

As shown in Figure 8, the irradiation at 350 nm of **26a** decreases the absorbance of the maximum at this wavelength to give a new maximum at 310 nm with a distinct shoulder at 450 nm. There is no change in the absorbance of this "photostationary" state after thermal relaxation or irradiation at 420 nm suggesting that the [2+2] photocycloaddition product is formed blocking the possible relaxation to **26a**.

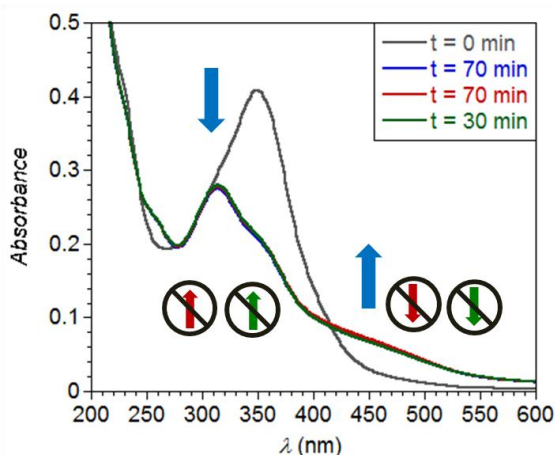


Figure 14. Evolution of the UV-vis spectra of **26a**: grey (initial compound), blue (excitation to 350 nm after 70 min), red (thermal relaxation after 70 min) and green (relaxation to 420 nm after 30 min) lines.

The change of the absorbance from the initial compound by irradiation at 350 nm and the lack of thermal relaxation are illustrated by Figure 15 which shows the study of this phenomenon after different times.

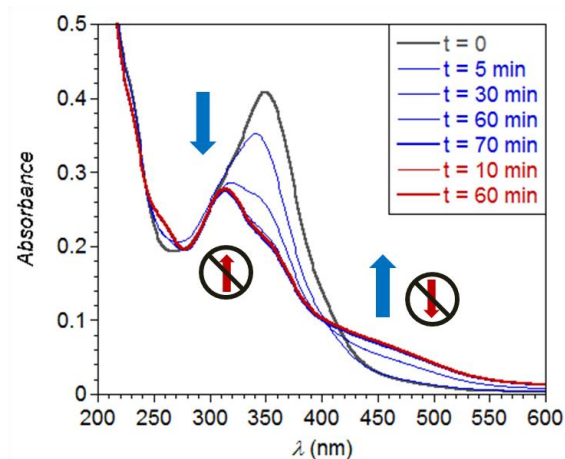


Figure 15. Evolution of the UV-vis spectra of **26a**: grey (initial compound), blue (after excitation to 350 nm as a function of time) and red (thermal relaxation as a function of time).

The evolution with time of the spectra after irradiation at 350 nm is shown in Figure 16. The presence of clear isosbestic points after 15 min of irradiation suggests an equilibrium between only two species up to the attainment of the photostationary state (blue lines in Figure 16).

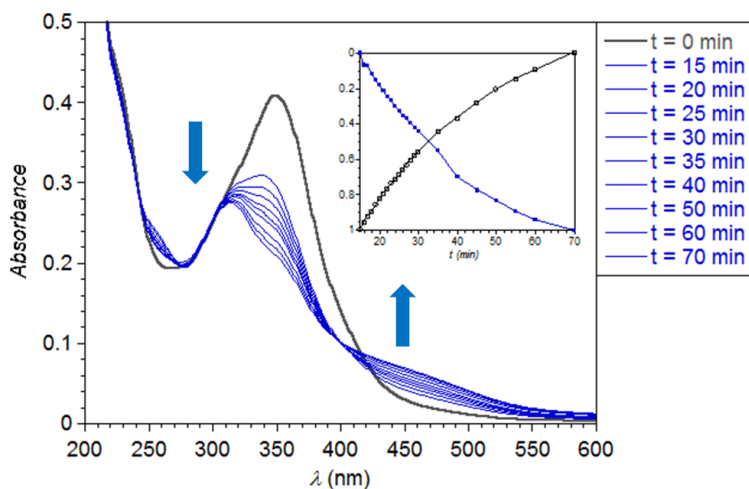


Figure 16. Evolution of the UV-vis spectra of **26a**: grey (initial compound) and blue (excitation to 350 nm as a function of time). (Inset) Curves of the normalized absorbance values at 333 and 450 nm.

This is supported by the curves of the normalized absorbance values at 333 and 450 nm with the irradiation time, which show a crossing point at an ordinate value close to 0.5 (inset of Figure 16). Yet the appearance of isosbestic points is preceded by a short induction period during the first 10 min of irradiation. This may indicate the formation of an intermediate in a preequilibrium process that is transformed into the final product or, more, likely, the presence of a mixture of both *syn* (*trans, trans*) and *anti* (*trans, trans*) isomers (E and F in scheme 5) at the initial stage.¹⁰⁰

Figure 17 shows the time evolution of the spectra of the irradiated samples after thermal relaxation. Once the photostationary state is reached, no further spectral changes were observed upon standing for 70 min at room temperature without irradiation (solid red lines in Figure 17), suggesting thus a very slow (if any) thermal relaxation in solution for the two possible photocycloaddition products (A and B in Scheme 5).

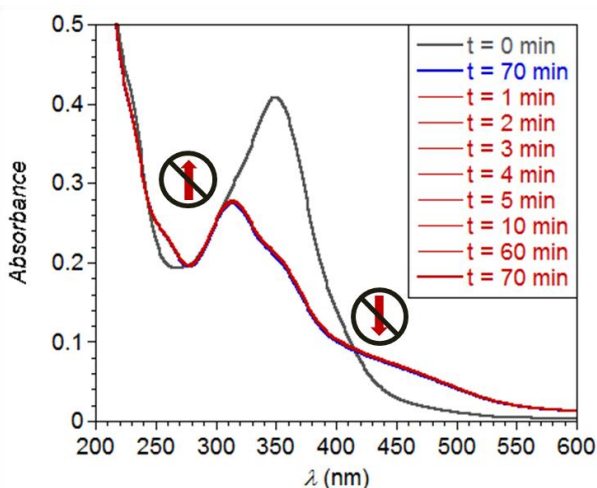


Figure 17. Evolution of the UV-vis spectra of **26a**: grey (initial compound) and red (thermal relaxation at the quoted times).

Although the absorption maximum of complex **26a** is located at 350 nm, excitation at 420 nm was also tested to check the possible wavelength effects on the photochemical activity. The time evolution of the spectra is qualitatively similar after 70 min of irradiation (blue line in Figure 18), but much slower than at 350 nm.

Besides the fact that excitation at 420 nm does not reduce the absorbance as downward as it does at 350 nm, no thermal relaxation occur after 50 minutes at room temperature (red line in Figure 18).

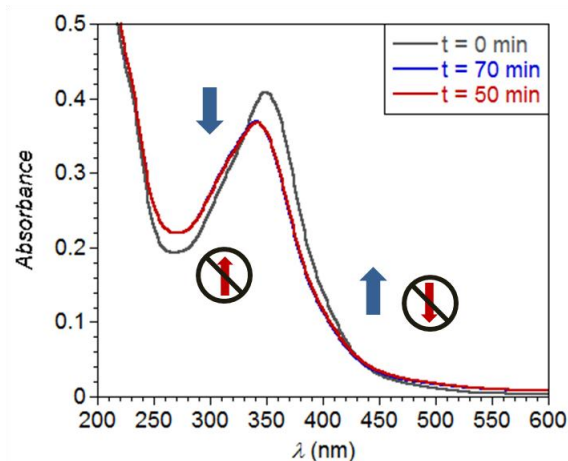


Figure 18. Evolution of the UV-vis spectra of **26a**: grey (initial compound), blue (excitation to 420 nm after 70 min) and red (thermal relaxation after 50 min) lines.

All these tests were performed in an inert atmosphere (Ar) but the same spectral changes are observed when the experiment is carried out in the open air, indicating that an inert atmosphere is no required to carry out these studies (Figure 19).

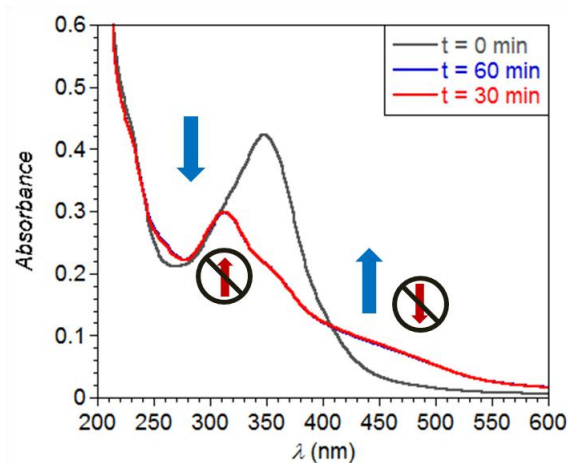


Figure 19. Evolution of the UV-vis spectra of **26a** carrying out the experiment in the open air: grey (initial compound), blue (excitation to 350 nm after 60 min) and red (thermal relaxation after 30 min).

Photo-chemistry of the $(n\text{-Bu}_4\text{N})_4[\text{Pd}_2(\text{dpazba})_2]$ (**27a**) dinuclear complex

As for the aforementioned complex **26**, the dipalladium(II) complex $(n\text{-Bu}_4\text{N})_4[\text{Pd}_2(\text{dpazba})_2]$ could also adopt two possible conformations in solution, either *syn (trans, trans)* or *anti (trans, trans)* (**A** and **B** in Scheme 6).

Only the *syn (trans, trans)* conformation has been observed for **27** in the solid state (see structural description above).

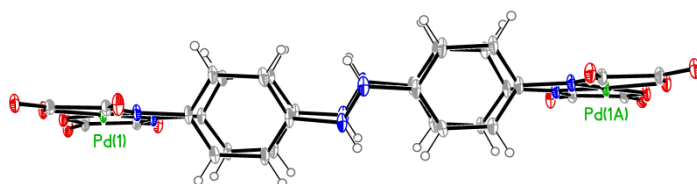
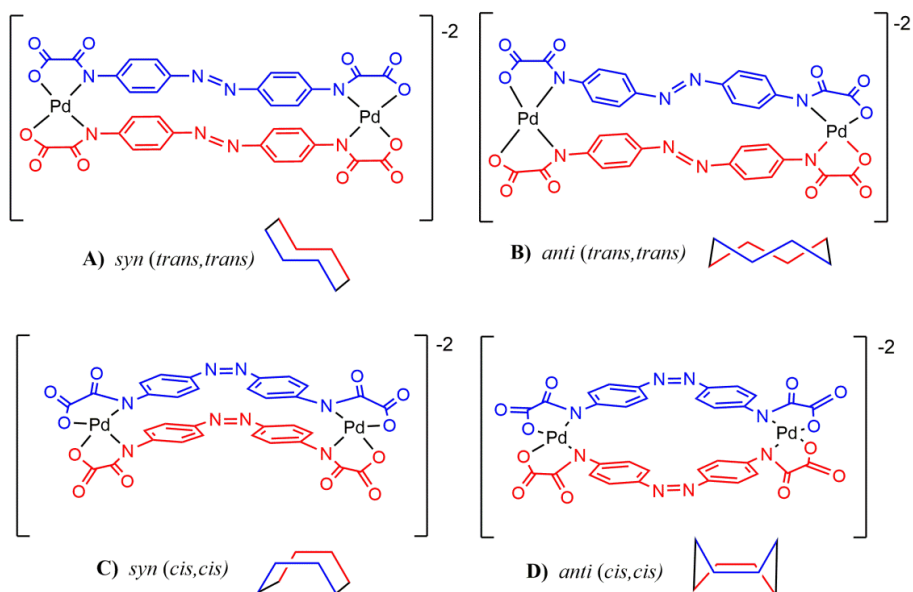


Figure 20. Perspective view of the anionic entity of **27**. Single crystals were grown at low temperature and in darkness adopting a *syn (trans, trans)* conformation (**A**, scheme 6).[†]

[†]The analogous $(n\text{-Bu}_4\text{N})_4[\text{Cu}_2(\text{dpazba})_2]$ complex was ceded to another PhD Thesis of our group which is underway.



Scheme 6. Possible conformation to the anionic entity $[\text{Pd}_2(\text{dpazba})_2]^{4-}$ (**27**).

Unlike complex **26a**, only geometric *trans/cis* photoisomerization to give the unstable *anti (cis, cis)* or *syn (cis, cis)* isomers (**C** and **D** in Scheme 6) is allowed for complex **27a** upon irradiation, the intramolecular (“pseudo-bimolecular”) [2+2] photocycloaddition being precluded in this case.

A solution of **27a** in acetonitrile [1×10^{-5} M] was purged with argon for 30 min and conveniently sealed prior to carry out the photo-spectrochemical measurements. The electronic absorption spectrum of the acetonitrile solution of **27a** was measured both before (grey line in Figure 21) and after irradiation (blue line in Figure 21) with UV light ($\lambda_{\max} = 350$ nm). Afterwards the sample was allowed to relax thermally at room temperature (red line in Figure 21). The reversible nature of the spectral changes supports a reversible transformation of the *syn (trans, trans)* isomer into the *syn (cis, cis)*.^{12,102-104}

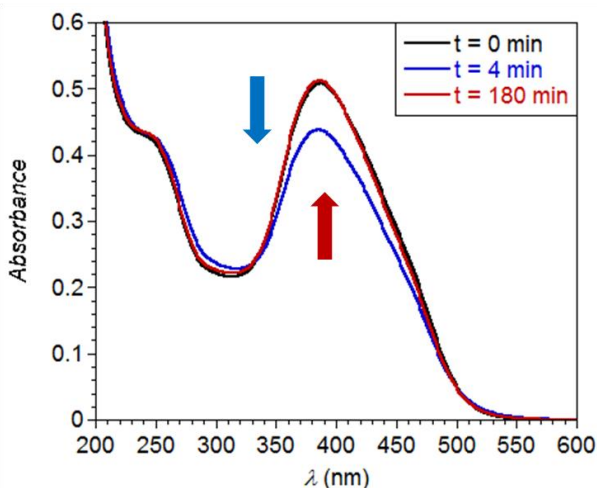


Figure 21. Evolution of the UV-vis spectra of **27a**: grey (initial compound), blue (excitation to 350 nm after 4 min) and red (thermal relaxation after 180 min).

Figures 22 and 23 show the time evolution of the electronic spectra of **27a** upon irradiation and thermal relaxation, respectively. As shown in Figure 22, the irradiation of **27a** at 350 nm leads to an immediate decrease of the intensity of the main peak located at 385 nm. No further spectral changes are observed after irradiation times greater than 4 min.

In contrast, the recovery of the original spectra by thermal relaxation occurs rather slowly after standing at room temperature without irradiation for up to 3 h (Figure 23).

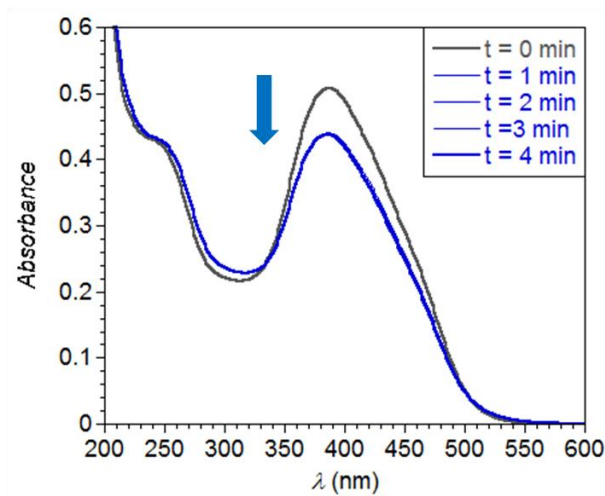


Figure 22. Evolution of the UV-vis spectra of **27a**: grey (initial compound) and blue (excitation to 350 nm during the quoted times).

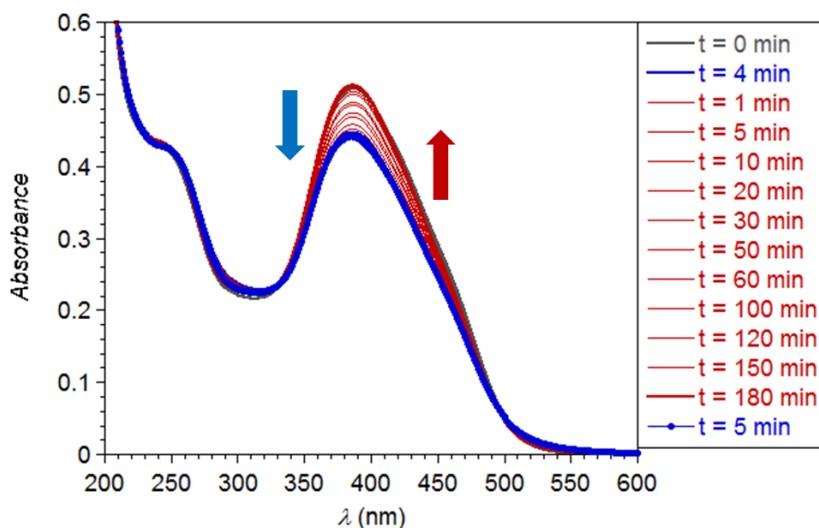


Figure 23. Evolution of the UV-vis spectra of **27a**: grey (initial compound), blue (excitation to 350 nm after 4 min) and red (thermal relaxation during the quoted times), blue dot-line (re-excitation to 350 nm after 5 min).

These two dramatically different kinetics of light excitation/thermal relaxations are nicely illustrated by Figure 24 (blue and red lines, respectively). Interestingly, we have also verified that the process of light excitation/thermal relaxation could be repeated again.

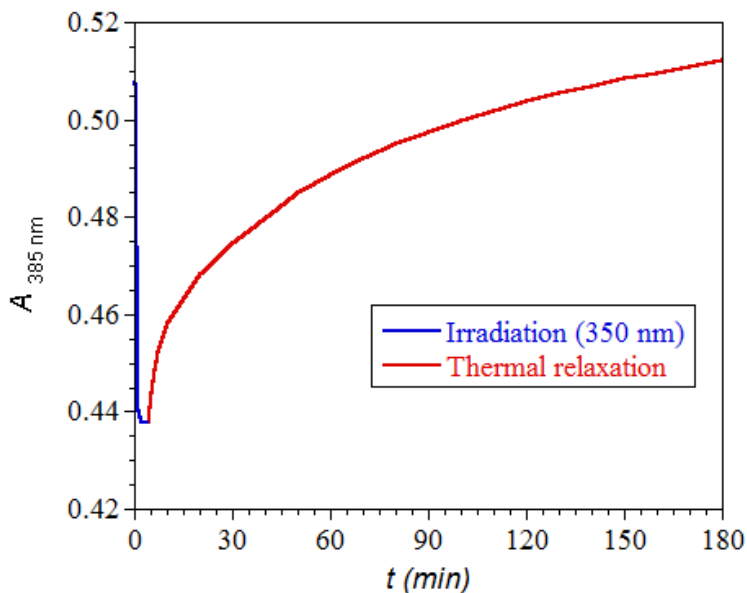


Figure 24. Recovering the original conformation of **27a** after irradiation at 350 nm (blue) and thermal relaxation (red) over the time.

On the other hand, we have also investigated the irradiation with UV light ($\lambda_{\max} = 350$ nm) and the subsequent relaxation by irradiation with UV light of a higher energy ($\lambda_{\max} = 308$ nm) (Figure 25). Surprisingly, the spectrum obtained after irradiation at 308 nm exhibits a small but non-negligible shift toward higher wavelengths of the main peak (grey and green lines in Figure 25). Moreover, a similar bathochromic shift of the main peak of the spectrum occurs with further excitation at 305 nm (deep and light blue lines in Figure 25). This induces us to think that the *syn (cis, cis)* isomer does not convert into the *syn (trans, trans)* one upon light relaxation at 308 nm but to the *anti (trans, trans)* isomer which then transforms into the *anti (cis, cis)* one upon further light excitation at 350 nm.

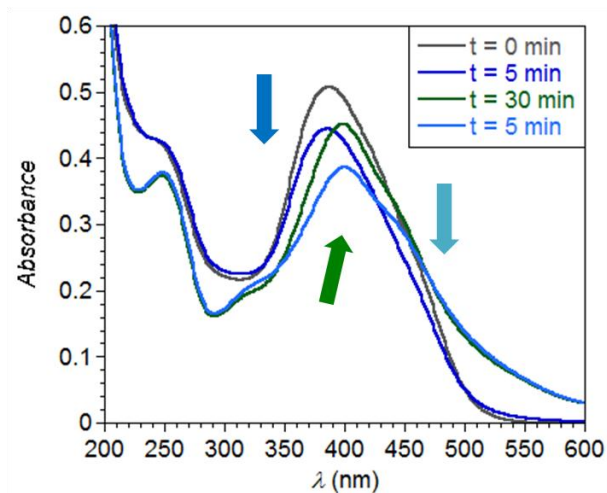


Figure 25. Evolution of the UV-vis spectra of **27a**: grey (initial compound), dark blue (excitation to 350 nm after 5 min), green (relaxation to 308 nm after 30 min) and light blue (re-excitation to 350 nm after 5 min).

Figure 26 shows the complex time evolution of the electronic spectra of **27a** upon two cycles of light excitation/light relaxation at 350 and 308 nm, respectively.

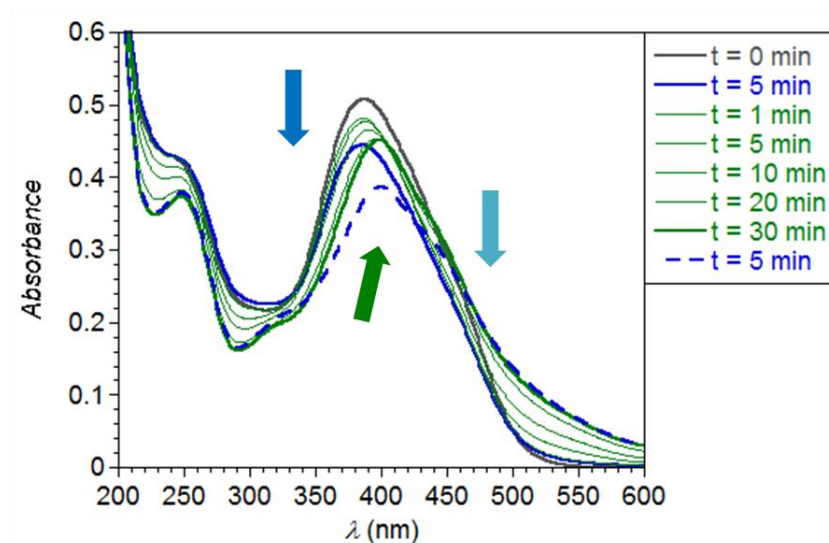


Figure 26. Evolution of the UV-vis spectra of **27a**: grey (initial compound), blue (excitation to 350 nm after 5 min), green (relaxation to 308 nm during the quoted times), blue dot-line (re-excitation to 350 nm after 5 min).

V.7. Cytotoxicity studies

A very preliminary cytotoxic activity against human carcinogenic cells is provided in this last part of the *Chapter* which illustrate a new function of the oxamate-containing Pd(II) complexes.

The complexes selected to check the effect in the growth of a chronic myelogenous leukemia cell line are the proligands and the mono- and dinuclear oxamate-containing Pd(II) complexes listed hereunder:

EtH-2-Mepma	
EtH-2,6-Me ₂ pma	Proligand
Et ₂ H ₂ -dpazba	
$(n\text{-Bu}_4\text{N})_2[\text{Pd}(2\text{-Mepma})_2]$ (9),	
$(n\text{-Bu}_4\text{N})_2[\text{Pd}(3,4\text{-Me}_2\text{pma})_2]$ (17)	
$\{\text{Na}(\text{H}_2\text{O})_2[\text{Pd}(2,6\text{-Me}_2\text{pma})_2]\}_n$ (1)	
$\{\text{K}_4(\text{H}_2\text{O})_3[\text{Pd}(2,6\text{-Me}_2\text{pma})_2]\}_n$ (2)	Mononuclear
$\{\text{Rb}_4(\text{H}_2\text{O})_3[\text{Pd}(2,6\text{-Me}_2\text{pma})_2]\}_n$ (3)	
$(n\text{-Bu}_4\text{N})_2[\text{Pd}(2,6\text{-Me}_2\text{pma})_2]$ (16)	
$(\text{AsPh}_4)_2[\text{Pd}(2,6\text{-Me}_2\text{pma})_2]$ (30)	
$(n\text{-Bu}_4\text{N})_4[\text{Pd}_2(\text{ppba})_2]$ (25)	
$(n\text{-Bu}_4\text{N})_4[\text{Pd}_2(\text{dpazba})_2]$ (27)	Dinuclear
$(n\text{-Bu}_4\text{N})_4[\text{Pd}_2(\text{dpeba})_2]$ (28)	
$(n\text{-Bu}_4\text{N})_4[\text{Pd}_2(\text{tpeba})_2]$ (29)	

These studies are performed in collaboration with a Brazilian Team headed by Prof. Dr. Elene Pereira-Maia. The first experiments concerning the solvent and the source of palladium(II) $\{\text{K}_2[\text{PdCl}_4]\}$ showed that they do not exhibit any cytotoxic effect at the level of concentration used. Then, the inhibition of cell growth determined is due to the complexes under investigation.

The concentrations of compounds necessary to inhibit 50% of cell growth, IC_{50} , determined after three days of incubation, are grouped in Table 6. For the sake of comparison, the values obtained with cisplatin, $AsPh_4Cl$ and $As(OH)_3$ are also shown. As_2O_3 , which is active against acute promyelocytic leukemia,¹⁰⁵⁻¹⁰⁷ exists mainly as $As(OH)_3$ in aqueous solution.

While all free pro-ligands tested did not affect cellular growth up to $100 \mu\text{mol L}^{-1}$, all palladium(II) complexes were able to inhibit tumoral cell growth in a concentration dependent manner. These results are very important as they evidence that Pd(II) coordination significantly improves the cytotoxic activity, which decreases in the order **30** > **16** > **25** > **29** > **17** > **9** > **28** > **27** ~ **3** ~ **1** ~ **2**. In order to look for a structure/activity relationship, the influence of the counter ion was also investigated. A comparison of the activity of compounds **1-3**, in which the counter ions alkaline cations, indicates that the nature of the counter ion does not interfere with the cytotoxic action, e.g., the active species is the $[Pd(2,6Me_2pma)_2]^{2-}$ anion. Interestingly, when the counter ion is the $n\text{-Bu}_4N^+$, the activity is improved. Complexes **16**, **17**, and **9** having this cation are more effective. To test this hypothesis, we have determined the IC_{50} value of $n\text{-Bu}_4NOH$ and it is $63 \mu\text{mol L}^{-1}$, whereas $NaCl$, KCl and $RbCl$ are not cytotoxic at the concentrations used in the assays. The most important result is the high activity of compound **30**, with an IC_{50} of 300 nM, approximately 170 times as active as complexes **1-3**, which also have the $[Pd(2,6Me_2pma)_2]^{2-}$ anion. Given that $AsPh_4Cl$ and PPh_4Cl are both active at the same range, it seems that the effect is not due to arsenic itself, but to an interaction of $AsPh_4^+$ or PPh_4^+ with cellular targets, such as DNA intercalation.

The comparison between mono- and dinuclear complexes is not easy because the quaternary amine cation has also cytotoxicity activity.¹⁰⁸⁻¹¹³ The fact that the dipalladium(II) are significantly active is meaningful as their mechanism of action can be different from that of the mononuclear ones. Otherwise, a deeper inspection of these results show somehow the importance of the intramolecular Pd(II)··Pd(II) distance in the cytotoxic activity, order being **25** ~ **29** > **27** ~ **28**. Anyway, a further study of these dinuclear species with alkaline countercations would be required to get a clearer picture of their cytotoxicity.

Table 9 IC₅₀* of the selected proligands (green), mono- (blue) and dinuclear (orange) palladium(II) complexes, reagent precursors (entries 15-19) and cisplatin (entry 20).

Entry	Compounds	IC ₅₀ (μM ± s.d.)
1	EtH-2-Mepma	> 100 ± 0.0
2	EtH-2,6-Me ₂ pma	> 100 ± 0.0
3	Et ₂ H ₂ -dpazba	> 100 ± 0.0
4	9	30.00 ± 3.0
5	17	28.08 ± 3.0
6	1	53.34 ± 4.1
7	2	64.28 ± 6.5
8	3	52.77 ± 4.5
9	16	15.90 ± 2.1
10	30	0.30 ± 0.02
11	27	42.70 ± 3.9
12	25	21.40 ± 2.0
13	28	40.8 ± 3.5
14	29	27.5 ± 3.0
15	<i>n</i> -Bu ₄ NOH	63.00 ± 5.0
16	<i>n</i> -Bu ₄ NCl	^a ±
17	AsPh ₄ Cl	0.32 ± 0.02
18	PPh ₄ Cl	0.18 ± 0.02
19	As(OH) ₃	3.01 ± 0.3
20	Cisplatin	1.10 ± 0.2

*IC₅₀ is the concentration required to inhibit 50% of cellular growth. The values are the mean of triplicate determinations. ^aAssays in current preparation

V.8. Conclusions

In conclusion, novel multifunctional oxamate-containing dipalladium(II) complexes were synthesized, consisting in dinucleating ligands with more or less rigid noninnocent separation between the metal ions. As for their analogous mononuclear species they exhibit several functionalities:

(i) they are environmentally friendly chemicals (in contrast to phosphines),

(ii) their easy and cheap preparation (in contrast to carbenes) makes them perfect as proligands and complexes,

(iii) they are highly robust (even working without an inert atmosphere) in carbon-carbon cross-coupling reactions or in photo-chemical and photo-switchphysical activities,

(iv) and they are also greatly stable in water where they can remain for months without any dissociation or formation of inactive palladium black.

In general, better results are obtained for the carbon-carbon cross-coupling reactions by using oxamate-containing palladium(II) complexes with $n\text{-Bu}_4\text{N}^+$ counter ion as catalysts in the Heck reaction compared to the Suzuki ones.

Explicitly, Heck carbon-carbon cross-coupling reactions using aryl iodides and $n\text{-Bu}_4\text{NBr}$ as ionic liquid medium allow working with 0.5 mol% of cat. [1 mol% of Pd(II)] in good yields (ca. 99%) and TON of ca. 198 besides let to accomplish reaction times of 10 min (TOF ca. 1188 h⁻¹).

To address upcoming environmental concerns, $n\text{-Bu}_4\text{NBr}$ serves as an alternative, greener medium to perform the Heck and Suzuki reactions. The strategy developed in this PhD Thesis in the carbon-carbon cross-coupling reactions by using oxamate-containing palladium(II) complex demonstrates that these complexes are active catalysts and they work very well with aryl halides that considering energy costs, the reactions occurring at short times and under mild temperatures.

Focusing on photochemical activity, the complexes (*n*-Bu₄N)₄[Pd₂(dpvba)₂] (**26**) and (*n*-Bu₄N)₄[Pd₂(dpazba)₂] (**27**) seem excellent candidates to continue with additional NMR, powder and X-ray diffraction studies in order to characterize the possible theoretical conformations of these kind of complexes and explain better the results of the solution studies.

A preliminary cytotoxicity study has been undertaken in order to establish the relevance of the oxamate-containing palladium(II) complexes in bio- and medical chemistry. Further studies may be required in order to understand better the value of these type of complexes. Due to the fact that the oxamate-containing palladium(II) complexes are very stable in solution as illustrate the parent copper(II) complexes^{114,115} no dissociation would be involved in the solution experiments. However, it deserves to point out that the election of quaternary amines, AsPh₄⁺ and PPh₄⁺ counteractions could mask the palladium cytotoxicity.^{105-107,116-118}

V.9. References

- (1) Steel, P. J. *Acc. Chem. Res.* **2005**, *38*, 243–250.
- (2) Pardo, E.; Ruiz-García, R.; Lloret, F.; Faus, J.; Julve, M.; Journaux, Y.; Novak, M. A.; Delgado, F. S.; Ruiz-Pérez, C. *Chem. Eur. J.* **2007**, *13*, 2054–2066.
- (3) Pardo, E.; Ruiz-García, R.; Cano, J.; Ottenwaelder, X.; Lescouëzec, R.; Journaux, Y.; Lloret, F.; Julve, M. *Dalt. Trans.* **2008**, 2780–2805.
- (4) Lu, Y.; Liu, Y.; Xu, Z.; Li, H.; Liu, H.; Zhu, W. *Expert Opin. Drug Discov.* **2012**, *7*, 375–383.
- (5) Decurtins, S.; Pellaux, R.; Antorrena, G.; Palacio, F. *Coord. Chem. Rev.* **1999**, *190-192*, 841–854.
- (6) In *Multifunctional Molecular Materials*; Ouahab, L., Ed.; Pan Stanford Publishing, Singapore, 2013.
- (7) Pardo, E.; Train, C.; Gontard, G.; Boubekour, K.; Fabelo, O.; Liu, H.; Dkhil, B.; Lloret, F.; Nakagawa, K.; Tokoro, H.; Ohkoshi, S.; Verdagner, M. *J. Am. Chem. Soc.* **2011**, *133*, 15328–15331.
- (8) Martínez-Lillo, J.; Armentano, D.; Fortea-Pérez, F. R.; Stiriba, S.-E.; De Munno, G.; Lloret, F.; Julve, M.; Faus, J. *Inorg. Chem.* **2015**, *54*, 4594–4596.
- (9) McCullough, J. J. *Chem. Soc. Rev.* **1987**, *87*, 811–860.
- (10) Becker, H. D. *Chem. Soc. Rev.* **1993**, *93*, 145–172.
- (11) Bouas-Laurent, H.; Desvergne, J.-P.; Castellan, A.; Lapouyade, R. *Chem. Soc. Rev.* **2000**, *29*, 43–55.
- (12) Griffiths, J. *Chem. Soc. Rev.* **1972**, *1*, 481.
- (13) Ulrich, H.; Rao, D. V.; Stuber, F. A.; Sayigh, A. A. R. *J. Org. Chem.* **1970**, *35*, 1121–1125.
- (14) Ciamician, G.; Silber, P. *Berichte der Dtsch. Chem. Gesellschaft* **1902**, *35*, 4128–4131.
- (15) Shechter, H.; Link, W. J.; Tiers, G. V. D. *J. Am. Chem. Soc.* **1963**, *85*, 1601–1605.
- (16) Syamala, M. S.; Ramamurthy, V. *J. Org. Chem.* **1986**, *51*, 3712–3715.
- (17) MacGillivray, L. R.; Reid, J. L.; Ripmeester, J. A. *J. Am. Chem. Soc.* **2000**, *122*, 7817–7818.
- (18) Papaefstathiou, G. S.; Zhong, Z.; Geng, L.; MacGillivray, L. R. *J. Am. Chem. Soc.* **2004**, *126*, 9158–9159.
- (19) Oliveira, W. X. C.; da Costa, M. M.; Fontes, A. P. S.; Pinheiro, C. B.; de Paula, F. C. S.; Jaimes, E. H. L.; Pedroso, E. F.; de Souza, P. P.; Pereira-Maia, E. C.; Pereira, C. L. M. *Polyhedron* **2014**, *76*, 16–21.
- (20) Rosenberg, B.; Vancamp, L.; Krigas, T. *Nature* **1965**, *205*, 698–699.
- (21) Rosenberg, B.; VanCamp, L.; Trosko, J. E.; Mansour, V. H. *Nature* **1969**, *222*, 385–386.
- (22) Dasari, S.; Bernard Tchounwou, P. *Eur. J. Pharmacol.* **2014**, *740*, 364–378.
- (23) Medici, S.; Peana, M.; Nurchi, V. M.; Lachowicz, J. I.; Crisponi, G.; Zoroddu, M. A. *Coord. Chem. Rev.* **2015**, *284*, 329–350.

- (24) Casini, A.; Reedijk, J. *Chem. Sci.* **2012**, *3*, 3135.
- (25) Wang, X.; Guo, Z. *Chem. Soc. Rev.* **2013**, *42*, 202-224.
- (26) Oun, R.; Wheate, N. J. In *Encyclopedia of Metalloproteins*; 2013; pp. 1710-1714.
- (27) Pinato, O.; Musetti, C.; Sissi, C. *Metallomics* **2014**, *6*, 380-395.
- (28) Schilling, T.; Keppler, K. B.; Heim, M. E.; Niebch, G.; Dietzfelbinger, H.; Rastetter, J.; Hanauske, A. R. *Invest. New Drugs* **1995**, *13*, 327-332.
- (29) Clarke, M. J.; Zhu, F.; Frasca, D. R. *Chem. Soc. Rev.* **1999**, *99*, 2511-2533.
- (30) Lainé, A.-L.; Passirani, C. *Curr. Opin. Pharmacol.* **2012**, *12*, 420-426.
- (31) Muhammad, N.; Guo, Z. *Curr. Opin. Chem. Biol.* **2014**, *19*, 144-153.
- (32) Caires, A. C. F. *Anticancer. Agents Med. Chem.* **2007**, *7*, 484-491.
- (33) Quirante, J.; Ruiz, D.; Gonzalez, A.; López, C.; Cascante, M.; Cortés, R.; Messeguer, R.; Calvis, C.; Baldomà, L.; Pascual, A.; Guérardel, Y.; Pradines, B.; Font-Bardía, M.; Calvet, T.; Biot, C. *J. Inorg. Biochem.* **2011**, *105*, 1720-1728.
- (34) MacGillivray, L. R.; Papaefstathiou, G. S.; Friscià, T.; Hamilton, T. D.; Bucar, D.-K.; Chu, Q.; Varshney, D. B.; Georgiev, I. G. *Acc. Chem. Res.* **2008**, *41*, 280-291.
- (35) Santurri, P.; Robbins, F.; Stubbings, R. *Org. Synth.* **1960**, *40*, 18.
- (36) Deeming, A. J.; Hogarth, G.; Lee, M. (Venus); Saha, M.; Redmond, S. P.; Phetmung, H. (Taya); Orpen, A. G. *Inorg. Chim. Acta*, **2000**, *309*, 109-122.
- (37) Dominguez, Z.; Khuong, T.-A. V.; Dang, H.; Sanrame, C. N.; Nuñez, J. E.; Garcia-Garibay, M. a. *J. Am. Chem. Soc.* **2003**, *125*, 8827-8837.
- (38) Fasina, T. M.; Collings, J. C.; Burke, J. M.; Batsanov, A. S.; Ward, R. M.; Albesa-Jove, D.; Porres, L.; Beeby, A.; Howard, J. a. K.; Scott, A. J.; Clegg, W.; W., S.; Christopher; Marder, T. B. *J. Mater. Chem.* **2005**, *15*, 690.
- (39) Gadzikwa, T.; Zeng, B.-S.; Hupp, J. T.; Nguyen, T. S. *Chem. Commun.* **2008**, 3672-3674.
- (40) Fortea-Pérez, F. R.; Marino, N.; Armentano, D.; De Munno, G.; Julve, M.; Stiriba, S.-E. *Cryst.Eng.Comm* **2014**, *16*, 6971.
- (41) Fortea-Pérez, F. R.; Schlegel, I.; Julve, M.; Armentano, D.; De Munno, G.; Stiriba, S.-E. *J. Organomet. Chem.* **2013**, *743*, 102-108.
- (42) Kivekas, R.; Pajunen, A.; Navarrete, A.; Colacio, E. *Inorg. Chim. Acta*, **1999**, *284*, 292-295.
- (43) Oliveira, W. X. C.; Ribeiro, M. A.; Pinheiro, C. B.; Nunes, W. C.; Julve, M.; Journaux, Y.; Stumpf, H. O.; Pereira, C. L. M. *Eur. J. Inorg. Chem.* **2012**, *2012*, 5685-5693.
- (44) **Angles definition:** Castellano, M.; Barros, W. P.; Acosta, A.; Julve, M.; Lloret, F.; Li, Y.; Journaux, Y.; De Munno, G.; Armentano, D.; Ruiz-García, R.; Cano, J. *Chem. Eur. J.* **2014**, *20*, 13965-13975.
- (45) Scudder, M.; Dance, I. J. *Chem. Soc. Dalt. Trans.* **1998**, 3155-3166.
- (46) Dance, I.; Scudder, M. J. *Chem. Soc. Dalt. Trans.* **1996**, 3755.
- (47) Castellano, M.; Fortea-Pérez, F. R.; Stiriba, S.-E.; Julve, M.; Lloret, F.; Armentano, D.; De Munno, G.; Ruiz-García, R.; Cano, J. *Inorg. Chem.* **2011**, *50*, 11279-11281.

- (48) Rogers, R. D.; Seddon, K. R. *Science* **2003**, *302*, 792–793.
- (49) Ranke, J.; Stolte, S.; Störmann, R.; Arning, J.; Jastorff, B. *Chem. Soc. Rev.* **2007**, *107*, 2183–2206.
- (50) Olivier-Bourbigou, H.; Magna, L.; Morvan, D. *Appl. Catal. A Gen.* **2010**, *373*, 1–56.
- (51) Calò, V.; Nacci, A.; Monopoli, A. *European J. Org. Chem.* **2006**, *2006*, 3791–3802.
- (52) Pârvulescu, V. I.; Hardacre, C. *Chem. Soc. Rev.* **2007**, *107*, 2615–2665.
- (53) Gordon, C. M. *Appl. Catal. A Gen.* **2001**, *222*, 101–117.
- (54) Welton, T. *Coord. Chem. Rev.* **2004**, *248*, 2459–2477.
- (55) Sheldon, R. *Chem. Commun.* **2001**, 2399–2407.
- (56) Steinrück, H.-P.; Wasserscheid, P. *Catal. Letters* **2014**, *145*, 380–397.
- (57) Zhao, D.; Wu, M.; Kou, Y.; Min, E. *Catal. Today* **2002**, *74*, 157–189.
- (58) Holbrey John D.; Turner Megan B.; Rogers Robin D. *Ionic Liquids as Green Solvents*; Rogers, R. D.; Seddon, K. R., Eds.; ACS Symposium Series; American Chemical Society: Washington, DC, 2003; Vol. 856.
- (59) Bellina, F.; Chiappe, C. *Molecules* **2010**, *15*, 2211–2245.
- (60) Böhm, V. P. W.; Herrmann, W. A. W.; Bohm, V.; Herrmann, W. A. W. *Chem. - A Eur. J.* **2000**, *6*, 1017–1025.
- (61) Hajipour, A. R.; Rafiee, F. *Appl. Organomet. Chem.* **2011**, *25*, 542–551.
- (62) Hornillos, V.; van Zijl, A. W.; Feringa, B. L. *Chem. Commun.* **2012**, *48*, 3712.
- (63) Ataei, A.; Nadri, S.; Rafiee, E.; Jamali, S.; Joshaghani, M. *J. Mol. Catal. A Chem.* **2013**, *366*, 30–35.
- (64) Gannon, T. J.; Law, G.; Watson, P. R.; Carmichael, A. J.; Seddon, K. R. *Langmuir* **1999**, *15*, 8429–8434.
- (65) Fry, A. J. *J. Electroanal. Chem.* **2003**, *546*, 35–39.
- (66) Herrmann, W. V. P. W. B. A.; Böhm, V. P. W. *J. Organomet. Chem.* **1999**, *572*, 141–145.
- (67) Calò, V.; Nacci, A.; Monopoli, A.; Ieva, E.; Cioffi, N. *Org. Lett.* **2005**, *7*, 617–620.
- (68) Islam, S. M.; Mondal, P.; Roy, A. S.; Mondal, S.; Hossain, D. *Tetrahedron Lett.* **2010**, *51*, 2067–2070.
- (69) Nájera, C.; Gil-Moltó, J.; Karlström, S.; Falvello, L. R. *Org. Lett.* **2003**, *5*, 1451–1454.
- (70) Susanto, W.; Chu, C.-Y.; Ang, W. J.; Chou, T.-C.; Lo, L.-C.; Lam, Y. a. *Green Chem.* **2012**, *14*, 77.
- (71) Yao, Q.; Kinney, E. P.; Zheng, C. *Org. Lett.* **2004**, *6*, 2997–2999.
- (72) Wolf, C.; Lerebours, R. *Org. Biomol. Chem.* **2004**, *2*, 2161–2164.
- (73) Alonso, F.; Beletskaya, I. P.; Yus, M. *Tetrahedron* **2005**, *61*, 11771–11835.
- (74) Bedford, R. B.; Blake, M. E.; Butts, C. P.; Holder, D. *Chem. Commun.* **2003**, 466–467.
- (75) Alonso, F.; Beletskaya, I. P.; Yus, M. *Tetrahedron* **2008**, *64*, 3047–3101.
- (76) Kumar, G. S.; Neckers, D. C. *Chem. Soc. Rev.* **1989**, *89*, 1915–1925.

- (77) Tsutsumi, O.; Shiono, T.; Ikeda, T.; Galli, G. *J. Phys. Chem. B* **1997**, *101*, 1332–1337.
- (78) Cattaneo, P.; Persico, M. *Phys. Chem. Chem. Phys.* **1999**, *1*, 4739–4743.
- (79) Bandara, H. M. D.; Cawley, S.; Gascón, J. A.; Burdette, S. C. *Eur. J. Org. Chem.* **2011**, *2011*, 2916–2919.
- (80) Bao, J.; Weber, P. M. *J. Am. Chem. Soc.* **2011**, *133*, 4164–4167.
- (81) Cusati, T.; Granucci, G.; Martínez-Núñez, E.; Martini, F.; Persico, M.; Vázquez, S. *J. Phys. Chem. A* **2012**, *116*, 98–110.
- (82) Lee, K. M.; White, T. J. *Macromolecules* **2012**, *45*, 7163–7170.
- (83) Mukhopadhyay, R. D.; Praveen, V. K.; Ajayaghosh, A. *Mater. Horizons* **2014**.
- (84) Semionova, V. V.; Glebov, E. M.; Korolev, V. V.; Sapchenko, S. A.; Samsonenko, D. G.; Fedin, V. P. *Inorg. Chim. Acta*, **2014**, *409*, 342–348.
- (85) Suzuki, M.; Momotake, A.; Kanna, Y.; Nishimura, Y.; Hirota, K.; Morihashi, K.; Arai, T. *J. Photochem. Photobiol. A Chem.* **2013**, *252*, 203–210.
- (86) Yang, P.-C.; Wang, Y.-H.; Wu, H. *J. Appl. Polym. Sci.* **2012**, *124*, 4193–4205.
- (87) Yager, K. G.; Barrett, C. J. *J. Photochem. Photobiol. A Chem.* **2006**, *182*, 250–261.
- (88) Clark, A. E. *J. Phys. Chem. A* **2006**, *110*, 3790–3796.
- (89) Sadowski, O.; Beharry, A. A.; Zhang, F.; Woolley, G. A. *Angew. Chem. Int. Ed. Engl.* **2009**, *48*, 1484–1486.
- (90) Castellano, M.; Ferrando-Soria, J.; Pardo, E.; Julve, M.; Lloret, F.; Mathonière, C.; Pasán, J.; Ruiz-Pérez, C.; Cañadillas-Delgado, L.; Ruiz-García, R.; Cano, J. *Chem. Commun.* **2011**, *47*, 11035–11037.
- (91) Beharry, A. A.; Woolley, G. A. *Chem. Soc. Rev.* **2011**, *40*, 4422–4437.
- (92) Beharry, A. A.; Sadowski, O.; Woolley, G. A. *J. Am. Chem. Soc.* **2011**, *133*, 19684–19687.
- (93) Lin, J.-L.; Chen, C.-W.; Sun, S.-S.; Lees, A. J. *Chem. Commun.* **2011**, *47*, 6030–6032.
- (94) Yamamura, M.; Okazaki, Y.; Nabeshima, T. *Chem. Commun.* **2012**, *48*, 5724–5726.
- (95) Imahori, T.; Yamaguchi, R.; Kurihara, S. *Chem. Eur. J.* **2012**, *18*, 10802–10807.
- (96) Doran, T. M.; Anderson, E. A.; Latchney, S. E.; Opanashuk, L. A.; Nilsson, B. L. *ACS Chem. Neurosci.* **2012**, *3*, 211–220.
- (97) *Supramolecular Chemistry*; Gale, P. A.; Steed, J. W., Eds.; John Wiley & Sons, Ltd: Chichester, UK, 2012.
- (98) Kienzler, M. A.; Reiner, A.; Trautman, E.; Yoo, S.; Trauner, D.; Isacoff, E. Y. *J. Am. Chem. Soc.* **2013**, *135*, 17683–17686.
- (99) Tsai, F. J.; Torkelson, J. M.; Lewis, F. D.; Holman, B. *Macromolecules* **1990**, *23*, 1487–1493.
- (100) Schraub, M.; Gray, H.; Hampp, N. *Macromolecules* **2011**, *44*, 8755–8762.
- (101) Liao, L.; Li, Y.; Zhang, X.; Geng, Y.; Zhang, J.; Xie, J.; Zeng, Q.; Wang, C. *J. Phys. Chem. C* **2014**, *118*, 15963–15969.
- (102) Wakatsuki, Y.; Yamazaki, H.; Grutsch, P. A.; Santhanam, M.; Kotal, C. *J. Am. Chem. Soc.* **1985**, *107*, 8153–8159.

- (103) Yutaka, T.; Mori, I.; Kurihara, M.; Mizutani, J.; Kubo, K.; Furusho, S.; Matsumura, K.; Tamai, N.; Nishihara, H. *Inorg. Chem.* **2001**, *40*, 4986–4995.
- (104) Yutaka, T.; Mori, I.; Kurihara, M.; Tamai, N.; Nishihara, H. *Inorg. Chem.* **2003**, *42*, 6306–6313.
- (105) Chen, G. Q.; Shi, X. G.; Tang, W.; Xiong, S. M.; Zhu, J.; Cai, X.; Han, Z. G.; Ni, J. H.; Shi, G. Y.; Jia, P. M.; Liu, M. M.; He, K. L.; Niu, C.; Ma, J.; Zhang, P.; Zhang, T. D.; Paul, P.; Naoe, T.; Kitamura, K.; Miller, W.; Waxman, S.; Wang, Z. Y.; de The, H.; Chen, S. J.; Chen, Z. *Blood* **1997**, *89*, 3345–3353.
- (106) Shen, Z. X.; Chen, G. Q.; Ni, J. H.; Li, X. S.; Xiong, S. M.; Qiu, Q. Y.; Zhu, J.; Tang, W.; Sun, G. L.; Yang, K. Q.; Chen, Y.; Zhou, L.; Fang, Z. W.; Wang, Y. T.; Ma, J.; Zhang, P.; Zhang, T. D.; Chen, S. J.; Chen, Z.; Wang, Z. Y. *Blood* **1997**, *89*, 3354–3360.
- (107) Soignet, S. L.; Frankel, S. R.; Douer, D.; Tallman, M. S.; Kantarjian, H.; Calleja, E.; Stone, R. M.; Kalaycio, M.; Scheinberg, D. A.; Steinherz, P.; Sievers, E. L.; Coutre, S.; Dahlberg, S.; Ellison, R.; Warrell, R. P. . *J. Clin. Oncol.* **2001**, *19*, 3852–3860.
- (108) Pinnaduwege, P.; Schmitt, L.; Huang, L. *Biochim. Biophys. Acta - Biomembr.* **1989**, *985*, 33–37.
- (109) Dimmock, J. R.; Arora, V. K.; Quail, J. W.; Pugazhenthii, U.; Allen, T. M.; Kao, G. Y.; De Clercq, E. *J. Pharm. Sci.* **1994**, *83*, 1124–1130.
- (110) Imazato, S. *Biomaterials* **1999**, *20*, 899–903.
- (111) Nagamune, H.; Maeda, T.; Ohkura, K.; Yamamoto, K.; Nakajima, M.; Kourai, H. *Toxicol. Vitro.* **2000**, *14*, 139–147.
- (112) Antonucci, J. M.; Zeiger, D. N.; Tang, K.; Lin-Gibson, S.; Fowler, B. O.; Lin, N. J. *Dent. Mater.* **2012**, *28*, 219–228.
- (113) Li, F.; Weir, M. D.; Chen, J.; Xu, H. H. K. *Dent. Mater.* **2013**, *29*, 450–461.
- (114) Ruiz, R.; Faus, J.; Lloret, F.; Julve, M.; Journaux, Y. *Coord. Chem. Rev.* **1999**, *193-195*, 1069–1117.
- (115) Julve, M. *Under Preparation*.
- (116) Basu, A.; Mahata, J.; Gupta, S.; Giri, A. K. *Mutat. Res. Mutat. Res.* **2001**, *488*, 171–194.
- (117) Sun, H.-J.; Rathinasabapathi, B.; Wu, B.; Luo, J.; Pu, L.-P.; Ma, L. Q. *Environ. Int.* **2014**, *69*, 148–158.
- (118) Xie, H.; Huang, S.; Martin, S.; Wise, J. P. *Mutat. Res. Toxicol. Environ. Mutagen.* **2014**, *760*, 33–41.

Conclusions and new horizons

Oxamate-containing palladium(II) complexes

The work presented in this manuscript is an attempt to summarise the efforts that involve to create a new palladium(II)-based oxamato chemistry.

Twenty-nine novel examples of mono- and dinuclear palladium(II) complexes have been prepared in this PhD Thesis by rational design. This series of compounds allowed us:

(i) to illustrate the advantage of the building blocks for the *bottom up* approach in metallosupramolecular chemistry;

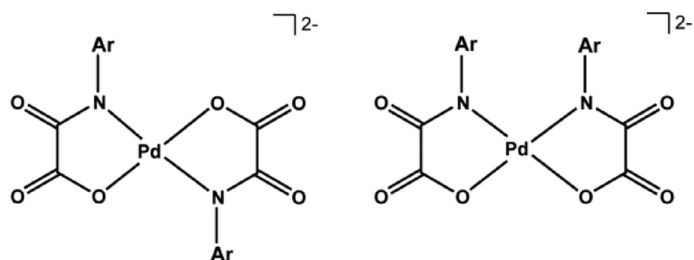
(ii) to provide noteworthy catalysts for carbon-carbon cross-coupling reactions with remarkable catalytic properties,

(iii) to produce complexes for molecular recognition to trap the elusive $[\text{Pd}(\text{H}_2\text{O})_4]^{2+}$ species;

(iv) to get suitable candidates to study photochemical activities

(v) and to have new water soluble anionic complexes with cytotoxicity activity.

Our research group has been focused on oxamato-containing copper(II) complexes as building blocks in molecular magnetism since more than fifteen years. The *trans*- conformation of the bis(oxamato)cuprate(II) is the only one observed in all the determinate structures. However, the use of Pd(II) instead of Cu(II) has allowed us to demonstrate that a new possibility of different conformation can be achieved opening thus a new possibility of different MOFs structures based on the use of stereochemically directed oxamato-containing palladium(II) mononuclear complexes as building blocks.



Scheme 1. *Trans*- (left) and *cis*-isomers (right) of bis(oxamato)palladate(II) complexes.

A wonderful family of coordination polymers developed by Pardo and co-workers has been built based on the use of mononuclear oxamato-containing copper(II) complexes with the *trans* conformation. The knowledge of the *cis*- one opens new possibilities in designing this type of materials.

Concerning the bis(oxamato)palladate(II) complexes with $n\text{-Bu}_4\text{N}^+$ as counter cations (Figure 1) the present study shows that they are to be suitable catalysts for Heck carbon-carbon cross-coupling reactions by using aryl halides as reagents and an alternative solvent (*ionic liquid*) such as $n\text{-Bu}_4\text{NBr}$.

The relevance of this family of oxamate complexes is that we have demonstrated that they are catalytically active, even using more expensive reagents (comparing aryl halides to aryl bromides and chlorides); the energy cost is significantly reduced because our reactions require at very short reaction times.

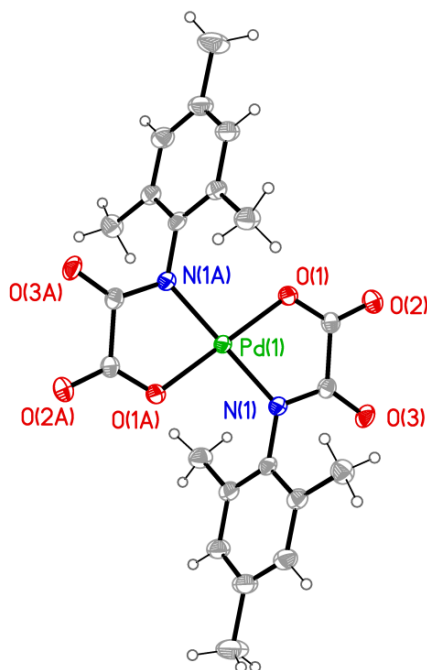


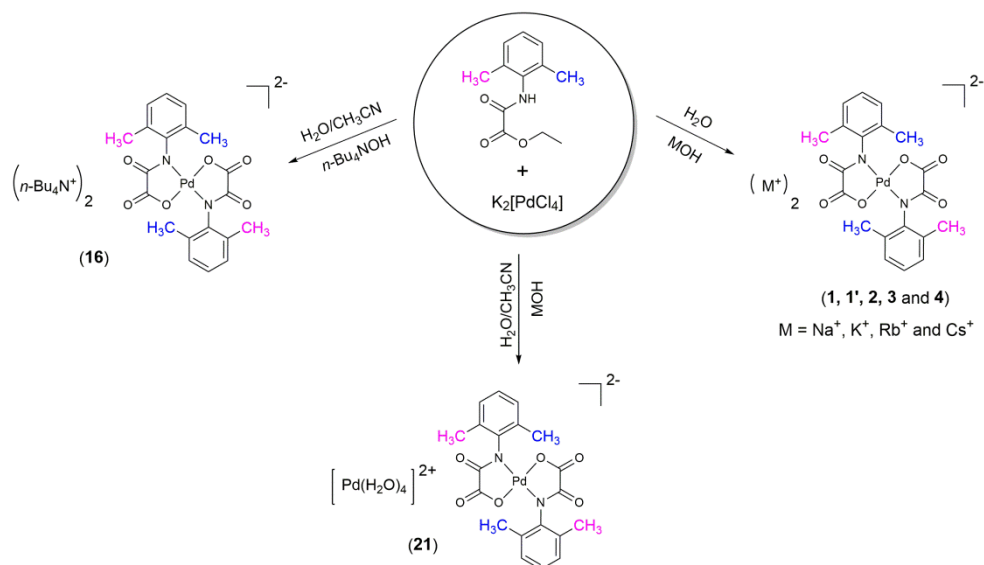
Figure 1. Perspective view of an example of anionic bis(*N*-substituted oxamato)palladate(II) complex.

Our efforts have been focused on alternative solvents such as *ionic liquids*, but this kind of complexes, which are extremely soluble in water, could be excellent candidates for homogeneous catalysis in such media. Besides, further studies will be needed to determine the stability constant of the palladium(II)-oxamate and try to shed some light on the possibility of an intermediate Pd(IV) step in Heck or Suzuki cross-coupling reactions.

In addition, the chemistry of palladium(II) catalysts is very rich and a other catalytic reactions could be tested with them.

It deserves to point out that trapping the $[\text{Pd}(\text{H}_2\text{O})_4]^{2+}$ counter-ion has been a hot topic over the years and it had been studied only by spectroscopy techniques. With the help of the oxamate-containing palladium(II) complexes, the tetraaquapalladium(II) cation has been characterized by single crystal X-ray diffraction for the first time in this PhD Thesis.

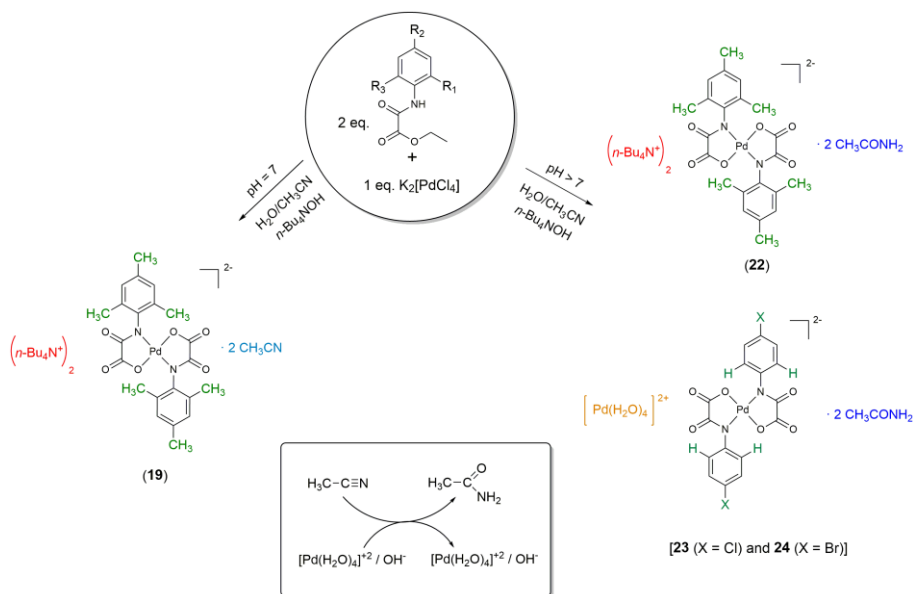
$[\text{Pd}(\text{H}_2\text{O})_4]^{2+}$ is present as counter-ion in the $[\text{Pd}(2,6\text{-Me}_2\text{pma})]^{2-}$ complexes when the solvents of the reaction of complex formation were changed (see Scheme 2).



Scheme 2. Simplified preparative route of the complexes with 2,6-Me₂pma as ligand.

The low solubility of the complex $[\text{Pd}(\text{H}_2\text{O})_4][\text{Pd}(2,6\text{-Me}_2\text{pma})_2]$ accounts for its crystallization within a couple of days under ambient conditions. From the point of view of Suzuki carbon-carbon cross-coupling reactions, both palladium(II) units are catalytic active. However, $[\text{Pd}(\text{H}_2\text{O})_4]^{2+}$ turns into the inactive palladium black after the reaction is finished.

$[\text{Pd}(\text{H}_2\text{O})_4]^{2+}$ was also present in the structure of the complexes of formula $[\text{Pd}(\text{H}_2\text{O})_4][\text{Pd}(4\text{-Xpma})_2] \cdot 2\text{CH}_3\text{CONH}_2$ ($\text{X} = \text{Cl}$ or Br) being an intermediate species of the nitrile hydration reaction. In our case, the hydration process is stopped at in the amide as product instead of an over-hydrolysis leading to the corresponding carboxylate product (Scheme 3).

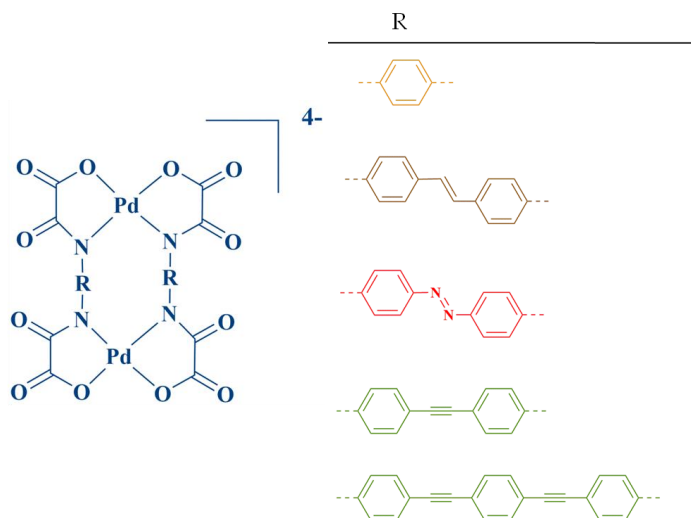


Scheme 3. Simplified reaction pathway with $\text{R} = \text{R} = \text{R} = \text{CH}_3$ for **19** and **22** and $\text{R} = \text{R} = \text{H}$ and $\text{R} = \text{Cl}, \text{Br}$ for **23** and **24**.

Once again, the low solubility of the complex accounts for the crystallization in a couple of days. This phenomenon prevents that the excess of oxamate dianion could fully give the bis(oxamato)palladate(II) entity as occurs with $(n\text{-Bu}_4\text{N})_2[\text{Pd}(2,6\text{-Me}_2\text{pma})_2] \cdot 2\text{CH}_3\text{CONH}_2$ which crystallizes in a couple of weeks.

On the one hand, we have demonstrated the presence of $[\text{Pd}(\text{H}_2\text{O})_4]^{2+}$ cation carrying out the acetonitrile hydration. The next step will be to perform these reactions within catalytic proportions and with a large number of nitrile reagents. Besides, may be necessary to check if this kind of reaction may be carried out without the presence of oxamate dianions or on the contrary, a catalytic presence of $[\text{PdCl}_4]^{2-}/\text{OH}^-$ may be enough to achieve the nitrile hydration to amide without an over hydrolysis to the corresponding carboxylic acid. On the other hand, new theoretical models could be proposed based on the information provided by structural knowledge of the $[\text{Pd}(\text{H}_2\text{O})_4]^{2+}$ cation.

In relation to the dipalladium(II) oxamate metallacyclophanes (Scheme 4), novel complexes based on dinucleating ligands with two oxamate donor groups separated by more or less rigid noninnocent spacers that self-assemble with palladium(II) ions to form double-stranded dipalladium(II) metallacyclic complexes of the cyclophane type were prepared and characterized. The intramolecular Pd··Pd separation can be trowed depending on the length and topology of the spacer.



Scheme 4. Dinuclear palladium(II) metallacyclophane complexes of general formula $[\text{Pd}_2\text{L}_2]^{4-}$.

Interestingly, these complexes have also proved to be good catalysts for Heck carbon-carbon cross-coupling reactions using aryl halides as reagents and an alternative solvent (*ionic liquid*) such as $n\text{-Bu}_4\text{NBr}$. Besides, preliminary studies have shown that this type of complexes are photoactive and being diamagnetic systems, they could complete the analogous studies for copper(II) complexes that are subject of current work in our research group by using the same ligands.

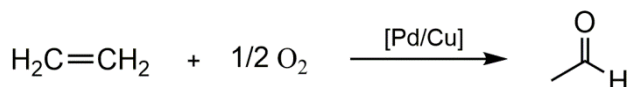
From discrete structures to metal-organic frameworks

Pardo and coworkers have achieved new structures of 3D oxamate-containing MOFs by using a single crystal-to-single crystal transmetallation approach. Similar results have been obtained by us using the same technique were the Pd(II) ion is incorporated into the MOF (Figure 2).

If the oxamate-copper(II) unit is transformed into the corresponding palladium(II) unit means that the stability constant of the Pd(II)-oxamate is greater than that with Cu(II). So, a careful control of the transmetallation time would allow to replace all the copper(II) ion by the palladium(II) ones.

These robust palladium(II)-MOFs based on oxamate ligands can be viewed as suitable hosts to carry out a large number of heterogeneous catalytic reactions such as the formation of carbon-carbon, carbon-oxygen, carbon-nitrogen, carbon-sulfur bonds as well as hydrogenation, hydrogenolysis, carbonylation and cycloisomerization reactions

In addition, the copper(II) ion is not fully transmetallated from the metal-organic framework precursor, a phenomenon that could allow us to envisage other reactions such as the Wacker process (Scheme 4).



Scheme 4. Wacker process originally described as oxidation of ethylene to acetaldehyde by dioxygen in water.

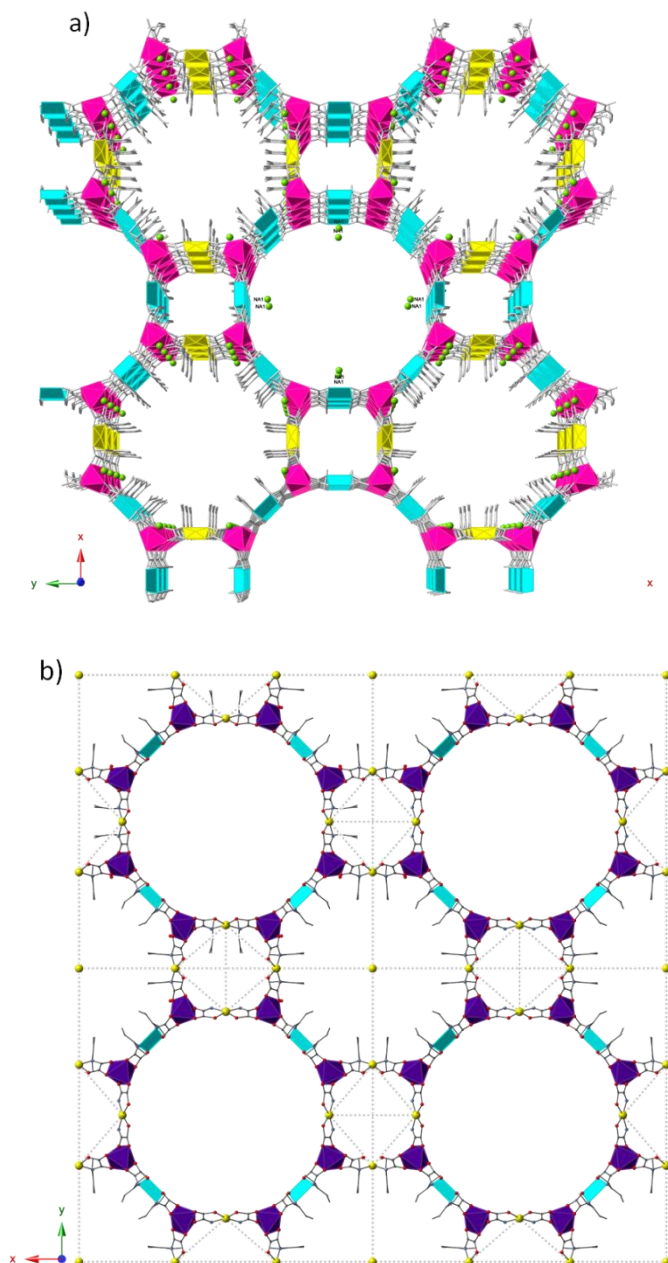


Figure 2. Perspective view of *preliminary results* of anionic 3D a) $\text{Cu}_x\text{Mn}_x\text{Na}_x\text{Pd}_x$ and b) $\text{Co}_x\text{Cu}_x\text{Pd}_x$ networks achieved by single crystal to single crystal transmetallation . Polyhedral colors: yellow (Pd), blue (Cu), pink (Mn) and purple (Co). Sphere colors: green (Na) and Yellow (Pd).

Appendixes

Appendix A

Supporting information for Chapter 1

A1.	Materials and characterization	243
A2.	Synthesis of the proligands	243
A3.	Characterization of the proligands	244
A4.	X-ray data collection and structure determination	245
A5.	Procedure for the Suzuki cross coupling reaction	246
A6.	General FT-IR and ¹ H NMR spectra of the proligands	247
A7.	FT-IR spectra of the complexes 1-4 (<i>Part I</i>)	248
A8.	General FT-IR spectra of the complexes 5-7 (<i>Part II</i>)	250
A9.	Powder diffraction (PXRD) of the complexes 1, 1' and 2-4	251
A10.	References	253

A1. Materials and characterization.

2,6-Dimethylaniline, 4-Xaniline (X = fluoro, chloro and bromo), $K_2[PdCl_4]$, MOH (M = Na, K, Cs and Rb), *n*-Bu₄NOH, ethyl chlorooxalate and all the solvents for the syntheses were purchased from commercial sources and used without further purification.

FT-IR spectra (KBr pellets) were performed with a Nicolet 5700 FT-IR instrument (4000 - 450 cm⁻¹). NMR spectra (¹H, ¹³C) were recorded on an Avance DRX 300 Bruker instrument at room temperature. All ¹H and ¹³C NMR spectra were measured relative to the signal for residual chloroform (7.26 ppm) in CDCl₃ or deuteriochloroform (77.23 ppm), respectively. The elemental analysis (C, H and N) was carried out on a EuroEA3000 analyzer by the Servei Central d'Instrumentació Científica at the University of Jaume I. A value of 2:1 for the M:Pd molar ratio was determined through electron probe X-ray microanalysis by using a Philips XL-30 scanning electron microscope (SEM) from the Central Service for Support to Experimental Research (SCSIE) at the University of Valencia. All GC analyses were performed on an Agilent 6890N gas chromatograph equipped with capillary columns pertaining to the SCSIE.

A2. Synthesis of the proligands.

The ethyl ester derivative of the proligands (EtH-2,6-Me₂pma, EtH-4-F-pma, EtH-4-Cl-pma and EtH-4-Br-pma) were prepared by following a previously reported procedure.¹ The corresponding aniline derivative (83 mmol) was dissolved in THF (250 mL) under nitrogen in a two round flask equipped a condenser and the resulting solution was treated with ethyl chlorooxoacetate (9.3 mL, 83 mmol) in presence of triethylamine (12 mL, 83 mmol) at room temperature under continuous stirring for 30 min.

The resulting solution was filtered and the solvent was removed under vacuum to afford oily crude, which quickly becomes solid. The obtained white solid was suspended in water and filtered off, then washed with a small amount of diethyl ether and dried under vacuum.

A3. Characterization of the proligands.

EtH-2,6-Me₂pma. Yield: 96%. IR(KBr/cm⁻¹): 3244 (N-H), 3027, 2977, 2923 (C-H), 1727, 1677 (C=O). ¹H NMR (CDCl₃) δ (ppm): 1.42-1.45 (t, 3H, CH₃), 2.25 (s, 6H, CH₃), 4.42-4.46 (q, 2H, CH₂), 7.11-7.13 (m, 3H, H_{aryl}), 8.46 (s, 1H, NH); ¹³C NMR (CDCl₃) δ (ppm): 14.4, 18.8, 64.0, 128.3, 128.6, 132.5, 135.4, 155., 161.3. Anal. Calcd. for C₁₂H₁₆NO₃: C 64.85, H 7.26, N 6.30. Found: C 65.31, H 7.23, N 6.40%.

EtH-4-F-pma. Yield: 85%. IR (KBr/cm⁻¹): 3322 (N-H), 3116, 2987, 2944, 2905 (C-H), 1732, 1687 (C=O). ¹H NMR (CDCl₃) δ (ppm): 1.41-1.46 (t, 3H, CH₃), 4.39 - 4.46 (q, 2H, CH₂), 7.05 - 7.11 (m, 2H, H_{aryl}), 7.60 - 7.64 (m, 2H, H_{aryl}), 8.86 (s, 1H, NH); ¹³C NMR (CDCl₃) δ (ppm): 14.41, 64.26, 116.28, 116.58, 121.90, 122.01, 161.35, 192.25. Anal. Calcd. for C₁₀H₁₀FNO₃: C 56.87, H 4.77, N 6.63. Found: C 57.19, H 5.58, N 6.46%.

EtH-4-Cl-pma. Yield: 90%. IR (KBr/cm⁻¹): 3334 (N-H), 3122, 2984, 2908, (C-H), 1729, 1698 (C=O). ¹H NMR (CDCl₃) δ (ppm): 1.29 - 1.34 (t, 3H, CH₃), 4.27 - 4.35 (q, 2H, CH₂), 7.41 - 7.44 (d, 2H, H_{aryl}), 7.77 - 7.80 (d, 2H, H_{aryl}), 10.93 (s, 1H, NH); ¹³C NMR (CDCl₃) δ (ppm): 14.20, 62.85, 122.4, 128.1, 129.1, 136.8, 155.9, 160.8. Anal. Calcd. for C₁₀H₁₀ClNO₃: C 52.76, H 4.43, N 6.15. Found: C 51.26, H 5.45, N 5.62%.

EtH-4-Br-pma. Yield: 95%. IR (KBr/cm⁻¹): 3334 (N-H), 3129, 2981, 2905, (C-H), 1729, 1705 (C=O). ¹H NMR (CDCl₃) δ (ppm): 1.29 - 1.34 (t, 3H, CH₃), 4.27 - 4.34 (q, 2H, CH₂), 7.54 - 7.57 (m, 2H, H_{aryl}), 7.71 - 7.74 (m, 2H, H_{aryl}), 10.92 (s, 1H, NH); ¹³C NMR (CDCl₃) δ (ppm): 14.2, 62.85, 116.99, 122.75, 131.99, 137.26, 155.89, 160.77. Anal. Calcd. for C₁₀H₁₀BrNO₃: C 44.14, H 3.70, N 5.15. Found: C 47.74, H 4.99, N 5.42%.

A4. X-ray data collection and structure determination.

(Chapter I, Part I). Single crystal X-ray diffraction data for **1/1'** and **2-4** were collected either at 100 (**1**, **1'** and **2**) or 296 K (**3** and **4**) on a Bruker-Nonius X8-APEXII CCD area detector system using graphite-monochromated Mo-K α radiation ($\lambda = 0.71073 \text{ \AA}$), and processed through the SAINT² reduction and SADABS³ absorption software.

The structures were solved by direct methods and subsequently completed by Fourier recycling using the SHELXTL⁴ software packages, then refined by the full-matrix least-squares refinements based on F^2 with all observed reflections, using established methods.⁵ All non-hydrogen atoms but the oxygen belonging to the water molecule O(1w) in both **2** and **4** were refined anisotropically. The latter were found disordered over two positions [O(1w) and O(1wA)] and refined freely within SHELXL while constraining the sum of the occupancies to unity; the relative occupancies of the two alternative positions reached values of 0.76:0.24 (**2**) and 0.57:0.43 (**4**) at convergence. The hydrogen atoms on the 2,6-dimethylphenyl substituent on the oxamate ligand were included at geometrically calculated positions and refined using a riding model. The hydrogen atoms on the water molecules in **1** and **2** were located on the ΔF map and refined with restraints, with thermal factors fixed to 1.5 times the U value of O(1w). The hydrogen atoms on the water molecules in **1'**, **3** and **4** were not placed. Similarity restraints on 1-2 and 1-3 distances³⁴ were applied in **2** and **3** to the alkaline cations-crystallization water molecules array to help to stabilize the refinement. The residual maxima and minima in the final Fourier-difference maps noted in **3** as 3.227 and -3.259 e \AA^{-3} were near the Pd(2) and Rb(4) atoms, respectively; the residual maxima and minima in **4**, noted as 3.025 and -4.547 e \AA^{-3} , were close to the Cs(3) and Cs(1) atoms, respectively. Crystal data and refinements conditions for **1**, **1'**, **2**, **3** and **4** are summarized in Table 1 whereas selected bond lengths and angles are listed in Tables 2 (**1**), 3 (**1'**), 4 (**2**), 5 (**3**) and 6 (**4**) (see Chapter 1). CCDC numbers are 992677 (**1**), 992678 (**2**), 992679 (**3**) 992680 (**4**) and 1002975 (**1'**).

A5. Procedure for the Suzuki cross-coupling reaction.

A test-tube with screw cap and valve was charged with a magnetic stir bar, the pre-catalyst (complexes **1** and **2-4**, 1 mol% Pd with respect to the reaction substrate), the aryl halide (0.50 mmol), Et₃N (1.00 mmol), the aryl boronic acid (0.75 mmol) and DMF (4 mL). The mixture was heated under continuous stirring during 5 min for the aryl iodides and 20 min for the aryl bromides at 150 °C at the open air. The reaction was monitored using thin liquid chromatography on silica gel. The reaction mixture was cooled, diluted with water (3 mL) and extracted three times (3 x 5 mL) with *n*-pentane. The extracts were combined and dried over magnesium sulphate. The products were examined by GC-MS using perfluorotributylamine (PFTBA) as internal standard.

A6. General FT-IR and ^1H NMR spectra of the proligands.

For the sake of brevity, a unique illustration of a proligand is given, in order to show the characteristic FT-IR and ^1H NMR peaks for this family of oxamate proligands.

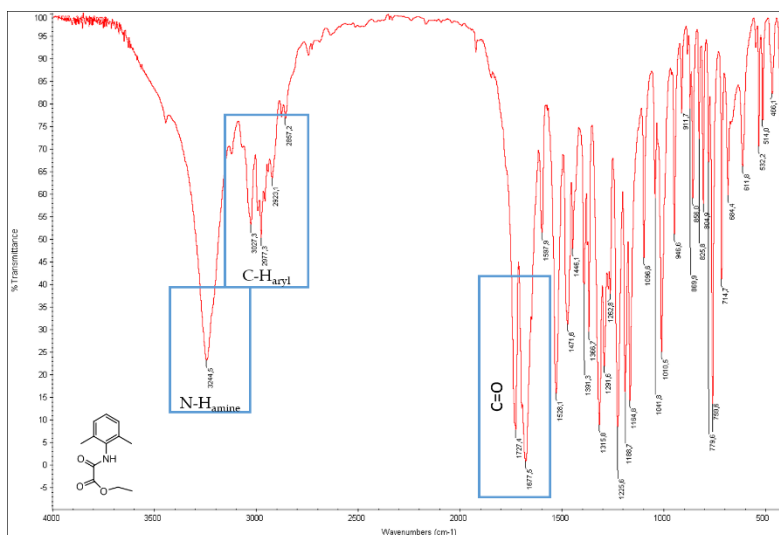


Figure S1. FT-IR spectrum for EtH-2,6-Me₂pma proligand

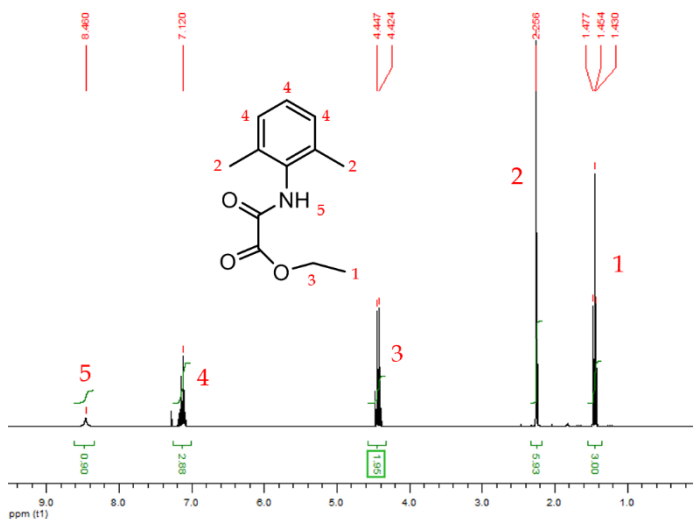
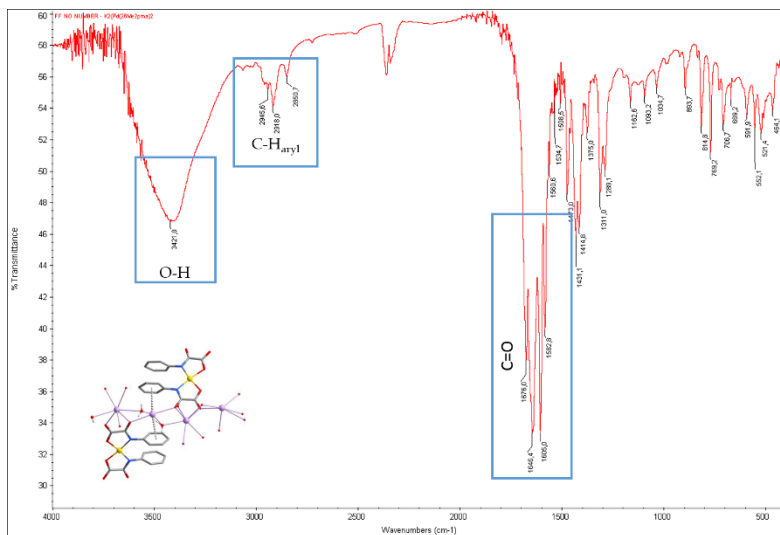
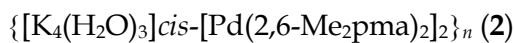
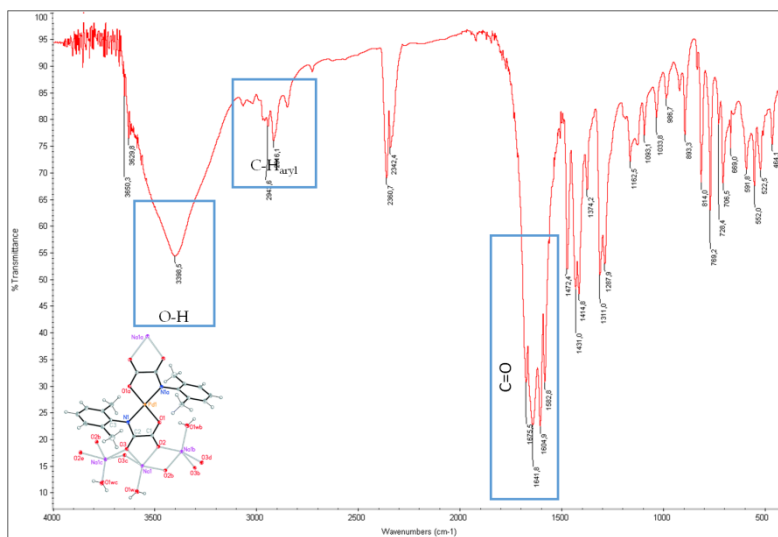
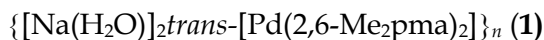
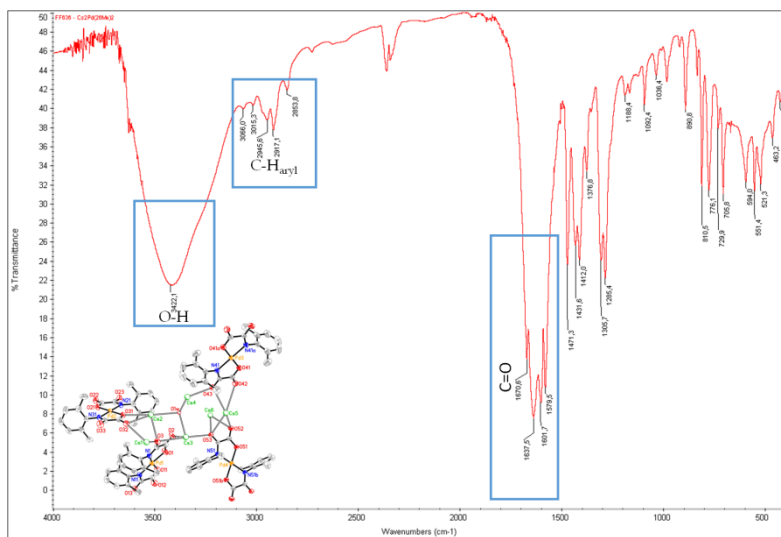
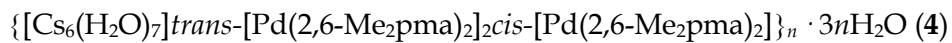
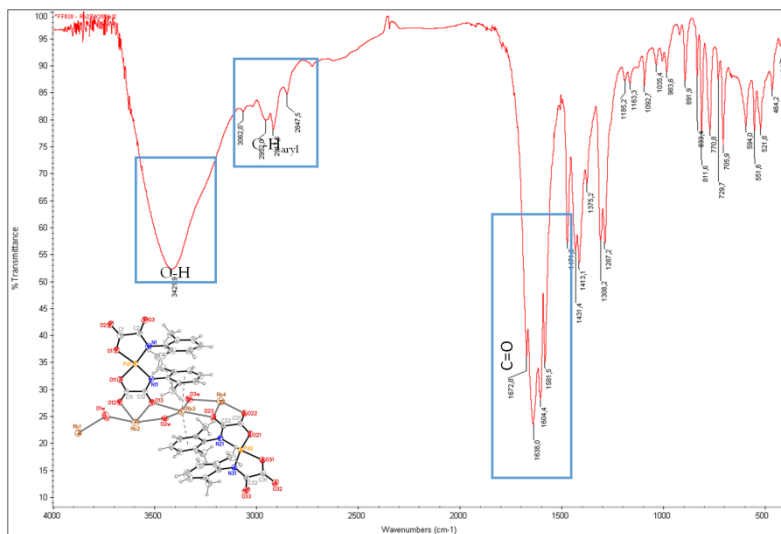
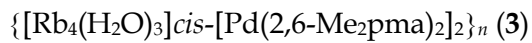


Figure S2. ^1H NMR spectrum for EtH-2,6-Me₂pma proligand

A7. FT-IR spectra of the complexes 1-4 (Part I).

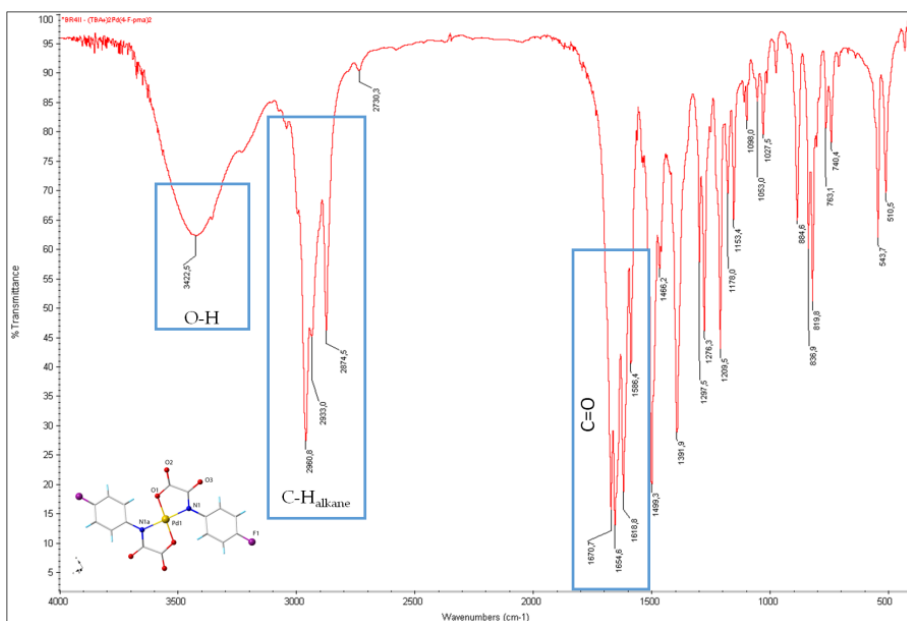
FT-IR spectra of the bis(oxamato)palladate complexes (**1-4**) of general formula $[M(H_2O)_n]_2[Pd(2,6-Me_2pma)_2]$ (where M = alkaline element) are given in order to show the most characteristic infrared peaks of these complexes.





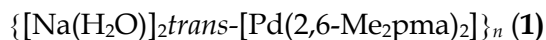
A8. General FT-IR spectra of the complexes 5-7 (Part II).

For the sake of brevity a unique illustration of bis(oxamato)palladate(II) complexes with halogen derivative proligands of general formula $(n\text{-Bu}_4\text{N})_2[\text{Pd}(4\text{-Xpma})_2]$ (where 4-Xpma = halogen derivative proligand) is given hereunder in order to show the most typical FT-IR peaks of these type of complexes.

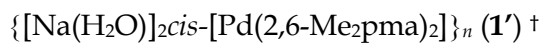
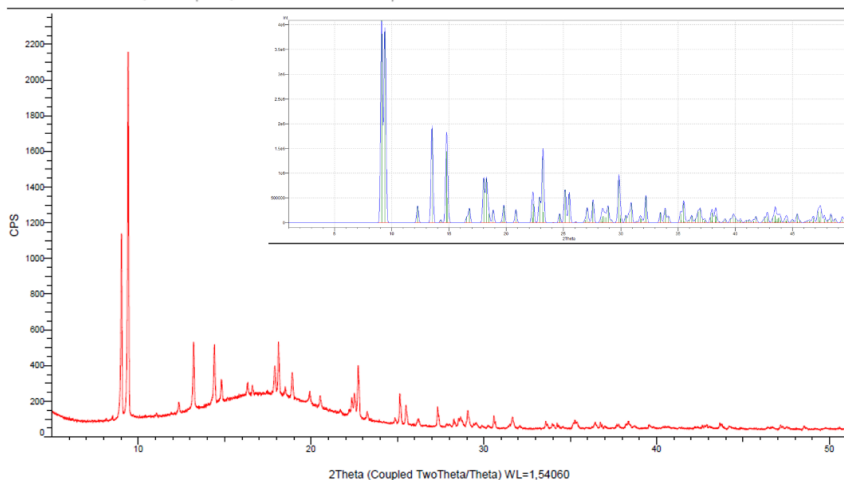
 $(n\text{-Bu}_4\text{N})_2\text{trans-}[\text{Pd}(4\text{-Fpma})_2]$ (5)

A9. Powder diffraction (PXRD) of the complexes 1, 1' and 2-4.

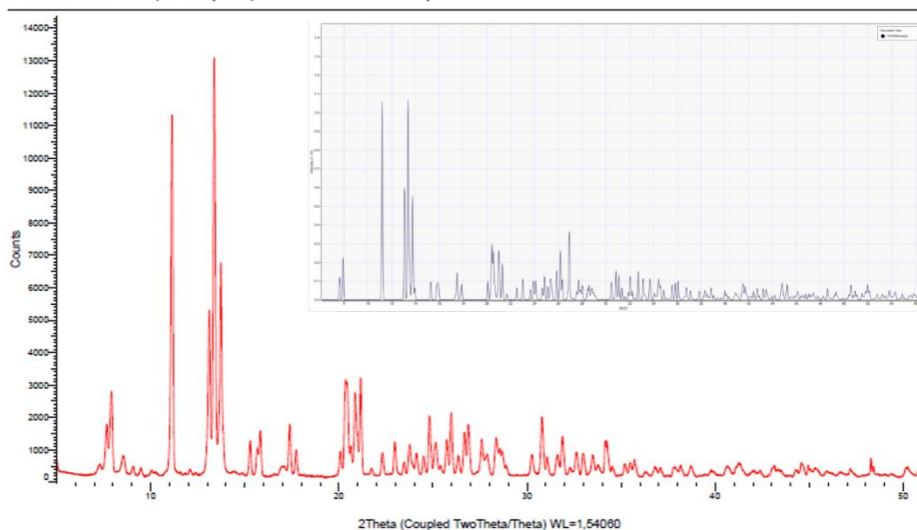
The figures hereunder show the experimental powder diffraction measurements (the inset corresponds to the simulated patterns).



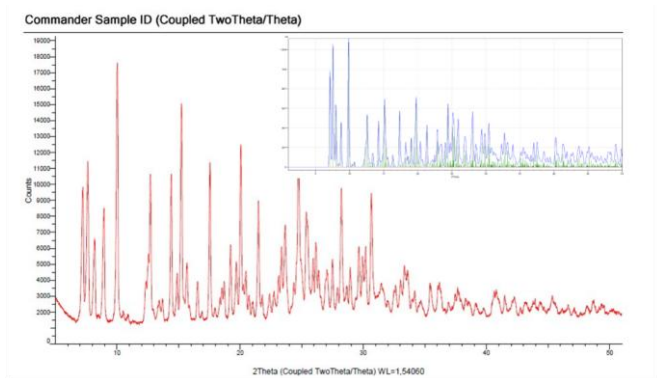
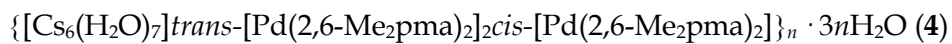
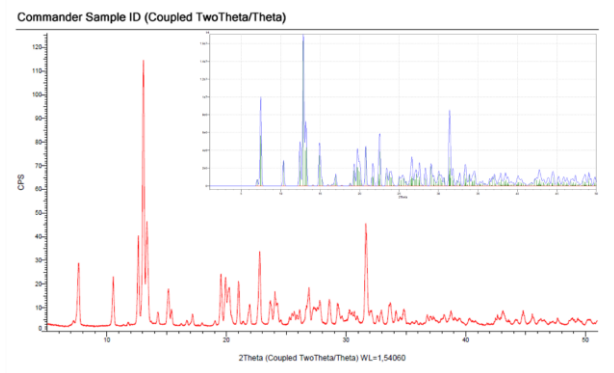
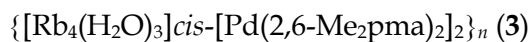
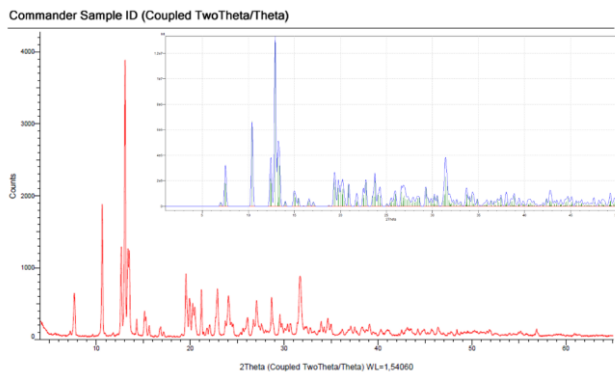
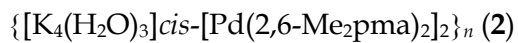
Commander Sample ID (Coupled TwoTheta/Theta)



Commander Sample ID (Coupled TwoTheta/Theta)



[†]Author note: compound 1' was first detected by powder diffraction.



A10. References.

- (1) Pardo, E.; Ruiz-García, R.; Cano, J.; Ottenwaelder, X.; Lescouëzec, R.; Journaux, Y.; Lloret, F.; Julve, M. *Dalt. Trans.***2008**, 2780–805.
- (2) SAINT Version 6.45; Bruker Analytical X-ray Systems: Madison, WI; 2003.
- (3) Sheldrick, G. M. SADABS Program for Absorption Correction, version 2.10; Analytical X-ray Systems: Madison, WI; 1998.
- (4) Sheldrick, G. M. *Acta Crystallogr. A.***2008**, 64, 112–22.
- (5) Müller, P. *Crystallogr. Rev.***2009**, 15, 57–83.

Appendix B

Supporting information for Chapter 2

B1.	Materials and characterization	257
B2.	Synthesis of the proligands	257
B3.	Characterization of the proligands	258
B4.	General procedures for carbon-carbon cross-coupling reactions	260
B5.	Crystal packing of 11	262
B6.	Supplementary results of Heck reactions	263
B7.	NMR characterization of the Heck and Suzuki crudes	268
B8.	References	277

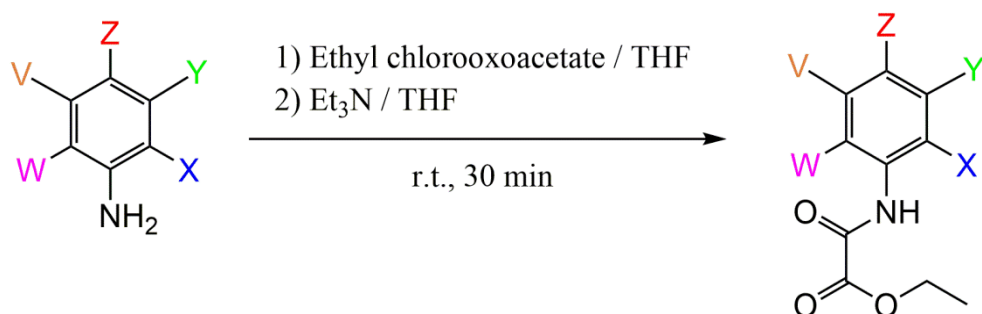
Appendix B - Study of the influence of the substituents and solvents on the catalytic properties of bis(oxamato)palladate(II) complexes

B1. Materials and characterization.

Aniline derivatives, $K_2[PdCl_4]$, $n\text{-Bu}_4\text{NOH}$, ethyl chlorooxalate and all the solvents for the syntheses were purchased from commercial sources and used without further purification. The general characterization is given in Appendix A, section A1.

B2. Synthesis of the proligands.

The synthesis of the proligands is described in Appendix A, section A2. Following the color code for the aniline derivatives which was given in Chapter 2 (Schemes 1 and 2), a concise synthetic pathway is shown in Scheme S1.



Scheme S1. Synthetic route for the proligands.

B3. Characterization of the proligands.

The characterization of EtH-2,6-Me₂pma, EtH-4-F-pma, EtH-4-Cl-pma and EtH-4-Br-pma is provided in Appendix A, section A3.

EtHpma. Yield: 80%. IR(KBr/cm⁻¹): 3352 (N-H), 3062, 2983, 2907 (C-H), 1727, 1706 (C=O). ¹H NMR (DMSO-d₆) δ (ppm): 1.42-1.46 (t, 3H, CH₃), 4.40-4.48 (q, 2H, CH₂), 7.19-7.26 (t, H, H_{aryl}), 7.30-7.38 (t, 2H, H_{aryl}), 7.64-7.75 (d, 2H, H_{aryl}), 8.96 (s, 1H, NH); ¹³C NMR (CDCl₃) δ (ppm): 14.4, 64.1, 120.2, 125.9, 129.6, 136.8, 154.3, 161.4. Anal. Calcd. for C₁₀H₁₂NO₃: C 61.85, H 6.23, N 7.21. Found C 62.39, H 6.43, N 7.27%.

EtH-2-Mepma. Yield: 95%. IR(KBr/cm⁻¹): 3216 (N-H), 3033, 2983, 2920 (C-H), 1735, 1699 (C=O). ¹H NMR (CDCl₃) δ (ppm): 1.35-1.42 (t, 3H, CH₃), 2.31 (s, 6H, CH₃), 4.39-4.48 (q, 2H, CH₂), 7.11-7.19 (m, 1H, H_{aryl}), 7.21-7.30 (m, 2H, H_{aryl}), 7.9-8.0 (d, 1H, H_{aryl}), 8.83 (s, 1H, NH); ¹³C NMR (CDCl₃) δ (ppm): 14.4, 17.7, 64.1, 122.3, 127.3, 128.8, 130.8, 134.8, 154.3, 161.6. Anal. Calcd. for C₁₁H₁₄NO₃: C 63.45, H 6.78, N 6.73. Found: C 62.98, H 7.02, N 6.78%.

EtH-4-Mepma. Yield: 95%. IR(KBr/cm⁻¹): 3338 (N-H), 3120, 2978, 2908 (C-H), 1732, 1705 (C=O). ¹H NMR (DMSO-d₆) δ (ppm): 1.28-1.33 (t, 3H, CH₃), 2.27 (s, 3H, CH₃), 4.28-4.31 (q, 2H, CH₂), 7.14-7.14 (d, 2H, H_{aryl}), 7.61-7.64 (d, 2H, H_{aryl}), 10.68 (s, 1H, NH); ¹³C NMR (DMSO-d₆) δ (ppm): 14.2, 20.9, 62.7, 120.7, 129.5, 134.2, 135.3, 155.7, 161.1. Anal. Calcd. for C₁₁H₁₄NO₃: C 63.45, H 6.78, N 6.73. Found: C 63.36, H 6.94, N 6.77%.

EtH-4-OMepma. Yield: 94%. IR(KBr/cm⁻¹): 3352 (N-H), 3117, 2977, 2901, 2848 (C-H), 1724, 1697 (C=O). ¹H NMR (CDCl₃) δ (ppm): 1.40 - 1.45 (t, 3H, CH₃), 3.81 (s, 3H, OCH₃), 4.37 - 4.45 (q, 2H, CH₂), 6.89 - 6.92 (m, 2H, H_{aryl}), 7.54 - 7.59 (m, 2H, H_{aryl}), 8.82 (s, 1H, NH); ¹³C NMR (CDCl₃) δ (ppm): 14.40, 55.88, 64.03, 114.75, 121.78, 129.94, 154.05, 157.57, 161.58. Anal. Calcd. for C₁₁H₁₃NO₄: C 59.19, H 5.87, N 6.27. Found: C 59.83, H 6.81, N 6.13%.

EtH-4-*i*-Prpma. Yield: 82%. IR(KBr/cm⁻¹): 3303 (N-H), 3050, 2960, 2870 (C-H), 1739, 1691 (C=O). ¹H NMR (CDCl₃) δ (ppm): 1.23 - 1.25 (d, 6H, CH₃), 1.41 - 1.45 (t, 3H, CH₃), 2.86 - 2.95 (m, 1H, CH), 4.38 - 4.45 (q, 2H, CH₂), 7.22 - 7.26 (m, 2H, H_{aryl}), 7.53 - 7.58 (m, 2H, H_{aryl}), 8.83 (s, 1H, NH); ¹³C NMR (CDCl₃) δ (ppm): 14.41, 24.34, 34.08, 64.08, 120.28, 127.54, 134.44, 146.74, 154.15, 161.54. Anal. Calcd. for C₁₃H₁₇NO₃: C 66.36, H 7.28, N 5.95. Found: C 66.43, H 7.73, N 5.87%.

EtH-2,3-Me₂pma. Yield: 92%. IR(KBr/cm⁻¹): (N-H), 3040, 2985, 2920 (C-H), 1736, 1681 (C=O). ¹H NMR (CDCl₃) δ (ppm): 1.42-1.47 (t, 3H, CH₃), 2.31 (s, 6H, CH₃), 4.42-4.45 (q, 2H, CH₂), 7.04-7.07 (m, 2H, H_{aryl}), 7.85-7.88 (d, 1H, H_{aryl}), 8.78 (s, 1H, NH); ¹³C NMR (CDCl₃) δ (ppm): 14.4, 17.8, 21.3, 64.1, 122.2, 127.9, 128.9, 131.7, 132.2, 136.1, 154.3, 161.6. Anal. Calcd. for C₁₂H₁₆NO₃: C 64.85, H 7.26, N 6.30. Found: C 65.28, H 7.12, N 6.32%.

EtH-2,4-Me₂pma. Yield: 92%. IR(KBr/cm⁻¹): 3220 (N-H), 3024, 2982, 2922 (C-H), 1735, 1685 (C=O). ¹H NMR (CDCl₃) δ (ppm): 1.41-1.50 (t, 3H, CH₃), 2.19-2.35 (d, 6H, CH₃), 4.35-4.48 (q, 2H, CH₂), 6.98-7.11 (t, 2H, H_{aryl}), 7.90-7.81 (d, 1H, H_{aryl}), 8.79 (s, 1H, NH); ¹³C NMR (CDCl₃) δ (ppm): 14.4, 17.8, 21.3, 64.0, 122.2, 127.9, 128.9, 131.7, 132.2, 136.1, 154.3, 161.6. Anal. Calcd. for C₁₂H₁₆NO₃: C 64.85, H 7.26, N 6.30. Found: C 64.95, H 7.19, N 6.37%.

EtH-2,5-Me₂pma. Yield: 91%. IR(KBr/cm⁻¹): 3391 (N-H), 3023, 2992, 2914 (C-H), 1738, 1680 (C=O). ¹H NMR (CDCl₃) δ (ppm): 1.37-1.43 (t, 3H, CH₃), 2.28 (s, 3H, CH₃), 2.32 (s, 3H, CH₃), 4.32-4.47 (q, 2H, CH₂), 6.89-6.95 (d, 1H, H_{aryl}), 7.02-7.11 (d, 1H, H_{aryl}), 7.82 (s, 1H, H_{aryl}), 8.82 (s, 1H, NH); ¹³C NMR (CDCl₃) δ (ppm): 14.4, 17.4, 21.5, 64.0, 122.7, 125.8, 127.0, 130.8, 134.5, 137.1, 154.3, 161.6. Anal. Calcd. for C₁₂H₁₆NO₃: C 64.85, H 7.26, N 6.30. Found: C 64.81, H 7.29, N 6.32%.

EtH-3,4-Me₂pma. Yield: 90%. IR(KBr/cm⁻¹): 3342 (N-H), 2985, 2940, 2901 (C-H), 1714, 1697 (C=O). ¹H NMR (CDCl₃) δ (ppm): 1.44-1.45 (t, 3H, CH₃), 2.20-2.30 (d, 6H, CH₃), 4.43-4.45 (q, 2H, CH₂), 7.11-7.12 (d, 1H, H_{aryl}), 7.4-7.5 (d, 2H, H_{aryl}), 8.80 (s, 1H, NH); ¹³C NMR (CDCl₃) δ (ppm): 14.4, 19.7, 20.3, 64.0, 117.7, 121.4, 130.5, 134.3, 134.4, 137.9, 154.1, 161.5. Anal. Calcd. for C₁₂H₁₆NO₃: C 64.85, H 7.26, N 6.30. Found: C 64.90, H 7.20, N 6.38%.

EtH-3,5-Me₂pma. Yield: 91%. IR(KBr/cm⁻¹): 3349 (N-H), 3100, 2998, 2920 (C-H), 1702, 1698 (C=O). ¹H NMR (CDCl₃) δ (ppm): 1.40-1.48 (t, 3H, CH₃), 2.30 (s, 6H, CH₃), 4.40-4.48 (q, 2H, CH₂), 6.8 (s, 1H, H_{aryl}), 7.2-7.3 (d, 2H, H_{aryl}), 8.85 (s, 1H, NH); ¹³C NMR (CDCl₃) δ (ppm): 14.4, 21.7, 64.1, 118., 127.7, 127.7, 136.6, 139.4, 154.2, 161.5. Anal. Calcd. for C₁₂H₁₆NO₃: C 64.85, H 7.26, N 6.30. Found: C 64.98, H 7.22, N 6.29%.

EtH-2,4,6-Me₃pma. Yield: 96%. IR(KBr/cm⁻¹): 3257 (N-H), 3019, 2977, 2919 (C-H), 1727, 1679 (C=O). ¹H NMR (CDCl₃) δ (ppm): 1.42-1.49 (t, 3H, CH₃), 2.19 (s, 6H, CH₃), 2.29 (s, 3H, CH₃), 4.41-4.48 (q, 2H, CH₂), 6.91 (s, 2H, H_{aryl}), 8.41 (s, 1H, NH); ¹³C NMR (CDCl₃) δ (ppm): 14.4, 18.7, 21.3, 64., 129.5, 129.9, 135.1, 138.1, 155.2, 161.4. Anal. Calcd. for C₁₃H₁₈NO₃: C 66.08, H 7.68, N 5.93. Found: C 65.36, H 7.76, N 5.97%.

EtH-2,4,6-Ph₃pma. Yield: 74%. IR(KBr/cm⁻¹): 3246 (N-H), 3056, 3031, 2887 (C-H), 1753, 1735, 1694 (C=O). ¹H NMR (DMSO-d₆) δ (ppm): 1.19-1.23 (t, 3H, CH₃), 4.16-4.18 (q, 2H, CH₂), 7.42-7.53 (m, 7H, H_{aryl}), 7.55-7.60 (m, 5H, H_{aryl}), 7.69 (s, 2H, H_{aromatic}), 7.86-7.88 (q, 2H, H_{aromatic}), 10.54 (s, 1H, NH); ¹³C NMR (CDCl₃) δ (ppm): 14.10, 62.40, 127.45, 127.79, 128.27, 129.18, 129.36, 130.47, 139.28, 139.60, 140.58, 141.84, 156.62, 160.47. Anal. Calcd. for C₂₈H₂₃NO₃: C 79.79, H 5.50, N 3.32. Found: C 80.01, H 6.23, N 3.47%.

B4. General procedures for carbon-carbon cross coupling reactions.

Heck cross coupling reaction (*Homogeneous catalysis/DMF*). A one neck round flask was charged with the pre-catalyst 5 mol% (0.05 mmol), an appropriate amount of aryl iodide (0.5 mmol), olefin (0.075 mmol), Et₃N (1 mmol), and DMF (4 mL) and a magnetic stir bar. The mixture was heated to 80 °C with stirring during different times. The reaction was monitored using thin liquid chromatography on silica gel. The reaction mixture was cooled, diluted with water (5 mL) and extracted (3 mL) with *n*-pentane. The *n*-pentane was kept for further characterizations.

Suzuki cross-coupling reaction (*Homogeneous catalysis/DMF*): Details in Appendix A, section A5.

Heck cross-coupling reaction (*ionic liquid medium*) A test-tube with screw cap and valve was charged with a magnetic stir bar, the precatalyst 0.5 mol%, aryl halide (0.50 mmol), Et₃N (1.00 mmol) and the olefin (0.75 mmol), prepared in 3–4 g of *n*-Bu₄NBr as ionic liquid. The mixture was heated with stirring during different times at 120 °C. The reaction was monitored using thin liquid chromatography on silica gel. The reaction mixture was cooled and extracted with 5 mL of *n*-pentane. After the extraction, the test-tube was charged again with the corresponding aryl halide (0.50 mmol), Et₃N (1.00 mmol) and the corresponding olefin (0.75 mmol) to start another run (a total of 3 – 8 runs).

Suzuki cross-coupling reaction (*ionic liquid medium*) A test-tube with screw cap and valve was charged with a magnetic stir bar, the precatalyst 0.5 mol%, aryl halide (0.50 mmol), Et₃N (1.00 mmol) and the phenylboronic acid (0.75 mmol), prepared in 3–4 g of *n*-Bu₄NBr as ionic liquid. The mixture was heated with stirring during different times at 120 °C. The reaction was monitored using thin liquid chromatography on silica gel. The reaction mixture was cooled and extracted with 5 mL of *n*-pentane. After the extraction, the test-tube was charged again with the corresponding aryl halide (0.50 mmol), Et₃N (1.00 mmol) and the phenylboronic acid (0.75 mmol) to start another run (a total of 3–8 runs).

For all procedures: the yields of the reactions were determined by GC-MS analysis using perfluorotributylamine (PFTBA) as internal standard and the crude was characterized by ¹H, ¹³C and DEPT NMR.

B5. Crystal packing of 11

For the sake of brevity, a unique supplementary illustration of the crystal packing is given for this family of bis(oxamato)palladate(II) complexes.

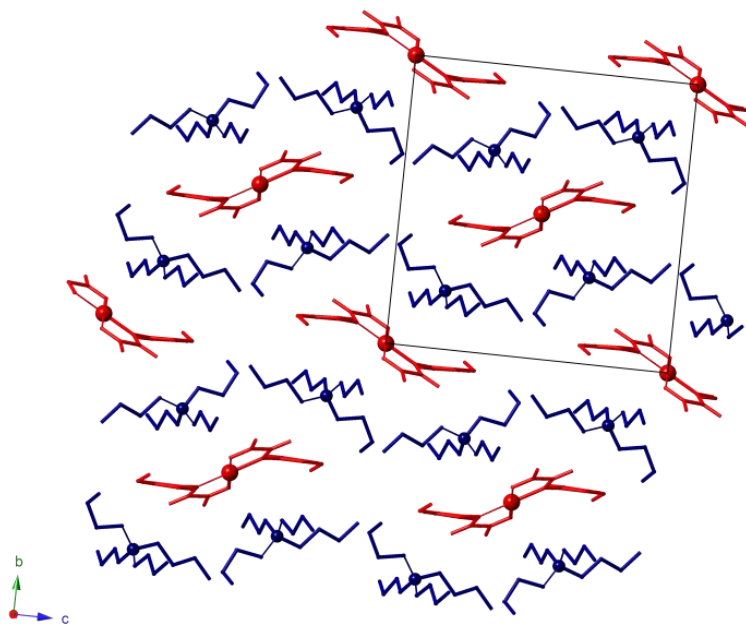
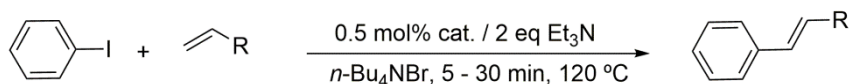


Figure S1. Crystal packing of **11a** showing the relative positions of the anionic complexes (red) and tetra-*n*-butylammonium cations (blue). The solvent molecules have been omitted for clarity).

B6. Supplementary results of Heck reactions

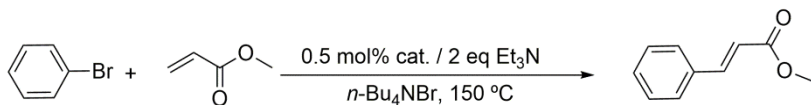
Table S1. Heck reaction of iodobenzene and olefins after different runs.



Entry ^a	Olefine	Catalyst	Time (min)	Runs - Yield ^b (%)							
				1	2	3	4	5	6	7	8
1		5a	5	99	99	99	99	99	99	99	99
2		6a	5	99	99	99	99	99	99	99	99
3		7a	5	99	99	99	99	99	99	99	-
4		11a	5	98	99	99	99	99	99	98	92
5		12a	5	92	99	99	99	99	98	98	96
6		5a	30	99	97	99	99	99	99	99	99
7		6a	30	70	95	96	99	99	98	98	98
8		7a	30	99	99	99	98	90	90	97	95
9		11a	30	86	99	99	99	98	98	99	99
10		12a	30	88	77	99	99	99	99	99	96

^a Reaction conditions: 0.5 mmol bromobenzene, 0.75 mmol ethyl acrylate, 0.5 mmol% cat., 1 mmol of Et₃N, 5-30 min, 120 °C in *n*-Bu₄NBr. ^bDetermined by GC-MS analysis using perfluorotributylamine (PFTBA) as internal standard.

Table S2. Example test of finding best reaction time conditions for heck reaction of bromobenzene and ethyl acrylate in *n*-Bu₄NBr at 150°C.

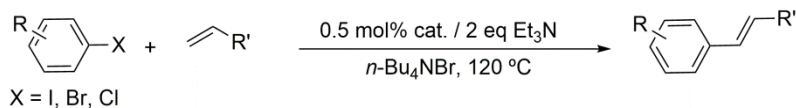


Entry ^a	Catalyst	Time (min)	Yield (%)	TON	TOF (h ⁻¹)
1	6a	10	75	150	900
2	11a	10	87	174	1044
3	6a	15	91	182	728
4	11a	15	92	184	736
5	6a	30	94	188	376
6	11a	30	93	186	372
7	6a	60	92	184	184
8	11a	60	91	182	182
9	6a	120	81	162	81
10	11a	120	88	164	82

^a Reaction conditions: 0.5 mmol bromobenzene, 0.75 mmol ethyl acrylate, 0.5 mmol% cat., 1 mmol of Et₃N, different times (min), 150 °C in *n*-Bu₄NBr. ^bDetermined by GC-MS analysis using perfluorotributylamine (PFTBA) as internal standard.

Appendix B - Study of the influence of the substituents and solvents on the catalytic properties of bis(oxamato)palladate(II) complexes

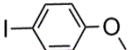
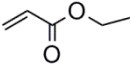
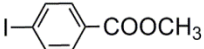
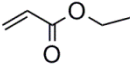
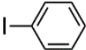
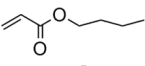
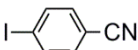
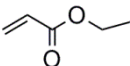
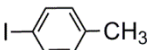
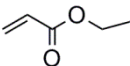
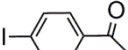
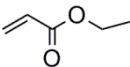
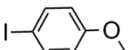
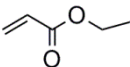
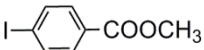
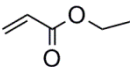
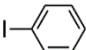
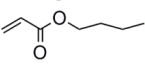
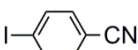
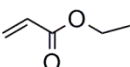
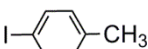
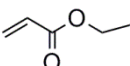
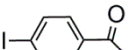
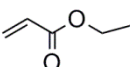
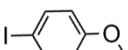
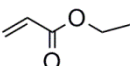
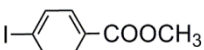
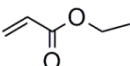

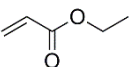
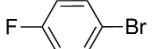
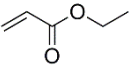
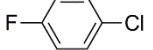
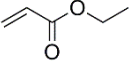

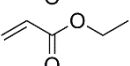

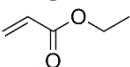
Table S3. Heck reaction of aryl halides and olefins in *n*-Bu₄NBr.



Entry ^a	Catalyst	Aryl iodide	Olefin	Time (min)	Runs - Yield ^b (%)		
					1	2	3
1	5a			5	0	14	65
2	5a			5	71	86	89
3	5a			5	0	70	90
4	5a			5	0	81	93
5	5a			5	0	92	93
6	5a			15	89	85	85
7	6a			5	19	86	88
8	6a			5	99	53	87
9	6a			5	41	47	85
10	6a			5	47	89	93
11	6a			5	17	43	92
10	6a			15	99	-	98
13	7a			5	26	90	97
14	7a			5	99	99	-
15	7a			5	96	2	58
16	7a			5	53	96	98

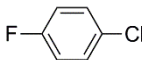
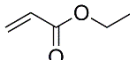
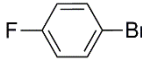
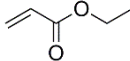
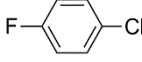
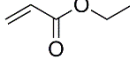
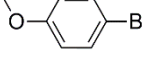
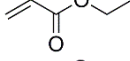
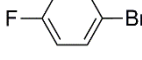
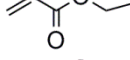
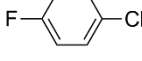
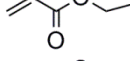
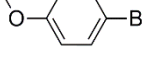
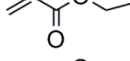
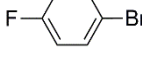
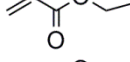
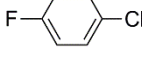
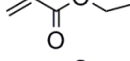
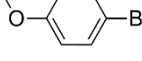
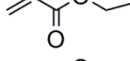
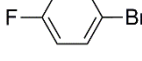
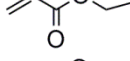
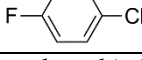
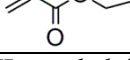
Appendix B - Study of the influence of the substituents and solvents on the catalytic properties of bis(oxamato)palladate(II) complexes

Table S3 contn

7	7a			5	37	93	99
18	7a			15	83	95	94
19	11a			5	47	75	90
20	11a			5	51	87	83
21	11a			5	74	99	94
22	11a			5	99	96	89
23	11a			5	41	94	99
24	11a			15	99	99	99
25	12a			5	80	87	92
26	12a			5	-	86	88
27	12a			5	37	90	99
28	12a			5	75	93	99
29	12a			5	69	99	99
30	12a			15 h	99	99	99
31	5a			1.5 h	99	*c	*c
32	5a			4 h	92	*c	*c
33	5a			72 h	*c	*c	*c
34	6a			1.5 h	99	*c	*c
35	6a			4 h	94	*c	*c

Appendix B - Study of the influence of the substituents and solvents on the catalytic properties of bis(oxamato)palladate(II) complexes

Table S3 contn

36	6a			72 h	13	* _c	* _c
35	6a			4 h	94	* _c	* _c
36	6a			72 h	13	* _c	* _c
37	7a			1.5 h	99	* _c	* _c
38	7a			4 h	93	* _c	* _c
39	7a			72 h	* _c	* _c	* _c
40	11a			1.5 h	99	* _c	* _c
41	11a			4 h	91	* _c	* _c
42	11a			72 h	* _c	* _c	* _c
43	12a			1.5 h	99	* _c	* _c
44	12a			4 h	94	* _c	* _c
45	12a			72 h	* _c	* _c	* _c

^a Reaction conditions: 0.5 mmol aryl iodide, 0.75 mmol olefins, 0.5 mmol% cat., 1 mmol Et₃N, 120 °C in *n*-Bu₄NBr. ^b Determined by GC-MS analysis using perfluorotributylamine (PFTBA) as internal standard. ^c Not tested.

Appendix B – Study of the influence of the substituents and solvents on the catalytic properties of bis(oxamato)palladate(II) complexes

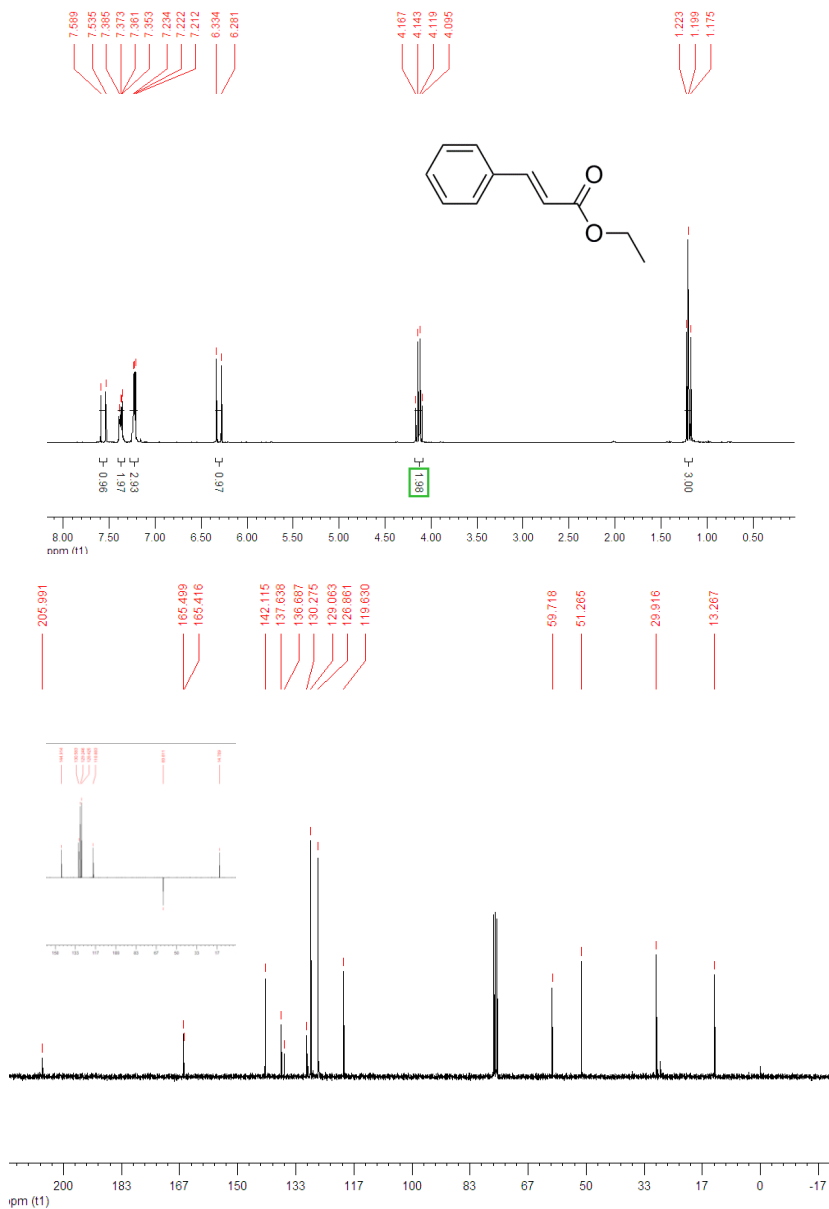


Figure S3: ¹H-NMR, ¹³C-NMR and Dept-135-NMR spectra of ethyl (2E)-2-phenylprop-2-enoate.

Appendix B – Study of the influence of the substituents and solvents on the catalytic properties of bis(oxamato)palladate(II) complexes

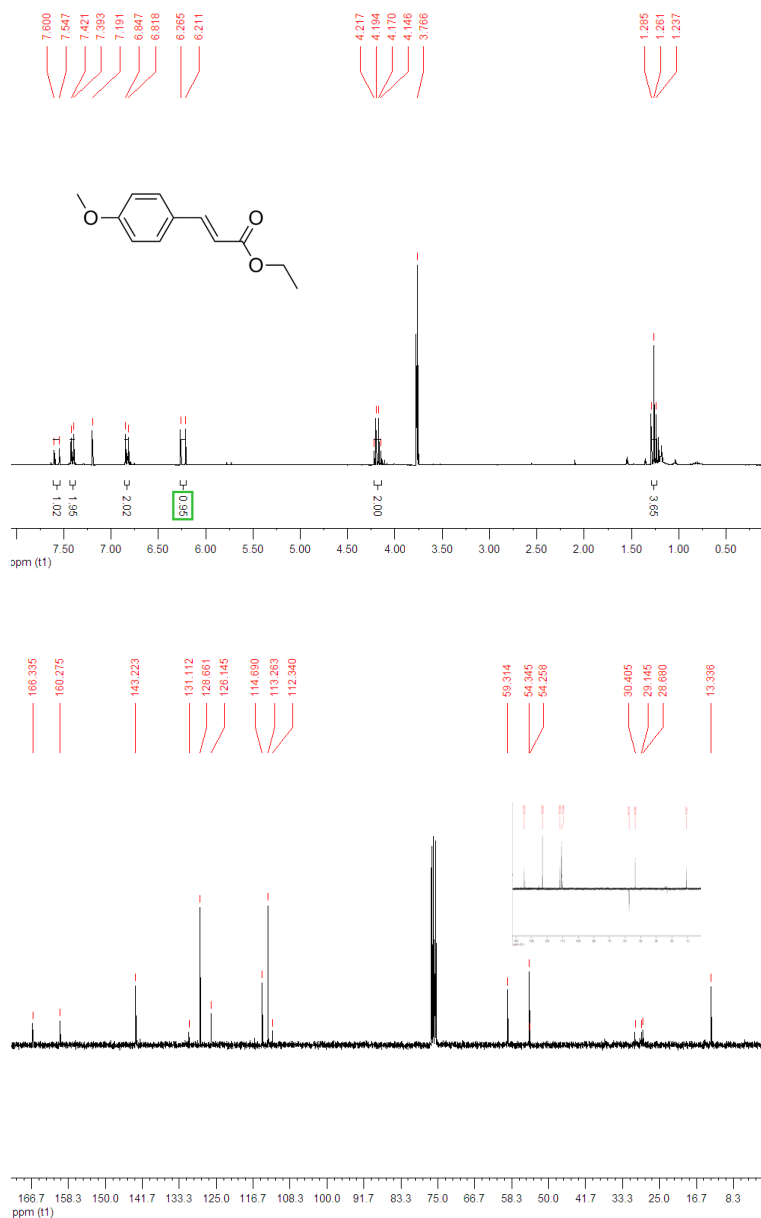


Figure S4: ¹H-NMR, ¹³C-NMR and Dept-135-NMR spectra of ethyl (2E)-3-(4-methoxyphenyl)prop-2-enoate.

Appendix B – Study of the influence of the substituents and solvents on the catalytic properties of bis(oxamato)palladate(II) complexes

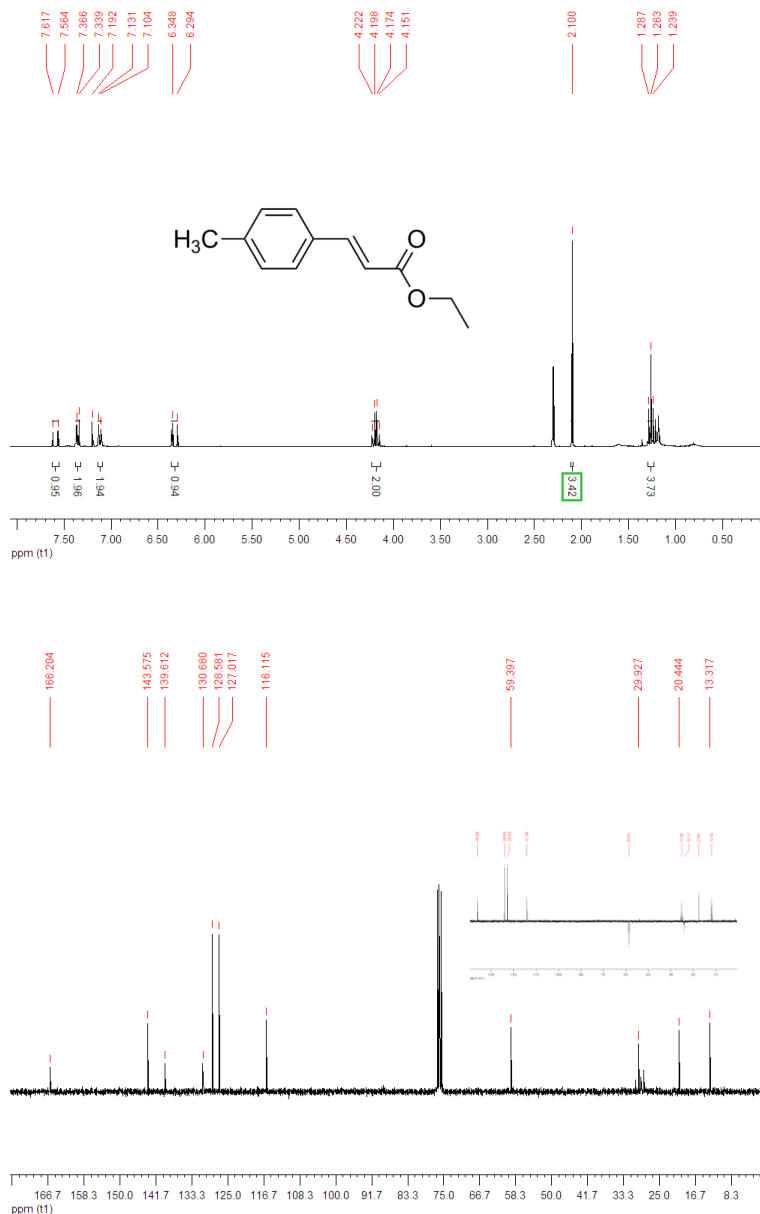


Figure S5: ¹H-NMR, ¹³C-NMR and Dept-135-NMR spectra of ethyl (2E)-3-(4-methylphenyl)prop-2-enoate.

Appendix B - Study of the influence of the substituents and solvents on the catalytic properties of bis(oxamato)palladate(II) complexes

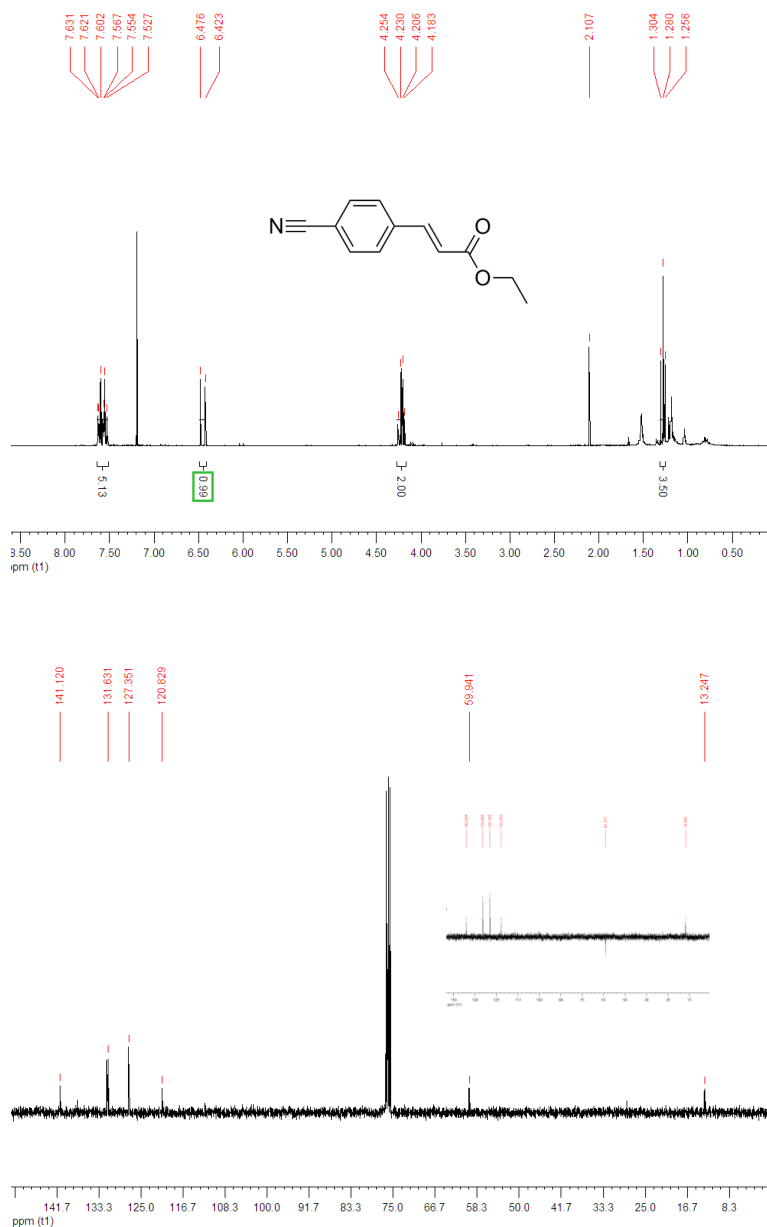


Figure S7: ¹H-NMR; ¹³C-NMR and Dept-135-NMR spectra of ethyl (2E)-3-(4-cyanophenyl)prop-2-enoate.

Appendix B – Study of the influence of the substituents and solvents on the catalytic properties of bis(oxamato)palladate(II) complexes

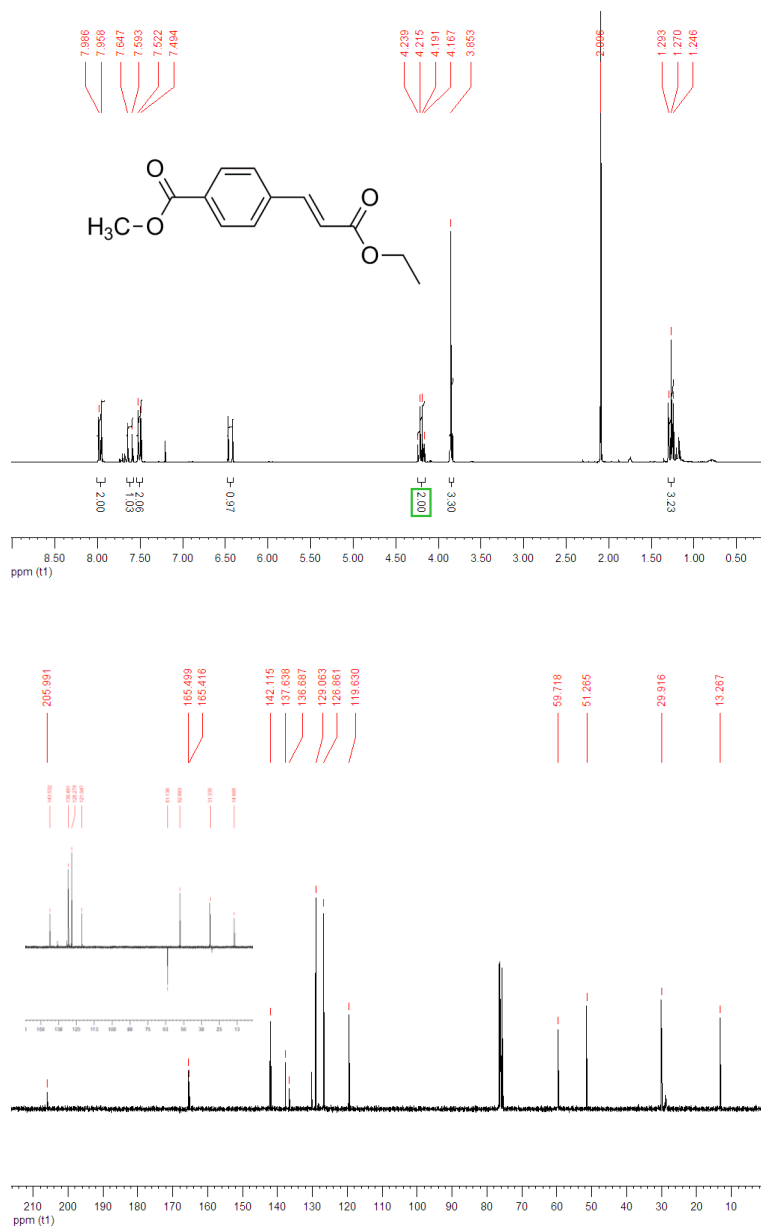


Figure S8: ¹H-NMR, ¹³C-NMR and DEPT-135-NMR spectra of methyl 4-[(1E)-3-ethoxy-3-oxoprop-1-en-1-yl]benzoate.

Appendix B – Study of the influence of the substituents and solvents on the catalytic properties of bis(oxamato)palladate(II) complexes

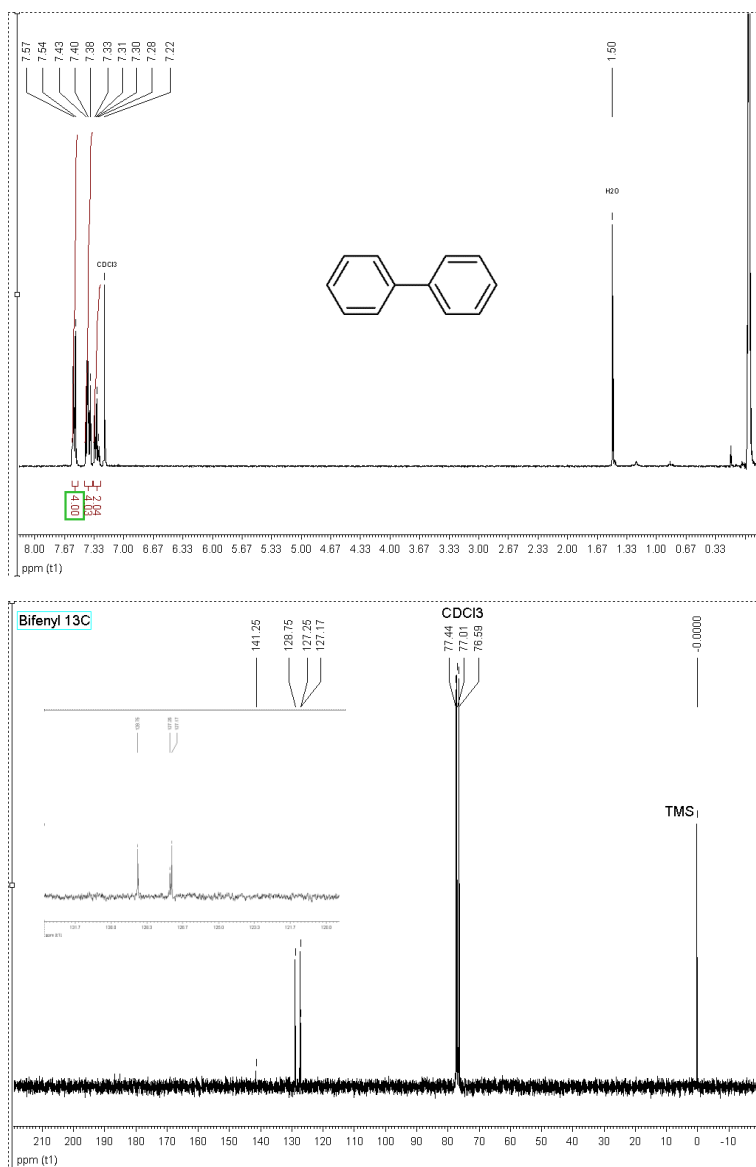


Figure S9: $^1\text{H-NMR}$, $^{13}\text{C-NMR}$ and Dept-135-NMR spectra of biphenyl

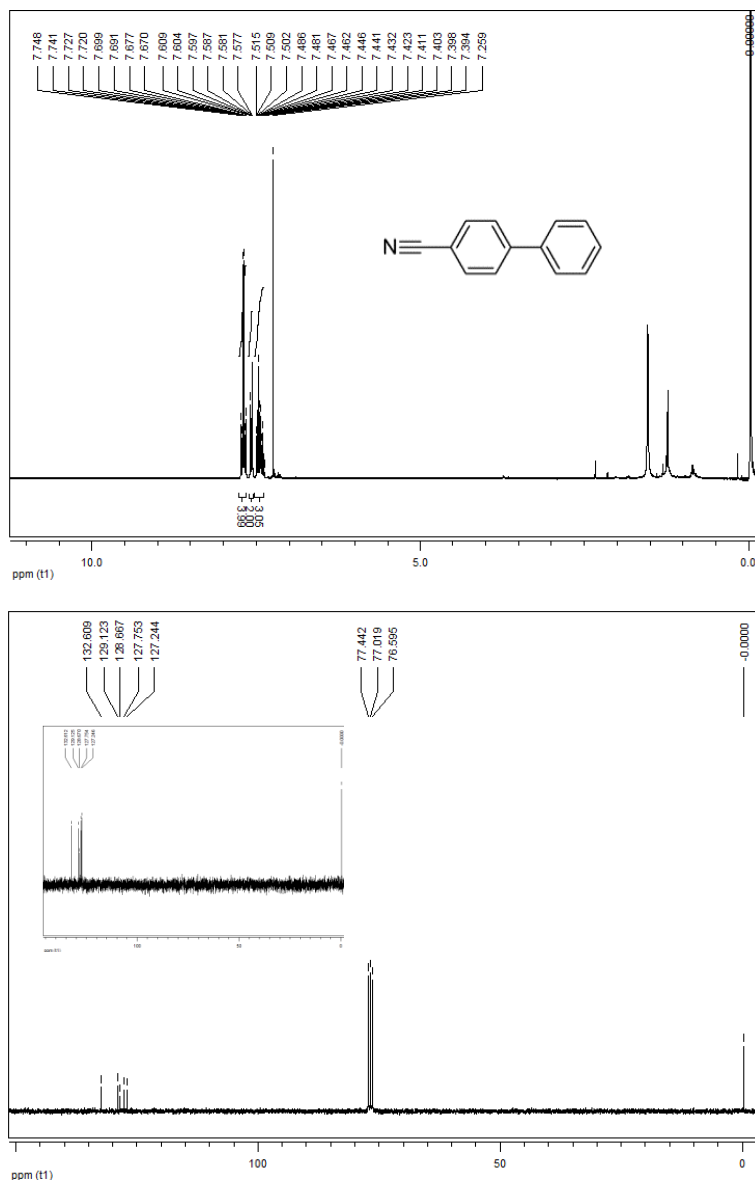


Figure S10: ¹H-NMR, ¹³C-NMR and Dept-135-NMR spectra of biphenyl-4-carbonitrile

B8. References

- (1) Pardo, E.; Ruiz-García, R.; Cano, J.; Ottenwaelder, X.; Lescouëzec, R.; Journaux, Y.; Lloret, F.; Julve, M. *Dalt. Trans.***2008**, 2780–805.
- (2) SAINT Version 6.45; Bruker Analytical X-ray Systems: Madison, WI; 2003.
- (3) Sheldrick, G. M. SADABS Program for Absorption Correction, version 2.10; Analytical X-ray Systems: Madison, WI; 1998.
- (4) Sheldrick, G. M. *Acta Crystallogr. A.***2008**, 64, 112–22.
- (5) Müller, P. *Crystallogr. Rev.***2009**, 15, 57–83.

Appendix B - Study of the influence of the substituents and solvents on the catalytic properties of bis(oxamato)palladate(II) complexes

Appendix C

Supporting information for Chapter 3

C1.	Materials and characterization	281
C2.	Synthesis of the proligands	281
C3.	Characterization of the proligands	281
C4.	Procedure for the Suzuki cross-coupling reaction	281
C5.	FT-IR spectra of the complex 21 (<i>Part I</i>)	282
C6.	FT-IR spectra of the complexes 19 and 22- 24 (<i>Part II</i>)	283
C7.	Crystallographic tables for complex 23	285
C8.	Crystal packing of 19 and 22	286
C9.	Perspective drawings of the centro- and non-centrosymmetric bis(oxamate)palladate(II) units and different views of the crystal packing of 23	287

C1. Materials and characterization.

Aniline derivatives, $K_2[PdCl_4]$, KOH, *n*-Bu₄NOH, ethyl chlorooxalate and all the solvents for the syntheses were purchased from commercial sources and used without further purification. The general characterization is given in Appendix A, section A1.

C2. Synthesis of the proligands.

The synthesis of the proligands is described in Appendix A, section A2.

C3. Characterization of the proligands.

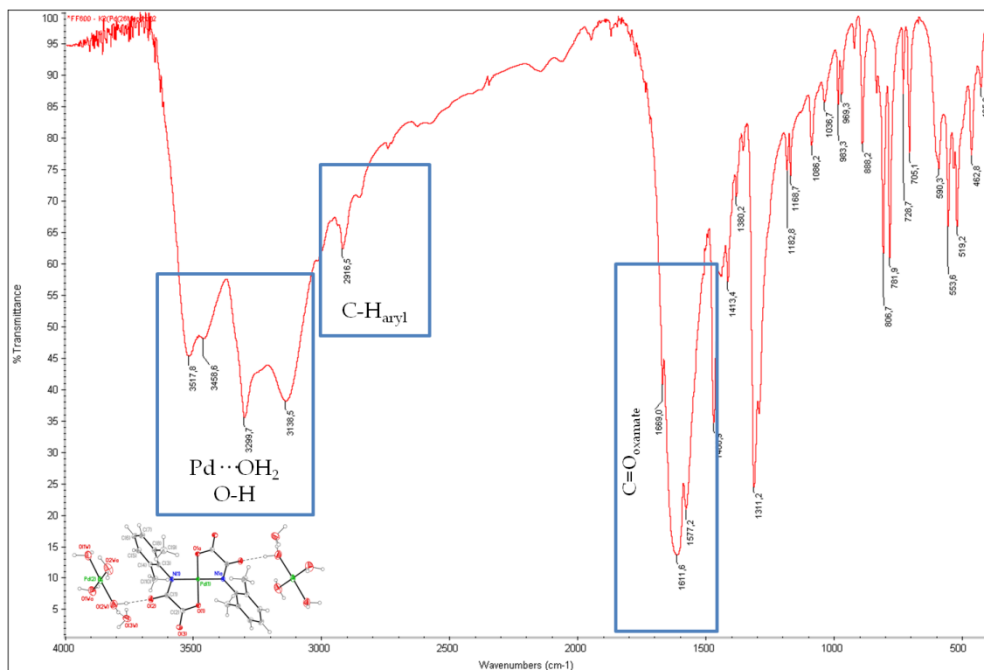
The characterization of EtH-2,6-Me₂pma, EtH-2,4,6-Me₃pma, EtH-4-F-pma, EtH-4-Cl-pma and EtH-4-Br-pma is detailed in Appendix A, section A3.

C4. Procedure for the Suzuki cross-coupling reaction.

Suzuki cross-coupling reaction (*Homogeneous catalysis/DMF*): Described in Appendix A, section A5. Note: The yields of the reactions were determined by GC-MS analysis using perfluorotributylamine (PFTBA) as internal standard and the crude was characterized by ¹H, ¹³C and DEPT NMR.

C5. FT-IR spectra of the complex **21** (Part I).

Illustration of the aquapalladate(II) and bis(oxamato)palladate complex (**21**) is provided in order to show the most characteristic FT-IR peaks of these complexes.

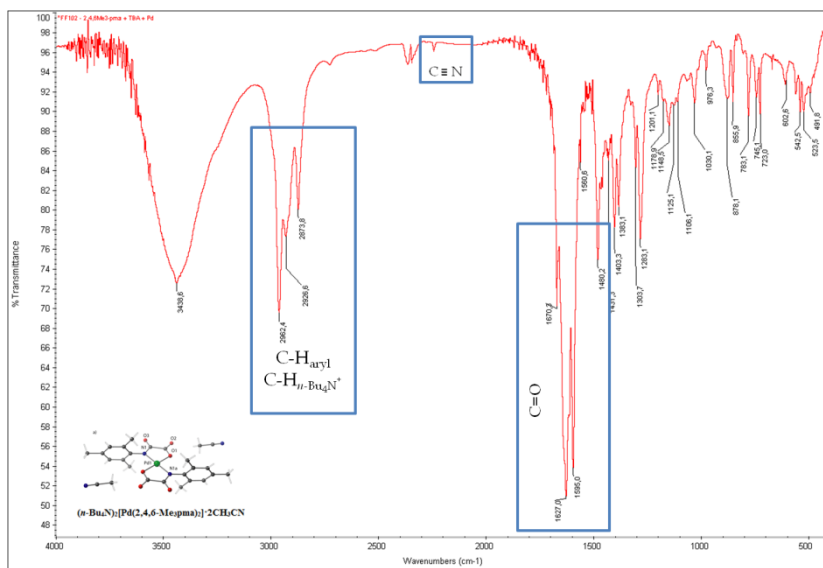


A general FT-IR spectra of bis(oxamato)palladate complexes with *n*-Bu₄N⁺ as counter cation is given in Appendix A, section A8.

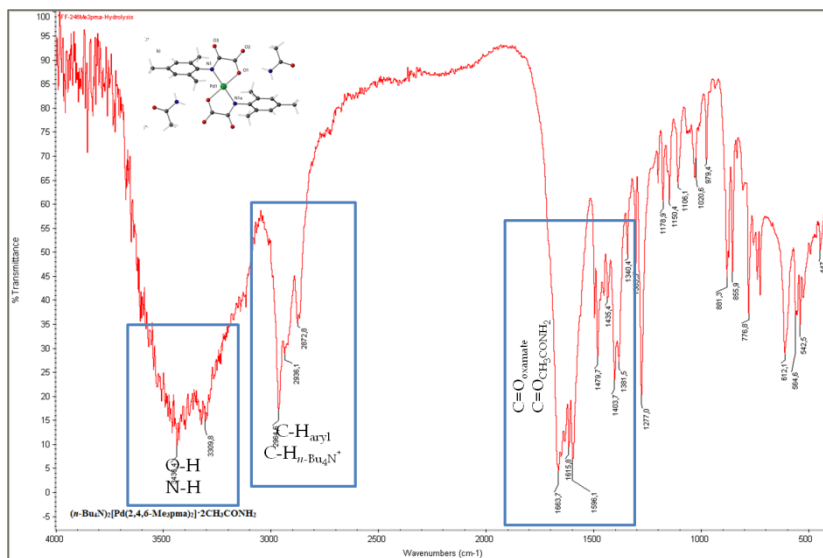
C6. FT-IR spectra of the complexes **19** and **22-24** (Part II).

Illustrations of bis(oxamato)palladate complexes (**19** and **22-24**) are provided in order to show the most characteristic FT-IR peaks of these complexes.

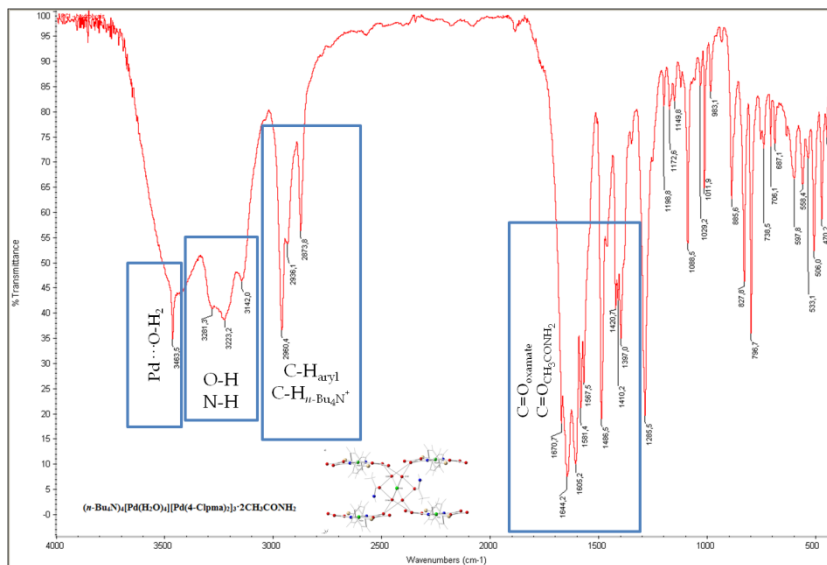
$[(n\text{-Bu}_4\text{N})_2[\text{Pd}(2,4,6\text{-Me}_3\text{pma})_2] \cdot 2\text{CH}_3\text{CN}$ (**19**)



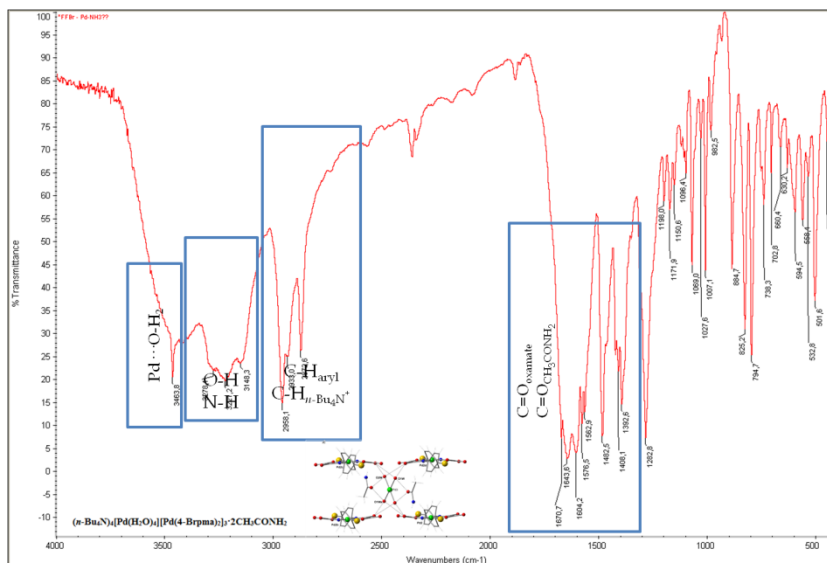
$(n\text{-Bu}_4\text{N})_2[\text{Pd}(2,4,6\text{-Me}_3\text{pma})_2] \cdot 2\text{CH}_3\text{CONH}_2$ (**22**)



$(n\text{-Bu}_4\text{N})_4[\text{Pd}(\text{H}_2\text{O})_4][\text{Pd}(4\text{-Clpma})_2]_3 \cdot 2\text{CH}_3\text{CONH}_2$ (**23**)



$(n\text{-Bu}_4\text{N})_4[\text{Pd}(\text{H}_2\text{O})_4][\text{Pd}(4\text{-Brpma})_2]_3 \cdot 2\text{CH}_3\text{CONH}_2$ (**24**)



C7. Crystallographic tables for complex 23.**Table S1.** Selected bond lengths (Å) and angles (deg) for **23***

Pd(1)-O(7)	2.007(3)	Pd(2)-O(1)	2.010(3)
Pd(1)-N(3)	2.026(4)	Pd(2)-N(1)	2.013(4)
Pd(2)-O(4)	2.003(3)	Pd(3)-O(1W)	2.082(4)
Pd(2)-N(2)	2.009(4)	Pd(3)-O(2W)	2.087(4)
O(7a)-Pd(1)-O(7)	180.0	N(2)-Pd(2)-N(1)	177.06(16)
O(7)-Pd(1)-N(3)	81.36(16)	O(1)-Pd(2)-N(1)	82.29(14)
O(7)-Pd(1)-N(3a)	98.64(16)	O(1W)-Pd(3)-O(1Wb)	180.0(2)
N(3)-Pd(1)-N(3a)	180.0	O(1W)-Pd(3)-O(2Wb)	93.22(17)
O(4)-Pd(2)-N(2)	81.70(15)	O(1Wb)-Pd(3)-O(2Wb)	86.78(17)
O(4)-Pd(2)-O(1)	178.33(14)	O(1Wb)-Pd(3)-O(2W)	93.22(17)
N(2)-Pd(2)-O(1)	97.86(15)	O(2Wb)-Pd(3)-O(2W)	180.0
O(4)-Pd(2)-N(1)	98.07(15)		

*Symmetry transformations used to generate equivalent atoms:

(a) = -x, -y+1, -z+3; (b) = -x, -y+2, -z+2.

Table S2. Hydrogen bonds lengths (Å) for **23***

O(1W)··O(3)	2.899(4)	O(2W)··O(3)	3.083(4)
O(1W)··O(5b)	3.103(4)	O(2W)··O(6a)	2.888(4)
O(1W)··O(6b)	3.060(4)	O(2W)··O(1Ha)	2.972(4)
O(1W)··O(1H)	3.000(4)	N(1H)··O(8)	2.919(7)
O(2W)··O(2)	3.258(4)	N(1H)··O(9)	3.117(7)

*Symmetry transformations used to generate equivalent atoms:

(a) = -x, -y+1, -z+3; (b) = -x, -y+2, -z+2.

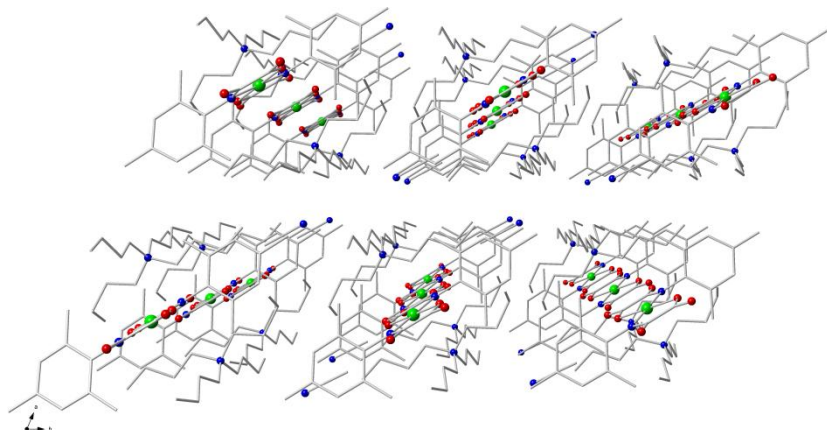
C8. Crystal packing for complexes 19 and 22.

Figure S1. Crystal packing of **19** showing the relative positions of the anionic entities, the organic cations and the acetonitrile molecules of crystallization. The hydrogen atoms have been omitted for clarity.

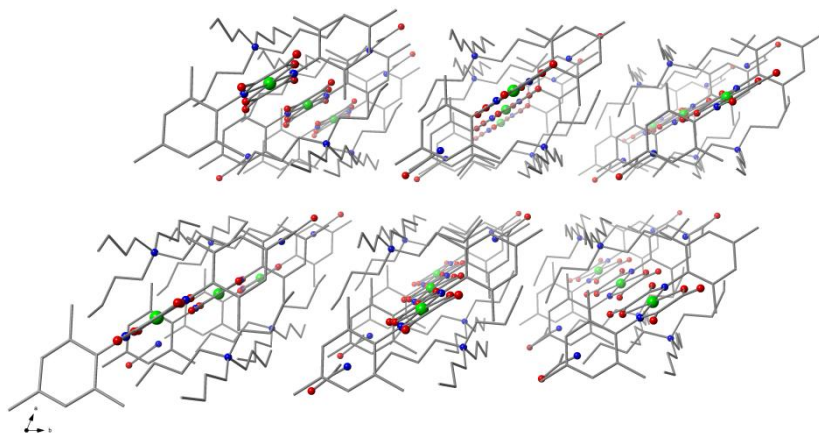


Figure S2. Crystal packing of **2** showing the relative arrangements of the anionic entities, organic cations and acetamide molecules of crystallization. The hydrogen atoms have been omitted for clarity.

C9. Perspective drawings of the centro- and non-centrosymmetric bis(oxamate)palladate(II) units and different views of the crystal packing of **23.**

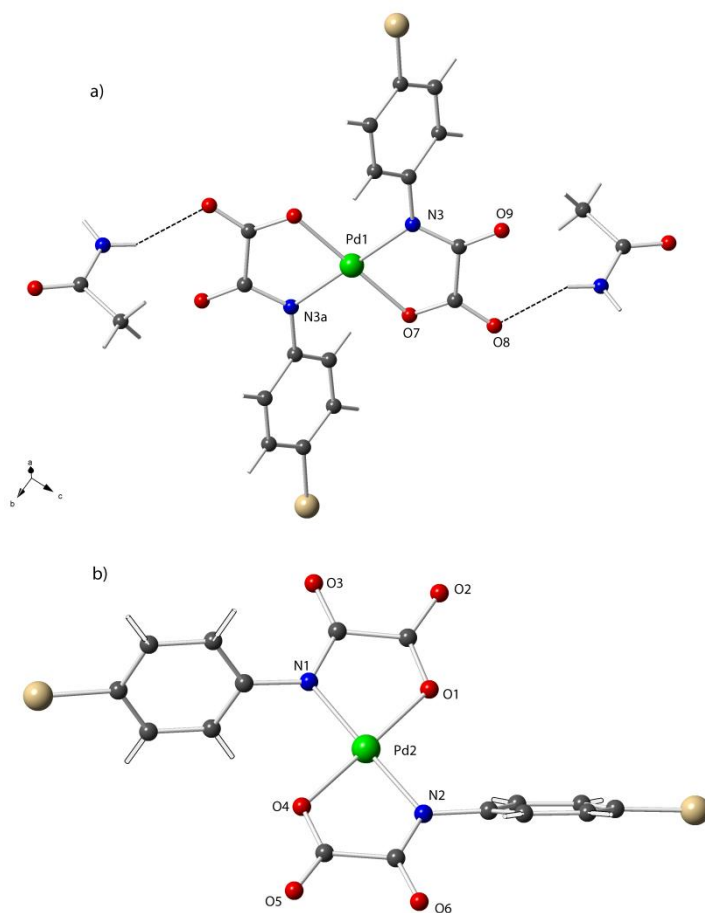


Figure S3. Perspective views of the (a) centro- [Pd(1)] and (b) non-centrosymmetric [Pd(2)] oxamate units of **23** [Symmetry code: (a) = $-x, -y+1, -z+3$].

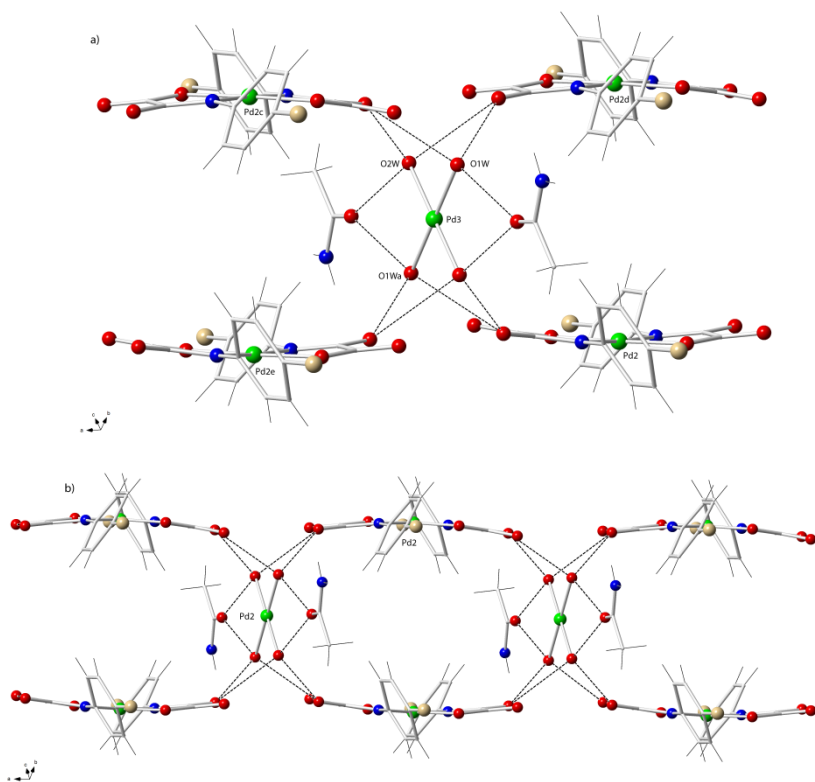


Figure S4. (a) Perspective view of the $[\text{Pd}(\text{H}_2\text{O})_4]^{2+}$ unit linked by hydrogen bonds to the acetamide molecules and $[\text{Pd}(\text{oxamato})_2]^{2-}$ species in **23**. The organic counter cations have been omitted for clarity. The values of the Pd(3)⋯Pd(2) and Pd(3)⋯Pd(2e) distances are 6.920(1) and 6.927(1) Å, respectively. (b) View of the supramolecular chains in **23** generated by hydrogen bonds (broken lines) involving the $[\text{Pd}(\text{H}_2\text{O})_4]^{2+}$ cations, acetamide molecules and distorted bis(oxamato)palladate(II) units [Symmetry code: (c) = $x, 1+y, 1+z$; (d) = $1-x, y, z$].

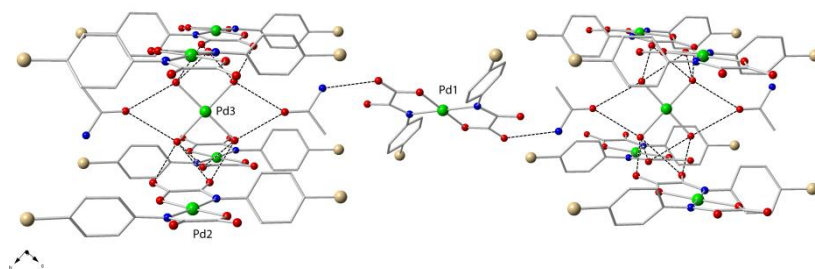


Figure S5. Perspective view of adjacent supramolecular chains in **23** connected by acetamide H-bonds involving bis(oxamato)palladate(II) units. The organic counter cations and hydrogen atoms have been omitted for clarity. The Pd(3)···Pd(1) distance is equal to 12.161(1) Å.

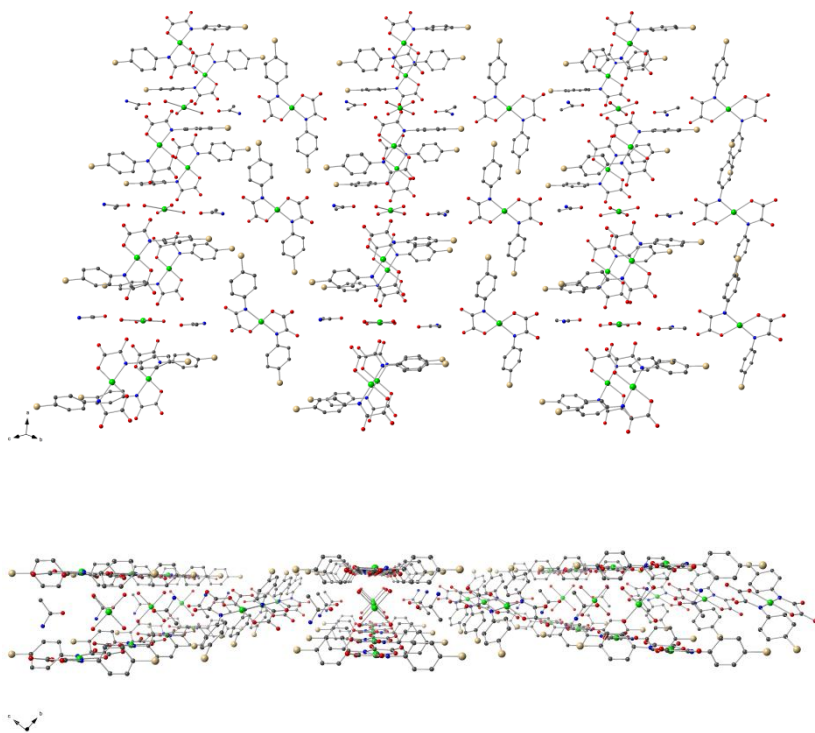


Figure S6. (Top) Perspective view of the packing in **23**. (Bottom) View along the crystallographic *a* axis of **23** showing the layers developing in the (1 -1 1) plane, which are built by centrosymmetric bis(oxamato)palladate(II) anions as spacers for different chains (Figure S5) connected to acetamide molecules [Pd(3)···Pd(1) 12.161(1) Å].

Appendix D

Supporting information for Chapter 4

D1.	Materials and characterization	293
D2.	Synthesis of the proligands	293
D3.	Characterization of the proligands	294
D4.	General procedures for carbon-carbon cross coupling reactions	295
D5.	General procedure for photochemical studies	295
D6.	Cells and Culture	295
D7.	Drug sensitive assay	295
D8.	Supplementary results of the carbon-carbon cross coupling reactions	296
D9.	Histograms of recovery and recyclability for the complexes 26-28	297
D10.	Study of the reaction time in 26 and 27 for the Suzuki cross-coupling reaction	299
D11.	References	299

Appendix D - Dinuclear palladium(II) oxamate metallacyclophanes

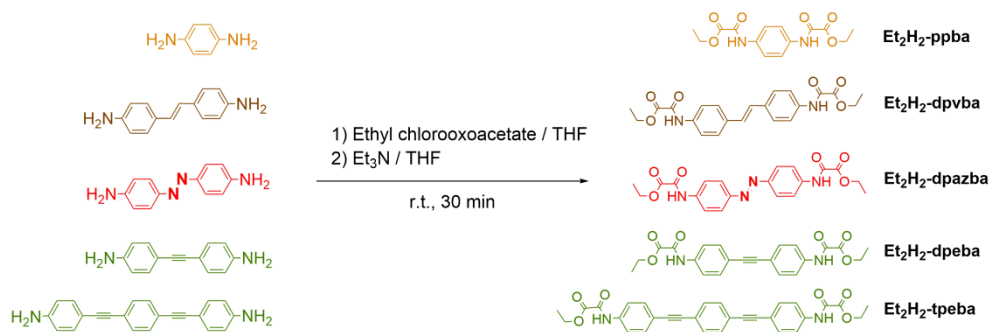
D1. Materials and characterization

All chemicals were purchased from commercial sources as reagents pure for analysis and they were used as received. The amines 1,4-phenylenediamine, 4-4'-diaminostilbene dihydrochloride were purchased and used as received. Otherwise, the amine precursor 4-4'-diaminobenzene was prepared by $\text{NaBO}_3/\text{H}_3\text{BO}_3$, through diazo coupling reaction of *para*-aminoacetanilide as reported in the literature.¹ As 4-4'-diphenylethyndiamine and 4-4'-triphenylethyndiamine which were prepared by the Pd/Cu catalyzed, Sonogashira-type cross-coupling reaction of *para*-ethynylaniline and *para*-iodoaniline/1-4-diiodobenzene, as reported in the literature.²⁻⁵

The general characterization could be found in Appendix A, section A1.

D2. Synthesis of the proligands

The synthesis of the proligands is described in Appendix A, section A2. Scheme S1 provides an overview on their synthetic pathway.



Scheme S1. Synthetic route for the proligands.

D3. Characterization of the proligands

Et₂H₂-ppba. Yield: 90%. IR (KBr/cm⁻¹): 3250 (N-H), 3056, 2986, 2943 (C-H), 1733, 1682 (C=O). ¹H NMR (DMSO-d₆) δ(ppm): 1.30-1.34 (t, 6H, CH₃), 4.30-4.32 (q, 4H, CH₂), 7.72 (s, 4H, H_{aryl}), 10.80 (s, 2H, NH); ¹³C NMR (DMSO-d₆) δ(ppm): 14.2, 62.7, 121.2, 134.4, 155.7, 161.03. Anal. Calcd. for C₁₄H₁₆N₂O₆: C 54.54, H 5.23, N 9.09. Found: C 53.69, H 5.73, N 9.02%.

Et₂H₂-dppvba. Yield: 94%. IR (KBr/cm⁻¹): 3333 (N-H), 3110, 3031, 2991, 2943, 2904 (C-H), 1730, 1701 (C=O). ¹H NMR (DMSO-d₆) δ(ppm): 1.30-1.35 (t, 6H, CH₃), 4.30-4.33 (q, 4H, CH₂), 7.18 (s, 2H, CH), 7.57-7.60 (d, 4H, H_{aryl}), 7.75-7.78 (d, 4H, H_{aryl}), 10.83 (s, 2H, NH); ¹³C NMR (DMSO-d₆) δ(ppm): 14.2, 62.7, 120.9, 127.1, 133.1, 137.1, 155.7, 160.98. Anal. Calcd. for C₂₂H₂₀N₂O₆: C 64.70, H 4.94, N 6.86. Found: C 64.75, H 5.03, N 6.90%.

Et₂H₂-dpazba. Yield: 95%. IR (KBr/cm⁻¹): 3332 (N-H), 3140, 2993, 2901 (C-H), 1729, 1701 (C=O). ¹H NMR (DMSO-d₆) δ(ppm): 1.30-1.35 (t, 6H, CH₃), 4.30-4.33 (q, 4H, CH₂), 7.53-7.65 (d, 4H, H_{aryl}), 7.71-7.74 (d, 4H, H_{aryl}), 10.85 (s, 2H, NH); ¹³C NMR (DMSO-d₆) δ(ppm): 14.2, 62.7, 127.1, 134.1, 137.1, 155.8, 161.5. Anal. Calcd. for C₂₀H₂₀N₄O₆: C 58.25, H 4.89, N 13.59. Found: C 58.40, H 5.01, N 13.66%.

Et₂H₂-dpeba. Yield: 96%. IR (KBr/cm⁻¹): 3335 (N-H), 3113, 2984, 2905 (C-H), 1729, 1706 (C=O). ¹H NMR (DMSO-d₆) δ(ppm): 1.30-1.34 (t, 6H, CH₃), 4.28-4.33 (q, 4H, CH₂), 7.53-7.55 (m, 4H, H_{aryl}), 7.80-7.83 (m, 4H, H_{aryl}), 10.96 (s, 2H, NH); ¹³C NMR (DMSO-d₆) δ(ppm): 14.2, 62.8, 89.3, 120.7, 132.3, 138.2, 154.7, 178.7. Anal. Calcd. for C₂₂H₂₀N₂O₆: C 64.70, H 4.94, N 6.86. Found: C 64.79, H 5.02, N 6.90%.

Et₂H₂-tpeba. Yield: 93%. IR (KBr/cm⁻¹): 3335 (N-H), 3104, 3050, 2973, 2923 (C-H), 1725, 1700 (C=O). ¹H NMR (DMSO-d₆) δ(ppm): 1.30-1.34 (t, 6H, CH₃), 4.28-4.33 (q, 4H, CH₂), 7.50-7.53 (m, 4H, H_{aryl}), 7.68-7.71 (d, 4H, H_{aryl}), 7.81-7.84 (m, 4H, H_{aryl}), 10.92 (s, 2H, NH); ¹³C NMR (DMSO-d₆) δ(ppm): 14.2, 62.8, 89.5, 120.7, 129.3, 132.3, 138.2, 154.0, 168.7. Anal. Calcd. for C₃₃H₃₆N₂O₆: C 71.20, H 6.52, N 5.03. Found: C 71.26, H 6.57, N 4.99%.

D4. General procedures for carbon-carbon cross coupling reactions

The general procedures for carbon-carbon cross coupling reactions are given in Appendixes A and B, sections A5 and B4, respectively.

D5. General procedure for photochemical studies

A acetonitrile solution ($5 \cdot 10^{-6}$ M) of the corresponding dinuclear palladium(II) oxamate metallacyclophane was purged with argon for 30 min and its electronic spectrums of the degassed solutions were measured at its corresponding wavelength. Afterwards, the samples were irradiated with different UV lights, relaxing by thermal or light relaxations and its electronic spectrum were studied.

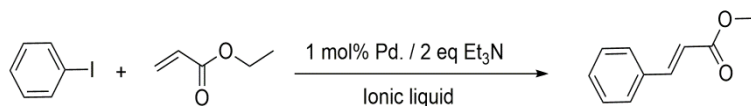
D6. Cells and Culture

The K562 cell line was derived from pleural effusion of a 53 year-old female with chronic myelogenous leukemia in terminal blast crisis in the Rio de Janeiro Cell Bank (number CR083 of the RJCB collection). The cell line was cultured in RPMI 1640 (Sigma) medium supplemented with 10 % fetal calf serum (CULTILAB, São Paulo, Brazil) at 37°C in a humidified 5 % CO₂ atmosphere. Cultures were initiated at 1×10^5 cells mL⁻¹ and grew exponentially to about 8×10^5 cells mL⁻¹ in 3 days. The viability of the cells was checked by Trypan Blue exclusion. The cell number was determined by Coulter counter analysis.

D7. Drug sensitivity assay

Dose-response curves were obtained by incubating 1×10^5 cells mL⁻¹ for 72 h, in the absence and presence of various concentrations of each palladium-based compound. The sensitivity to the drug was evaluated by the compound concentration required to inhibit cell growth by 50 %, the IC₅₀.

D8. Supplementary results of carbon-carbon cross coupling reactions

Table S2. Screening of Heck reaction with complexes **25** to **29** in different ionic liquids.

Entry ^a	Complex	Temp. (°C)	Ionic Liquid	Yield (%) ^b
1	25	120	<i>n</i> -Bu ₄ NBr	97
2	25	80	<i>n</i> -Bu ₄ NCl	26
3	25	80	BMIM-Br	6
4	25	80	BMIM-PF ₆	-
5	26	120	<i>n</i> -Bu ₄ NBr	99
6	26	80	<i>n</i> -Bu ₄ NCl	45
7	26	80	BMIM-Br	1
8	26	80	BMIM-PF ₆	-
9	27	120	<i>n</i> -Bu ₄ NBr	99
10	27	80	<i>n</i> -Bu ₄ NCl	42
11	27	80	BMIM-Br	1
12	27	80	BMIM-PF ₆	-
13	28	120	<i>n</i> -Bu ₄ NBr	98
14	28	80	<i>n</i> -Bu ₄ NCl	40
15	28	80	BMIM-Br	7
16	28	80	BMIM-PF ₆	-
17	29	120	<i>n</i> -Bu ₄ NBr	99
18	29	80	<i>n</i> -Bu ₄ NCl	30
19	29	80	BMIM-Br	4
20	29	80	BMIM-PF ₆	-

^aReaction conditions: 0.75 mmol ethyl acrylate, 1 mmol% Pd, 1 mmol Et₃N, in ionic liquids. ^b Determined by GC-MS analysis using PFTBA as internal standard.

D9. Histograms of recovery and recyclability for complexes 26-29

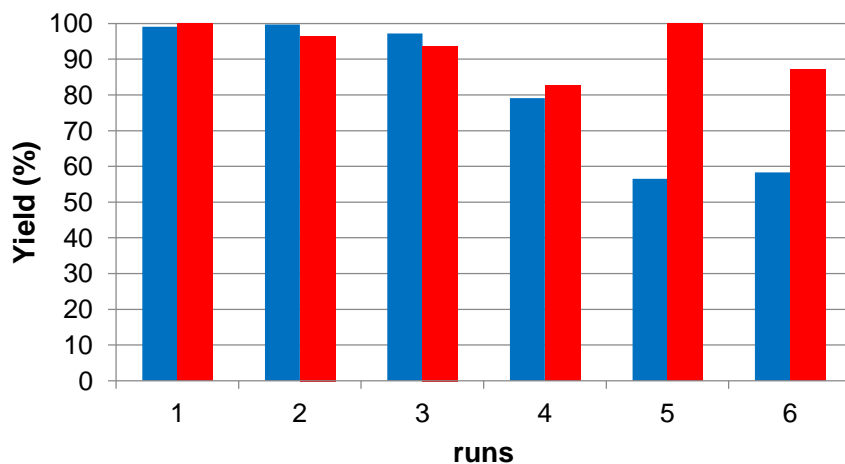


Figure S1. Histogram of recycling experiment of Heck reaction of iodoaryl and ethyl acrylate with 0.5 mmol% of **26** (blue) and for Suzuki reaction of iodoaryl and phenylboronic with 5 mmol% of **26** (red).

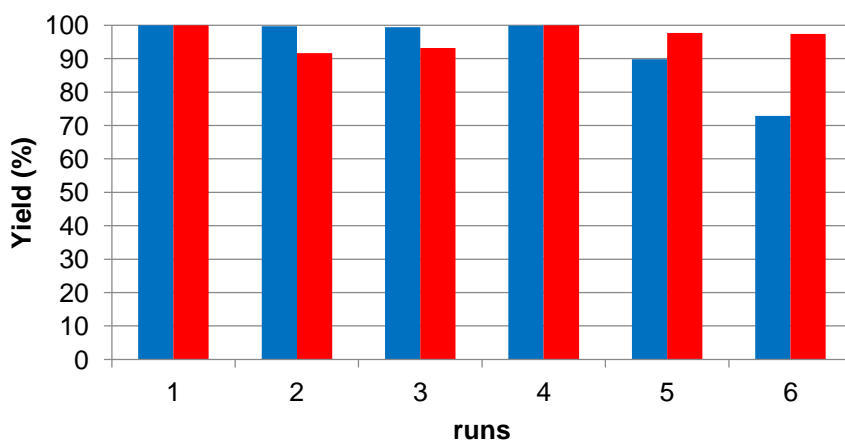


Figure S2. Histogram of recycling experiment of Heck reaction of iodoaryl and ethyl acrylate with 0.5 mmol% of **27** (blue) and for Suzuki reaction of iodoaryl and phenylboronic with 5 mmol% of **27** (red).

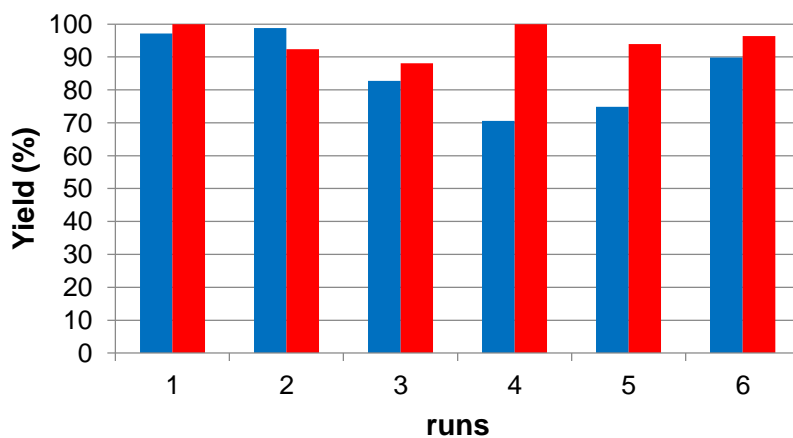
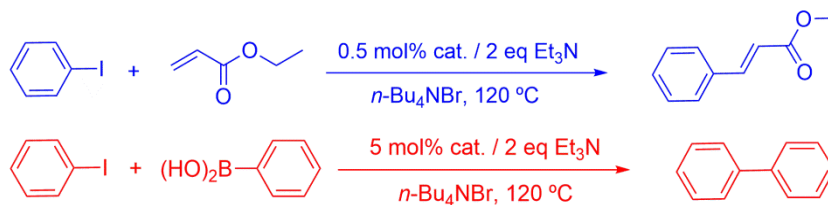


Figure S3. Histogram of recycling experiment of Heck reaction of iodoaryl and ethyl acrylate with 0.5 mmol% of **28** (blue) and for Suzuki reaction of iodoaryl and phenylboronic with 5 mmol% of **28** (red).

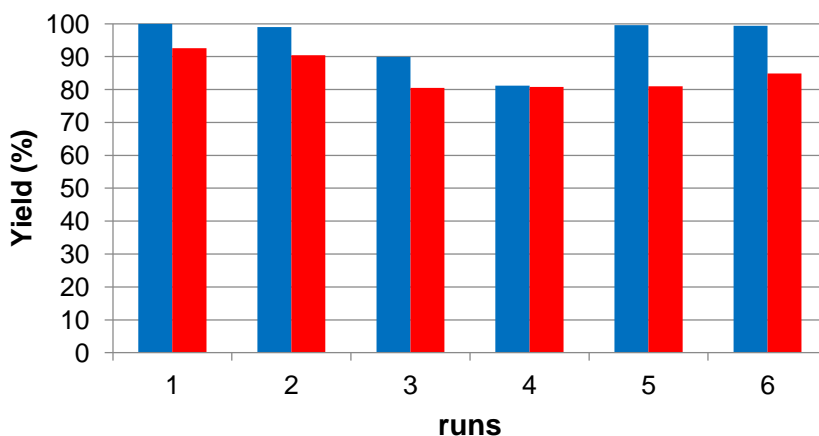


Figure S4. Histogram of recycling experiment of Heck reaction of iodoaryl and ethyl acrylate with 0.5 mmol% of **29** (blue) and for Suzuki reaction of iodoaryl and phenylboronic with 5 mmol% of **29** (red).

D10. Study of the reaction time in 26 and 27 for the Suzuki cross coupling reaction.

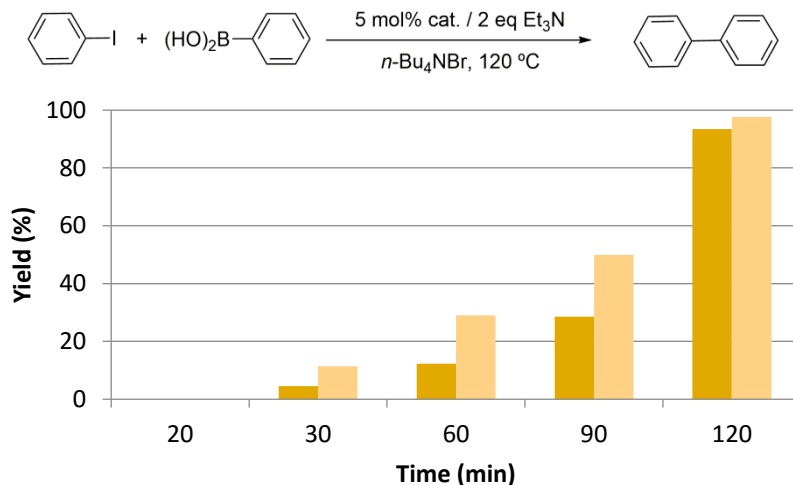


Figure S5. Histogram of the importance of finding the ideal reaction time in a cross coupling reaction exemplified by for the complexes **26** (left) and **27** (right).

D11. References

- (1) Santurri, P.; Robbins, F.; Stubbings, R. *Org. Synth.* **1960**, *40*, 18.
- (2) Deeming, A. J.; Hogarth, G.; Lee, M. (Venus); Saha, M.; Redmond, S. P.; Phetmung, H. (Taya); Orpen, A. G. *Inorganica Chim. Acta* **2000**, *309*, 109–122.
- (3) Dominguez, Z.; Khuong, T.-A. V.; Dang, H.; Sanrame, C. N.; Nuñez, J. E.; Garcia-Garibay, M. a. J. *Am. Chem. Soc.* **2003**, *125*, 8827–8837.
- (4) Fasina, T. M.; Collings, J. C.; Burke, J. M.; Batsanov, A. S.; Ward, R. M.; Albesa-Jové, D.; Porrès, L.; Beeby, A.; Howard, J. a. K.; Scott, A. J.; Clegg, W.; W., S.; Christopher; Marder, T. B. *Journal of Materials Chemistry*, 2005, *15*, 690.
- (5) Gadzikwa, T.; Zeng, B.-S.; Hupp, J. T.; Nguyen, T. S. *Chem. Commun.* **2008**, 3672–3674.

Appendix D - Dinuclear palladium(II) oxamate metallacyclophanes
